

Detection of Cardiorespiratory Interaction for Clinical Research Applications

by

Muammar Muhammad Kabir

B. Eng. (Electrical and Electronic, with Honours),
The University of Adelaide, Australia, 2007

Thesis submitted for the degree of

Doctor of Philosophy

in

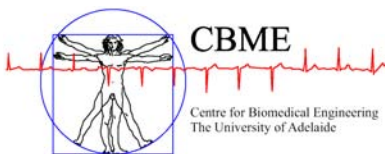
Electrical and Electronic Engineering,
Faculty of Engineering, Computer and Mathematical Sciences
The University of Adelaide, Australia

April, 2012

Supervisors:

Dr Mathias Baumert, School of Electrical & Electronic Engineering

Prof Derek Abbott, School of Electrical & Electronic Engineering



© 2012

Muammar Muhammad Kabir
All Rights Reserved



THE UNIVERSITY
of ADELAIDE

This Thesis is dedicated to my parents for their love, encouragement and endless support.

“To laugh often and much; To win the respect of intelligent people and the affection of children; To earn the appreciation of honest critics and endure the betrayal of false friends; To appreciate beauty, to find the best in others; To leave the world a bit better, whether by a healthy child, a garden patch, or a redeemed social condition; To know even one life has breathed easier because you have lived. This is to have succeeded.” -Ralph Waldo Emerson

Contents

Contents	v
Abstract	xiii
Statement of Originality	xv
Acknowledgments	xvii
Thesis Conventions	xix
Bibliography	xxi
List of Figures	xxiii
List of Tables	xxvii
Chapter 1. Introduction	1
1.1 Introduction	2
1.2 Open questions to address	3
1.3 Thesis overview	3
1.4 Physiological systems	5
1.4.1 Electrocardiogram (ECG)	5
1.4.2 Respiration	6
1.5 Processing of physiological signals	8
1.5.1 Hilbert transform	8
1.5.2 Empirical mode decomposition	9
1.6 Concept of synchronization	12
1.7 Analysis of synchronization	13
1.7.1 Cardioventilatory coupling—Detection via quantification of distribution of inspiratory onsets	13

1.7.2	Cardiorespiratory coordination—Synchrogram	16
1.7.3	Respiratory sinus arrhythmia	21
1.8	Statement of original contribution	23
1.9	Chapter summary	24
Chapter 2. Factors affecting cardiorespiratory coordination		25
2.1	Introduction	26
2.2	Methods	27
2.2.1	Ethics statement	27
2.2.2	Animal preparation and data recording	27
2.2.3	Data analysis	28
2.3	Results—Effect of anesthetic	30
2.3.1	Effect of isoflurane concentration on heart rate and respiratory rate	30
2.3.2	Effect of isoflurane concentration on cardiorespiratory coordina- tion	31
2.3.3	Effect of ventilation rate on heart rate, percentage of coordina- tion, and duration of coordinated epochs	31
2.4	Results—Effect of autonomic blockade	32
2.4.1	Effect of autonomic blockade on heart rate and respiratory fre- quency	32
2.4.2	Effect of autonomic blockade on heart rate variability	33
2.4.3	Effect of autonomic blockade on cardiorespiratory coordination .	34
2.5	Discussion	35
2.6	Chapter summary	37
Chapter 3. Respiratory pattern during voluntary movement in awake rats		39
3.1	Introduction	40
3.2	Methods	41
3.2.1	Ethical approval and preliminary surgery	41
3.2.2	Recordings of respiration and gross motor activity	42
3.2.3	Experimental protocol	42
3.2.4	Data acquisition and analysis	43

3.3	Results	46
3.3.1	Assessment of respiratory indices and motor indices	47
3.3.2	Relationship between motor activity and respiratory pattern . . .	48
3.3.3	Heart rate during basal conditions and its association with motor activity	50
3.3.4	Effect of motor activity on cardiorespiratory coordination	51
3.4	Discussion	53
3.5	Chapter summary	57
Chapter 4. Phase-coupling and sleep apnea		59
4.1	Introduction	60
4.2	Methods	61
4.2.1	Ethics statement	61
4.2.2	Subjects	62
4.2.3	Data recordings and analysis	64
4.3	Results—Adults	68
4.3.1	Polysomnographic findings	69
4.3.2	Predominant phase locking ratios	69
4.3.3	Sleep stage effects on respiratory and RR intervals and cardiorespiratory coordination in OSAS patients	71
4.3.4	Surrogate data analysis in OSAS patients	72
4.3.5	Age effects on cardiorespiratory coordination in OSAS patients .	73
4.3.6	Gender effects on cardiorespiratory coordination in OSAS patients	75
4.3.7	BMI effects on cardiorespiratory coordination in OSAS patients .	75
4.3.8	Effect of respiratory signal source on the quantification of CRC .	76
4.3.9	Correlation between CRC and heart and respiratory parameters .	77
4.3.10	Effect of sleep stage and severity of OSAS on HF power of heart rate	77
4.4	Results—Children	77
4.4.1	Polysomnographic findings	78
4.4.2	Predominant phase locking ratios in children	78

4.4.3	Sleep stage effects on respiratory and RR intervals and cardiorespiratory coordination in children	80
4.4.4	Age, BMI and gender effects on cardiorespiratory coordination in healthy children	82
4.5	Discussion	82
4.6	Chapter summary	87
Chapter 5. Time delay correction of the synchrogram technique		89
5.1	Introduction	90
5.2	Methods	90
5.2.1	Subjects / Experimental protocol	90
5.2.2	Processing of ECG and respiratory signal	92
5.2.3	Cardiorespiratory coordination analysis	92
5.2.4	Calculation of time delays for enhanced detection of coordination	93
5.2.5	Statistical analysis	95
5.3	Results	95
5.3.1	Effect of changes in body posture on RR interval	95
5.3.2	Effect of changes in body posture on respiratory interval	96
5.3.3	Calculation of time-delay using cross-correlation analysis and symbolic coupling traces	96
5.3.4	Percentage of cardiorespiratory coordination	97
5.3.5	Average duration of coordinated epochs	99
5.3.6	Phase-locking ratio	99
5.3.7	Cardiorespiratory coordination in patients with OSAS using modified synchrogram	99
5.4	Discussion	100
5.5	Chapter summary	104
Chapter 6. Cardiorespiratory interaction using joint symbolic dynamics		107
6.1	Introduction	108
6.2	Methods	109
6.2.1	Simulated data analysis using Lorenz system and an autoregressive model	109

6.2.2	Subjects / Experimental protocol	110
6.2.3	Data analysis	110
6.3	Results	115
6.3.1	Theoretical probability analysis	115
6.3.2	Analysis of joint symbolic dynamics of the non-linearly coupled system	116
6.3.3	Effect of changes in body posture on respiratory and RR interval	116
6.3.4	Symbolic dynamics approach—Optimisation of word length and threshold value, and analysis of cardiorespiratory interaction	116
6.3.5	Effect of changes in body posture on RSA	119
6.3.6	Correlation between results obtained using symbolic dynamics and RSA analysis	121
6.4	Discussion	122
6.5	Chapter summary	124
Chapter 7. Sleep apnea detection using joint symbolic dynamics		127
7.1	Introduction	128
7.2	Methods	129
7.2.1	Subjects	129
7.2.2	Overnight polysomnography and data processing	129
7.2.3	Joint symbolic dynamics	130
7.2.4	Statistical analysis	130
7.3	Results—Adults	133
7.3.1	Sleep stage effects on cardiorespiratory interaction in adults with OSAS	133
7.3.2	Group effects on cardiorespiratory interaction in adults with OSAS	133
7.3.3	Age, gender and BMI effects on cardiorespiratory interaction in adults	134
7.4	Results—Children	135
7.4.1	Effect of SDB—Group effects on cardiorespiratory interaction between healthy children and children with SDB	135
7.4.2	Analysis of cardiorespiratory interaction in healthy children and in children with SDB after excluding SDB related events	137

7.4.3	Analysis of cardiorespiratory response to spontaneous arousals in healthy children	138
7.5	Discussion	139
7.6	Chapter summary	141
Chapter 8. Respiratory sinus arrhythmia in children		143
8.1	Introduction	144
8.2	Methods	144
8.2.1	Subjects	145
8.2.2	Overnight polysomnography and data processing	145
8.2.3	Phase-averaged RSA	146
8.2.4	Statistical analysis	146
8.3	Results	147
8.3.1	Effect of sleep stage on RSA in healthy children	147
8.3.2	Effect of spontaneous arousals on RSA in healthy children	148
8.3.3	Effect of age, gender and BMI on RSA in healthy children	148
8.3.4	Effect of sleep stage on RSA in SDB children before removing SDB related events and comparison with healthy controls	149
8.3.5	Effect of sleep stage on RSA in SDB children after removing SDB related events and comparison with healthy controls	151
8.4	Discussion	152
8.5	Chapter Summary	153
Chapter 9. Thesis conclusion and future work		155
9.1	Introduction	156
9.2	Thesis summary and conclusions	156
9.3	Potential future directions	159
9.3.1	Early detection of diseases	159
9.3.2	Assessment of stress and mental-disorders	159
9.3.3	Cardiorespiratory interaction during inspiration and expiration	159
9.4	Summary of author's original contributions	160
9.5	In closing	161

Appendix A. Influence of age on cardiorespiratory interaction	163
A.1 Introduction	164
A.2 Methods	164
A.2.1 Subjects	164
A.2.2 Processing of ECG and respiratory signal	164
A.2.3 Calculation of time delays for enhanced detection of cardiorespi- ratory interaction	165
A.2.4 Joint symbolic dynamics	165
A.2.5 Statistical analysis	165
A.3 Results	166
A.3.1 Age effect on cardiorespiratory interaction using original RR in- terval	166
A.3.2 Age effect on cardiorespiratory interaction using delayed RR in- terval	166
A.4 Discussion	167
A.5 Summary	168
Appendix B. Respiratory sinus arrhythmia and cardiorespiratory phase coordina- tion	169
B.1 Introduction	170
B.2 Methods	170
B.2.1 Subjects / Experimental protocol	170
B.2.2 Processing of ECG and Respiratory signal	171
B.2.3 Cardiorespiratory phase coordination and RSA pattern analysis .	171
B.3 Results	172
B.3.1 Duration of coordinated epochs	172
B.3.2 Association between RSA and cardiorespiratory phase coordina- tion	172
B.4 Discussion	173
B.5 Summary	174
Appendix C. Matlab Codes	175

Contents

C.1	Detection of R-peaks	176
C.2	Detection of inspiratory and expiratory onsets	179
C.3	Respiration analysis during movement in rats	188
C.4	Phase-averaged RSA analysis	196
C.5	Joint symbolic dynamics approach	206
	Bibliography	215
	Glossary	233
	Index	235
	Biography	237

Abstract

Human physiological systems are a widely studied topic in the field of Biomedical Engineering. There is a particular interest in the study of human cardiovascular and respiratory systems since these two systems do not act independently; there exists a strong coupling between them. Experimental studies use the concept of synchronization to demonstrate the interaction between different physiological systems. Synchronization is the appearance of some relationship between two periodic oscillators in the form of locking of their phases or adjustment of rhythms. Cardiorespiratory coordination is an aspect of the interaction between heart and respiratory rhythm that has been reported not only at rest or during exercise, but also in subjects under the influence of anesthesia and drugs. Through the quantification of cardiorespiratory coordination we can achieve a better understanding of its physiological functioning.

Some of the conventional signal-processing techniques such as power spectral density and cross-correlation analysis have shown linear dependencies between heart and respiratory rate. However, as these biological signals are inherently non-linear, non-stationary, and contain superimposed noise, the techniques mentioned above often prove to be inadequate for characterizing their complex dynamics. Therefore, to overcome these issues, it is required to develop a technique that is less sensitive to noise, robust and possibly provides additional information about the interaction between cardiac rhythms and respiration. This Thesis introduces a new and relatively simple approach for the quantification of cardiorespiratory interaction based on joint symbolic dynamics, which provides an easy interpretation of physiological data by a simplified description of the system's dynamics. Furthermore, this Thesis investigates the association between cardiorespiratory coordination and some of the physiological mechanisms, and assesses cardiorespiratory coordination as a marker of cardiorespiratory system disturbances.

Statement of Originality

This work contains no material that has been accepted for the award of any other degree or diploma in any university or other tertiary institution to Muammar Muhammad Kabir and, to the best of my knowledge and belief, contains no material previously published or written by another person, except where due reference has been made in the text.

I give consent to this copy of the thesis, when deposited in the University Library, being available for loan, photocopying, and dissemination through the library digital thesis collection, subject to the provisions of the Copyright Act 1968.

I also give permission for the digital version of my thesis to be made available on the web, via the Universitys digital research repository, the Library catalogue, the Australasian Digital Thesis Program (ADTP) and also through web search engines, unless permission has been granted by the University to restrict access for a period of time.

24 February 2012

Signed

Date

Acknowledgments

I would like to take the opportunity to express my gratitude to all those people whose support, skills and encouragement has helped me to complete this Thesis successfully.

First, I would like to convey my deep gratitude to my supervisors **Dr Mathias Baumert** and **Prof Derek Abbott** for their guidance and support throughout my candidature. Their remarkable skills and encouraging attitude has broadened my knowledge in the field of Biomedical Engineering and Signal Processing. Their continuous support, motivation and enthusiasm have helped me to gain many positive and life time skills throughout my candidature. A special thanks to **Dr Mathias Baumert** for his pioneering idea about joint symbolic dynamics. His continuous flow of ideas and insightful comments has helped me to build my confidence in research and become a successful scientist.

I am grateful to Prof Douglas A. Gray, A/Prof Chris Coleman, A/Prof Christophe Fumeaux and Dr Brian W.-H. Ng from School of Electrical & Electronic Engineering for their informative discussions and valuable suggestions.

My PhD has been a memorable journey. It has given me the opportunity to meet and work with many scientists all over the world. I would like to thank A/Prof Eugene Nalivaiko (School of Biomedical Sciences and Pharmacy, University of Newcastle) and his research group from Flinders University, South Australia and University of Newcastle, New South Wales, for their assistance with data collection from rats and interpretation of results. A/Prof Eugene's vast knowledge about medical physiology has helped me to understand some of the basic physiological mechanisms in human body. I am also grateful to Dr David A. Saint (School of Medical Sciences, The University of Adelaide), Prof Prashanthan Sanders (Royal Adelaide Hospital, The University of Adelaide) and his research group, Dr Hany Dimitri (Royal Adelaide Hospital, The University of Adelaide), Dr Declan Kennedy (Women's and Children Hospital, The University of Adelaide) and his research group, and Dr Mark Kohler (School of Psychology, Social Work and Social Policy, University of South Australia) for their support in collecting data from human subjects and valuable suggestions.

I would also like to express my utmost gratitude to all my friends and colleagues from the School of Electrical & Electronic Engineering at the University of Adelaide:

Acknowledgments

Dr Withawat Withayachumnankul, Dr Jegathisvaran Balakrishnan, Mr Henry Ho, Mr Mayank Kaushik, Mr Benjamin S. Y. Ung, Mr Hungyen Lin, Mr Muhammad Asrafal Hasan, Mrs Sarah A. Immanuel, Mr Omid Kavehei, Mr Syed Mostafa Rahimi Azghadi, and Mr Ali Karami for their constant support and encouragement throughout my candidature.

I am grateful to Ms Rose-Marie Descalzi, Ms Colleen Greenwood, Ms Philomena Jensen-Schmidt, Ms Ivana Rebellato, Mr Danny Di Giacomo, and Mr Stephen Guest at School of Electrical & Electronic Engineering for their assistance in administrative work during my candidature. I would also like to thank IT support and technical officers from School of Electrical & Electronic Engineering, Mr David Bowler, Mr Mark J. Innes, Mr Ryan King, Mr Ian R. Linke, Mr Alban P. O'Brien, and Mr Pavel Simcik for their valuable technical support.

I gratefully acknowledge the School of Electrical & Electronic Engineering at the University of Adelaide, IEEE South Australia and Walter and Dorothy Duncan Trust Fund for their financial support and travel grants. I would also like to thank Australian Research Council for its support in research studies discussed in Chapters 5 & 6 (grant # DP 110102049).

I owe special thanks to my parents, Dr S. M. Alamgir Kabir and Dr G. T. J. Afrooz Begum, my brother-in-law, Engr. Zahedur Rahman, my sister, Dr Nadia Afroz Kabir and my lovely nephew, Nafiur Rahman for their generosity, encouragement and tremendous support.

Last but not the least, I would like to take the opportunity to extend my deepest gratitude to all of my family members, and childhood friends, especially Nafees Mosharref, Paul Damouni, Nabeel Mosharref, Shafaat S. Giasuddin, Rubaiyat S. Giasuddin, Mohammad A. Kochi, Tanveer Ahmed, Mahmood Shafique, Nayeem Mohammad, Shahriar Kabir, Tauseef Zaman, Nabil Mohammad, Nadia Kalam, Tahira Zaman, Sumaiya Zaman, Humaira Choudhury, Kaniz Khan, and Rania Fatima for their continuous support and encouragement in building my confidence and helping me create another success story for my life.

Muammar M. Kabir

Thesis Conventions

The following conventions have been adopted in this Thesis:

1. **Spelling.** Australian English spelling conventions have been used, as defined in the Macquarie English Dictionary, A. Delbridge (Ed.), Macquarie Library, North Ryde, NSW, Australia, 2001.
2. **Typesetting.** This document was compiled using $\text{\LaTeX}2\text{e}$. TeXnicCenter was used as text editor interfaced to $\text{\LaTeX}2\text{e}$. Adobe Illustrator CS2 and Inkscape was used to produce schematic diagrams and other drawings.
3. **Mathematics.** MATLAB code was written using MATLAB Version R2007b/R2008a; URL: <http://www.mathworks.com>.
4. **Referencing.** The Harvard style has been adopted for referencing.
5. **URLs.** Universal Resource Locators are provided in this Thesis for finding information on the world wide web using hypertext transfer protocol (HTTP). The information at the locations listed was current on 17 December 2009.

Bibliography

Journal Articles

- KABIR M. M., SAINT D. A., NALIVAICO E., ABBOTT D., & BAUMERT M. (2011). Time delay correction of the synchrogram for optimized detection of cardiorespiratory coordination, *Med. Biol. Eng. Comput.*, **49**, pp. 1249–1259.
- KABIR M. M., SAINT D. A., NALIVAICO E., ABBOTT D., VOSS A., & BAUMERT M. (2011). Quantification of cardiorespiratory interactions based on joint symbolic dynamics, *Ann. Biomed. Eng.*, **39**(10), pp. 2604–2614.
- BAUMERT M., KOHLER M., KABIR M. M., SANDERS P., KENNEDY D., MARTIN J., & PAMULA Y. (2011). Altered cardio-respiratory response to spontaneous cortical arousals in children with upper airway obstruction, *Sleep Med.*, **12**, pp. 230–238.
- KABIR M. M., DIMITRI H., SANDERS P., ANTIC R., NALIVAICO E., ABBOTT D., & BAUMERT M. (2010). Cardiorespiratory phase-coupling is reduced in patients with obstructive sleep apnea, *PLoS ONE*, **13**(5), art. no. e10602.
- KABIR M. M., BEIG M. I., BAUMERT M., TROMBINI M., MASTORCI F., SGOIFO A., WALKER F. R., DAY T. A., & NALIVAICO E. (2010). Respiratory pattern in awake rats: Effects of motor activity and of alerting stimuli, *Physiol. Behav.*, **101**, pp. 22–31.
- BAUMERT M., KOHLER M., KABIR M. M., KENNEDY D., & PAMULA Y. (2010). Cardiorespiratory response to spontaneous cortical arousals during stage 2 and REM sleep in healthy children, *J. Sleep Res.*, **19**, pp. 415–424.

Conference Articles

- KABIR M. M., ABBOTT D., & BAUMERT M. (2011). Influence of age on cardiorespiratory interactions assessed by joint symbolic dynamics, *Seventh International Conference on Intelligent Sensors, Sensor Networks and Information Processing—Symposium on Biomedical Sensing and Sensors 2011*, Adelaide, Australia, pp. 41–45.

- KABIR M. M., DIMITRI H., SANDERS P., ANTIC R., ABBOTT D., & BAUMERT M. (2011). Quantification of cardio-respiratory interactions in patients with mild obstructive sleep apnea syndrome using joint symbolic dynamics, *Computing in Cardiology 2011*, Hangzhou, China, **38**, pp. 41–44.
- KABIR M. M., KOHLER M., ABBOTT D., & BAUMERT M. (2011). Quantification of cardiorespiratory interactions in healthy children during night-time sleep using joint symbolic dynamics, *Proceedings of the 33rd IEEE Engineering in Medicine and Biology Society*, Boston, USA, pp. 1459–1462.
- KABIR M. M., SAINT D. A., ABBOTT D., & BAUMERT M. (2011). Effect of postural changes on cardiorespiratory coordination in humans, *Proceedings of 3rd International Conference on Signal Acquisition and Processing*, Singapore, pp. V1-76–V1-80.
- KABIR M. M., NALIVAICO E., ABBOTT D., & BAUMERT M. (2010). Impact of movement on cardiorespiratory coordination in conscious rats, *Proceedings of the 32nd IEEE Engineering in Medicine and Biology Society*, Buenos Aires, Argentina, pp. 1938-1941.
- KABIR M. M., BEIG M. I., NALIVAICO E., ABBOTT D., & BAUMERT M. (2008). Cardiorespiratory coordination in rats is influenced by autonomic blockade, *13th International Conference on Biomedical Engineering*, Singapore, pp. 456-459.
- KABIR M. M., BEIG M. I., NALIVAICO E., ABBOTT D., & BAUMERT M. (2008). Isoflurane increases cardiorespiratory coordination in rats, *Proceedings SPIE Biomedical Applications of Micro- and Nanoengineering IV and Complex Systems*, Melbourne, Australia, **6416**, art. no. 72700Y.

List of Figures

1.1	ECG signal	6
1.2	Respiratory signal	7
1.3	Empirical mode decomposition	11
1.4	Difference between synchronized and desynchronized signals	13
1.5	Respiratory wave, ECG and the times of R-peaks and inspiratory onsets	14
1.6	Synchrogram plot	17
1.7	Respiratory sinus arrhythmia	22
<hr/>		
2.1	Heart rate and concentration of isoflurane	30
2.2	Respiratory frequency and concentration of isoflurane	31
2.3	Cardiorespiratory coordination and concentration of isoflurane	32
2.4	Heart rate, respiratory rate and autonomic blockade	33
2.5	Coherence plot	34
2.6	Low-frequency and high-frequency power	35
2.7	Cardiorespiratory coordination and autonomic blockade	36
<hr/>		
3.1	Wavelet analysis of respiration and motor activity	44
3.2	Motor activity, respiratory and heart rate	45
3.3	Record of respiration, ECG and gross spontaneous motor activity	46
3.4	Histogram of respiratory intervals	47
3.5	Relationship between respiration and motor activity	49
3.6	Relationship between total time of rapid breathing and movement	51
3.7	Relationship between the duration of motor act and changes in heart rate	52
3.8	RR and respiratory intervals vs. low and high intensity movement	54
3.9	Motor activity and cardiorespiratory coordination	55

List of Figures

4.1	Sleep stages and synchrogram	65
4.2	Cardiorespiratory coordination in adults	69
4.3	RR and respiratory intervals in adults/OSAS patients	71
4.4	Cardiorespiratory coordination	72
4.5	Cardiorespiratory coordination	73
4.6	High Frequency Power	77
4.7	RR interval in healthy and SDB children	78
4.8	Respiratory intervals in healthy and SDB children	80
4.9	Percentage of cardiorespiratory coordination	81
4.10	Average duration of coordinated epochs	82
4.11	Healthy children—Age, BMI and gender effects	83
<hr/>		
5.1	Respirace	91
5.2	PowerLab data acquisition system	92
5.3	Time delay between ECG and respiration	93
5.4	Correlation plots	96
5.5	Probability plots	97
5.6	Percentage of coordination for different body positions	98
5.7	Average duration of coordination for different body positions	100
5.8	Percentage of coordination in patients with OSAS	102
<hr/>		
6.1	Simulated data analysis	110
6.2	Schematic illustration of symbolic dynamics	111
6.3	Phase-averaged respiratory sinus arrhythmia plot	114
6.4	Interaction between coupled systems using symbolic dynamics	115
6.5	Significance test results	118
6.6	Cardiorespiratory coordination using symbolic dynamics	119
6.7	RSA in supine and upright posture	120
6.8	RSA during head-up tilt	121

7.1	Sleep related comparison of cardiorespiratory interaction in adults with OSA	132
7.2	Association between cardiorespiratory interaction and severity of OSA in adults	133
7.3	Association between cardiorespiratory interaction and age, BMI or gender in adults	134
7.4	Analysis of cardiorespiratory interaction in children considering respiratory arousal episodes	135
7.5	Analysis of cardiorespiratory interaction in children after excluding SDB related events	136
7.6	Cardiorespiratory response to spontaneous arousals in healthy children	138
7.7	Cardiorespiratory response to spontaneous arousals in healthy children	139

8.1	Sleep stages effects on RSA in healthy children	146
8.2	Effect of spontaneous arousals on RSA in healthy children	147
8.3	Age effect on RSA in healthy children	148
8.4	Gender and BMI effects on RSA in healthy children	149
8.5	Group and sleep stage effects on RSA in children before removing SDB related events	150
8.6	Group and sleep stage effects on RSA in children after removing SDB related events	151

A.1	Cardiorespiratory interaction vs. age	166
A.2	Cardiorespiratory interaction vs. age using delayed RR interval	167

B.1	RSA magnitude and cardiorespiratory phase coordination	172
B.2	RSA phase and cardiorespiratory phase coordination	173

List of Tables

2.1	Ventilation rates	33
3.1	Temporal characteristics of motor activity	48
4.1	Cardiorespiratory coordination in patients with and without heart diseases	63
4.2	Overnight polysomnography in adults	67
4.3	Predominant phase locking ratios in adults	70
4.4	Cardiorespiratory coordination: Original vs. surrogate data	74
4.5	Abdominal vs. thoracic respiratory signals: Percentage of coordination	76
4.6	Abdominal vs. thoracic respiratory signals: Duration of coordination	76
4.7	Overnight polysomnography in children	79
4.8	Predominant phase locking ratios in children	80
5.1	Respiratory intervals	95
5.2	Frequent phase locking ratios	101
6.1	Joint symbolic dynamics approach	117
6.2	Correlation analysis	122
7.1	Word formations using joint symbolic dynamics	131
7.2	Comparison of cardiorespiratory interaction in healthy children	137
8.1	Correlation analysis	148

Chapter 1



Introduction



CARDIAC and respiratory rhythms reveal transient phases of phase-locking, which are thought to be an important aspect of cardiorespiratory control. This Chapter provides an outline of all the Chapters in this Thesis. Here we discuss some of the physiological aspects of heart rate and respiration and the processing of their signals. This Chapter reviews the theoretical underlay of cardiorespiratory coordination. It also discusses recent research in this field.

1.1 Introduction

Physiological systems are a widely studied topic in the field of Biomedical Engineering. While every physiological system is important, there is much interest in the study of human cardiovascular and respiratory systems (Rosenblum *et al.* 2004, Wu and Hu 2006) due to the central function of these systems in the human body. According to Wu and Hu (2006), these two systems do not act independently; there exists a strong coupling between them.

Synchronization is a basic phenomenon in nature (Rosenblum *et al.* 1996, Rosenblum and Kurths 1998, Rosenblum *et al.* 2001, Bettermann *et al.* 2002, Kotani *et al.* 2002, Rosenblum *et al.* 2002, Rzecziński *et al.* 2002, Cysarz *et al.* 2004a, Rosenblum *et al.* 2004). Experimental studies use the concept of synchronization to demonstrate the interaction between different physiological systems. Through the detection of synchronization we may achieve a better understanding of physiological functioning.

The association between cardiac and respiratory rhythms has long been recognized. Several methods have been developed to detect cardiorespiratory synchronization. Since human cardiovascular and respiratory systems are very complex, the proposed methods come with certain limitations, for example, they are highly sensitive to noise and inadequate to characterize the complex dynamics of cardiorespiratory synchronization. Moreover, some of the methods fail to detect the actual strength of synchronization (Hoyer *et al.* 1998a, Wu and Hu 2006). In addition, although there has been a substantial amount of research on heart and respiration, the underlying mechanisms causing cardiorespiratory synchronization have been little explored. Due to the lack of validation of the methods and inconsistent results, their use in practical applications has not yet gained popularity.

This Thesis discusses some nonlinear data processing techniques, analyzes cardiac and respiratory signals under various conditions to determine factors causing or responsible for cardiorespiratory synchronization, and introduces a modified as well as novel technique that is robust and provides an effective and easy interpretation of cardiorespiratory synchronization. Developing this effective methodology and analyzing the dynamics of the physiological systems can provide a better detection of physiological interactions and understanding about the underlying mechanisms in human body, which can be used for other experimental studies and clinical applications.

1.2 Open questions to address

To understand the underlying physiological mechanisms responsible for the interaction between cardiac rhythm and respiration, this Thesis will address the following questions.

- Do anesthetics affect the interaction between cardiac rhythm and respiration?
- Does the autonomic nervous system (ANS), which influences the heart rate, have any influence on cardiorespiratory synchronization?
- Can controlled breathing (paced respiration) increase cardiorespiratory synchronization?
- How does voluntary movement affect respiration, heart rate and cardiorespiratory synchronization?
- Can the quantification of cardiorespiratory synchronization be used as a marker for determining the severity of obstructive sleep apnea syndrome?
- Can a robust and effective methodology be developed that would provide improved performance in the quantification of cardiorespiratory synchronization compared to previous techniques?

1.3 Thesis overview

This Thesis consists of 9 chapters. Basic fundamentals necessary for understanding the main topic are discussed in Chapter 1. The novel technique for the detection of cardiorespiratory coordination is discussed in Chapter 6. A detailed description for each Chapter of this Thesis is as follows.

Chapter 1 gives an overview of relevant physiological systems and elucidates the fundamental concept of synchronization. It also discusses some of the techniques of signal processing.

Chapter 2 investigates the influence of anesthetic and respiratory ventilation rates on the interaction between heart rhythm and respiration in rats. It also examines the influence of autonomic nervous system (ANS) on cardiorespiratory synchronization. This

study is necessary to understand the factors responsible for cardiorespiratory coordination and the physiology underlying this interaction.

Chapter 3 discusses the impact of voluntary movement on respiration and cardiorespiratory synchronization in awake and free-moving rats. This study elucidates how external factors can affect the interaction between cardiac and respiratory cycles, which should be taken into consideration during cardiorespiratory synchronization analysis.

Chapter 4 aims at quantification of cardiorespiratory synchronization in adults with obstructive sleep apnea and in children with sleep disordered breathing.

Chapter 5 introduces a modified version of a well-known technique for better quantification of cardiorespiratory synchronization.

Chapter 6 introduces a novel technique to investigate the interactions between heart rhythms and respiration based on their joint symbolic dynamics (JSD). The results are validated by comparing them with a different technique, which shows that the novel technique is more sensitive and provides an improved performance in detecting changes in cardiorespiratory synchronization.

Chapter 7 explores cardiorespiratory synchronization in adults with obstructive sleep apnea and in children with sleep disordered breathing (discussed in Chapter 4) using the novel technique introduced in Chapter 6. The relationship between cardiorespiratory interaction and spontaneous arousal in healthy children is studied. The study also verifies the claim in Chapter 6 that the novel technique provides improved performance in detecting changes in the interaction between heart rhythm and respiration.

Chapter 8 investigates respiratory sinus arrhythmia in healthy children and children with sleep disordered breathing.

Chapter 9 summarizes the work in this Thesis and provides possible future directions for further development.

Appendix A investigates the influence of age on the interaction between cardiac and respiratory cycles in healthy subjects using the approach based on joint symbolic dynamics.

Appendix B investigates the relation between respiratory sinus arrhythmia (RSA) and cardiorespiratory coordination (CRC) by comparing RSA during CRC, with the RSA immediately before and after the CRC episode.

Appendix C elaborates some of the software program developed as a part of this research.

In order to study the interaction between cardiac rhythm and respiration, we now give a brief description about the essential physiological systems and some of the techniques required for the processing of signals from physiological systems and for the quantification of cardiorespiratory synchronization.

1.4 Physiological systems

1.4.1 Electrocardiogram (ECG)

The electrocardiogram (ECG) is the graphical recording of electrical activity of the heart over time as seen at the surface of the epidermis and expresses certain electrophysiologic phenomena manifested by the heart during the process of contraction and relaxation of cardiac muscle (Sigler 1957). The first human ECG was recorded in 1887 by Waller using a mercury capillary electrometer arrangement (Waller 1887). The instrumentation used to record ECG and the basic nomenclature that describes the characteristics of ECG was later introduced by Einthoven *et al.* (1950)—they also proposed a set of bipolar limb leads (leads I,II and III) to capture the cardiac electrical activity in the frontal plane. These three leads are internationally known as the standard leads:

Lead I - tracing obtained by leading off from the right and left arms

Lead II - tracing obtained by leading off from the right arm and left leg

Lead III - tracing obtained by leading off from the left arm and left leg.

The standard bipolar leads, however, cannot always accurately determine the exact events occurring in specific locations of the heart. As a result, unipolar leads were introduced, based on the work by Wilson *et al.* (1926). Different areas of the chest are used for different unipolar leads, each of which can provide vital information regarding the heart physiology (Sigler 1957). The most common leads used are V1, V2, V3, V4, V5 and V6 leads, as recommended by Standardization of precordial leads (1938). Details about the placement of the leads are discussed by Sigler (1957).

In the ECG, the main characteristic waves are the P-wave, the QRS-complex and the T-wave (see Fig. 1.1). For the purpose of study, intervals between characteristics waves, such as QT, ST and RR segments, are measured as shown in Figure 1.1. The variation in heart rate or RR interval with time can be termed as the heart rate variability (HRV).

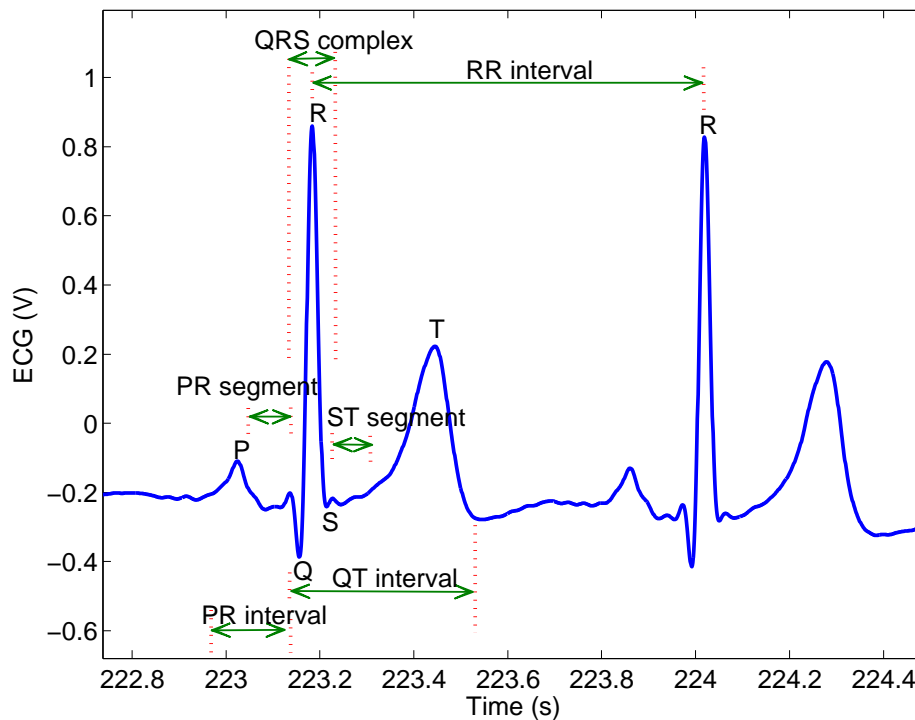


Figure 1.1. ECG signal. An example of ECG signal showing R-peaks and the corresponding R-R interval.

Processing of ECG

In this Thesis, custom written computer software developed under MATLAB[®] (see Appendix C) is used to detect the R-peaks from the recorded ECG signal using parabolic fitting, where a parabola of specific length, based on the sampling frequency, is fitted around the R-wave to determine the R-wave maximum (Manriquez and Zhang 2007). The R-R time series are visually scanned for artifacts.

1.4.2 Respiration

Respiration can be defined as the transport of oxygen from the atmosphere into the human body and the release of carbon-dioxide in the opposite direction. The main function of the respiratory system is to supply oxygen to the blood, which carries the oxygen to other parts of the body.

Biomedical signals are non-linear, non-stationary and usually contaminated with noise. A reliable measure of respiration is required for clinical studies. For example, the clinical significance of some of the heart rate variability can only be understood by studying

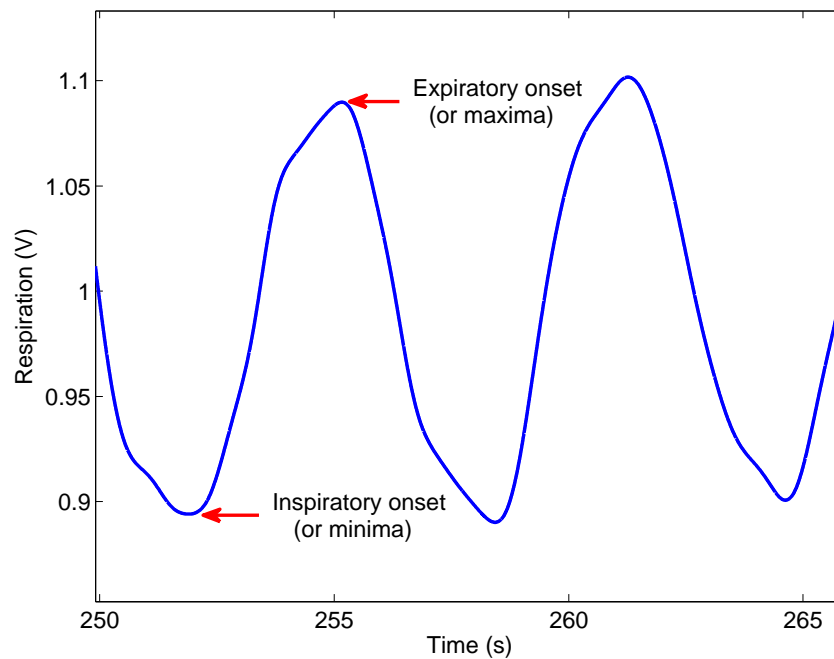


Figure 1.2. Respiratory signal. An example of respiratory signal inspiratory onset/minima and expiratory onset/maxima.

the corresponding respiratory signal (Moody *et al.* 1985). Similarly, knowledge of respiration is necessary to study its interaction with the heart rhythms (Schafer *et al.* 1998).

Processing of respiratory signal

The minimum and maximum points in the respiratory cycle are termed as inspiratory and expiratory onsets, respectively, as seen in Figure 1.2. In this Thesis, to remove noise, respiratory signals are low-pass filtered using a zero-phase forward and reverse digital filter, which first filters the raw signal in the forward direction using an n^{th} order Butterworth filter, and subsequently filters the reversed signal. The resultant signal will have zero phase distortion. In this Thesis, custom written computer software developed under MATLAB[®] (see Appendix C) is used to detect inspiratory onsets for each respiratory cycle. First, the offset of the signal is removed by subtracting the mean value. Subsequently, the inspiratory and expiratory onsets are determined as the zero-crossings of the first derivative of the respiratory signal.

1.5 Processing of physiological signals

1.5.1 Hilbert transform

The phases of a signal can be calculated using Hilbert transform. According to Gabor (1946), the instantaneous phase and amplitude for a signal $s(t)$ can be obtained from the analytic signal $\zeta(t)$, represented as

$$\zeta(t) = s(t) + j\tilde{s}(t) = A(t)e^{j\phi t}, \quad (1.1)$$

where $\tilde{s}(t)$ is the Hilbert transform of $s(t)$.

For a discrete signal $x[n]$ with samples N , if the discrete Fourier transform is given as

$$F(x[n]) = X[k] = \sum_{n=0}^{N-1} x[n]e^{-jnk\frac{2\pi}{N}}, k \in 0, N-1, \quad (1.2)$$

then the discrete Hilbert transform can be defined as

$$H(x[n]) = \hat{x}[k] = \frac{1}{N} \sum_{k=0}^{N-1} \hat{X}[k]e^{jnk\frac{2\pi}{N}}, k \in 0, N-1, \quad (1.3)$$

where for N —even

$$\hat{X}(k) = \begin{cases} -jX[k], k = 1, \frac{N}{2} - 1 & \text{for } N \text{ even,} \\ jX[k], k = \frac{N}{2} + 1, N - 1 & \text{for } N \text{ even.} \end{cases} \quad (1.4)$$

Here, the continuous and Nyquist components are excluded (for $k = 0$ and $k = N/2$).

while for N —odd

$$\hat{X}(k) = \begin{cases} -jX[k], k = 1, \frac{N-1}{2} & \text{for } N \text{ odd,} \\ jX[k], k = \frac{N+1}{2}, N - 1 & \text{for } N \text{ odd.} \end{cases} \quad (1.5)$$

Here, the continuous component is excluded.

1.5.2 Empirical mode decomposition

Classically Fourier based methods/spectral analysis provide simplest model for examining the global energy-frequency distributions of oscillatory waveform based on sinusoid. Although the Fourier spectral analysis has gained much popularity, it can only be applied to stationary signals and linear time invariant systems. However, physiological signals are often non-stationary and generated by systems which are inherently nonlinear.

The Empirical Mode Decomposition (EMD) method was developed based on the assumption that any time series data consist of different simple intrinsic modes of oscillation. The decomposition is based on the direct extraction of the energy associated with various intrinsic modes. During the process, the intrinsic oscillatory modes are identified by their characteristic time scales in the data empirically, and subsequently the data is decomposed accordingly (Huang *et al.* 1998).

Empirical mode decomposition separates data into non-overlapping time scale components (Huang *et al.* 1998, Wu and Hu 2006). It decomposes the multi-component signal into a series of well-behaved intrinsic modes known as intrinsic mode functions (IMF) (Maragos *et al.* 1993a). According to Huang *et al.* (1998), these functions satisfy the following two conditions:

1. the number of extrema and the number of zero crossings must either be equal or differ at most by one in the whole data set,
2. at any point, the mean value of the envelope defined by the local maxima and the envelope defined by the local minima is zero.

In other words, an IMF represents a simple oscillatory mode embedded in the data (Maragos *et al.* 1993b, Huang *et al.* 1998). An IMF is not restricted to a narrow band signal, and can have a variable amplitude and frequency at different functions of time i.e. it can be non-stationary and both amplitude and frequency modulated.

For a signal $x(t)$, the algorithm to create IMFs in EMD can be explained as follows (Huang *et al.* 1998):

1. Identify the local extremas in the time series $x(t)$

1.5 Processing of physiological signals

2. Interpolate (e.g. cubic spline) among all maximas and minimas to generate the upper and lower envelope of the time series respectively. The upper and lower envelopes should cover all the data between them.
3. Compute the running mean series $m_1(t)$ by point-by-point averaging of the two envelopes, $\Psi(t)$

$$m_1(t) = \frac{\Psi_{\max}(t) + \Psi_{\min}(t)}{2} . \quad (1.6)$$

4. Determine the first component, $h_1(t)$ by subtracting the running mean $m_1(t)$ from the original time series $x(t)$

$$h_1(t) = x(t) - m_1(t) \quad (1.7)$$

- if the conditions for IMF are satisfied then the resultant component $h_1(t)$ is an IMF
 - if the conditions for IMF are not satisfied then the whole process from step 1 (also known as sifting process) is repeated until an IMF component is obtained.
5. Subtract the first IMF from the original data to evaluate the residue, $r_1(t)$

$$r_1(t) = x(t) - h_1(t) . \quad (1.8)$$

6. Repeat the sifting process, replacing the original signal with the residual signal $r_1(t)$.
7. Continue the process to determine all the intrinsic modes h_i . The final residue is a constant or monotonic function which represents the general trend of the original time series.

At the end of the process there will be a residue, r and a series of IMFs, h_i (where $i = 1,2,3,\dots,n$), as seen in Figure 1.3. The IMFs are generated in descending order of frequency and therefore h_1 is the one associated with the locally highest frequency

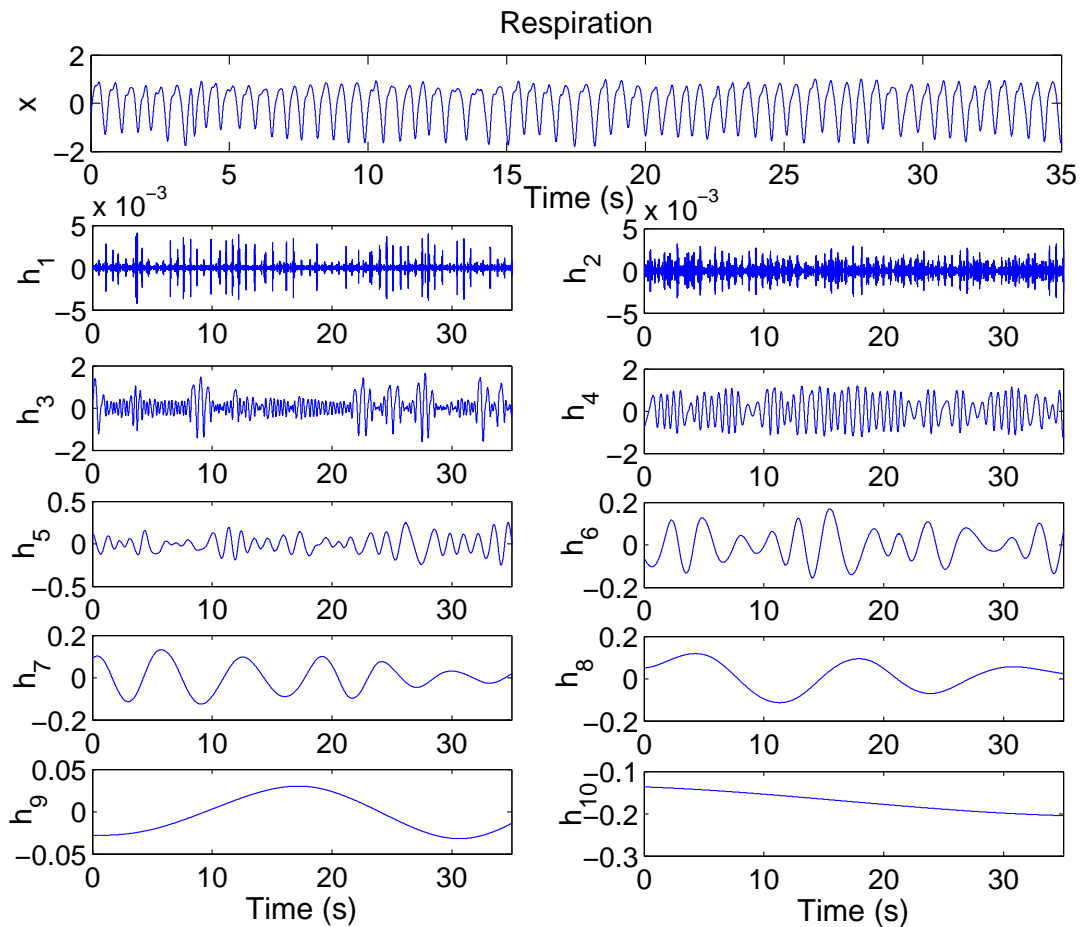


Figure 1.3. Empirical mode decomposition. A respiratory signal and the subsequent intrinsic mode functions.

(Balocchi *et al.* 2004). After the sifting process is accomplished, the original data can be $x(t)$ expressed as:

$$x(t) = \sum_{i=1}^N h_i(t) + r_n(t), \quad (1.9)$$

where, the residual signal is given by

$$r_i(t) = r_{i-1}(t) + h_i(t). \quad (1.10)$$

The IMF that best fits the original signal is used for the purpose of further analysis. The EMD method has been successfully applied to biomedical signals in several studies (Echeverria *et al.* 2001, Zhang *et al.* 2008, Bhuiyan *et al.* 2010).

1.6 Concept of synchronization

Synchronization can be defined as the appearance of some relationship between the characteristics of two or more systems (Hoyer *et al.* 2000, Schafer *et al.* 1999, Rzecziński *et al.* 2002, Cysarz *et al.* 2004a, Rosenblum and Kurths 1998, Rosenblum *et al.* 2004, Rosenblum *et al.* 1996). There are different types of synchronization such as amplitude synchronization, frequency synchronization and phase synchronization. However, it has been suggested that the properties of phase synchronization in chaotic systems are similar to those of synchronization in periodic noisy oscillators (Pikovsky *et al.* 1997) and thus the analysis of phase synchronization allows us to study and describe both chaotic and noisy oscillators within a common framework (Rosenblum *et al.* 2001). Hence, this research will focus on the phase synchronization.

Dynamic phase synchronization between different physiological systems have been the subject of interest in the field of biomedical engineering. The physiological interactions between systems cause an adjustment of rhythms and this process is termed as cardiorespiratory synchronization (Wu and Hu 2006, Rosenblum *et al.* 2001, Hoyer *et al.* 1998a, Hoyer *et al.* 1998c). Synchronized signals are characterized by the presence of increased order among the signals.

The following figure indicates the difference between the synchronized and the desynchronized state of respiration, heart rate and blood pressure. During the desynchronized state, the signals do not follow any pattern and are quite random while during the synchronized state some relationship can be observed among the signals.

Earlier studies support the existence of cardiorespiratory synchronization (Wu and Hu 2006, Rosenblum *et al.* 2004, Bartsch *et al.* 2007). Although respiratory signals can be considered as sinusoidal wave, the cardiac excitations tend to be more regular than respiratory oscillations (Wu and Hu 2006, Rosenblum *et al.* 2002). It has been observed that synchronization usually occurs or becomes stronger when the cardiac and respiratory signals become regular enough (Rzecziński *et al.* 2002).

Factors such as noise and changing frequency ratios of synchronized intervals complicate the detection of dynamic phase synchronization (Hoyer *et al.* 2000). Wu and Hu (2006) and Hoyer *et al.* (1998c) made an important contribution by describing the technical problems in the analysis of respiratory signals. According to them, over-filtered signals have the possibility of losing their original characteristics while poorly-filtered

NOTE:
This figure is included on page 13 of the print copy of
the thesis held in the University of Adelaide Library.

Figure 1.4. Difference between synchronized and desynchronized signals. The above figure represents the respiration, heart rate variability and blood pressure of an individual before and after a state of appreciation. Before having a feeling of appreciation, the patterns of the rhythms were random and no relationship was observed. On the other hand, the patterns of the rhythms were regular and synchronized at the time of appreciation. After emwave (2011)

signals might still contain some noise that would affect the detection of synchronization.

1.7 Analysis of synchronization

1.7.1 Cardioventilatory coupling—Detection via quantification of distribution of inspiratory onsets

Cardioventilatory coupling (CVC) is a concept, which specifically refers to the influence of timing of breathing on cardiac activity (Galletly and Larsen 1997, Galletly and Larsen 1999, Tzeng *et al.* 2003). Cardioventilatory coupling is quantified based on the temporary alignment between the R waves of the ECG and inspiratory onsets of respiration, using the R-peak to Inspiratory-onset interval (RI) plot (see Figure 1.5). Galletly and Larsen (1998) showed that during anaesthesia CVC places the heart beats and

1.7 Analysis of synchronization

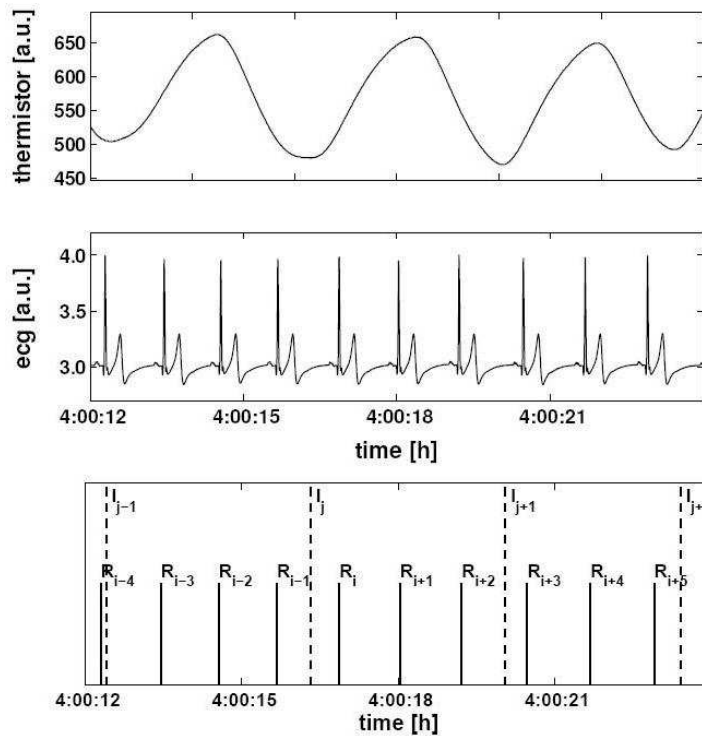


Figure 1.5. Respiratory wave, ECG and the times of R-peaks and inspiratory onsets. The top and middle section of the figure represents the respiration and ECG respectively. The bottom section shows the identified R peaks and the inspiratory onsets. After Cysarz *et al.* (2004a)

inspiratory onsets such that they are maximally affected by vagal modulation of respiratory sinus arrhythmia (RSA)—discussed in Section 1.7.3—implying common physiological roles and significant relationship between CVC and RSA.

This method has been used in the early studies (Bettermann *et al.* 2002, Cysarz *et al.* 2004a) and is based on the calculation of temporal distances between the event markers of the two time series. In the case of analyzing the interaction between heart rhythm and respiration, two different possibilities need to be considered:

1. Temporal distance between inspiratory onset, I , and the successive R-peak, R . The absolute distance t_i and relative distance ϕ_i between the inspiratory onsets and successive R-peaks is given as

$$t_i = R_i - I_j, \quad (1.11)$$

$$\phi_i = \left(\frac{R_i - I_j}{I_{j+1} - I_j} + j \right) \bmod n . \quad (1.12)$$

Here, ϕ_i corresponds to the definition of phase angle of an oscillator, which, when multiplied by 2π is equivalent to the cyclic phase obtained by performing the Hilbert transform of the signal (Rosenblum and Kurths 1998, Lotric and Stefanovska 2000, Rosenblum *et al.* 2001, Cysarz *et al.* 2004a). However, considering that Hilbert transform is an alternative approach to relative distance and that it provides the phase for every point of the time series, using the Hilbert transform for the estimation of phases and the ultimate detection of synchronization would prove to be more effective (Rosenblum *et al.* 2001).

2. Temporal distance between inspiratory onset and the preceding R-peak. The absolute distance t_j and relative distance β_j between the inspiratory onsets and the preceding R-peaks is given as

$$t_j = I_j - R_{i-1} , \quad (1.13)$$

$$\beta_j = \left(\frac{I_j - R_{i-1}}{R_i - R_{i-1}} \right) . \quad (1.14)$$

In one of the studies Tzeng *et al.* (2003) observed that CVC coupling is strongest when the low ventilatory frequency and short-term HRV is high. In another study Tzeng *et al.* (2007) showed that arterial baroreceptors play a role in the process of CVC with very little contribution from vagal afferents and suggested CVC as a determinant of consecutive differences in respiratory period (Tzeng *et al.* 2007). Alternatively, changes in breathing rate by mechanical ventilation can alter the chaotic properties of the coupling patterns and hence can also be used in determining the CVC process (Mangin *et al.* 2009).

However, the proposed method does not work with signals containing one distinct frequency. In the statistical calculation white noise is included, but nonstationarities overlying the physiological coordination mechanisms have been overlooked. Also, Tzeng *et al.* (2007) suggested that, in addition to the RI plot, the respiratory period and the ratio of heart rate to respiratory rate should also be considered for accurate determination of CVC, since the presence of CVC on the RI plot was observed to be

dependent on the ratio of heart rate to respiratory rate and hence would not accurately reflect the strength of coupling.

1.7.2 Cardiorespiratory coordination—Synchrogram

In physics, synchronization is considered as a locking process due to interaction between two systems (Schafer *et al.* 1999, Rosenblum *et al.* 1998). But since the durations of synchronization are usually very short and the underlying mechanisms causing the synchronization are not yet completely understood, it is difficult to claim that the adjustments in rhythms are caused by coupling mechanisms. As explained by Bettermann *et al.* (2000), the term coordination is less restrictive and hence has been used in a broad sense in this Thesis. Cardiorespiratory coordination is a concept based on the physics of coupled oscillators that aims to quantify the interaction (Toledo *et al.* 2002) between respiratory and heart rhythm, assuming they are generated by two independent systems. It was initially described as short intermittent periods (Schafer *et al.* 1998, Hoyer *et al.* 1997, Bettermann *et al.* 2002) during which the phases of heart rate and respiratory rate coincide with different integer ratios known as phase locking ratios (Schafer *et al.* 1999, Censi *et al.* 2000, Lotric and Stefanovska 2000).

The interaction between heartbeat and respiration occurs at different levels (Hoyer *et al.* 1998a, Schafer *et al.* 1999, Rzecziński *et al.* 2002). Each level corresponds to a particular $m : n$ ratio, where m is the number of heart beats and n is the number of respiratory cycles (Rosenblum *et al.* 2004). The number of heart beats is determined by identifying the R-peaks in the electrocardiogram recording while one respiratory cycle corresponds to one breathing cycle. Cardiorespiratory phase coordination/synchronization has been reported in healthy adults (Lotric and Stefanovska 2000, Kotani *et al.* 2002), athletes (Schafer *et al.* 1998, Schafer *et al.* 1999), sleeping humans (Cysarz *et al.* 2004a, Bartsch *et al.* 2007), infants (Mrowka *et al.* 2000), and in anesthetized (Stefanovska *et al.* 2000) and conscious rats (Kabir *et al.* 2010c). Rodent studies demonstrated that the underlying mechanism could be the excitatory effects from arterial baroreceptors of the central respiratory pattern generator (Tzeng *et al.* 2007). Although the mechanisms and physiological significance underlying coordination between respiration and heart rate are not understood, its quantification might have clinical merit, e.g. estimating the prognosis of cardiac diseases after myocardial infarction in patients (Hoyer *et al.* 2002, Leder *et al.* 2000).

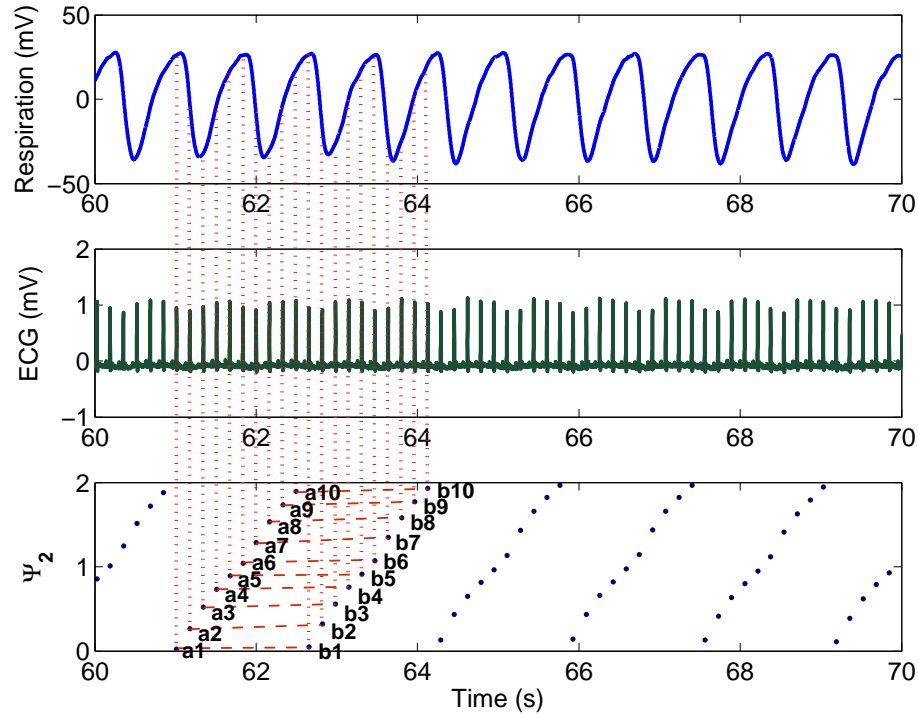


Figure 1.6. Synchrogram plot. Generation of synchrogram from the respiratory and ECG signals. a_1, a_2, \dots, a_{10} and b_1, b_2, \dots, b_{10} in the synchrogram plot represent the respiratory phases, based on the time points of R-peaks, for the first two and the following two respiratory cycles.

If we denote the phase of heartbeat as ϕ_c and of respiratory signal as ϕ_r and considering that the heart beats m times in n respiratory cycles, then phase coordination is defined as the locking of the corresponding phases given by

$$|m\phi_c - n\phi_r| \leq i, \quad (1.15)$$

where i is a constant.

In other words, if the phase difference between the two oscillators is within a certain threshold value i , and remains stable for n respiratory cycles, the oscillators can be considered as coordinated. If t_k is the time of the appearance of a k^{th} R-peak, then we can generate the cardiorespiratory synchrogram by observing the phase of the respiration at the instants t_k , denoted by $\phi_r(t_k)$ and wrapping the respiratory phase into a

1.7 Analysis of synchronization

$[0, 2\pi m]$ interval. This approach provides also a visual tool to detect cardiorespiratory coordination (Fig. 1.6, bottom panel) by plotting ψ_n , given by equation

$$\psi_n = \frac{1}{2\pi}(\phi_r(t_k) \bmod 2\pi n) , \quad (1.16)$$

against t_k . In case of $m : n$ coordination, the plot displays m horizontal lines (Fig. 1.6, bottom panel). Some of the techniques based on mathematical models or heuristic approaches suggested for the detection of horizontal lines in the plots to determine the presence of cardiorespiratory coordination are discussed below (Cysarz *et al.* 2004a).

Detection using synchronization- λ

This process is based on a mathematical model proposed in a number of earlier studies (Tass *et al.* 1998, Mrowka *et al.* 2000, Rosenblum *et al.* 2001). According to this approach if two oscillators with phases ϕ_1 and ϕ_2 are synchronized then the difference in their phases should be a constant or fluctuate around a constant (Bettermann *et al.* 2002, Cysarz *et al.* 2004a). In this process the phase ϕ_2 is registered each time the phase ϕ_1 exceeds a pre-defined value θ . The values of ϕ_2 remain almost constant during synchronization while in other cases spread equally over the interval $[0, 2\pi]$. Given a $m : n$ coordination the phases can be represented as ϕ_1/m and ϕ_2/n . The mathematical calculation for determining λ can be given as follows:

If we consider the phases ϕ_2 at the time points where $\phi_1 = \theta$,

$$\tilde{\zeta}_i = \phi_2(t)|_{\phi_1(t)=\theta} , \quad (1.17)$$

then the fast Fourier mode of the distribution of $\tilde{\zeta}_i$, known as circular variance (Fisher 1993), can be defined as

$$\lambda^2 = \frac{1}{M^2} \left(\sum_{j=1}^M \sin \tilde{\zeta}_j \right)^2 + \frac{1}{M^2} \left(\sum_{j=1}^M \cos \tilde{\zeta}_j \right)^2 , \quad (1.18)$$

where M is the total number of observed values for ϕ_2 .

In case of synchronization, the value of λ will be 1, while $\lambda = 0$ represents de-synchronized oscillators.

Although this technique can detect synchronization, it is unable to identify the variation in the strength of coupling as it lacks supplementary information (Cysarz *et al.* 2004a).

Detection using quantification of histograms

This technique makes use of a sliding window (Rosenblum *et al.* 2001, Cysarz *et al.* 2004a). The sliding window, consisting of a calculated distribution of phases, is moved over the complete series of phases. When the sliding window encounters a structure with parallel horizontal lines, some distinct peaks, at equal distances, are observed in the distribution of phases. In the power spectrum plot, the presence of these peaks (also termed as local maxima) is used for the detection of cardiorespiratory coordination (Cysarz *et al.* 2004a). The procedure can be described as follows.

First, the length of the sliding window, n_F and the number of bins, k , to calculate the distribution are chosen. In case of the absence of synchronization between the two series, the value of each bin, x_l would be n_F/k . On the other hand, if a $m:n$ is observed, x_l can be given by following distribution

$$x_l = \begin{cases} n_F/m & \text{if } l \in (l_0 + n/mkz) \bmod k, z = 0, \dots, m-1, \\ 0 & \text{otherwise,} \end{cases} \quad (1.19)$$

where l_0 represents the index of the bin containing the first local maximum of the distribution (Cysarz *et al.* 2004a). Using Fourier transform, the distribution can be quantified as:

$$P_x(f) = \left| \frac{1}{k} \sum_{l=0}^{k-1} \left(x_l - \frac{n_F}{k} \right) e^{-2\pi i f l / k} \right|. \quad (1.20)$$

In order to avoid the dc-component in the power spectrum, the average of all bins n_F/k is subtracted from each bin. In case of $m:n$ coordination, m local maxima at the frequencies $f = am, a \leq k/2m$ would be observed while $P_x(f) = 0$ would mean that the two series are uncoordinated. However, the local maxima would even be observed even if the parallel horizontal lines are not mapped into m bins (Cysarz *et al.* 2004a). As a result, the difference between the maximum and the minimum of the magnitude of power spectrum is considered to determine cardiorespiratory coordination,

$$\Delta(P_x) = \max(P_x) - \min(P_x). \quad (1.21)$$

A larger difference would indicate coordination between the two oscillators.

Although this method does not require a pre-selection of the integer values m and n , choosing the length of the sliding window with the distribution of phases is a crucial task because it has to be carried out by trial and error method.

Detection through quantification of the distribution of inspiratory onsets in RR intervals

Instead of the coordinated R-peaks of the cardiac signal, this technique yields the coordinated inspiratory onsets of the respiratory signal, and has been successfully used in some of the studies (Galletly and Larsen 1997, Galletly and Larsen 1998, Galletly and Larsen 1999, Galletly and Larsen 2001). This techniques also uses the relative distance β_j as explained in Section 1.7.1. However, since inspiratory onsets are used, the values of β_j lie in the interval $[0, 1]$, but can be mapped onto the interval $[0, 2\pi]$ by multiplying the values with 2π . The distribution of β_j in the data window of length n_F can be quantified by calculating the circular variance

$$\gamma^2 = \frac{1}{n_F} \left(\sum_{k=1}^{n_F} \sin 2\pi\beta_k \right)^2 + \frac{1}{n_F} \left(\sum_{k=1}^{n_F} \cos 2\pi\beta_k \right)^2 . \quad (1.22)$$

Here, the range of γ is $[0, 1]$. In the presence of coordination, β_j would remain constant within the data window, giving $\gamma = 1$. On the other hand, an equal distribution of β_j would result in $\gamma = 0$, indicating no coordination between the two oscillators.

Detection via phase recurrences

The phase recurrence method detects synchronization by identifying the recurrence in the phases of the oscillators. From the synchrogram plot this method looks for parallel horizontal lines. If the phases or relative distances of a sequence of R-peaks are approximately the same, then parallel horizontal lines should appear in the synchrogram plot (Cysarz *et al.* 2004a). The advantage of this technique is that it can also detect synchronization within a short interval of time (Rosenblum *et al.* 2001, Cysarz *et al.* 2004a).

First, the value of n is preselected while m is varied to determine cardiorespiratory coordination. The values are chosen based on the possible number of heart beats in textitn respiratory cycles and such that there is no overlap between the chosen $m : n$ ratios—for example, a $m : n$ ratio of $6 : 2$ is equivalent to $3 : 1$ and hence the selection of

$m = 6$ is redundant for $n = 2$. Consequently, the studies are carried for the following $m : n$ coordination: $n = 1$: $m = 2, 3, \dots, 8$; $n = 2$: $m = 5, 7, 9, 11, 13$ and $n = 3$: $m = 7, 8, 10, 11, 13, 14, 16, 17, 19, 20$. A threshold value of $i = 0.025$ was suggested by Cysarz *et al.* (2004a) for the phase difference.

This technique is used in the first three Chapters of this Thesis. For this, we have presented an illustration in Figure 1.6 on how the synchrogram is generated from respiratory and ECG signals. The phases of the respiratory signal corresponding to the time points of the R-peaks are plotted as normalized phases between 0 and 2 radians. Subsequently, the phases for every two respiratory cycles form a relatively vertical line, e.g. a_1, a_2, \dots, a_{10} ; b_1, b_2, \dots, b_{10} . We then determine the differences between each point of one line to each corresponding point of the next line, e.g. $a_1 - b_1, a_2 - b_2, \dots, a_{10} - b_{10}$. If the differences between all the corresponding points are below the threshold value of 0.025, the respective R-peaks are considered as coordinated with respiration. In Fig. 1.6 (bottom panel), for visual analysis, if we draw lines joining the respective points a_1, b_1 ; $a_2, b_2, \dots, a_{10}, b_{10}$, a structure of parallel horizontal lines, as termed by Cysarz *et al.* (2004a), would be observed. Similarly, from the example in Fig. 1.6, it can be observed that every two respiratory cycles consists of ten equidistant R-peaks, indicating a phase locking ratio of 10:2 (or 5:1).

1.7.3 Respiratory sinus arrhythmia

The best known phenomenon of cardiorespiratory interaction is respiratory sinus arrhythmia (RSA) (Berntson *et al.* 1993)—cyclic oscillation of heart rate, with acceleration (or decrease in R-R interval length) during the inspiratory phase and deceleration (or acceleration in R-R interval) during expiration (Bernardi *et al.* 2001), as seen in Fig. 1.7. In other words, it is a modulation of the heart rate resulting from interaction between the process of respiration and the generation of heart rhythm. This interaction is different but can cause related phenomenon of synchronization (Rzeczinski *et al.* 2002).

Respiratory sinus arrhythmia (RSA) has been observed in humans as well as in mammals. Although the physiological significance of RSA is yet to be established there is clinical evidence that reduced RSA is a prognostic indicator for cardiac mortality (Casolo *et al.* 1992, Moser *et al.* 1994). It has been suggested that RSA enhances pulmonary gas exchange and thereby improves the energy efficiency of pulmonary circulation (Hayano *et al.* 1996). Moderate exercise has shown an increase in the magnitude

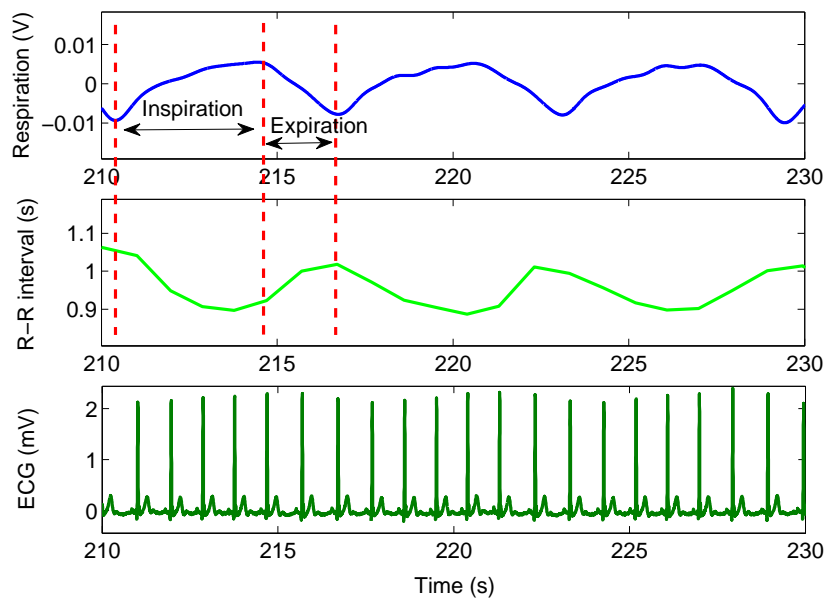


Figure 1.7. Respiratory sinus arrhythmia. Figure showing deceleration in R-R interval during inspiration and acceleration in R-R interval during expiration.

of RSA recorded at rest (De Meersman 1992). The RSA has a significant effect on the rate of decay of vagal baroreflex responses (Eckberg 2003), which might also affect synchronization. Neural RSA mechanisms are well established: it is vagally-mediated, with inputs to cardiac vagal neurons from both central pattern generator (Neff *et al.* 2003) and from peripheral airways and lung stretch receptors (Taha *et al.* 1995). Experiments performed by Eckberg (2003) indicate that the sensitivity of both sympathetic and vagal system to changes of baroreceptor input is controlled by respiration. On the other hand, the level of stimulation of sympathetic and vagal motoneurons, influenced by brain activities, affects the magnitude of respiratory gate (Eckberg 2003). As a result, synchronization not only depends on the regularity of the respiratory signal, but also on the influence of the activity of higher brain regions on cardiac and respiratory oscillators.

The difference between the longest and the shortest heart beat interval within a respiratory cycle is defined as the amplitude of RSA and is the quantitative index of parasympathetic cardiac control (Hayano *et al.* 1994). The amplitude of RSA usually increases with the length of respiratory cycle (Hayano *et al.* 1994). However, the phase shift between heart rate and respiration, which also varies with respiratory cycle length, are comparatively less variable between different individuals than RSA amplitude (Schiek *et al.* 1998).

1.8 Statement of original contribution

The key contributions in this Thesis are summarized as follows.

- **Influence of autonomic nervous system (ANS) and isoflurane on cardiorespiratory coordination:** Experimental studies are carried out in rats, using ECG and respiratory signals (1) for different levels of isoflurane (an anesthetic); (2) changing the rate of respiration (forced ventilation) at a particular level of isoflurane; and (3) by blocking the sympathetic nervous system or vagal system or both. This Thesis demonstrates that isoflurane, forced ventilation and ANS have influence on cardiorespiratory coordination (Kabir *et al.* 2008, Kabir *et al.* 2009),
- **Effect of voluntary movement on respiration:** This Thesis introduces a novel framework for analysing relations between respiration and movement in small laboratory animals. It illustrates a strong association between voluntary movement and respiration, and also between movement and cardiorespiratory coordination (Kabir *et al.* 2010a, Kabir *et al.* 2010c),
- **Cardiorespiratory coordination as a marker for sleep apnea:** This Thesis investigates cardiorespiratory coordination in children and adults suffering from obstructive sleep apnea syndrome (OSAS). It demonstrates that quantification of cardiorespiratory coordination in patients suffering for OSAS can be used to identify the severity of OSAS (Kabir *et al.* 2010b),
- **Time delay correction of synchrogram:** This Thesis investigates cardiorespiratory coordination for different body postures in adults, using modified synchrogram technique by including an adaptive delay in the cardiac oscillator. It illustrates that the modification substantially enhances the sensitivity of the detection of cardiorespiratory coordination (Kabir *et al.* 2011c),
- **Joint symbolic dynamics:** This Thesis introduces a novel approach to quantify cardiorespiratory coordination that is based on the joint symbolic dynamics of respiratory phase and heart rate. It illustrates the technique's ability to provide improved performance by comparing it with other techniques (Kabir *et al.* 2011d, Kabir *et al.* 2011b, Kabir *et al.* 2011a),

1.9 Chapter summary

- **Respiratory sinus arrhythmia in children:** This Thesis provides a detailed study on respiratory sinus arrhythmia (RSA) during sleep in healthy children and children suffering from sleep disordered breathing (SDB). It demonstrates that RSA is associated with sleep stages and SDB in children.

1.9 Chapter summary

This Thesis focuses on the interaction between heart rhythms and respiration and aims to identify some of the underlying physiological mechanisms causing or affecting this interaction.

The original contribution in this Thesis is a novel methodology for analysing cardiorespiratory coordination. The proposed technique in this Thesis appears to be less sensitive to noise, easier to interpret and shows improved performance over other well-known methods.

In the next Chapter, we will investigate the influence of isoflurane, paced respiration, and autonomic nervous system on cardiorespiratory coordination.

Chapter 2



Factors affecting cardiorespiratory coordination



ANESTHETICS and autonomic disturbance create changes in the modulation of heart rate. This chapter investigates the influence of anesthetic and respiratory ventilation rates on the interaction between heart rhythm and respiration in rats. It also examines the effect of sympathetic and parasympathetic blockade on cardiorespiratory coordination.

2.1 Introduction

In living creatures, the peripheral nervous system (PNS) consists of nerves, whose main function is to connect the central nervous system to the limbs and organs. The autonomic nervous system (ANS) is a part of the PNS which is responsible for control of involuntary body functions (below the level of consciousness) including body temperature, cardiovascular and respiratory activities. The ANS transmits autonomic signals to various organs of the body through two major subdivisions: the sympathetic nervous system (SNS) and the parasympathetic (vagal) nervous system (PSNS). The SNS responds to impending danger and is responsible for functioning of body under stress, increase of heart rate and blood pressure together with the sense of excitement. On the other hand, the PSNS works in opposition to SNS and is responsible for the slowing of the heart and stimulation of the digestive systems (controls the vegetative functions) (Guyton and Hall 2006).

Power spectral analysis of heart rate has gained increasing interest as an index of autonomic nervous function (Akselrod *et al.* 1981, Cerutti *et al.* 1991, Malliani *et al.* 1991, Montano *et al.* 1992, Kuwahara *et al.* 1996). The heart rate power spectrum that appears in the respiratory frequency range is termed the high-frequency (HF) power and is considered to reflect the PSNS (Kuwahara *et al.* 1996). On the other hand, low-frequency power (LF) of heart rate variability is reported to be influenced by the activities of the SNS or a mixture of both the SNS and PSNS (Akselrod *et al.* 1981, Kuwahara *et al.* 1996).

While anesthetics adversely affect heart rate, autonomic disturbance creates changes in the modulation of heart rate. Isoflurane, a volatile anesthetic, has been reported to cause a marked increase in heart rate and decrease in high frequency spectral power of HRV (Marano *et al.* 1996). General anesthetics could also provide information about the affect of consciousness on cardiorespiratory coordination (CRC), which is required to investigate the effect of breathing rates on CRC. Also, the parasympathetic (vagal) system is known to have a great influence on heart rate (Marano *et al.* 1996) and heart rate variability (Baumert *et al.* 2007a). However, the effects of general anesthetic, rate of breathing, and autonomic blockade on the phase-locking between heart rate and respiration have not been fully investigated.

This Chapter explores the effect of general anesthetic (isoflurane), breathing rates and autonomic blockade on CRC in rats.

2.2 Methods

The experiments on rats and data recordings were carried out by scientists and laboratory technicians of Flinders University, South Australia.

2.2.1 Ethics statement

Experiments were conducted in accordance with the European Community Council Directive of 24 November 1986 (86/609/EEC), and were approved by the Flinders University Animal Welfare Committee.

2.2.2 Animal preparation and data recording

The signals were acquired using a MacLab interface and Chart software (ADInstruments, Sydney, Australia). Respiratory and ECG signals were sampled at 500 Hz.

Effect of anesthetic

Two male Wistar Hooded rats, weighing 275 g and 293 g (obtained from Flinders University Animal House, Bedford Park, South Australia), are used for this experiment. General anesthesia was induced by placing rats in a container perfused with 3% isoflurane in O₂. Following induction, the trachea was cannulated, and gas mixture was delivered to the lungs via the trachea tube. The CO₂ level in the expired air was measured using a DATEK monitor, and the respiratory frequency was derived from the CO₂ signal. Also the ECG was recorded using two stainless-steel subcutaneous electrodes connected to BioAmp amplifier and PowerLab data acquisition system (ADInstruments, Australia). Rats were placed in a supine position on a heating pad, and their body temperature (measured with a rectal thermometer) was maintained at 37-38°C.

During the experiment ECG and respiratory rate, obtained from spontaneous breathing of the rats, were recorded continuously while changing the concentration of isoflurane at 15-min intervals. To analyze the affect of paced respiration on cardiorespiratory coordination, the level of isoflurane concentration was set to 1.5 mg/kg and respiratory frequency was increased by 5 cycles per minute (cpm) every 15 minutes starting from 35 cpm, while recording the ECG and respiration continuously.

2.2 Methods

Effect of autonomic blockade

Seven male Wistar Hooded rats, weighing 250-300 g (obtained from Flinders University, Bedford Park, South Australia), are used for this experiment. During the experiment, ECG, respiratory rate and blood pressure were recorded continuously before and after autonomic blockade. In order to differentiate the influences of both the components of ANS (i.e. sympathetic and parasympathetic), atenolol or/and methylscopolamine were used to block either the sympathetic nervous system or the vagal system or both. This was achieved by carrying out two separate recordings/experiments in each rat. First, after 50 minutes of baseline recording, each rat was injected with atenolol to block the sympathetic nervous system and recorded for another 40 minutes. It was followed by a further 40 minutes of recording with an additional blockade of vagal system, obtained by injecting methylscopolamine. Second, after a period of two weeks, the same protocol was followed except that the vagal system was first blocked followed by the blockade of sympathetic nervous system.

For the purpose of analysis before and after blockade, we select a 30 minute interval of the baseline data after eliminating the first 10 minutes of the recording and 30 minute epochs each after vagal blockade with methylscopolamine or sympathetic nervous system blockade with atenolol or both, starting 5 minutes after the injection.

2.2.3 Data analysis

Processing of ECG and Respiration

The R-peaks are extracted from the ECG signal using parabolic fitting as described in Chapter 1, Section 1.4.1. For the time-frequency adaptive analysis of non-linear and non-stationary respiratory signals by extracting the essential respiratory rhythm related components, we use empirical mode decomposition (EMD), described in Chapter 1, Section 1.5.2.

Coherence analysis

Each set of data of 512 points for RR and respiratory time series, from the rats under investigation for studying the effect of autonomic blockade, are resampled at 10 Hz and a Hamming window and the fast Fourier transform are applied to obtain the power

spectrum of the fluctuation. The spectral estimates are obtained by averaging the respective squared magnitudes and the products of the computed discrete Fourier transforms. Subsequently, coherence between the two spectra are computed by taking the ratio of the magnitude square of the cross-spectra and dividing by the product of the autospectra.

Coherence is a function of frequency and a linear relationship between two variables. In the presence of no noise it would result in a coherence of one, while non-linear or random relationships or the presence of noise would decrease coherence of the two variables toward zero. For the analysis of the effect of autonomic blockade on heart rate variability (HRV), we define two frequency bands of interest: low-frequency (LF)—0.25-0.8 Hz and high-frequency (HF)—0.8-3 Hz (Fauchier *et al.* 2006).

Cardiorespiratory coordination analysis

We study the coordination between cardiac and respiratory cycles using cardiorespiratory coordination analysis described in Chapter 1.1, Section 1.7.2.

We select only artifact-free recording segments to generate the results. We employed three parameters for characterising cardiorespiratory coordination: Firstly, we calculate the percentage of coordination by adding up the time of all coordinated epochs observed and then dividing it by the total duration of the segments. Secondly, we measure the average duration of all coordinated epochs by calculating the arithmetic mean of the durations of coordinated epochs. Further, the phase locking ratio for each coordinated epoch was recorded.

Statistical analysis

Statistical analysis is performed with GraphPad Prism version 5.01 for Windows (GraphPad Software, San Diego California USA, www.graphpad.com). To test the effect of isoflurane on heart rate, respiratory rate, percentage of cardiorespiratory coordination and duration of coordinated epochs, the linear regression model is performed by taking the mean values of the corresponding results from both rats for different isoflurane concentrations. However, since only two rats are used and cardiorespiratory coordination show a high increase at a particular ventilation rate, it is not possible to use linear regression model to study the effect of mechanical ventilation on cardiorespiratory coordination, as linear regression model determines the association between two variables of interest, X and Y , by producing estimates for slope and intercept.

2.3 Results—Effect of anesthetic

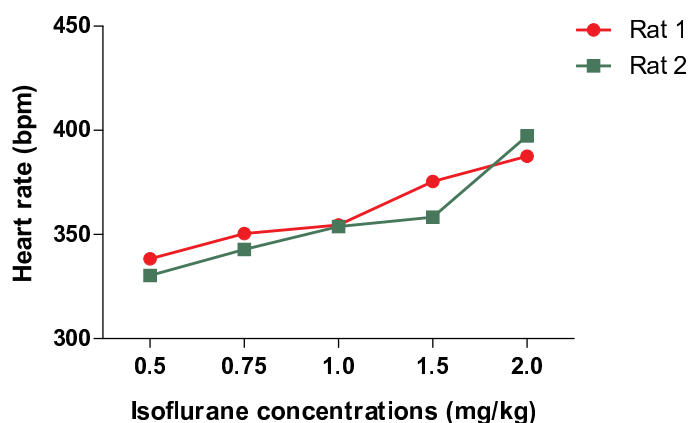


Figure 2.1. Heart rate and concentration of isoflurane. Changes in heart rate (beats per minute) obtained from two rats at different levels of isoflurane concentrations. Heart rate shows a marked increase with the increase in the concentration of isoflurane.

The differences before and after autonomic blockade are analyzed by one-way analysis of variance (ANOVA) for multiple measurements and Wilcoxon test for paired comparisons.

Data are expressed as the mean \pm SD. For the analysis, $p < 0.05$ is considered statistically significant.

2.3 Results—Effect of anesthetic

2.3.1 Effect of isoflurane concentration on heart rate and respiratory rate

Heart rate shows an increase with the increase in the concentration of isoflurane (Fig. 2.1). Using linear regression it is observed that the heart rate is significantly associated with isoflurane ($r^2 = 0.98$, $F(1,3) = 160.3$, $p < 0.001$). However, no significant change in respiratory frequency is observed with the increase in the level of isoflurane (Fig. 2.2) ($r^2 = 0.53$, $F(1,3) = 3.52$, $p > 0.05$).

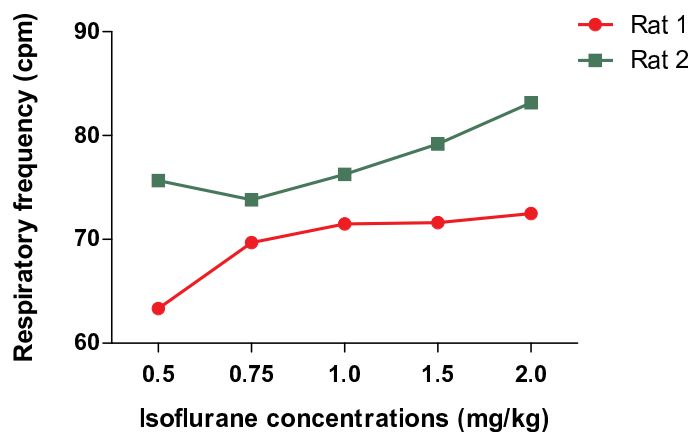


Figure 2.2. Respiratory frequency and concentration of isoflurane. Changes in respiratory frequency (cycles per minute) obtained from two rats at different levels of isoflurane concentrations. Respiratory rate shows a slight increase with the increase in the concentration of isoflurane.

2.3.2 Effect of isoflurane concentration on cardiorespiratory coordination

Isoflurane causes a significant dose-dependent increase in the percentage of coordination ($r^2 = 0.99$, $F(1, 3) = 350.30$, $p < 0.001$) and duration of synchronized epochs ($r^2 = 0.84$, $F(1, 3) = 15.9$, $p < 0.05$) as seen in Fig. 2.3.

2.3.3 Effect of ventilation rate on heart rate, percentage of coordination, and duration of coordinated epochs

The change in ventilation rate causes a change in heart rate, percentage of synchronization and duration of synchronized epochs. Both rats show a decrease in heart rate and a considerable increase in percentage and duration of synchronized epochs at the ventilation rates of 50 and 55 cycles per minute (Table 2.1).

2.4 Results—Effect of autonomic blockade

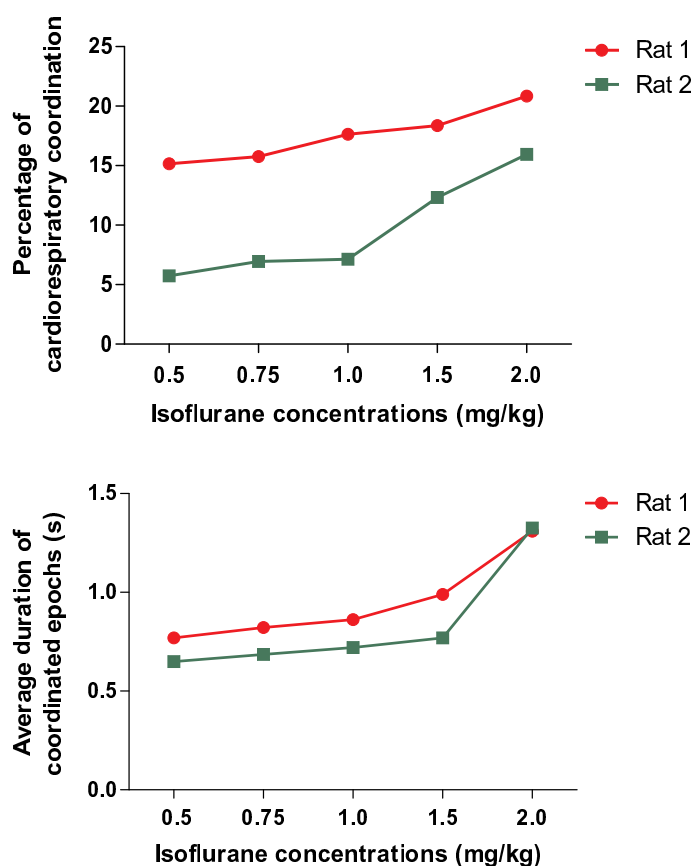


Figure 2.3. Cardiorespiratory coordination and concentration of isoflurane. Changes in percentage of coordination (top panel) and duration of coordinated epochs (bottom panel) obtained from two rats at different levels of isoflurane concentrations. Both graphs show an increase with the increase in the concentration of isoflurane.

2.4 Results—Effect of autonomic blockade

2.4.1 Effect of autonomic blockade on heart rate and respiratory frequency

Atenolol, which is used to block the sympathetic nervous system, has caused a significant decrease (350 ± 39 vs. 321 ± 24 , $p < 0.0001$), while methyl-scopolamine, used to block the parasympathetic nervous system, has caused a significant increase (350 ± 39 vs. 421 ± 33 , $p < 0.0001$) in heart rate compared to baseline (Fig. 2.4(a)). The blockade of both the sympathetic and vagal system has caused a slight but significant increase in heart rate (350 ± 39 vs. 357 ± 28 , $p < 0.05$) as seen in Fig. 2.4(a).

Although, there is no significant effect of either sympathetic or vagal blockade on the respiratory frequency, the blockade of both the systems cause a significant decrease

Table 2.1. Ventilation rates. Heart rate (HR), percentage of coordination (PoC) and average duration of coordinated epochs (AvDur) for different rates of ventilation.

	Ventilation rate (cpm)					
	35	40	45	50	55	60
HR (bpm)	346±16	369±14	358±21	349±13	350±11	362±11
PoC (%)	7.6±4.1	1.9±6.9	7.9±6.9	22.0±6.4	15.0±10.1	9.5±2.4
AvDur (s)	1.2±0.3	0.9±0.3	1.5±0.8	1.6±0.6	1.5±0.5	1.2±0.2

in respiratory frequency compared to baseline values (70.9 ± 26.6 vs. 63.3 ± 19.2 , $p < 0.05$), see Fig. 2.4(b).

2.4.2 Effect of autonomic blockade on heart rate variability

A selection of time series of RR interval and respiration together with their respective power spectra and coherence is shown in Fig. 2.5. Two major spectral components were observed at low-frequency (LF) and high-frequency (HF) power in the power spectra plot for RR time series. The power spectra peak of respiration occurred at the

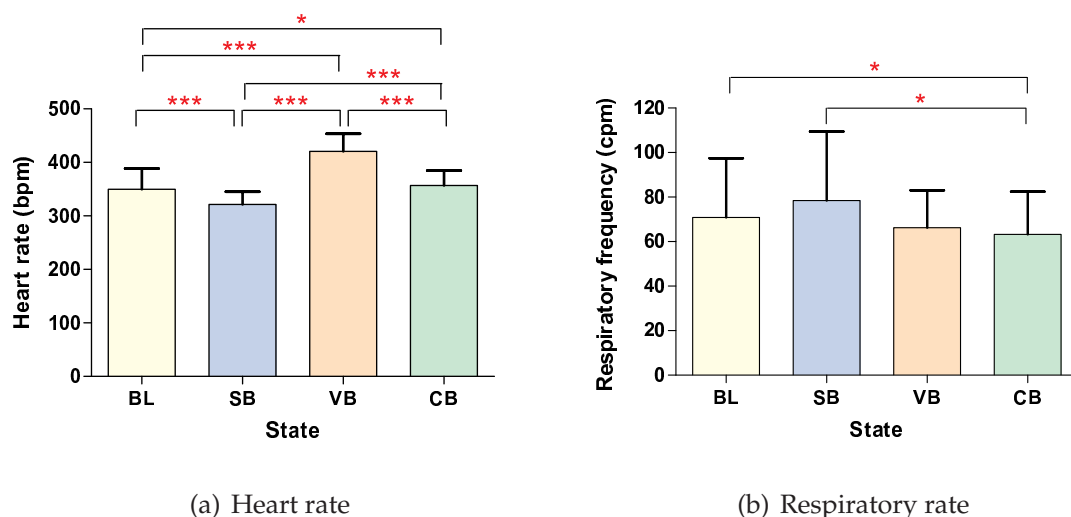


Figure 2.4. Heart rate, respiratory rate and autonomic blockade. Mean+SD of heart rate and respiratory rate in seven rats during the baseline state (BL) and after sympathetic (SB), vagal (VB), and complete blockade (CB). The symbols * and *** represent $p < 0.05$ and $p < 0.0001$, respectively. The means are represented by the coloured bars and the standard deviations (SD) by the thin error bars.

2.4 Results—Effect of autonomic blockade

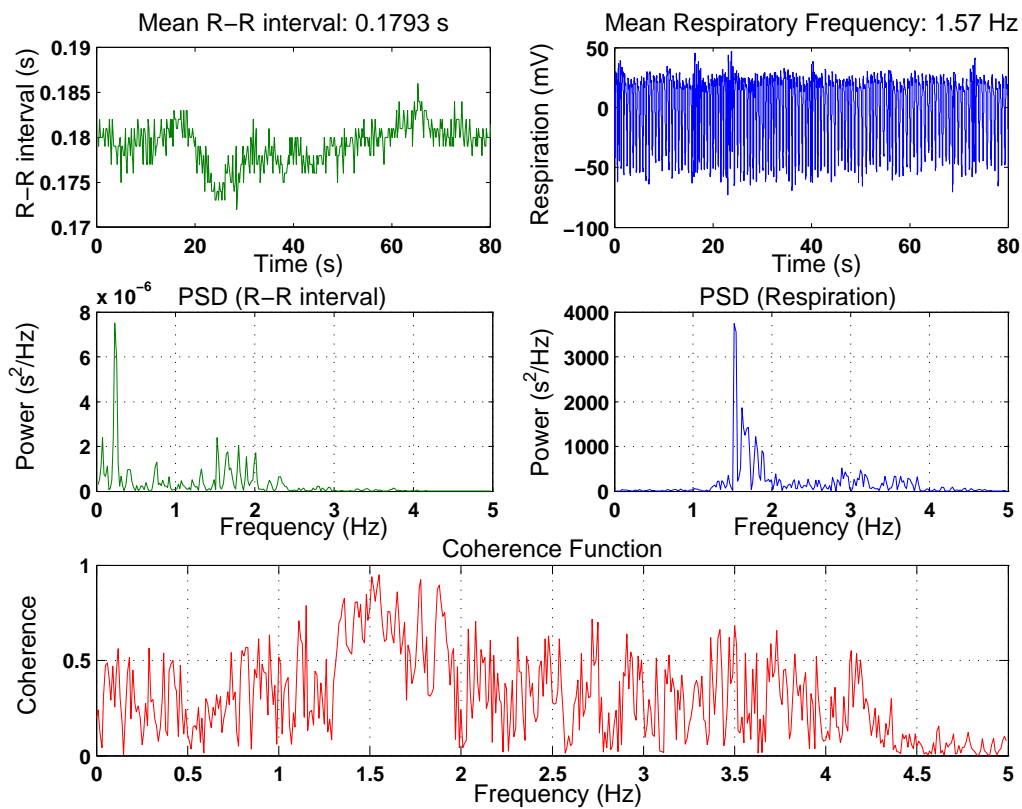


Figure 2.5. Coherence plot. Coherence function between RR interval and respiration.

HF range. A high coherence between RR and respiration variabilities was observed at about 1.5 Hz. The effects of autonomic nervous blockade on heart rate variability (HRV) are shown in Fig. 2.6. Sympathetic blockade caused a significant increase in the low-frequency (LF) power of HRV ($4.2 \pm 4.3 \times 10^{-4}$ vs. $7.9 \pm 7.5 \times 10^{-4} s^2$, $p < 0.05$). The high-frequency (HF) power of HRV also shows an increase after sympathetic blockade, but it is not statistically significant ($1.3 \pm 1.3 \times 10^{-4}$ vs. $1.89 \pm 1.3 \times 10^{-4} s^2$, $p > 0.05$). On the other hand vagal blockade significantly reduced both the LF and HF power of HRV ($4.2 \pm 4.3 \times 10^{-4}$ vs. $1.1 \pm 1.2 \times 10^{-4}$, $p < 0.05$, and $1.3 \pm 1.3 \times 10^{-4}$ vs. $0.5 \pm 0.4 \times 10^{-4}$, $p < 0.05$, respectively), see Fig. 2.6.

2.4.3 Effect of autonomic blockade on cardiorespiratory coordination

Although an increase and decrease in the overall percentage of cardiorespiratory coordination is observed after the respective blockade of sympathetic and vagal systems, the differences are not statistically significant (Fig. 2.7(a)).

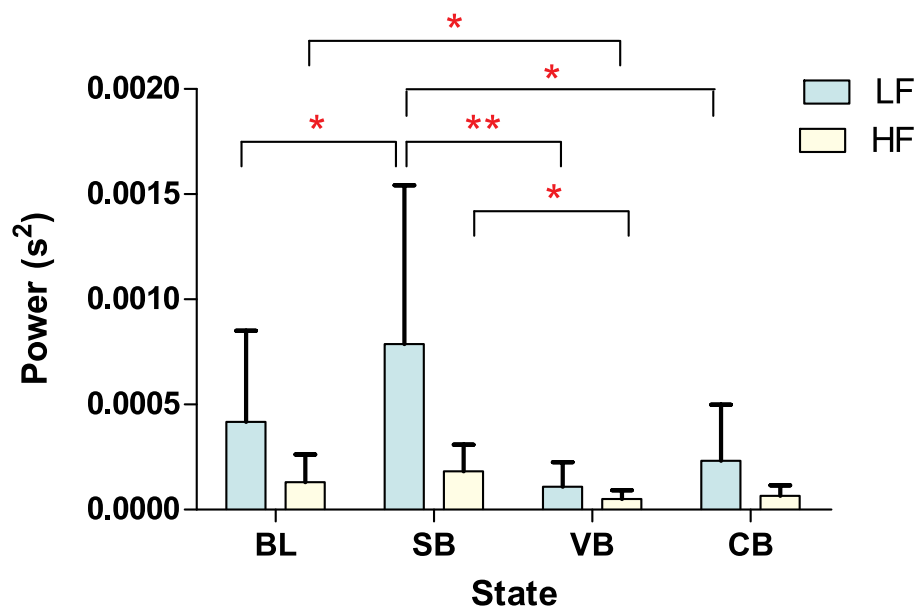


Figure 2.6. Low-frequency and high-frequency power. Mean+SD of low-frequency and high-frequency power of heart rate variability during the baseline state (BL) and after sympathetic (SB), vagal (VB), and complete blockade (CB). The symbols * and ** represent $p < 0.05$ and $p < 0.01$, respectively.

The average duration of coordinated epochs is significantly shorter after injecting with methyl-scopolamine compared to baseline (1.1 ± 0.3 vs. 0.9 ± 0.2 s, $p < 0.05$), see Fig. 2.7(b). On the other hand, average duration of coordinated epochs is significantly longer after sympathetic blockade compared to vagal blockade and blockade of both sympathetic and vagal systems (1.2 ± 0.3 vs. 0.9 ± 0.2 , $p < 0.0001$ and 1.0 ± 0.3 s, $p < 0.01$, respectively), but is not significantly different from the baseline state (Fig. 2.7(b)).

Here, cardiorespiratory coordination has occurred for the phase-locking ratios of 2:1, 3:1, 4:1, 5:2 and 7:2. The 3:1 phase-locked state is frequently observed and is not significantly affected by autonomic blockade.

2.5 Discussion

In this chapter we investigate the effect of anesthetic concentrations and breathing ventilation rates as well as the affect of autonomic blockade on cardiorespiratory phase coordination in rats to understand or identify the underlying mechanism responsible for the locking of phases between cardiac and respiratory cycles. It is observed that

2.5 Discussion

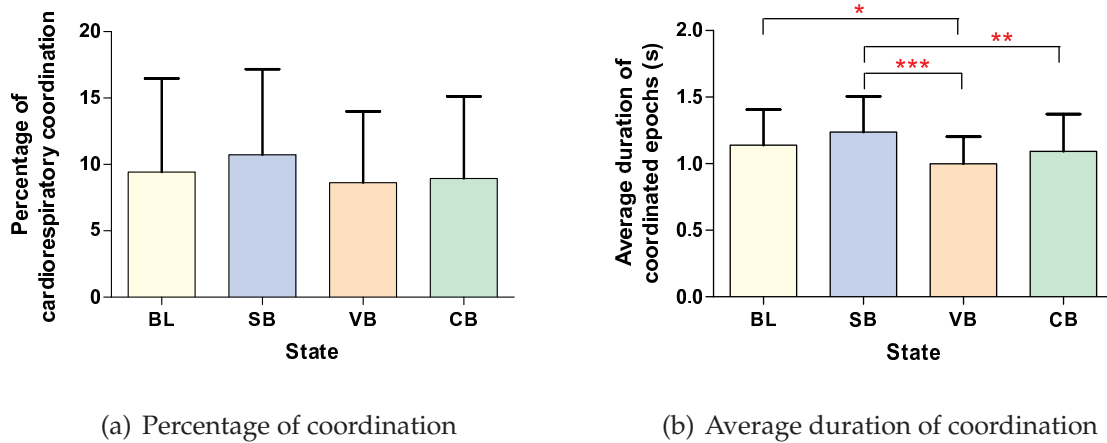


Figure 2.7. Cardiorespiratory coordination and autonomic blockade. Cardiorespiratory coordination in seven rats during baseline state (BL) and after sympathetic (SB), vagal (VB) and complete blockade (CB). The symbols *, ** and *** represent $p < 0.05$, $p < 0.01$ and $p < 0.0001$, respectively.

isoflurane caused a dose-dependent increase in heart rate, respiratory frequency and cardiorespiratory coordination. Also, individual and joint blockade of sympathetic and vagal systems cause significant changes in heart rate, respiratory rate and average duration of coordination but has no significant effect on the percentage of cardiorespiratory coordination.

Isoflurane causes a dose-dependent increase in heart rate, which is in accordance with the results reported by Marano *et al.* (1996). The increase in heart rate suggests that although isoflurane causes an overall reduction in autonomic tone (Marano *et al.* 1996), the sympathetic tone becomes the predominant factor under isoflurane. While concentration of isoflurane also causes an increase in cardiorespiratory coordination, the respiratory rate remained almost unaffected. This would suggest that the heart rate rather than respiratory rate is the predominant factor causing the phenomenon of phase-locking between heart rate and respiration.

Cardiorespiratory coordination and RSA are caused by cardiorespiratory coupling (Bettermann *et al.* 2002). With the increase in concentration of isoflurane, the increase of cardiorespiratory coupling after the reduction in vagal tone is contradictory with the observation that vagal outflow to the sinus node of the heart is the predominant driver of RSA. Also, RSA results from modulation of heart rate by respiration which is uni-directional. On the other hand, synchronization can occur from a bi-directional

interaction between heart rate and respiration. This suggests that RSA might not be an important factor responsible for cardiorespiratory coordination.

Rzeczinski *et al.* (2002) studied cardiorespiratory coordination in human subjects under paced respiration and observed that, for a suitable choice of respiratory frequency, a higher cardiorespiratory coordination can be achieved. In this study an increase in cardiorespiratory coordination at the ventilation rates of 50-55 cycles per minute in both the rats supports the observation by Rzeczinski *et al.* (2002) that the phase-locking between heart rate and respiration is maximized at a particular respiratory frequency.

Autonomic blockade has also produced changes in heart rate, which is in accordance with the results reported earlier in the literature (Marano *et al.* 1996, Beckers *et al.* 2006, Baumert *et al.* 2007a). The overall reduction of cardiorespiratory coordination after vagal blockade is in line with the observation that vagal outflow to the sinus node of the heart is the predominant driver of RSA. However, the increase of cardiorespiratory coordination after sympathetic blockade is unexpected. Possibly, sympathetic effects on heart rate disturb the respiratory sinus rhythm and a sympathetic blockade consequently increases the amount of observed phase locking between heart rate and respiration. Although the average duration of coordinated epochs and percentage of coordination is found to increase with sympathetic blockade and decrease with vagal blockade, the change in percentage of coordination do not reach statistical significance.

The results in this study are obtained by analyzing the data from a small number of rats. The results motivate the need for future validation in a larger group of rats.

2.6 Chapter summary

In this Chapter we have demonstrated that anesthetic (isoflurane), vagal and sympathetic blockade significantly affects heart rate, respiratory rate and cardiorespiratory coordination in rats. Also we have observed that the phase-locking between heart rate and respiration in rats increases at a certain ventilation rate, suggesting that the cardiorespiratory coordination occurs at a specific respiratory frequency.

From the study in this Chapter, we have observed that cardiorespiratory coordination in rats is influenced by controlled breathing (paced respiration). However, the pattern of respiration in rats while at rest, but awake and freely behaving has received little attention. In the next Chapter we will investigate the influence of voluntary movement on respiration and cardiorespiratory coordination in rats.

Chapter 3

Respiratory pattern during voluntary movement in awake rats

THIS chapter aims at assessing the impact of motor activity on respiratory rate and cardiorespiratory coordination in the awake rat. All motor activity is found to be associated with an immediate increase in respiratory rate that remained elevated for the whole duration of movement. The extent of motor-related rapid breathing is significantly correlated with the intensity of associated movement. Cardiorespiratory coordination also shows a significant decrease with the increase in motor activity.

3.1 Introduction

Although rats are widely used for physiological studies, an important aspect of their respiratory physiology has received little attention—their pattern of respiration while at rest, but awake and freely behaving requires further investigation. It is generally assumed that we have a good knowledge of the rat's respiratory activity under 'resting' conditions. However, most previous studies investigating respiration in awake rats have focused on homeostatic (chemoreflex-induced) changes, and did not address the possibility that respiration could also be influenced by motor activity. Consequently, respiratory data either comprised average values including undiscriminated periods of motor activity (Roux *et al.* 2000, Antunes *et al.* 2005, Fournier *et al.* 2007) or were collected when the animals were immobile (Genest *et al.* 2007, Montandon *et al.* 2008). In reality, immobility is just one component of an animal's resting state; indeed, even when at rest, animals move about, groom and shift body position. This issue is significant because it has been established in studies of larger species, including humans, that respiration is closely linked to motor activity, with motor-related increases in respiratory rate being triggered by feed-forward central command in the brain and maintained by feedback mechanisms (Horn and Waldrop 1998, Eldridge and Waldrop 1991).

The possibility of motor-respiratory interaction was also out of the scope of studies that examined respiratory activity during various behaviours in rats (Welker 1964, Clarke and Trowill 1971, Ikemoto and Panksepp 1994, Kepecs *et al.* 2007). Similarly, although previous studies on animals, investigating respiration and heart rhythms, have focused on the effect of anesthesia, drugs and induced movements on the cardiorespiratory coordination (Marano *et al.* 1996, Galletly and Larsen 1997, Pereda *et al.* 2005, Kabir *et al.* 2008, Kabir *et al.* 2009), the association between movement and cardiorespiratory coordination in freely moving animals has never been established. Accordingly, this Chapter sought to document the pattern of respiratory rate in awake and freely behaving rats; in particular, its variability, how fast it changes in association with a motor act, whether it depends on the intensity of motor activity and its association with the heart rhythm.

In this Chapter we begin by examining, in two groups of conscious, freely-behaving rats, the relationship between respiratory rate, spontaneous motor activity, and heart rate. In designing our study we have confronted with several challenges, the main being the lack of an adequate framework for analyzing respiratory-motor relations in

small laboratory animals. We have developed such a framework and present it in detail.

A wavelet is used to divide a continuous or discrete time signal into different frequency components. Wavelets have advantages over Fourier transforms for representing functions that have discontinuities and for accurately re-constructing and de-constructing finite, non-periodic and non-stationary signals (Hubbard 1998, Eckberg 2003). They have the ability to examine the signal simultaneously in both time and frequency domains. The signal under investigation can be transformed or reconstructed by a suitable integration over all the resulting frequency components using wavelets that presents the signal information in a more useful form (Addison 2002). For our study, we initially performed wavelet analysis, using Daubechies 4 tap wavelet, to determine the influence of movement on respiration and heart rhythm.

While there are several techniques for assessing respiratory indices in conscious unrestrained rodents, we consider that whole-body plethysmography is the method of choice as it is entirely non-invasive and thus does not introduce any confounding factors. Using this method, we test our hypotheses: the intensity of motor activity is associated with changes in respiratory frequency and cardiorespiratory coordination.

3.2 Methods

The experiments on rats and data recordings were carried out by scientists and laboratory technicians of University of Newcastle, New South Wales, Australia.

3.2.1 Ethical approval and preliminary surgery

Male Hooded Wistar ($n = 5$) and Sprague Dawley rats ($n = 5$) weighing 280-320 g were used in all experiments. All efforts were made to reduce animal pain or discomfort. The experimental protocol was approved by the University of Newcastle Animal Ethics Committee, and is in compliance with the European Communities Council Directive of 24 November 1986 (86/609/EEC). Preparatory surgery was conducted under isoflurane (1.5% in 100% oxygen) anaesthesia, with carprofen (5 mg/kg) being used as a post-surgery analgesic. Telemetric ECG radio-transmitters (TA11CA-F40, Data Sciences International) were implanted in the peritoneal cavity, with electrodes positioned in accord with the method described by Sgoifo *et al.* (1996): one electrode on the

3.2 Methods

internal surface of the xiphoid process, another one and in the mediastinum, along the trachea at the level of the left ventricle. This placement dramatically reduces movement artifacts, even in vigorously moving animals. Upon recovery from anaesthesia, animals were returned to the animal house for at least one week before experiments began. They were held on a reverse 12h/12h light-dark cycle (lights on at 8 pm), with food and water *ad libitum*.

3.2.2 Recordings of respiration and gross motor activity

Respiratory movement was detected using a custom-built whole-body plethysmograph. This consisted of a transparent Perspex cylinder (inner diameter 95 mm, length 260 mm, volume 1.84 l, wall thickness 3 mm) that had both ends closed with removable plugs, and compressed medical air was constantly flushed through it at a flow rate of 2.5 l/min. Both input and output lines were fabricated from polyethylene tubing (outer diameter 1.45 mm, inner diameter 0.75 mm, about 1 m length) that were tightly fitted into the plugs. A plastic T-connector was inserted 20 cm away from the start of the output line and then linked to one input of a differential pressure amplifier (model 24PC01SMT, Honeywell Sensing and Control, Golden Valley, MN, USA), the second input being opened to the room air. An additional plastic tubing inserted into the “output” plug connected the plethysmograph chamber to the input of the CO₂ monitor (Normocap, Datex Instrumentarium Corp., Helsinki, Finland). In preliminary experiments we have established that keeping airflow at 2 l/min is sufficient to prevent any rise of CO₂ in the plethysmograph.

For semi-quantitative assessment of animals' motor activity, a piezoelectric pulse transducer (MLT1010/D, ADInstruments, Sydney, Australia) was placed under the plethysmograph. The transducer was sensitive enough to detect even minor movements (e.g. turning the head), while locomotion produced large oscillatory responses.

3.2.3 Experimental protocol

All experiments were carried out in the first half of the dark phase of the light/dark cycle, with just sufficient levels of red light to permit observation of the animals. Importantly, to limit the stressfulness of their transfer, plastic cylinders of the same size as the plethysmograph chamber had been placed in all home cages, allowing animals to habituate to them. Indeed animals often sat or slept inside these cylinders. On

the day of experiment, rats were placed in a plethysmographic chamber while still in their home cage. Presumably, as a result of their habituation process, animals entered the chamber willingly without being forced. The ECG probes were then switched on and the recording started. The experimental protocol consisted of a 40-min recording period.

3.2.4 Data acquisition and analysis

Analogue ECG, respiratory and motion signals were digitized at 1 kHz and acquired using a PowerLab A/D converter and ChartPro 6.0 software (ADInstruments, Sydney, Australia). Heart rate was calculated from the ECG records using the same software.

Custom written software developed with MATLAB[®] (see Appendix C) is used for the analysis of the respiratory pattern and its dependence on motor activity. We first compute time series for respiratory intervals, the inspiratory onsets being determined as the zero-crossings of the first derivative of the respiratory signal. Mean respiratory interval duration and coefficient of variation of respiratory interval are computed from the obtained breath-to-breath time series and respiratory interval histograms constructed with a bin width of 10 ms. These histograms are bimodal for all animals, and we characterize them by measuring mode values for the low- and high-frequency peaks; the best non-linear regression fit for these data is then determined using GraphPad Prism version 5.01 for Windows (GraphPad Software, San Diego California USA, www.graphpad.com).

We calculate three measures of motor activity after appropriate thresholding (30% above the noise level) of the movement sensor signal: i) total duration of activity (both in seconds/min and as a percentage of total time); ii) number of movements/min; and iii) average duration of individual movement (in seconds).

Analysis of relationship between respiratory rate and motor activity require us to develop a novel framework. The first task is to find a method of characterising the intensity of a movement. For this purpose we initially compute, for each respiratory interval, the movement power index (MPI):

$$\text{MPI}_n = \frac{1}{t_{n+1} - t_n} \sum_{i=t_n \Delta f}^{t_{n+1} \Delta f} P_i^2. \quad (3.1)$$

3.2 Methods

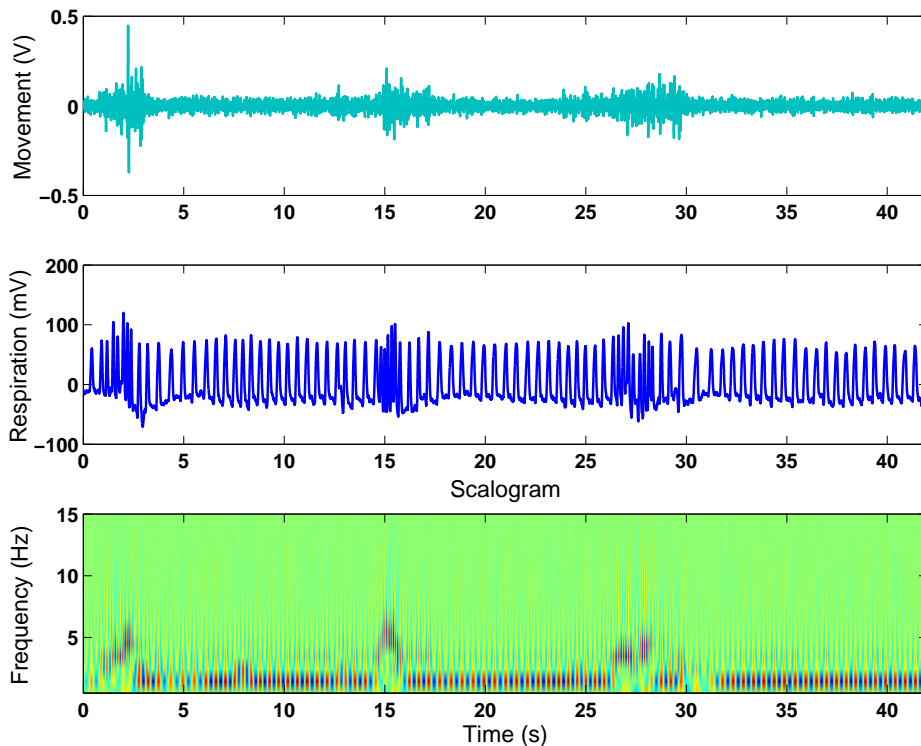


Figure 3.1. Wavelet analysis of respiration and motor activity. Wavelet analysis (Daubechies 4 tap) shows a high frequency in respiratory signal during motor activity.

where P is the piezoelectric sensor signal (V), t_n is the time of the n -th inspiratory onset ($n = 1, 2, 3, \dots, N - 1$) and Δf is the sampling frequency (s^{-1}). We then plot each respiratory interval against the corresponding MPI value for the whole record in each animal. To characterize these plots, and to permit inter-group comparisons, we dichotomize the respiratory interval time series based on the median, computing the average MPI value of respiratory intervals shorter than the median value and the average value of respiratory intervals longer than the median value. To further explore the relationship between the movement intensity and respiratory interval, we sort all measured MPI values into bins of $0.01 \text{ V}^2\text{s}^{-1}$ widths, computed the mean and the standard deviation of all respiratory intervals within each bin, plot these values against corresponding MPI values and determine the optimum regression function fit for these data (Graph-Pad Software, San Diego, CA, USA).

To investigate the presumed relationship between the duration of motor activity and the duration of elevated respiratory rate, we initially derive from the whole 30-min recording period 15-20 artefact-free segments, and calculate, for each such segment,

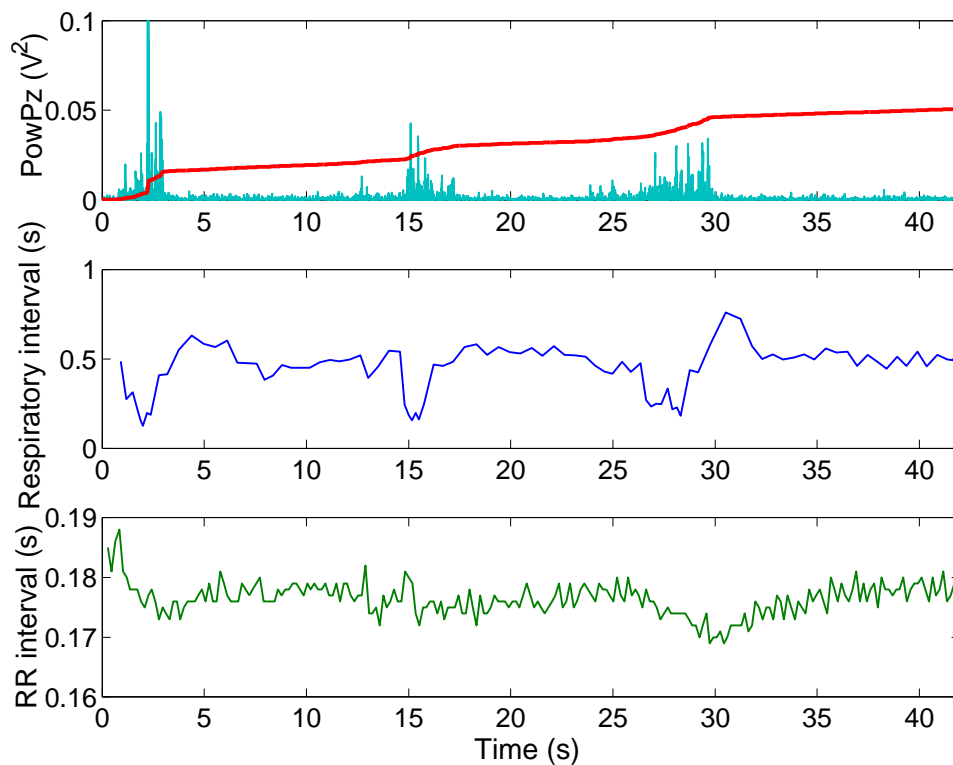


Figure 3.2. Motor activity, respiratory and heart rate. Power of piezoelectric signal (PowPz) (top panel) and the corresponding changes in respiratory and RR interval (middle and bottom panel, respectively). The red line in the top panel indicates the cumulative sum of PowPz (divided by 10^{-3} to fit in the graph). A shortening in respiratory and RR interval can be observed with the increase in the movement intensity.

the total movement time and the total time of rapid breathing. From these, we compute the total movement time and the total time of rapid breathing for each record.

To assess the relationship between motor activity and the heart rate, we measure RR intervals before and during a movement, compute the difference (Δ), and plot it against the duration of the associated movement. To characterize and compare this relationship we compute, for each record, mean values for Δ RR interval changes during short (<1 s), intermediate (1-5) and long (>5 s) movements.

Finally, to investigate the impact of motor activity on cardiorespiratory coordination, movement is dichotomized based on the threshold value of 10^{-2} V^2 for the slope of the cumulative sum of the power of piezoelectric signal: low-intensity movement ($\text{slope} \leq 10^{-2} \text{ V}^2$) and high-intensity movement ($\text{slope} > 10^{-2} \text{ V}^2$). Subsequently, we determine the coordination between cardiac and respiratory cycles during low-intensity

3.3 Results

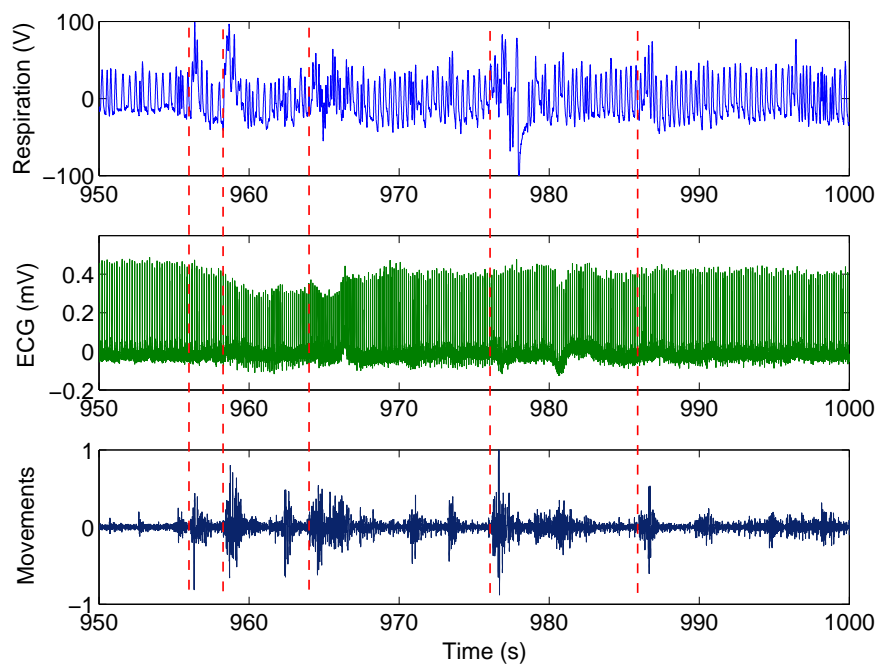


Figure 3.3. Record of respiration, ECG and gross spontaneous motor activity. Respiratory and cardiac activity changed during various individual motor acts. The onset of respiratory rate acceleration either coincide with the onset of a movement or slightly preceded it, as shown by the red dashed lines.

and high-intensity movements based on the cardiorespiratory coordination analysis described in Chapter 1, Section 1.7.2.

Group data are analysed by ANOVA with Fishers's protected t-tests, significance threshold being set at the 0.05 level. All data are presented as mean \pm SD; where possible, data values have been embedded in accompanying figures.

3.3 Results

Behaviours displayed by animals after entering the plethysmographic chamber do not differ noticeably from those displayed in the home cage. Periods of motor activity are intermingled with periods of relative quiescence. Sometimes the rats curled up and closed their eyes, suggesting that they are asleep. All sorts of body movements (eg. turning the head) are readily detectable by the piezoelectric sensor. Observations made during experiments, and subsequent visual inspection of our records, reveal a high extent of variability in the respiratory rate and heart rate, and a strong association

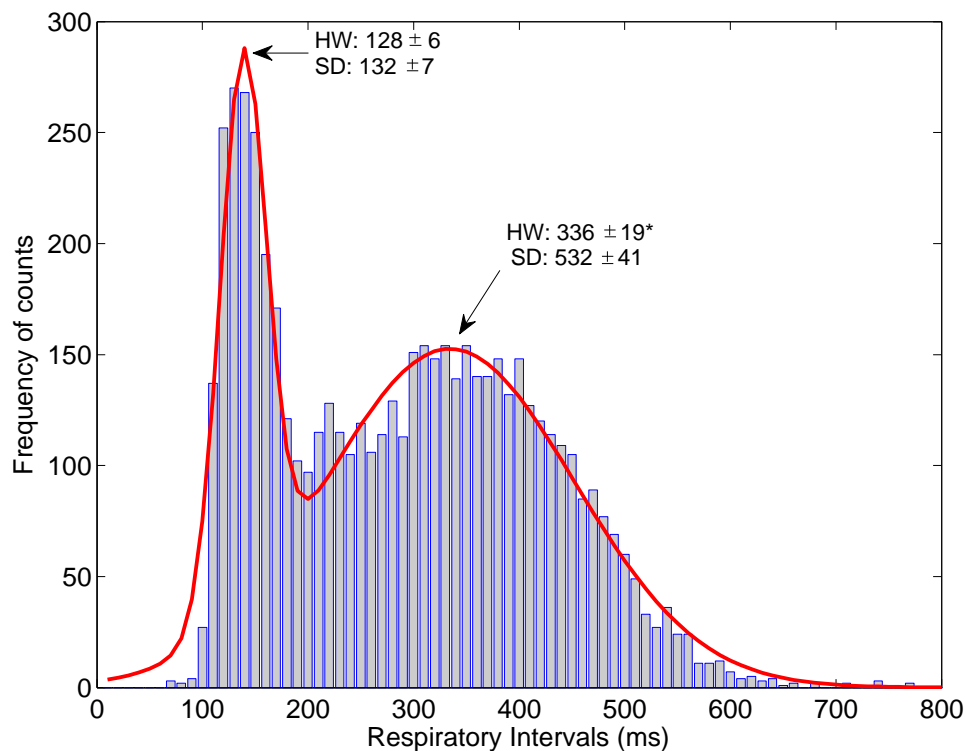


Figure 3.4. Histogram of respiratory intervals. Histogram of respiratory intervals recorded during spontaneous behaviour in one rat (HW3) showing a bimodal distribution. These data could be well approximated by the sum of two Gaussian functions (superimposed curve). Bin width = 10 ms; total number of intervals = 7213; duration of record = 30 min. The values near the arrowheads are the mean group data for the modes of the shorter and of the longer peak. HW—Hooded Wistar; SD—Sprague-Dawley: the symbol * indicates significant differences in results between two groups of rats, $p < 0.05$.

between respiration and motor activity. This is illustrated through wavelet analysis which reveals a high frequency in respiratory signal during movement (Fig. 3.1), and by plotting the respiratory and RR intervals against the power of piezoelectric signal (Fig. 3.2). The onset of respiratory rate acceleration either coincide with the onset of a movement or even slightly precede it, but is never delayed (see dashed lines in Fig. 3.3).

3.3.1 Assessment of respiratory indices and motor indices

The mean values for respiratory intervals differ between the two groups of rats ($F = 22$, $n = 5$, $p < 0.05$), being 421 ± 76 ms and 285 ± 18 ms for SD and HW rats, respectively. As seen in Fig. 3.3, respiratory intervals vary greatly during the recording period and this is reflected by high coefficient of variation values (44% and 38% for SD and HW,

3.3 Results

Table 3.1. Temporal characteristics of motor activity. Average duration of movement and total movement time in two groups of rats.

Rat strain	Mean movement duration (ms)	Total movement time	
		(s/min)	(%)
Hooded Wistar ($n = 5$)	683 ± 62	11.7 ± 0.7	19.4 ± 1.2
Sprague-Dawley ($n = 5$)	552 ± 28	10.3 ± 1.0	17.2 ± 1.7

respectively); there is no significant group effect ($F = 1.2$, $n = 5$, $p > 0.05$). The histograms of respiratory intervals constructed for each animal reveal a bimodal distribution that could be well approximated by the sum of two Gaussian functions (Fig. 3.4). While the mode values for the shorter peak do not differ between the groups (128 ± 6 vs. 132 ± 7 ms, $n = 5$, $p > 0.05$), the mode values for the longer peaks are larger in SD rats (532 ± 80 ms) compared to HW (336 ± 19 ms, $n = 5$, $F = 18$, $p < 0.05$). The small number of long (>1 s) respiratory intervals are not an experimental error; they originated from the apnoeic periods that followed augmented breaths (Fig. 3.3).

Temporal characteristics of motor activity recorded in the two group of rats are presented in Table 3.1. The indices comprised the average duration of an individual movement and the total movement time. While SD rats tended to be less active, there was no significant difference between the two groups.

3.3.2 Relationship between motor activity and respiratory pattern

We first determine whether the extent of rapid breathing depends on the intensity (power) of associated movements. To quantify motor activity, we have developed the “movement power index” (see Methods for details) and computed it for each respiratory interval. We then plot the value of each respiratory interval against the intensity of movement associated with (i.e. occurring during) this interval. An example of such a plot is presented in Fig. 3.5A; this relationship is similar in the other nine rats as evidenced by the fact that the mean values of the movement power index for respiratory intervals shorter than the median were significantly higher than corresponding index for all intervals longer than the median (see Fig. 3.5B). To further analyze these data we sort all measured MPI values into bins of $0.01 \text{ V}^2\text{s}^{-1}$ width, computed the mean respiratory interval and the standard deviation of all respiratory intervals within each bin, and plot these results against corresponding MPI values. Examples of these plots

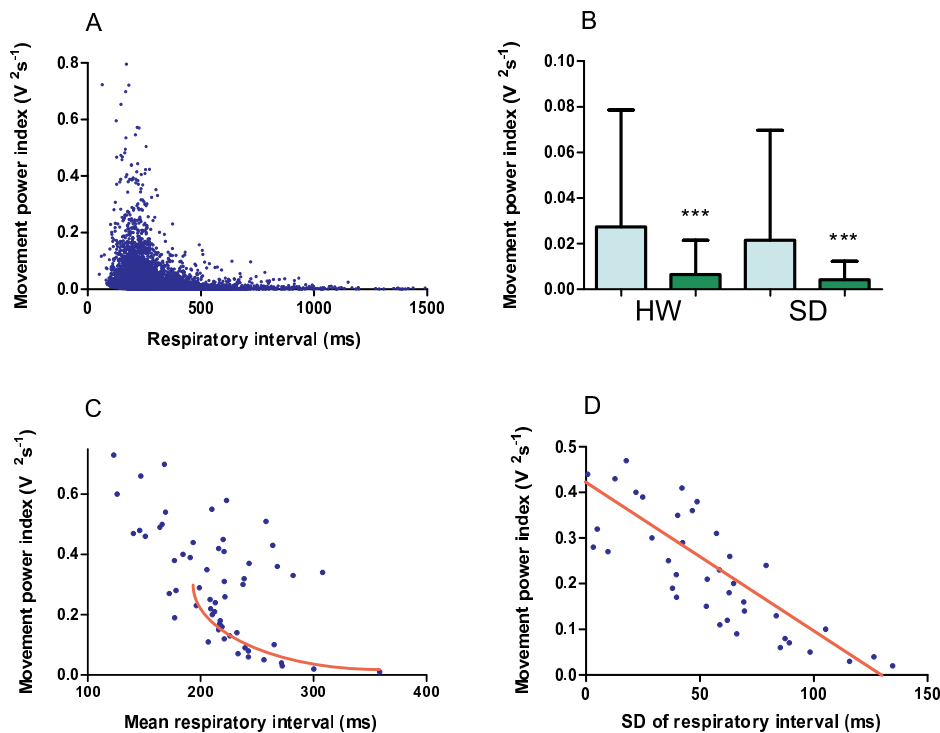


Figure 3.5. Relationship between respiration and motor activity. Relationship between respiration and motor activity in a spontaneously behaving rat. Example of analysis performed on the data from a single animal. A—Each data point represents the duration of a respiratory interval (abscissa) and an index reflecting the power of movement that occurred during this respiratory interval (ordinate; see Methods for the details of computing this index). Panel B shows group data for the mean movement power index computed separately for respiratory intervals that were shorter than the median (blue) and longer than the median (green). HW—Hooded Wistar; SD—Sprague-Dawley; ***—difference between MPIs below and above the median value, $p < 0.0001$. C—Dependence of the mean respiratory interval (computed from data shown in Panel A, with bin width of $0.01 \text{ V}^2\text{s}^{-1}$) on the movement power index. Data points with MPI values below $0.2 \text{ V}^2\text{s}^{-1}$ are fitted with parabolic curve ($r^2 = 0.56$, $p < 0.01$). Note that data points for $\text{MPI} > 0.2 \text{ V}^2\text{s}^{-1}$ that could be not satisfactory fitted represent a small fraction of all analysed respiratory intervals; this is evident from panels A and B. Panel D—Variability of rapid breathing is inversely correlated to the intensity of associated movement. Data points are standard deviations computed for each binned respiratory intervals. Data are fitted with linear equation ($r^2 = 0.62$, $p < 0.01$).

are presented in Fig. 3.5C and Fig. 3.5D. Data points with MPI values below $0.2 \text{ V}^2\text{s}^{-1}$ are fitted with parabolic curve. Note that data points for $\text{MPI} > 0.2 \text{ V}^2\text{s}^{-1}$ that could be

3.3 Results

not satisfactory fitted represent a small fraction of all analyzed respiratory intervals; this is evident from Fig. 3.5, panel A. The variation of respiratory intervals with regard to MPI bins follow an inverse linear trend (Fig. 3.5D). Thus, at rest or at low-intensity movements respiratory rate is lower and more variable compared to high-intensity movements when it is invariably high.

The next question we address is whether there is an association between the duration of motor activity and the duration of rapid breathing. To address this issue, data records from each animal are first split into 15-20 artefact-free segments, and movements and respiration are quantified individually in each of these segments. This analysis reveals that, for each such segment, duration of movements and of rapid breathing are highly correlated. An example of such analysis is presented in Fig. 3.6A; the results were very similar in the nine other animals, with a r^2 ranging 0.96-0.99 ($p < 0.001$). We then compute the total movement time and the total time of rapid breathing for the whole observation period in each animal. Again, we find a strong correlation between the two indices (Fig. 3.6B). Importantly, the value of total time of rapid breathing (348 ± 12 s) is slightly but significantly higher than the total movement time (316 ± 12 s; $p < 0.001$, $n = 10$), consistent with the fact that in some instances (in $7.1 \pm 1.6\%$ of total time of rapid breathing), the rise in the respiratory rate occurred without any detectable movement. There is no effect of strain on this motor-respiratory relationship.

3.3.3 Heart rate during basal conditions and its association with motor activity

The values for the mean RR intervals differ significantly between the two strains ($F = 17$, $p < 0.05$), being shorter for HW (155 ± 3 ms) compared to SD (187 ± 8 ms). There is, however, no between-strain difference in the coefficients of variation for RR intervals ($1.0 \pm 0.1\%$ and $0.7 \pm 0.1\%$ for HW and SD, respectively; $F = 2.7$, $p > 0.05$).

As illustrated in Fig. 3.3, the association between changes in heart rate and locomotion is not as obvious as it is for the respiratory-motor relationship. Overall, we find that longer bouts of locomotion are always associated with tachycardia, whereas during short-lasting movements (<1 s), there are no consistent changes in the HR. This relationship is reflected by the plot in Fig. 3.7A that is constructed from the data obtained in one rat, and by the results of group data analysis as shown in Fig. 3.7B.

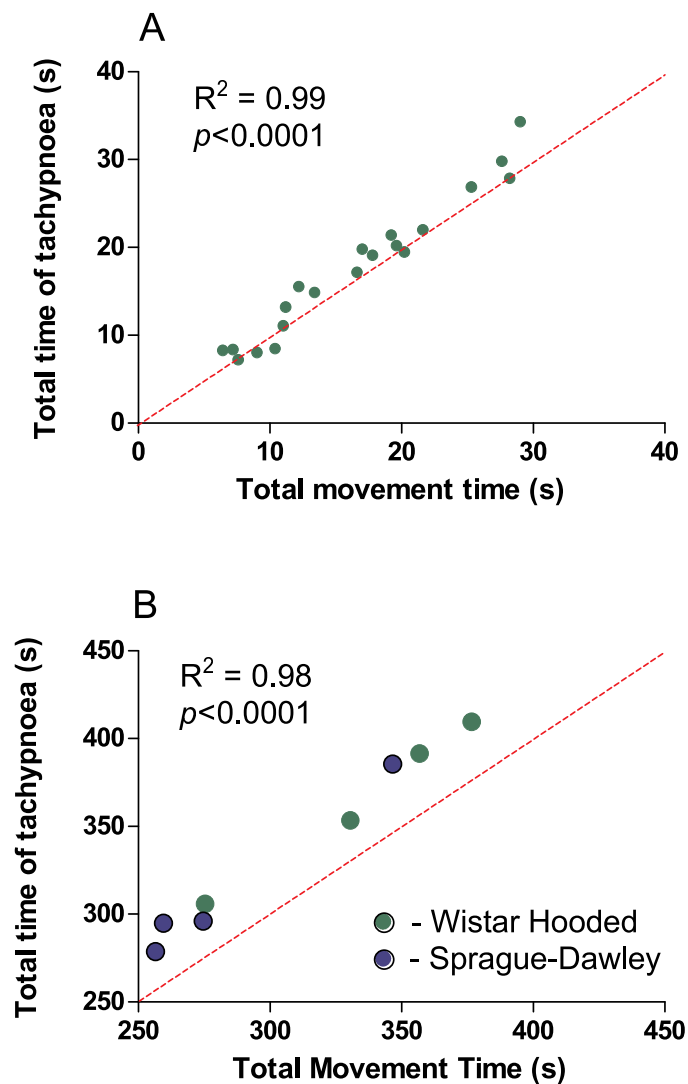


Figure 3.6. Relationship between total time of rapid breathing and movement. Relationship between the total movement time and total time of rapid breathing. A—example from an individual rat where the recording was split into 20 segments, and the pairs of movement and respiratory indices were plotted against each other for each such segment. B—group data; each point represents the pair of movement and respiratory indices derived from the whole recording period in a given animal. Note that in (A) most data points, and in (B) all of them are located above the line with the slope=1, indicating that the total time of rapid breathing consistently exceeded the total movement time.

3.3.4 Effect of motor activity on cardiorespiratory coordination

All rats show a significant shortening in the overall RR interval during high intensity movement as compared to low intensity movement (0.15 ± 0.01 vs. 0.16 ± 0.01 s, $p <$

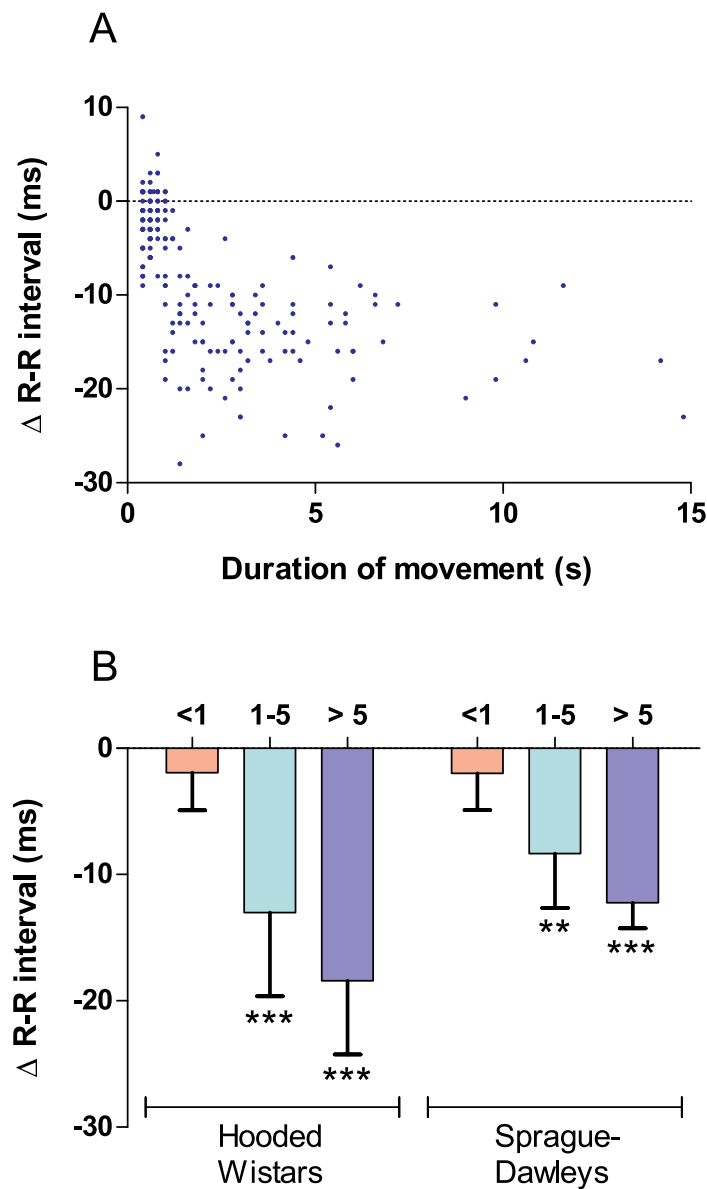


Figure 3.7. Relationship between the duration of motor act and changes in heart rate.

Relationship between the duration of an individual motor act and the changes in heart rate associated with it. A—example from an individual rat; each data point represents two values: change (Δ) in RR interval that occurred during or following a movement (abscissa), and the duration of corresponding movement (ordinate). B—group values for delta RR-intervals computed separately for short (<1 s, light-red columns), intermediate (1-5 s, cyan) and long (>5 s, purple) movements. The symbols ** and *** represent $p < 0.01$ and $p < 0.001$, respectively.

0.01 respectively in HW and 0.17 ± 0.01 vs. 0.19 ± 0.01 s, $p < 0.001$ respectively in SD), see Fig. 3.8(a). The respiratory interval is also shortened in all rats during high intensity movement as compared to low intensity movement (0.23 ± 0.1 vs. 0.34 ± 0.1 s, $p < 0.01$ respectively in HW and 0.27 ± 0.1 vs. 0.39 ± 0.1 s, $p < 0.05$ respectively in SD), see Fig. 3.8(b).

The total percentage of coordination between cardiac and respiratory signals is significantly higher during low-intensity movement as compared to high-intensity movement (13.6 ± 4.0 vs. 0.8 ± 1.6 %, $p < 0.001$ respectively in HW and 16.1 ± 3.6 vs. 1.2 ± 1.8 %, $p < 0.001$ respectively in SD), see Fig. 3.9(a). High-intensity movement also causes a slight but significant decrease in the duration of cardiorespiratory coordination (1.9 ± 0.3 vs. 0.7 ± 0.2 %, $p < 0.001$ respectively in HW and 1.9 ± 0.3 vs. 0.7 ± 0.2 s, $p < 0.001$ respectively in SD), see Fig. 3.9(b).

The phase-locking ratio of 3:1 is the most frequently ratio observed during low-intensity movement. Other phase-locking ratios for cardiorespiratory coordination are 2:1, 4:1, 5:2 and 7:2. However, 2:1 is the most frequently observed locking ratio during high-intensity movement.

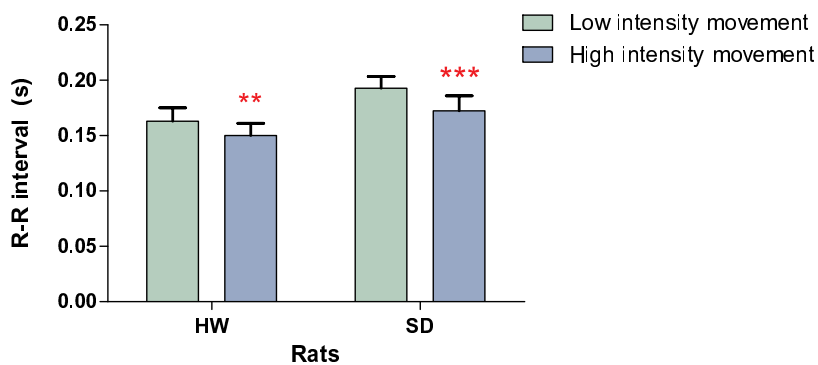
3.4 Discussion

The most important finding in this study is that motor activity is associated with an increase in the respiratory rate and a decrease in cardiorespiratory coordination. Further, we have discovered that the respiratory pattern in freely moving rats has several distinctive features including: i) high variability of the respiratory rate; ii) bimodal distribution of respiratory intervals; iii) dependence of motor-related rapid breathing on the intensity of associated movement; and iv) a tight correlation between the duration of motor-related rapid breathing and the duration of motor activity.

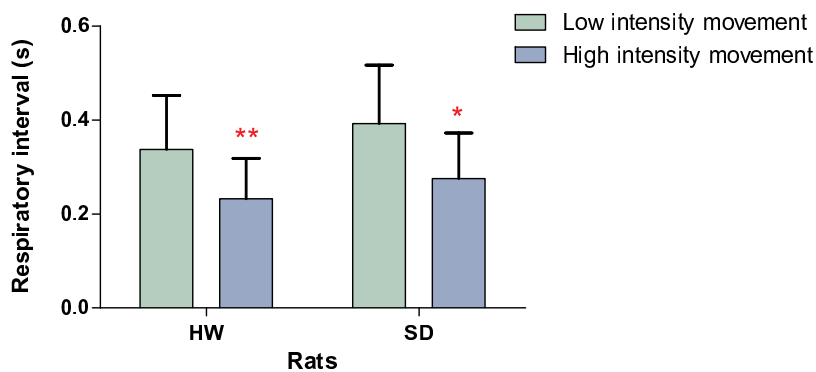
Respiratory rate in spontaneously behaving rats

Previous studies in humans have established the relation between respiration and body movement during certain activities such as exercise (Kenwright *et al.* 2008). However, most of previous studies investigating respiration in rats have focused on homeostatic changes (Roux *et al.* 2000, Antunes *et al.* 2005, Fournier *et al.* 2007, Genest *et al.* 2007, Montandon *et al.* 2008), and did not address the possibility that respiration could be also influenced by motor activity. The range of respiratory rate observed in our rats

3.4 Discussion



(a) RR interval

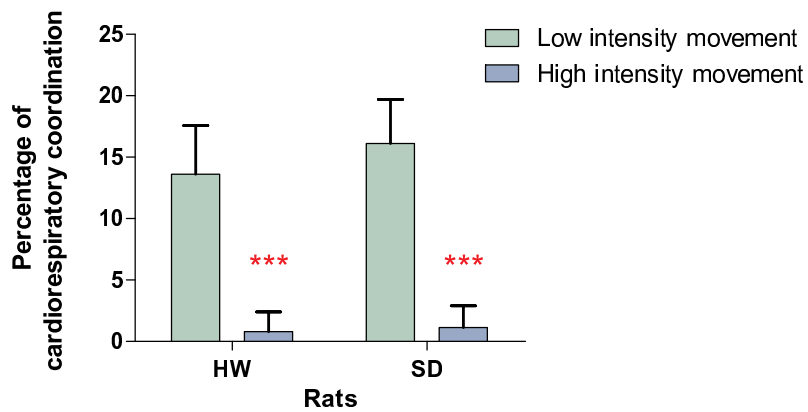


(b) Respiratory interval

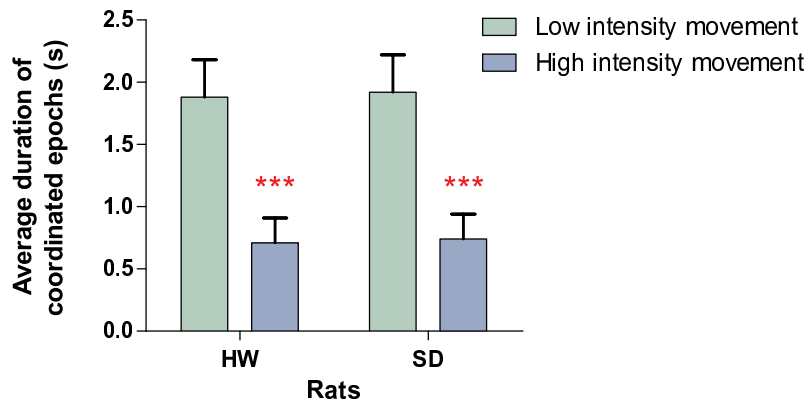
Figure 3.8. RR and respiratory intervals vs. low and high intensity movement. Overall average RR intervals and respiratory intervals in HW and SD rats during low-intensity and high-intensity movement presented as mean+SD. The symbols *, ** and *** represent $p < 0.05$, $p < 0.01$ and $p < 0.001$, respectively.

at rest (2-3 Hz) is in good accord with these previous reports. The slow and regular resting breathing was frequently intermingled with much faster respiratory movements.

We have studied our animals in the active phase (lights off), when they are frequently engaged in stereotyped behaviors or moved around the chamber. We have found that all motor acts are accompanied by rapid breathing, with the latter being grossly associated with the movement intensity. The dominant cause of the change in respiratory interval would be to facilitate high demand of oxygen in the lungs during movement as compared to non-movement. Nevertheless, the relation between the two appears to be quite complex: while vigorous movements are always accompanied by near maximal rises in respiratory rate, it is lower and varied greatly during low-intensity movements or during immobility. This relationship is reflected in the negative correlation between



(a) Percentage of coordination



(b) Duration of coordinated epochs

Figure 3.9. Motor activity and cardiorespiratory coordination. Percentage of coordination and duration of coordinated epochs in HW and SD rats during low-intensity and high-intensity movement presented as mean+SD. The symbol *** represents $p < 0.001$.

the movement power index and the dispersion of the mean respiratory interval. A tight correlation between the duration of motor activity and the duration of rapid breathing supports the idea that most respiratory changes observed in our animals were related to the former. All these findings are in a good accord with basic principles of exercise physiology (Horn and Waldrop 1998, Eldridge and Waldrop 1991).

We do not assess changes in tidal volume in this study mainly because method for its computing requires equilibration of the temperature of inspired air with body temperature (Mortola and Frappell 1998), which may not be the case during rapid breathing (Kepecs *et al.* 2007). We do not consider this as serious limitation of our study

3.4 Discussion

as it has been explicitly stated by Hilton that rapid breathing, rather than exercise-induced increase in breathing rate, is the usual component of the arousal reaction (Hilton *et al.* 1983).

Interaction between cardiac and respiratory signals during movement in conscious freely moving rats

In addition to a significant shortening in overall respiratory intervals, high-intensity movement also causes a significant shortening in RR intervals. Respiratory sinus arrhythmia (RSA), which is significantly influenced by respiratory rate (Rzeczinski *et al.* 2002, Hsieh *et al.* 2003) and mostly reflects the changes in cardiac vagal tone (Grossman and Taylor 2007), might be the cause of shortening in RR intervals. Furthermore, the shortening in RR interval during movement could also be due to the contraction of body muscles, which activates the muscle receptors causing a release from vagal tone, as reported in human subjects during exercise (Baum *et al.* 1995).

High-intensity movement also causes a significant decrease in cardiorespiratory coordination together with a change in the most frequent phase-locking ratio from 3:1 to 2:1. In Chapter 2 it is suggested that the phase-locking between the heart and respiratory rhythms is maximized at a particular respiratory frequency (Kabir *et al.* 2008). This would suggest that a change in respiratory interval during movement is the dominant cause of the decrease in cardiorespiratory coordination.

Group differences

The rationale for employing two groups of rat is the observation in previous studies that in HW rats, responses of rapid heart-rate to restraint stress are substantially higher compared to SD rats (Salome *et al.* 2007, Ngampramuan *et al.* 2008), and we thus tested the possibility that there might be also a group difference in respiratory responses to external stimuli. Our current findings suggest that there may be some genetically determined differences in the control of respiratory rate at rest (with lower basal values in SD compared to HW).

Physiological role of responses of rapid breathing

Motor-related rises in respiratory rate reported here can be interpreted in many ways. Close association between minute ventilation and exercise intensity is well established

in larger mammals, including humans, and our finding of dependence of rapid breathing amplitude and duration on the intensity and duration of associated movement suggests that its main physiological role is to facilitate gas exchange in the lungs. A possible way to further advance understanding of these complex relations is to perform ethologically-oriented experiments combined with more detailed assessment of the respiratory pattern.

3.5 Chapter summary

In this Chapter we have studied the association between movement and respiration. We conclude that voluntary movements in rats are associated with substantial and rapid increases in the respiratory rate. We have also observed a significant decrease in cardiorespiratory coordination during high-intensity movement. Our results add new information to the growing body of knowledge relating to fore-brain mechanisms that control respiratory rate in awake rats during their natural behavior.

From this study it is evident that voluntary movement affects respiration and cardiorespiratory coordination. Hence, depending on the aim of the study, movement epochs should be excluded during analysis as they might potentially confound our results. In the next Chapter we will investigate cardiorespiratory coordination as a marker of severity of obstructive sleep apnea syndrome in adults and children.

Chapter 4

Phase-coupling and sleep apnea

THIS chapter is aimed at quantification of cardiorespiratory phase-coordination in adults with obstructive sleep apnea syndrome (OSAS) and children with sleep disordered breathing (SDB). Overnight polysomnography data from two groups of subjects: one group containing 213 adults with suspected OSAS and another group containing 80 children (40 healthy and 40 with sleep disordered breathing), are investigated. Cardiorespiratory phase-coordination is associated with sleep stages and is significantly reduced during rapid-eye-movement (REM) sleep compared to slow-wave (SW) sleep in both the groups. A significant reduction in phase-coordination is also observed in adults with severe OSAS compared to adults with no or mild OSAS. There is, however, no effect of age and BMI on phase coupling. This study suggests that the assessment of cardiorespiratory phase coordination may be used as an ECG based screening tool for determining the severity of OSAS.

4.1 Introduction

Sleep can be defined as a state of unconsciousness in living beings from which one can be aroused by some sort of stimuli (Guyton and Hall 2006). There are different stages of sleep: very light sleep (stage 1) to very deep sleep (stage 4), and a further stage of rapid-eye-movement (REM) sleep. The four stages of sleep (stage 1 through to stage 4) together are known as non-rapid-eye-movement sleep (NREM), while stage 3 sleep together with stage 4 sleep are termed as slow-wave (SW) sleep, during which the brain waves are usually very strong and of very low frequency. Rapid-eye-movement sleep is characterized by rapid movements of eyes together with active bodily muscle movements, active brain, low muscle tone and irregular heart rate and respiratory rate (Guyton and Hall 2006). Rapid-eye-movement sleep is also known as paradoxical sleep due to the presence of marked activity in the brain even though the person is asleep (Guyton and Hall 2006). Throughout the night, sleep proceeds in cycles of NREM and REM, beginning with a short period of stage 1 sleep, then progressing through stage 2, followed by stages 3 and 4, and finally proceeding onto REM (Carskadon and Dement 2005). Normally, REM sleep lasts 5 to 30 minutes and appears every 90 minutes on average. The proportion of deep sleep (stage 3 and 4) is higher during the early stages of the sleep cycle, while that of REM sleep increases later in the sleep cycle and is longest in the last one-third of the sleep episode (Carskadon and Dement 2005). In healthy adults, NREM sleep constitutes about 75-80% while REM sleep constitutes the remaining 20-25% of total time spent in sleep.

Obstructive sleep apnea syndrome (OSAS) is a disorder of breathing during sleep that affects between 3-7% of adults (Young *et al.* 1993, Punjabi 2008) and 1-4% of children (Lumeng and Chervin 2008) with differing pathophysiology and presentation in the two groups (Marcus 2001). Obstructive sleep apnea syndrome (OSAS) is characterized by repetitive partial or complete closure of the upper airways that causes alterations in the functioning of cardiovascular and respiratory systems. In adults the association between OSAS and increased cardiovascular morbidity is now well recognised (McNicholas *et al.* 2007). While the mechanisms leading to cardiovascular morbidity are likely to be multifactorial, frequent arousals triggered by episodes of upper airway obstruction are believed to play a key role via repetitive sympathetic nervous system activation and destabilisation of cardiorespiratory control (Bradley and Floras 2009, Pack and Gislason 2009, Verrier and Josephson 2009). Evidence also suggests that children with upper airway obstruction may also be at increased risk

of developing cardiovascular disease (Aljadeff *et al.* 1997, O'Driscoll *et al.* 2009, Marcus *et al.* 1998).

Cardiac autonomic nerve activity in OSAS patients has been mainly studied using heart rate variability (HRV) methodology that is based on the assessment of ECG RR-interval changes (Roche *et al.* 1999). Patients with OSAS have elevated sympathetic nerve activity (Narkiewicz *et al.* 1998, Somers *et al.* 1995) and their HRV is altered (Narkiewicz *et al.* 1998), primarily by a great increase in very low frequency oscillations (VLF) that are caused by the heart rate bouts associated with repeated arousals (Baumert *et al.* 2008). Some indices of HRV were shown to be an independent predictor of cardiac mortality in different patient populations, including myocardial infarction (Tsuji *et al.* 1996), dilated cardiomyopathy (Hoffmann *et al.* 1996), and congestive heart failure (Sandercock and Brodie 2006). Autonomic modulation of the heart rate is altered during sleep in OSAS patients (Coruzzi *et al.* 2006, Wiklund *et al.* 2000, Aydin *et al.* 2004) and it has been proposed to use HRV as a screening tool (Roche *et al.* 1999, Roche *et al.* 2002).

This chapter explores cardiorespiratory coordination during sleep in a large cohort of adults with OSAS, healthy children and in children with sleep disordered breathing (SDB). A detailed statistical analysis was performed on the group of adults with suspected OSA. In children a rather simple analysis was performed by removing all the spontaneous arousal episodes and SDB related events—apnea, hypopnea and respiratory arousal episodes—to test whether cardiorespiratory coordination is affected during normal sleep episodes in children with SDB compared to healthy controls. It is hypothesized that cardiorespiratory coordination is reduced due to sleep apnea or disordered breathing and its assessment provides markers of cardiorespiratory system disturbances.

4.2 Methods

4.2.1 Ethics statement

The study conformed to principles outlined in the Declaration of Helsinki and was approved by the local ethics committee of Royal Adelaide Hospital and Women's and Children's Hospital, Adelaide, Australia. For children, parental consent and child assent were obtained for all participants. In the case of adults, since de-identified data

4.2 Methods

were collected from participants for this study, the ethics committee waived the need for written informed consents.

4.2.2 Subjects

Overnight sleep studies were performed in two separate groups of subjects—adults and children. The first group consisted of 312 adult patients with suspected obstructive sleep apnea syndrome (OSAS). The PSG data for 64 patients are excluded due to poor signal quality. From a total of 248 adults (157 males / 91 females) with suspected OSAS, another 35 with diabetes mellitus are excluded due to suspected diabetic autonomic neuropathy that might potentially confound our results (Javorka *et al.* 2008). The age and BMI of the patients ranged 20-77 years (mean±SD: 49.4 ± 12.3 yrs) and 20.1-73.3 kg/m² (mean±SD: 34.1 ± 8.14 kg/m²) respectively. In this cohort, 69 patients are reported to have cardiovascular disease. Initially, we separately analyse 144 patients without heart diseases and 69 patients with heart diseases and observe no significant differences in the results between the two groups (see Table 4.1). Accordingly, the subsequent results in OSAS patients are reported taking 213 subjects into account. However, the effect of age, gender and BMI are studied using linear regression model on the 144 patients without heart diseases.

In the second group, fifty-three healthy children and fifty-four children with sleep disordered breathing (SDB) were enrolled. Among the healthy children (controls), none were reported to snore regularly or were taking medication that would affect sleep architecture or cardiovascular physiology. The sub-group of fifty-four children with SDB are those who had a history of frequent snoring and were scheduled for adenotonsillectomy for suspected SDB, as diagnosed by an experienced paediatric otorhinolaryngologist at the Adelaide Women's and Children's Hospital. Children are excluded if they had undergone previous ear, nose, throat or craniofacial surgery; had a medical condition (other than SDB) associated with hypoxia or sleep fragmentation; or were taking medication known to affect sleep or cardiorespiratory physiology. The PSG data for 13 of the 53 control children and 4 of the 54 children with SDB are excluded due to poor signal quality. Of the remaining 50 children with SDB, a further 10 are excluded due to significantly greater age and lower socioeconomic status compared to the control children. The age and BMI z-score of the subjects ranged 3-12.9 years (mean±SD: 7.7 ± 2.6 yrs) and -1.7-2.3 (mean±SD: 0.3 ± 0.8) respectively.

Table 4.1. Cardiorespiratory coordination in patients with and without heart diseases. Percentage of coordination (%cordn) and duration of coordinated epochs (AvDurCordn) for different apnea/hypopnea index (AHI) groups and sleep stages using abdominal signal (ABDO) for patients with and without heart diseases.

		AHI \leq 15	15<AHI<30	AHI \geq 30	
Patients without heart disease (Total: 144)	Number	88	25	31	
	Age	43.1 \pm 10.6	51.7 \pm 12.4	43.0 \pm 8.9	
	Male	60.2%	60%	80.7%	
	BMI	31.3 \pm 7.1	32.0 \pm 5.9	36.5 \pm 8.3	
	%cordn	SS1	12.1 \pm 6.1	10.1 \pm 5.3	6.7 \pm 4.4
		SS2	14.7 \pm 6.5	11.3 \pm 4.1	7.8 \pm 3.6
		SW	18.6 \pm 7.6	16.4 \pm 6.8	14.1 \pm 5.8
		REM	11.3 \pm 4.5	8.9 \pm 3.2	7.2 \pm 2.7
	AvDurCordn	SS1	7.8 \pm 1.9	7.7 \pm 1.8	5.9 \pm 2.4
		SS2	8.6 \pm 1.6	8.6 \pm 2.1	6.3 \pm 2.1
		SW	9.1 \pm 1.6	9.4 \pm 1.8	7.9 \pm 2.2
		REM	7.7 \pm 1.8	7.4 \pm 1.9	6.1 \pm 1.7
Patients with heart disease (Total: 69)	Number	35	15	19	
	Age	54.1 \pm 9.7	61.9 \pm 8.0	56.1 \pm 12.5	
	Male	48.6%	73.3%	68.4%	
	BMI	34.6 \pm 10.2	32.4 \pm 2.4	41.8 \pm 8.3	
	%cordn	SS1	11.7 \pm 6.6	16.3 \pm 8.7	8.3 \pm 3.4
		SS2	15.0 \pm 6.2	12.3 \pm 5.4	9.0 \pm 4.6
		SW	18.9 \pm 9.3	16.1 \pm 9.0	15.1 \pm 6.3
		REM	11.0 \pm 4.0	10.4 \pm 4.7	6.8 \pm 4.1
	AvDurCordn	SS1	7.8 \pm 2.3	7.6 \pm 2.1	6.3 \pm 2.2
		SS2	8.5 \pm 2.2	7.9 \pm 2.3	6.8 \pm 2.1
		SW	9.6 \pm 2.1	8.4 \pm 2.2	7.5 \pm 1.7
		REM	7.2 \pm 1.7	6.9 \pm 1.9	6.2 \pm 1.6

4.2 Methods

4.2.3 Data recordings and analysis

Sleep stages were assigned to consecutive 30 s epochs. Sleep scoring was carried out according to standard rules (Rechtschaffen and Kales 1968).

Overnight polysomnography

Overnight polysomnography was performed using a E series[®] system (Compumedics, Australia). For sleep staging and arousal scoring standard surface, the following standard parameters were measured and recorded continuously utilizing the appropriate signal sampling and filtering protocols: electroencephalogram (EEG; C3-A2 or C4-A1); left and right electrooculogram (EOG); submental and diaphragmatic electromyogram with skin surface electrodes; leg movements by piezoelectric motion detection from surface electrodes on the tibialis anterior muscles of both legs; heart rate by electrocardiogram (ECG) using a modified lead II; oronasal airflow by thermistor and nasal pressure; respiratory movements of the chest and abdominal wall using uncalibrated respiratory inductive plethysmography bands; arterial oxygen saturation (SaO₂) by finger pulse oximetry (Nellcor N595 with an averaging time of 3 s); and transcutaneous CO₂ (TcCO₂) using a heated (41° C) transcutaneous electrode (TINA, Radiometer Pacific, Melbourne, Vic., Australia).

Overnight polysomnography (PSG) was conducted without sedation or sleep deprivation and was only performed if subjects were well on the night and free of any recent respiratory infection. Overnight PSG began at each subject's usual bedtime. In the case of children, a parent accompanied each child throughout the procedure. Each subject was continuously monitored and observed via infrared camera by a paediatric sleep technician who also documented observations of sleep behaviour, including the presence or absence of snoring.

All PSGs were visually scored by a sleep technician experienced in analyzing paediatric sleep studies. Sleep stages were assigned to consecutive 30 s epochs according to standard rules (Rechtschaffen and Kales 1968). For the purpose of this study, sleep stages 3 and 4 are combined and termed slow-wave sleep (SW). Epochs were scored as movement if the EEG and EOG signals were obscured for $\geq 50\%$ of the epoch by muscle tension or artefact associated with movement of the subject (Rechtschaffen and Kales 1968). Movement time was scored as a separate category, and was not included in either sleep or wake time. Wake time refers to time spent awake during the recording period after initial sleep onset. Respiratory variables were scored according

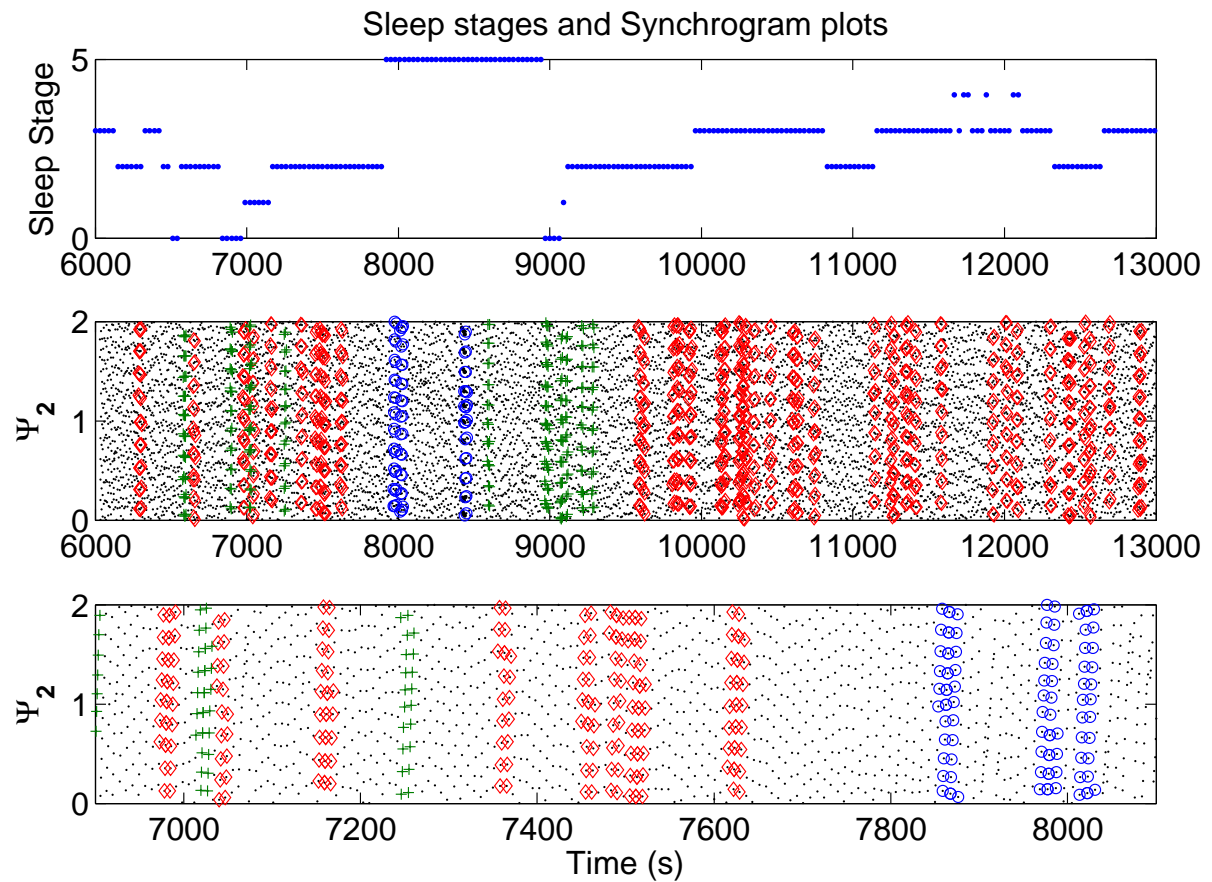


Figure 4.1. Sleep stages and synchrogram. Synchrogram plot (second panel) revealing cardiorespiratory locking at different frequency ratios and sleep stages (rated at the top panel). Small dots indicate the normalised phases. ‘Diamond’, ‘plus’, and ‘circle’ symbols indicate 9:2, 10:2 and 11:2 coordination respectively. The numbers 0-5 for sleep stage represent awake, stage 1, stage 2, stage 3, stage 4 and REM sleep respectively. The recorded data segment for this figure was selected such that all the sleep stages are available in order to compare the differences. For better visualisation, an expanded time scale version of the synchrogram plot (second panel) has been shown in the third panel.

to standard guidelines recommended for paediatric sleep studies (American Thoracic Society 1996). The apnea/hypopnea index (AHI) was calculated as the number of obstructive and nonobstructive events per hour of sleep. Cortical spontaneous arousals were scored according to the criteria of the American Sleep Disorders Task Force (1992), and are expressed as the total number of arousals per hour of sleep (arousal index). The point of arousal onset was determined visually from the EEG channel. Periodic limb movements (PLMS) were scored using standard criteria (American Sleep Disorders Association 1993). The PLM index (PLMI) was calculated as the number of PLMS per hour of sleep.

4.2 Methods

Artefact such as movements can potentially confound the results (as discussed in Chapter 3) and hence should be removed for data analysis. As a result, all 30 s epochs containing artifacts together with an artifact-free epoch immediately before and after each artifact-epoch are excluded from both the groups. In addition, SDB related events (apnea, hypopnea and respiratory arousal episodes) and spontaneous arousal epochs, together with one clean epoch each immediately before and after, are also excluded during data analyses in children with SDB.

Processing of ECG and respiratory signal

The ECG signal (lead II) was digitized at 128 Hz in adults and 500 Hz in healthy children and saved for off-line analysis. Herein, ECG R-wave peaks are detected using the programming library libRASCH (www.librasch.org). The RR intervals time series are visually scanned for artifacts and, if necessary, manually edited.

Abdominal and thoracic respiratory signals, digitized at 32 Hz, are used for the analysis of cardiorespiratory coordination. Respiratory signals are processed as described in Chapter 1, Section 1.4.2. To remove noise, the respiratory signals are low-pass filtered at 0.5 Hz.

Cardiorespiratory coordination analysis

We study the coordination between cardiac and respiratory cycles in all the subjects using cardiorespiratory synchrogram plot as described in Chapter 1, Section 1.7.2. The cardiorespiratory synchrogram provides a visual tool to detect cardiorespiratory coordination (Fig. 4.1, second panel).

We employ three parameters for every sleep stage—percentage of coordination (%cordn), average duration of coordinated epochs (AvDurCordn) and phase-locking ratio—for characterising cardiorespiratory coordination. If p_j and q_j are the start and end time points of the j^{th} coordinated epoch ($j = 1, 2, \dots, N$) and t_{total} is the total duration of the recording, then the equations for calculating the parameters can be given as

$$\text{Percentage of coordination} = \frac{\sum_{j=1}^N (q_j - p_j)}{t_{\text{total}}} \times 100 \quad (4.1)$$

$$\text{Average duration of coordinated epochs} = \frac{\sum_{j=1}^N (q_j - p_j)}{N} \quad (4.2)$$

Table 4.2. Overnight polysomnography in adults. Demographic data and overnight polysomnography findings in different groups of obstructive sleep apnea syndrome patients.

	AHI \leq 15	15<AHI<30	AHI \geq 30
Total number of patients, N_{Total}	133	51	64
Patients with diabetes mellitus, N_{DM}	10	11	14
Patients analysed, N ($N_{\text{Total}} - N_{\text{DM}}$)	123	40	50
Male	70	26	38
Age (yrs)	46 \pm 11	56 \pm 12	48 \pm 12
BMI (kg/m ²)	32 \pm 8	32 \pm 5	39 \pm 9
Weight (kg)	91.2 \pm 21.4	93.4 \pm 19.6	111.2 \pm 23.6
Height (cm)	168.6 \pm 9.2	170.2 \pm 10.2	170.6 \pm 8.3
RR interval (ms)	911 \pm 120	956 \pm 131	845 \pm 123
Respiratory interval (ms)	3797.5 \pm 335.5	3947.4 \pm 315.8	3703.7 \pm 434.2
Total length of recording (min)	428.8 \pm 53.4	431.1 \pm 64.6	438.2 \pm 27.1
Sleep time (min)	346.0 \pm 55.4	346.9 \pm 60.6	352.8 \pm 64.8
Wake time (min)	61.1 \pm 42.4	64.7 \pm 42.3	74.1 \pm 56.8
REM sleep (%)	14.7 \pm 4.1	14.6 \pm 3.8	12.3 \pm 4.5
Arousals (#/h)	16.4 \pm 8.4*	25.3 \pm 8.6*	50.7 \pm 19.6*
Total percentage of coordination (%)	13.5 \pm 6.2*	11.6 \pm 5.1*	8.8 \pm 4.5*
Mean duration of coordinated epochs (s)	8.3 \pm 1.8*	8.1 \pm 2.0*	6.5 \pm 2.1*
Hypertension	26	14	18
Structural heart disease	18	8	6
Smoker	14	2	8

$$\text{Phase-locking ratios} = m_j : n_j. \quad (4.3)$$

Surrogate data analysis

In order to determine whether randomness of heart rate variations play any role with respect to cardiorespiratory coordination, we use surrogate data in adults with suspected OSAS for our analysis. The surrogate data are obtained by randomizing the order of RR intervals separately for every sleep stage and constructing the new R time series by starting with the first original R time and cumulating the randomized RR intervals. Accordingly, the phases of the respiratory signal corresponding to the new

4.3 Results—Adults

time points of the R-peaks are calculated and analysed for cardiorespiratory coordination.

Statistical analysis

GraphPad Prism version 5.01 for Windows (GraphPad Software, San Diego California USA, www.graphpad.com) is used for statistical analysis.

In adults, in addition to GraphPad Prism, statistics computer software SPSS, Inc. version 15.0 is used to analyse the data. To determine the effects of age, gender, and BMI on cardiorespiratory coordination, linear regression models are developed for the 144 patients without heart disease. To determine the effect of OSAS severity on cardiorespiratory coordination, the cohort is trichotomized based on the apnea-hypopnea index (AHI): $AHI \leq 15$, $15 < AHI < 30$, and $AHI \geq 30$. Differences in cardiorespiratory coordination between the three OSAS groups as well as between different sleep stages are assessed with 2-way ANOVA for repeated measurements. For post-hoc analysis, Tukey's multiple comparison test is used.

In children, analysis of variance (ANOVA) is used to test for group differences in cardiorespiratory coordination. Repeated measures ANOVA is used to test for differences in cardiorespiratory coordination across groups and between sleep stages. Post-hoc analysis is performed using Student's t-tests.

Data are expressed as mean \pm standard deviation (SD) and *p* values are 2-tailed with statistical significance determined at $\alpha = 0.05$.

4.3 Results—Adults

Respiratory and RR intervals are significantly shortened in patients with severe OSAS compared to patients with no/mild OSAS (Table 4.2). Cardiorespiratory coordination is significantly associated with the degree of severity of OSAS. The AHI shows negative correlations with the mean RR interval ($r = -0.244$, $p < 0.001$), percentage of coordination (%cordn) ($r = -0.463$, $p < 0.001$) and average duration of coordinated epochs (AvDurCordn) ($r = -0.437$, $p < 0.001$). Patients with severe OSAS have a significantly lower percentage of heart rate - respiratory rate phase-locking states compared to patients with no or mild OSAS (Fig. 4.2(a)). The average duration of coordinated epochs is significantly decreased in patients with severe OSAS compared to patients with moderate or no/mild OSAS (Fig. 4.2(b)).

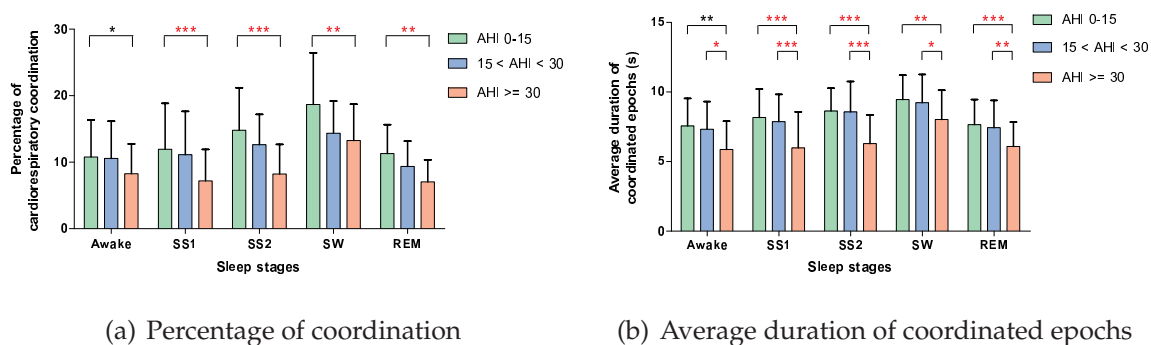


Figure 4.2. Cardiorespiratory coordination in adults. Group related comparison of percentage of coordination (%cordn, mean±SD) and average duration of coordinated epochs (Av-DurCordn, mean±SD) using original data from abdominal signal. Here, *, ** and *** represent $p < 0.05$, $p < 0.01$, and $p < 0.0001$, respectively.

4.3.1 Polysomnographic findings

Demographic and polysomnographic data are presented in Table 4.2. Of the 213 patients, 133 (70 male) presented with no or mild OSAS ($AHI \leq 15$), 40 (26 male) patients with mild to moderate OSAS ($15 < AHI < 30$) and 50 patients (38 male) with severe OSAS ($AHI \geq 30$). Neither age nor BMI are significantly different between the three subgroups.

Sleep time, wake time and percentage of REM sleep are not significant between the three OSAS subgroups ($p > 0.5$). The number of arousals per hour is significantly higher in patients with severe OSAS (50.7 ± 19.6 /h) compared to patients with moderate (25.3 ± 8.6 /h) or no/mild (16.4 ± 8.4 /h, $p < 0.0001$) OSAS.

4.3.2 Predominant phase locking ratios

The most frequent phase locking ratio observed in adults with mild and moderate OSAS was 4:1 (Table 4.3), followed by 5:1 and 3:1. In adults with severe OSAS, 2:1 was the most frequent phase locking ratio, followed by 4:1, 5:1 and 3:1.

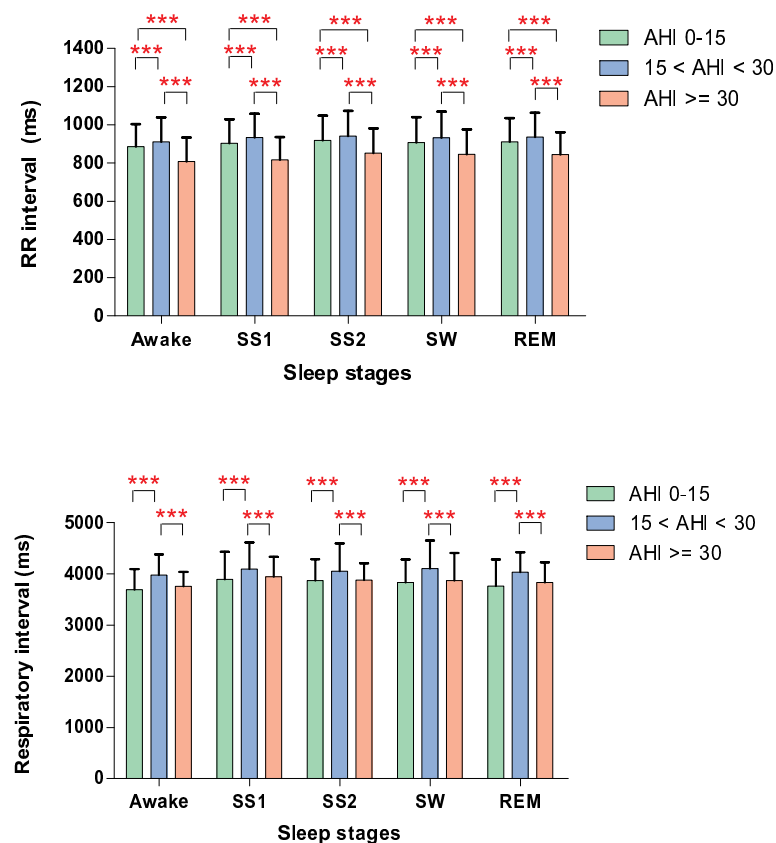


Figure 4.3. RR and respiratory intervals in adults/OSAS patients. Group and sleep related comparison of RR interval and respiratory interval. Here, *** represents $p < 0.0001$.

4.3.3 Sleep stage effects on respiratory and RR intervals and cardiorespiratory coordination in OSAS patients

Mean heart rate and respiratory rate are not significantly different between sleep stages (see Fig. 4.3). The percentage of coordination (%cordn) is nearly 50% higher during slow-wave sleep compared to REM sleep (18.7 ± 7.7 vs. 11.2 ± 4.3 %, $p < 0.0001$), see Figure 4.4. The average duration of coordinated epochs (AvDurCordn) also depend on the sleep stage (Fig. 4.5). Post-hoc analysis reveals: i) prolongation of coordinated epochs in slow-wave sleep compared to REM sleep; and ii) prolongation of coordinated epochs in stage 1, stage 2 and slow-wave sleep compared to wakefulness. There is no significant difference in the dominance of phase locking ratios during different sleep stages (Table 4.3).

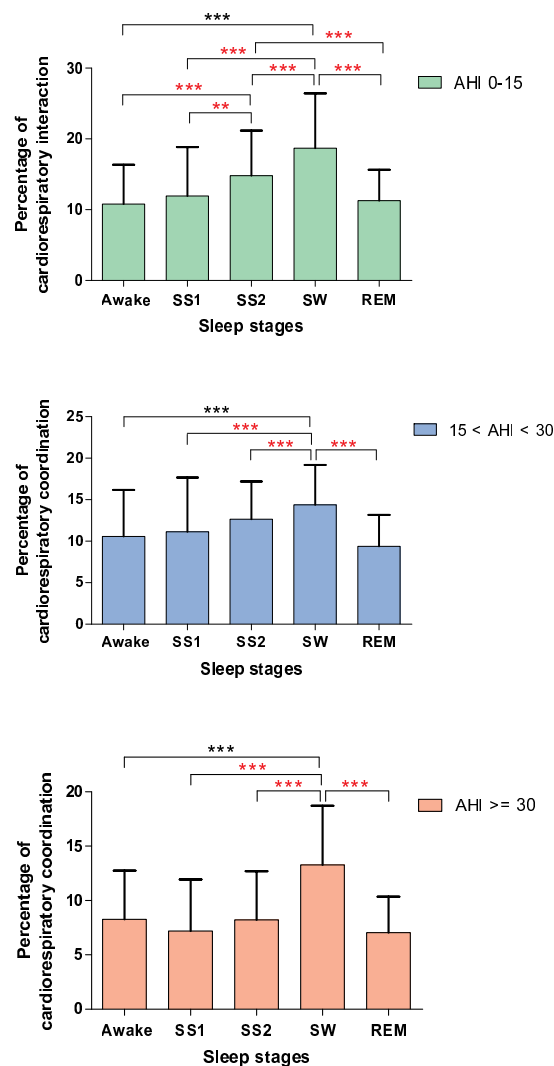


Figure 4.4. Cardiorespiratory coordination. Sleep related comparison of percentage of coordination (%cordn, mean±SD) using original data from abdominal signal. Here, *, ** and *** represent $p < 0.05$, $p < 0.01$ and $p < 0.0001$, respectively.

4.3.4 Surrogate data analysis in OSAS patients

The percentage of coordination (%cordn) and average duration of coordinated epochs (AvDurCordn) is significantly decreased ($p < 0.001$ and $p < 0.0001$ respectively) after randomizing the order of the R wave occurrence, see Table 4.4. Moreover, comparing the results obtained using surrogate data it is observed that they follow a similar pattern and significance among the different AHI groups and sleep stages as that of the results obtained using original data. The %cordn and AvDurCordn, obtained using surrogate data, is significantly higher during slow-wave sleep compared to REM sleep

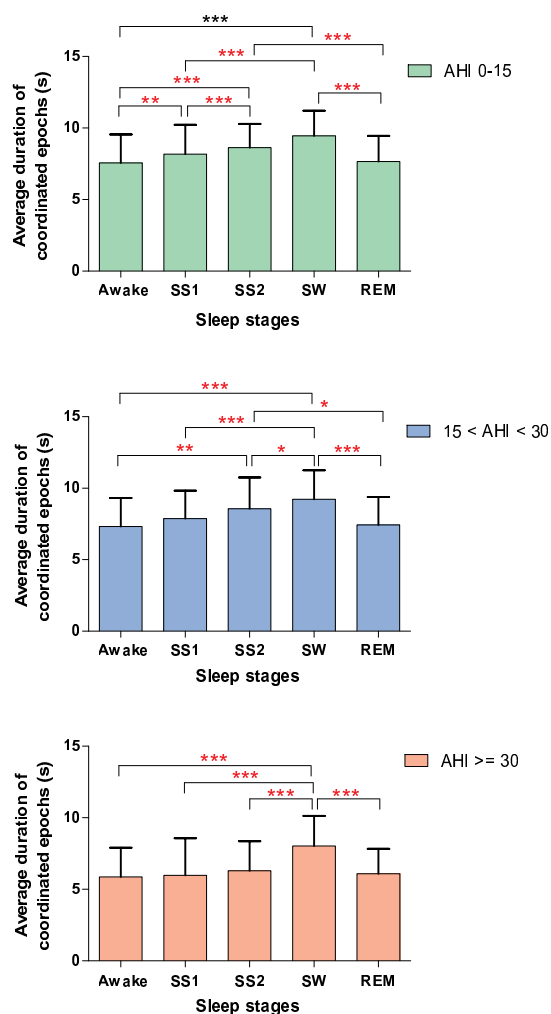


Figure 4.5. Cardiorespiratory coordination. Sleep related comparison of average duration of coordination (AvDurCordn, mean \pm SD) using original data from abdominal signal. Here, *, ** and *** represent $p < 0.05$, $p < 0.01$ and $p < 0.0001$, respectively.

(9.9 ± 3.9 vs. 5.7 ± 2.4 %, $p < 0.0001$ and 5.9 ± 1.9 vs. 4.4 ± 1.8 s, $p < 0.0001$ respectively, in patients with no/mild OSAS), see Table 4.4.

4.3.5 Age effects on cardiorespiratory coordination in OSAS patients

Using the linear regression model for the 144 patients without heart disease, we find no significant association between age and percentage of coordination (%cordn). Likewise, age is not significantly associated with the average duration of coordinated epochs

Table 4.4. Cardiorespiratory coordination: Original vs. surrogate data. Percentage of coordination and average duration of coordinated epochs for different AHI groups and sleep stages using original (ORG) and surrogate (SUR) data.

Percentage of coordination						
	AHI _≤ 15		15 < AHI < 30		AHI _≥ 30	
	ORG	SUR	ORG	SUR	ORG	SUR
Awake	10.8 ± 5.6 %	5.7 ± 2.1 % **	10.6 ± 5.6 %	4.8 ± 2.2 % **	8.3 ± 4.5 %	3.9 ± 1.5 % **
SS1	11.9 ± 6.9 %	6.2 ± 3.3 % **	11.1 ± 6.5 %	5.5 ± 2.8 % **	7.2 ± 4.8 %	4.3 ± 2.2 % **
SS2	14.8 ± 6.4 %	8.5 ± 3.1 % **	12.6 ± 4.6 %	6.1 ± 3.7 % **	8.2 ± 4.5 %	4.4 ± 2.4 % **
SW	18.7 ± 7.8 %	10.9 ± 4.4 % **	14.4 ± 4.8 %	8.1 ± 4.2 % **	13.3 ± 5.4 %	5.0 ± 2.5 % **
REM	11.3 ± 4.3 %	5.7 ± 2.4 % **	9.4 ± 3.8 %	4.9 ± 2.2 % **	7.1 ± 3.3 %	3.5 ± 2.2 % **
Average duration of coordination						
Awake	7.6 ± 1.9 s	4.1 ± 2.0 s ***	7.3 ± 1.9 s	3.5 ± 1.9 s ***	5.9 ± 2.1 s	2.4 ± 1.9 s ***
SS1	8.2 ± 2.1 s	4.7 ± 2.1 s ***	7.9 ± 1.9 s	3.9 ± 2.2 s ***	5.9 ± 2.5 s	2.5 ± 2.3 s ***
SS2	8.6 ± 1.6 s	5.4 ± 1.7 s ***	8.6 ± 2.2 s	4.3 ± 2.1 s ***	6.3 ± 2.1 s	3.0 ± 2.0 s ***
SW	9.5 ± 1.8 s	6.0 ± 1.9 s ***	9.2 ± 2.1 s	4.7 ± 2.2 s ***	8.1 ± 2.1 s	3.7 ± 2.0 s ***
REM	7.7 ± 1.8 s	4.4 ± 1.9 s ***	7.4 ± 1.9 s	3.6 ± 1.9 s ***	6.1 ± 1.7 s	2.4 ± 1.8 s ***

Asterisks indicate significant differences with ORG. Here, ** and *** represent $p < 0.01$ and $p < 0.0001$.

(AvDurCordn) and locking ratio. On the other hand, there is a significant positive correlation between the age and the mean RR interval ($r = 0.188$, $p < 0.01$) and a significant positive correlation between age and mean respiratory time interval ($r = 0.242$, $p < 0.001$). To further investigate the age effect on respiratory and RR intervals, the study group is divided into four arbitrary subgroups: <30 years, 30-45 years, 46-60 years and >60 years. The mean RR interval is significantly longer in patients above 60 years of age, compared to patients in the range of 30-45 years (967.92 ± 88.55 vs. 877.01 ± 114.32 ms). On the other hand, the mean respiratory time interval is significantly higher in patients above 60 years of age, compared to patients less than 30 years of age (4051.32 ± 173.67 vs. 3579.95 ± 325.63 ms).

4.3.6 Gender effects on cardiorespiratory coordination in OSAS patients

Analysing 144 patients without heart diseases, we observe that gender has no significant effect on RR interval ($r = -0.072$, $p > 0.1$) or respiratory time period ($r = 0.029$, $p > 0.1$). Males and females have similar patterns of coordination between heart rate and respiration. Considering '0' as females and '1' as males, a negative correlation is observed between gender and percentage of coordination (%cordn) ($r = -0.180$, $p < 0.01$), between gender and duration of coordinated epochs (AvDurCordn) ($r = -0.149$, $p < 0.05$) and between gender and locking ratio ($r = -0.204$, $p < 0.01$).

4.3.7 BMI effects on cardiorespiratory coordination in OSAS patients

Although BMI shows no correlation with percentage of coordination (%cordn) ($r = -0.007$, $p > 0.1$) in the 144 patients without heart diseases, a significant correlation is observed between BMI and duration of coordinated epochs ($r = -0.262$, $p < 0.01$). Notice that BMI shows significant negative correlations with both the mean RR interval ($r = -0.343$, $p < 0.001$) the mean respiratory time period ($r = -0.144$, $p < 0.05$). The association of heart rate and respiratory rate with BMI is further assessed by dividing the cohort into four groups based on the statistical categories of BMI values: underweight (<18.5 kg/m²), normal (18.5-25 kg/m²), overweight (25.1-30 kg/m²) and obese (>30 kg/m²). The RR interval and respiratory time period is significantly shorter in obese patients compared to patients with normal BMI (938.39 ± 135.75 vs. 881.61 ± 111.65 ms, $p < 0.001$ and 3997.34 ± 296.03 vs. 3888.53 ± 355.231 ms, $p < 0.01$). No

4.3 Results—Adults

Table 4.5. Abdominal vs. thoracic respiratory signals: Percentage of coordination. Percentage of coordination for different AHI groups and sleep stages using abdominal (ABDO) and thoracic (THOR) signals.

	AHI \leq 15		15<AHI<30		AHI \geq 30	
	ABDO	THOR	ABDO	THOR	ABDO	THOR
Awake	10.8 \pm 5.6 %	8.3 \pm 4.5 %	10.6 \pm 5.6 %	7.9 \pm 3.8 %	8.3 \pm 4.5 %	6.3 \pm 3.6 %
SS1	11.9 \pm 6.9 %	10.7 \pm 5.5 %	11.1 \pm 6.5 %	9.4 \pm 4.4 %	7.2 \pm 4.8 %	7.8 \pm 4.5 %
SS2	14.8 \pm 6.4 %	13.7 \pm 6.1 %	12.6 \pm 4.6 %	11.9 \pm 4.7 %	8.2 \pm 4.5 %	8.3 \pm 4.2 %
SW	18.7 \pm 7.8 %	17.1 \pm 7.5 %	14.4 \pm 4.8 %	13.7 \pm 5.2 %	13.3 \pm 5.4 %	11.8 \pm 5.9 %
REM	11.3 \pm 4.3 %	10.1 \pm 4.7 %	9.4 \pm 3.8 %	8.7 \pm 3.8 %	7.1 \pm 3.3 %	6.9 \pm 4.6 %

Table 4.6. Abdominal vs. thoracic respiratory signals: Duration of coordination. Duration of coordinated epochs for different AHI groups and sleep stages using abdominal (ABDO) and thoracic (THOR) signals.

	AHI \leq 15		15<AHI<30		AHI \geq 30	
	ABDO	THOR	ABDO	THOR	ABDO	THOR
Awake	7.6 \pm 1.9 s	7.2 \pm 4.5 s	7.3 \pm 1.9 s	7.2 \pm 1.8 s	5.9 \pm 2.1 s	6.5 \pm 2.1 s
SS1	8.2 \pm 2.1 s	7.9 \pm 2.3 s	7.9 \pm 1.9 s	7.8 \pm 2.7 s	5.9 \pm 2.5 s	5.7 \pm 1.7 s
SS2	8.6 \pm 1.6 s	9.1 \pm 1.8 s	8.6 \pm 2.2 s	8.7 \pm 2.4 s	6.3 \pm 2.1 s	6.2 \pm 2.1 s
SW	9.5 \pm 1.8 s	9.7 \pm 1.9 s	9.2 \pm 2.1 s	9.4 \pm 2.4 s	8.1 \pm 2.1 s	7.9 \pm 2.6 s
REM	7.7 \pm 1.8 s	7.5 \pm 2.1 s	7.4 \pm 1.9 s	7.4 \pm 1.8 s	6.1 \pm 1.7 s	5.1 \pm 1.5 s

significant difference in cardiorespiratory coordination is observed between the four BMI categories.

4.3.8 Effect of respiratory signal source on the quantification of CRC

All results reported above are based on analysing the abdominal respiratory signal. To determine whether the origin of the respiratory signal (abdomen vs. thorax) affects our results, we compare the percentage of coordination (%cordn) and average duration of coordinated epochs (AvDurCordn) obtained from the abdominal trace with those obtained from the thorax (Table 4.5 and 4.6). There is no significant difference in %cordn and AvDurCordn values obtained from thorax or abdomen ($p > 0.05$).

4.3.9 Correlation between CRC and heart and respiratory parameters

The mean RR interval and respiratory interval of the cohort is 906.1 ± 126.5 ms and 3821.66 ± 315.76 ms, respectively. The percentage of coordination (%cordn) shows no significant correlation with mean RR interval ($r = 0.095$, $p > 0.05$), respiratory rate ($r = 0.015$, $p > 0.05$) or high frequency power of the HRV (logHF), computed as the logarithm of power in the frequency range 0.15-0.4 Hz, ($r = 0.01$, $p > 0.05$). Average duration of coordinated epochs (AvDurCordn) is significantly correlated with mean RR interval ($r = 0.383$, $p < 0.001$) and respiratory time interval ($r = -0.492$, $p < 0.001$), but not with logHF ($r = 0.11$, $p > 0.05$).

4.3.10 Effect of sleep stage and severity of OSAS on HF power of heart rate

The high frequency power component of HRV (logHF), i.e. the magnitude of RSA, is significantly different between awake and stage 2 sleep (Fig. 4.6). The degree of OSAS had no significant effect on the magnitude of high frequency power.

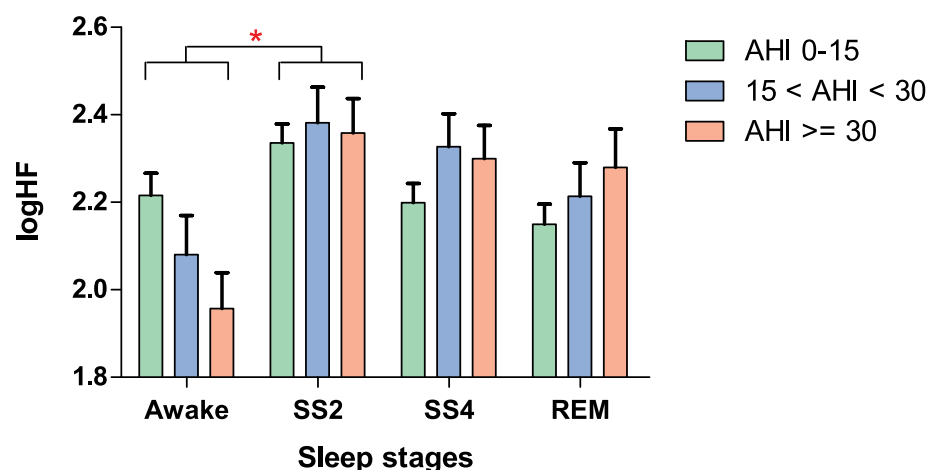


Figure 4.6. High Frequency Power. Group and sleep related comparisons of log transformed high frequency power (logHF) (mean+SD). Here, * represents $p < 0.05$

4.4 Results—Children

Data analyses in healthy controls and children with SDB are performed after excluding all the artefact, SDB related events and spontaneous arousal episodes together with an

4.4 Results—Children

artifact-free/SDB-event-free/arousal-free episode immediately before and after each above mentioned episode.

4.4.1 Polysomnographic findings

As anticipated baseline PSG confirms the presence of respiratory abnormalities in the SDB children who have a significantly higher obstructive apnoea hypopnoea index, elevated respiratory arousals, increased frequency of SaO₂ desaturations and a significantly lower mean SaO₂ nadir compared to controls. There are no significant differences between groups with respect to sleep architecture, spontaneous arousals or PLMS (Table 4.7).

4.4.2 Predominant phase locking ratios in children

In healthy children, 4:1 is the most frequent phase-locking ratio observed during stage 1 (45%), during stage 2 sleep (57.5%) and during slow-wave sleep (62.5%), followed by 5:1 (Table 4.8). In children with SDB, the most frequent phase-locking ratio is 5:1, observed during stage 1 (32.5%), stage 2 (45%) and REM sleep (40%), followed by 4:1 (Table 4.8). However, most of the control and SDB children show a phase-locking ratio of 2:1 during awake state (controls: 70% and SDB: 72.5%).

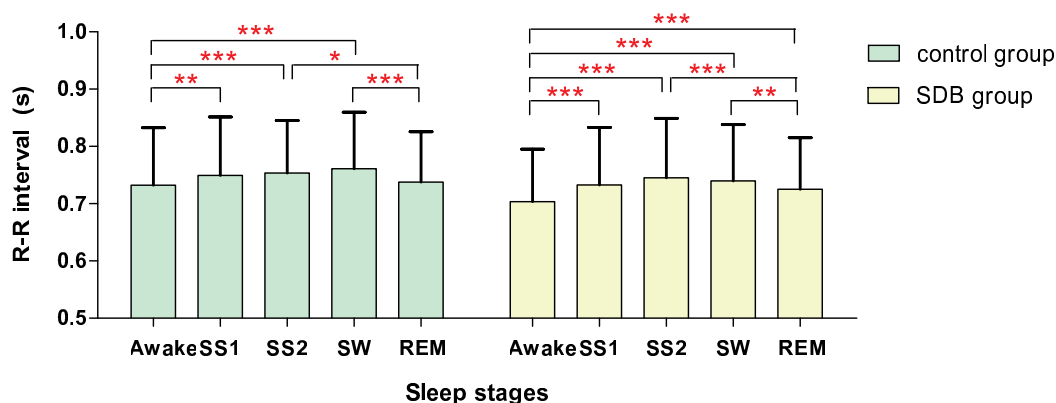


Figure 4.7. RR interval in healthy and SDB children. Group and sleep related comparison of RR interval (mean+SD) in healthy and SDB children. Here, *, ** and *** represent $p < 0.05$, $p < 0.001$ and $p < 0.0001$, respectively.

Table 4.7. Overnight polysomnography in children. Demographic data and overnight polysomnography findings in healthy and sleep disordered breathing children.

	Control <i>n</i> = 40	SDB <i>n</i> = 40
Age (yrs)	7.5 ± 2.6	7.5 ± 2.7
Male (%)	52.5	62.5
BMI percentile	60.7 ± 26.4	65.8 ± 31.9
Socio-economic status	994.9 ± 93.0	976.9 ± 93.9
Total sleep time, TST (min)	446.9 ± 37.3	425.6 ± 59.5
Stage 1 sleep (% of TST)	2.9 ± 1.5	3.3 ± 2.3
Stage 2 sleep (% of TST)	44.2 ± 6.9	42.4 ± 6.2
SW sleep (% of TST)	32.2 ± 6.3	34.6 ± 6.5
REM sleep (% of TST)	20.6 ± 3.9	19.7 ± 5.7
REM latency (min)	92.8 ± 22.0	85.8 ± 31.2
Movement time (min)	9.1 ± 4.9	8.7 ± 4.5
Wake after sleep onset time (min)	39.7 ± 30.9	53.4 ± 44.9
Periodic limb movement index (median, range)	3.3 ± 4.9 (1.2, 0-19.6)	4.9 ± 7.3 (1.3, 0-27.2)
Spontaneous arousal index	9.4 ± 2.7	8.4 ± 2.4
Respiratory arousal index (median, range)	0.4 ± 0.4 (0.3, 0-1.7)	3.2 ± 4.2 (1.1, 0-17.0)***
SaO ₂ nadir	92.9 ± 1.9	90.6 ± 5.7*
SaO ₂ desaturation index (median, range)	0.8 ± 0.8 (0.8, 0-4.9)	5.1 ± 9.4 (1.3, 0-53.1)***
Obstructive apnoea hypopnoea index (median, range)	0.1 ± 0.2 (0.1, 0-0.9)	5.0 ± 9.0 (0.9, 0-49.8)***

Here, * and *** represent $p < 0.05$ and $p < 0.001$, SDB vs. control

4.4 Results—Children

Table 4.8. Predominant phase locking ratios in children. Percentage of predominant phase locking ratios for different sleep stages in healthy and SDB children. '0' indicates no phase-locking observed for given ratio.

Phase locking ratios $m:n$	Healthy					SDB				
	Awake	SS1	SS2	SW	REM	Awake	SS1	SS2	SW	REM
2:1	70	2.5	0	0	0	72.5	15	0	0	0
3:1	7.5	10	10	10	5	2.5	2.5	2.5	2.5	0
4:1	17.5	45	57.5	62.5	37.5	12.5	27.5	32.5	37.5	22.5
5:1	2.5	30	27.5	22.5	47.5	12.5	32.5	45	35	40
6:1	2.5	12.5	5	5	10	0	17.5	17.5	25	37.5
7:1	0	0	0	0	0	0	0	2.5	0	0
5:2	0	0	0	0	0	0	0	0	0	0
7:2	0	0	0	0	0	0	0	0	0	0
9:2	0	0	0	0	0	0	0	0	0	0
8:3	0	0	0	0	0	0	0	0	0	0
11:3	0	0	0	0	0	0	0	0	0	0
14:3	0	0	0	0	0	0	0	0	0	0

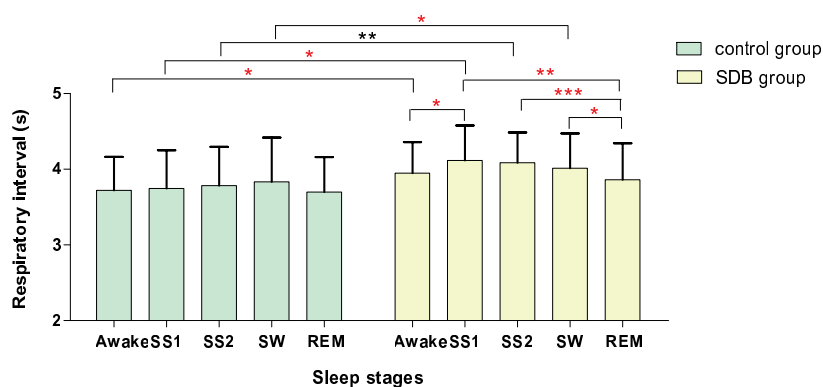


Figure 4.8. Respiratory intervals in healthy and SDB children. Group and sleep related comparison of respiratory intervals (mean+SD) in healthy and SDB children. Here, *, ** and *** represent $p < 0.05$, $p < 0.001$ and $p < 0.0001$, respectively.

4.4.3 Sleep stage effects on respiratory and RR intervals and cardiorespiratory coordination in children

There is no significant difference in mean RR interval between controls and the SDB children in any of the sleep stages. There is, however, significant shortening in average

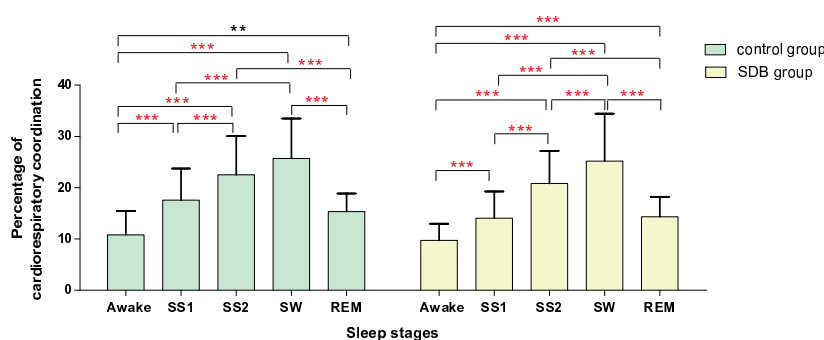


Figure 4.9. Percentage of cardiorespiratory coordination. Group and sleep related comparison of percentage of coordination (%cordn, mean+SD) in healthy and SDB children. Here, *, ** and *** represent $p < 0.05$, $p < 0.001$ and $p < 0.0001$, respectively.

RR interval during REM sleep as compared to SW sleep in control and SDB children (Controls: 0.74 ± 0.1 vs. 0.76 ± 0.1 s, $p < 0.0001$; SDB: 0.73 ± 0.1 vs. 0.74 ± 0.1 s, $p < 0.001$), see Figure 4.7. Awake state is associated with a significantly shorter RR interval as compared to stage 1, stage 2 and SW sleep (Figure 4.7).

On the other hand, children with SDB show a significant prolongation of respiratory intervals compared to controls for all the sleep stages except for REM sleep (Figure 4.8). There is also a significant shortening in mean respiratory interval during REM sleep as compared to stage 1, stage 2 and SW sleep in children with SDB (3.86 ± 0.5 vs. 4.11 ± 0.5 , 4.09 ± 0.4 and 4.01 ± 0.5 s, respectively). However, mean respiratory intervals are not significantly different between sleep stages in control group (Figure 4.8).

Percentage of cardiorespiratory coordination and the duration of coordinated of coordinated epochs is strongly associated with sleep stages. A significant increase in percentage of cardiorespiratory coordination is observed during SW sleep as compared to any other sleep stage in controls and children with SDB (SW vs. REM sleep—Controls: 25.7 ± 7.8 vs. 15.3 ± 3.5 %, $p < 0.0001$, SDB: 25.2 ± 9.2 vs. 14.3 ± 3.9 %, $p < 0.0001$), see Figure 4.9. Average duration of coordinated epochs is also higher during SW sleep as compared to stage 1 and REM sleep (SW vs. REM sleep—Controls: 8.1 ± 1.2 vs. 7.1 ± 1.4 and 6.8 ± 1.0 %, $p < 0.0001$, SDB: 8.4 ± 1.0 vs. 6.8 ± 1.6 and 7.1 ± 1.2 %, $p < 0.0001$, respectively), see Figure 4.10. However, there are no significant differences in cardiorespiratory coordination between controls and children with SDB (Figures 4.9 and 4.10).

4.5 Discussion

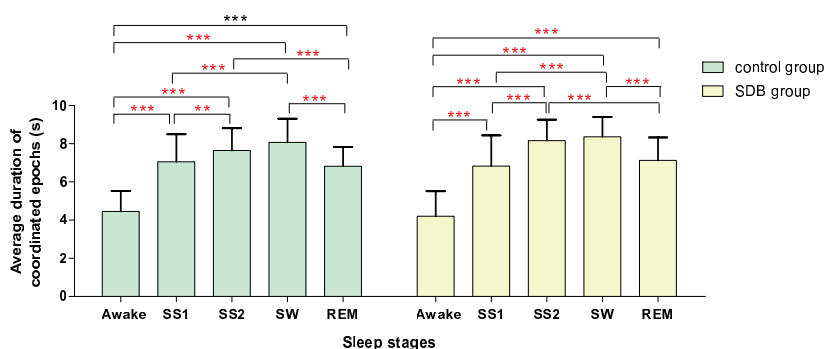


Figure 4.10. Average duration of coordinated epochs. Group and sleep related comparison of average duration of coordination (AvDurCordn, mean+SD) in healthy and SDB children. Here, *, ** and *** represent $p < 0.05$, $p < 0.001$, and $p < 0.0001$, respectively.

4.4.4 Age, BMI and gender effects on cardiorespiratory coordination in healthy children

The group of healthy children (40 controls) are further divided into sub-groups based on gender or either the median values of age (median: 7.3 yrs) or BMI z-score (median: 0.37) to study the effects of gender, age and BMI on cardiorespiratory coordination, respectively. No significant differences are observed in cardiorespiratory coordination between the corresponding sleep stages of the two groups (Figure 4.11).

4.5 Discussion

Our major findings are: (1) the phase-locking between cardiac and respiratory rhythms decreases with the severity of OSAS in adults; (2) cardiorespiratory coordination during normal sleep episodes remains unaffected in children with SDB compared to healthy controls; (3) the percentage of cardiorespiratory coordination and the duration of coordinated epochs is significantly higher during slow-wave sleep compared to REM sleep in adults with OSAS, healthy children and children with SDB; (4) 4:1 is the most frequent phase locked ratio for cardiorespiratory coordination; (5) cardiorespiratory coordination is not affected by age or BMI.

Respiratory sinus arrhythmia (RSA) is usually quantified by means of the high frequency power of HRV which is significantly influenced by breathing rate (Hirsch and

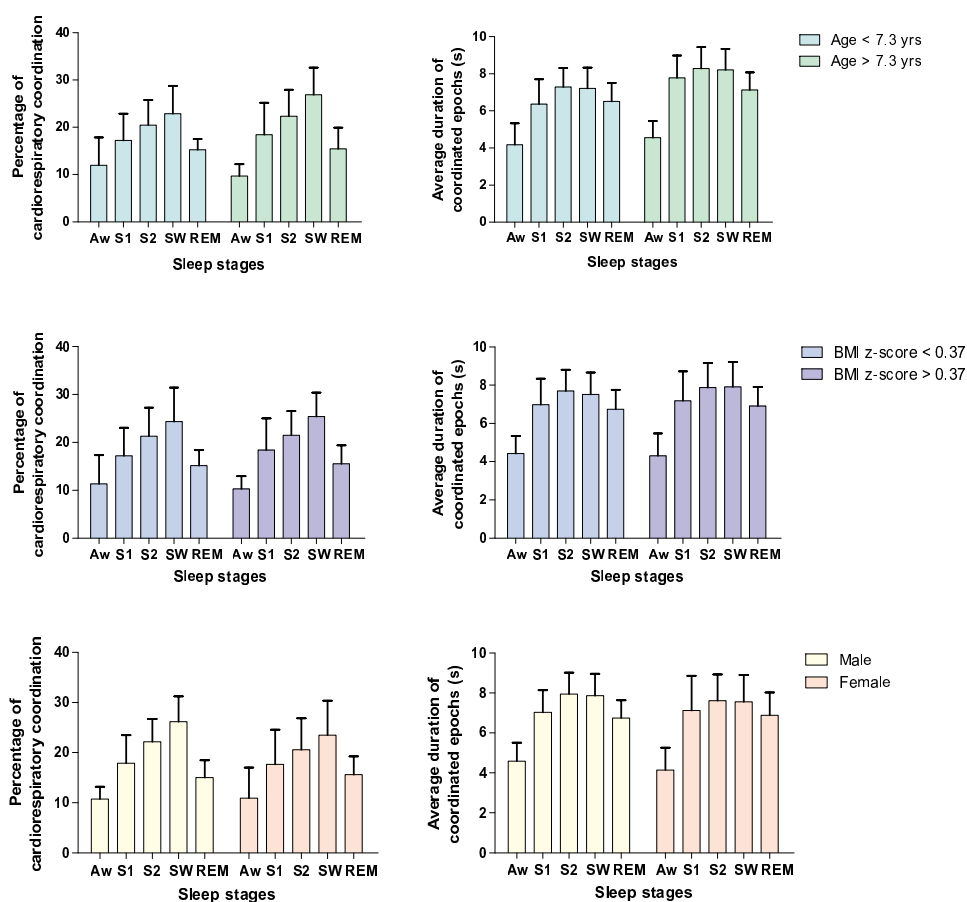


Figure 4.11. Healthy children—Age, BMI and gender effects. Comparison of cardiorespiratory coordination (mean+SD) between corresponding sleep stages of different sub-groups of healthy children. There are no significant differences in cardiorespiratory coordination between the sub-groups.

Bishop 1981, Penttila *et al.* 2001). It provides a basic surrogate, but completely lacks information on the respiratory system. We determine the effects of sleep stage and degree of OSAS on high frequency power of HRV (Fig. 4.6). Although a significant difference in high frequency power is observed between awake and stage 2 sleep, the degree of OSAS showed no effect on high frequency power. This suggests that cardiorespiratory coordination and RSA can be considered as two independent phenomena. However, according to Schafer *et al.*, cardiorespiratory coordination can be reduced by an increase in RSA (Schafer *et al.* 1998, Schafer *et al.* 1999).

The assessment of cardiorespiratory coordination using the Hilbert transform has some technical advantages over the traditional approach. Importantly, it does not require the detection of the inspiratory onset, which can be challenging, in particular when

4.5 Discussion

large amounts of data need to be processed, e.g. PSG recordings. The phase analysis technique has the advantage of tracing transitions between synchronous and non-synchronous epochs using the synchrogram plot (Rosenblum *et al.* 2001) and has been employed in earlier studies (Bahraminasab *et al.* 2008, Zhang *et al.* 2010). Although the detection of inspiratory onset is not required for the study of cardiorespiratory coordination, it has been used to determine the respiratory time period. The trade-off is that phase locking in general, independent of the phase between inspiratory onset and R wave, might not always be in line with the physiological model. Despite of this shortcoming, there is evidence that the quantification of phase-coordination might provide an useful tool to assess cardiorespiratory relationships (Pereda *et al.* 2005). Using a surrogate data approach, we find that the percentage of coordination and the average duration of coordinated epochs decrease significantly when the order of RR intervals is randomized. This suggests that cardiorespiratory coordination—as we have quantified and discussed below—indeed represents a deterministic feature of heart rate and respiration and is not a random observation. However, it also suggests that randomized RR intervals can show some coordination; up to 10% of the whole sleep duration, depending on the variability of the original RR interval series and probably also on the regularity of respiration. According to a recent study by Kenwright *et al.* (2008), the possibility of having an interaction between cardiac and respiratory oscillators is reduced by an increase in variation of respiratory frequency. It was shown that cardiorespiratory coordination is significantly decreased during exercise due to an increase in cardiac and respiratory frequencies as a result of greater demand for nutrients and oxygen from the blood by various body organs (Kenwright *et al.* 2008). From our results it appears that heart rate and/or respiration are more regular during slow-wave sleep compared to REM sleep, since cardiorespiratory coordination is higher in slow-wave sleep compared to REM sleep, even when the order of RR intervals is random.

In our study we find that phase coordination between heart and respiratory rhythms lasts for time intervals of on average 8.3 seconds in adults with no/mild OSAS and 8.1 seconds in healthy children. Although these phase-locked periods are rather short they account for up to 20% of the whole sleep duration. In accordance with a previous study (Bartsch *et al.* 2007), we observe a profound sleep stage effect on cardiorespiratory coordination. Phase-locking occurs more often and for longer periods in slow-wave sleep compared to REM sleep. This might be the effect of less regular breathing patterns in REM sleep paralleled by sympathetic cardiac activation, making both rhythms more erratic and therefore phase-locking less likely. This is in line with the fact that RSA

has shown to increase during SW sleep (Brandenberger *et al.* 2005). Note that REM sleep, characterized by irregular and high-frequency waves in the electroencephalogram is associated with a lack of synchrony between neuron firing rates, possibly due to desynchronized nervous activity (Guyton and Hall 2006, Gottesmann 1999).

It has been suggested by Hamann *et al.* (2009) that cardiorespiratory coordination can be observed as long as the noise from higher brain regions, which affects the cardiac and respiratory oscillators, is uncorrelated. However, during REM sleep, when the higher brain regions are more active, long-term correlated noise might be imposed on the two oscillators and thereby causing a reduction in the cardiorespiratory coordination (Hamann *et al.* 2009). It seems probable that the decrease in the amount of phase-locking between the cardiac and respiratory signals during REM sleep is caused by the desynchronized activity of the nervous system. Some of the earlier studies have also found changes in heart rate with the change in sleep stages (Snyder *et al.* 1964, Penzel *et al.* 2003, Nalivaiko *et al.* 2007). However, in this study, significant changes in RR intervals with sleep stages were only observed in healthy and SDB children but not adults. As almost one-third of our adult study group consisted of patients with heart disease their medication might partly explain the different heart rate behaviour.

In our study cardiorespiratory coordination is neither affected by age nor by BMI in adults as well as in children. These results are consistent with an earlier study by Bartsch *et al.* (2007). However, in a recent study by Shiogai *et al.* (2010), it was reported that although cardiorespiratory coordination showed no correlation with age for males, it significantly increased with age for females. A different approach for detection of phases with the Hilbert transform, used in this study, compared to marked events method used for cardiac phase detection by Shiogai *et al.* (2010), might be a possible cause of the variation in results. Similarly, the low sampling frequency and filtering approach to the respiratory signal used in this study could also be the contributing factors for the differences. According to another study, autonomic modulation of heart rate diminishes with age (Umetani *et al.* 1998). Interestingly, we have observed no significant effect of age on cardiorespiratory coordination, suggesting that there is little association between HRV and the phase-locking between heart and respiratory rhythms. Also, in our study, a positive correlation between age and RR interval is unexpected as heart rate (reciprocal of RR interval) was reported to increase with age (Penzel *et al.* 2003, Nalivaiko *et al.* 2007).

4.5 Discussion

The BMI has an effect on OSAS and is also associated with an increased cardiac sympathetic tone (Ferguson *et al.* 1995, Busetto *et al.* 2005). Patients with higher BMI are more likely to be affected by OSAS. However, in our study, although OSAS has an effect on the phase locking between heart rate and respiration, BMI shows no association with cardiorespiratory coordination. On the other hand, the respiratory time period has a negative correlation with BMI.

Autonomic modulation of heart rate is altered in OSAS patients (Narkiewicz *et al.* 1998). Our results indicate a significant increase in heart rate and respiratory rate in patients with moderate and severe OSAS compared to patients with mild or no OSAS. This increase in heart rate might be a result of a decrease in cardiac vagal outflow, of an increase in cardiac sympathetic outflow or both (Narkiewicz and Somers 2003). On the other hand cardiorespiratory coordination decreased significantly with the severity of OSAS. This suggests that the amount of phase locking is influenced by autonomic control, which is affected by the repetitive obstructive episodes in OSAS patients. Measures of cardiorespiratory coordination seem to be more sensitive to OSAS than conventional HRV metrics alone, since they incorporate both, respiratory and cardiac domains.

However, after removing sleep disordered-breathing related events and spontaneous arousal epochs, no significant differences in cardiorespiratory coordination are observed between healthy children (controls) and children with SDB. This would suggest that the coordination between cardiac and respiratory cycles in patients with OSAS is mainly affected by OSAS related events but remains almost unaffected during normal quiet sleep episodes.

The location of respiratory signal recording (abdomen vs. chest) might potentially influence cardiorespiratory coordination analysis. While the abdominal and thoracic excursions are approximately in phase during normal breathing, a higher difference in phase is typically observed during airway obstruction. It has been even suggested to use the phase difference between the two signals to detect sleep apnea (Varady *et al.* 2003). For the purpose of this study we have primarily used the respiratory signal obtained from the abdominal transducer. However, our analyses indicate that respiratory signals derived from the thorax can be equally used. There is no significant difference in the mean percentage of coordination for different AHI groups and sleep stages. Further, the sampling frequency has an influence on the accuracy of measurement of R-peaks, with a significant decrease in the amplitude of R-peak observed at

a sampling rate of 125 Hz, compared to 500 Hz, but with no significant influence on the RR interval (Pizzuti *et al.* 1985). The ECG sampling frequency of adults for this study was relatively low (128 Hz). This, together with the technique used for quantifying synchronization and the short intervals of synchronized epochs considered as signature for cardiorespiratory coordination, could have influenced our results.

4.6 Chapter summary

In this Chapter we have investigated cardiorespiratory coordination in children and adults suffering from obstructive sleep apnea syndrome. We have illustrated that OSAS (mainly OSAS related events) perturbs the phase locking between cardiac and respiratory rhythms. It thus appears that the assessment of cardiorespiratory coordination may provide an ECG based screening tool for OSAS.

Although the synchrogram technique—an established method for evaluating phase-locking between cardiac and respiratory oscillators—has been able to detect and show significant changes in cardiorespiratory coordination in patients suffering from OSAS, a slight modification by introducing an additional adaptive delay in the cardiac oscillator can improve the performance of the synchrogram technique, which will be discussed in the next Chapter.

Chapter 5

Time delay correction of the synchrogram technique

THE cardiorespiratory synchrogram, a graphical tool based on the stroboscopic technique, is an established method for evaluating phase-locking between cardiac and respiratory oscillators. In the original method, the phase of the respiratory oscillator is observed at the instants of time when the phase of the cardiac oscillator attains a certain value. In this Chapter, we introduce an additional adaptive delay in the cardiac oscillator based on the maximisation of the cross-correlation or symbolic coupling traces between the phases of respiration and the delayed RR intervals. We then investigate phase coordination in thirteen normal subjects (5 males, 8 females; age: 19-24 years) for different body postures. Cardiorespiratory coordination is observed to be significantly reduced in the upright position (supine vs. upright: 11.9 ± 5.1 vs. 6.9 ± 3.6 , $p < 0.05$). Compared to the original algorithm we observe an increase in the detection of average cardiorespiratory coordination (supine original vs. delay: 11.9 vs. 18.9 %), together with a decrease in standard deviation of the percentage of coordination in all the subjects, after introducing the heart rate delay (supine original vs. delay: 5.1 vs. 4.4 %). In conclusion, the performance of the synchrogram technique is improved by including an adaptive delay in the cardiac oscillator.

5.1 Introduction

It has previously been reported that delays in coupling between two systems can have significant influence on their dynamical behaviour (Niebur *et al.* 1991, Yeung and Strogatz 1999, Reddy *et al.* 2000). From the point of view of measurement it has been demonstrated that higher coordination between two time series of delayed systems can be observed by introducing a delay, e.g. a time-shifted synchronization index (Rybski *et al.* 2003).

Takahashi *et al.* (2000), Gilad *et al.* (2005), Takahashi *et al.* (2005) and Tzeng *et al.* (2009) have shown that there exists a delay between phase of respiration and RR interval, which is further affected by body posture (Gilad *et al.* 2005). Alvarez-Ramirez *et al.* (2009) suggested that the prolongation of phase delay in RR time series can be used to discriminate healthy subjects from patients with congestive heart failure. However, phase delay has never been considered in the synchrogram method—a standard visual tool for the detection of cardiorespiratory coordination.

This Chapter introduces a modification of the synchrogram method that incorporates an adaptive delay. The modified algorithm is validated by comparing its performance with that of the original method, investigating the phase-locking between cardiac and respiratory rhythms during postural changes in normal subjects.

5.2 Methods

5.2.1 Subjects / Experimental protocol

Thirteen healthy subjects (5 males, 8 females) participated in this study. The age of the subjects ranged between 19-24 years. The study conformed to the principles outlined in the Declaration of Helsinki and was approved by the institution's human research ethics committee. Subjects gave informed consent.

The protocol included 10 minutes of recording for different body postures. A group of eight subjects (4 males, 4 females) was investigated in the supine position and while standing during spontaneous normal breathing. A second group of five subjects (1 male, 4 females) underwent graded head-up tilt test at angles: 0, 30 and 60° during controlled metronomic breathing at 15 bpm. The subjects were instructed not to speak and to remain absolutely motionless during the recording.

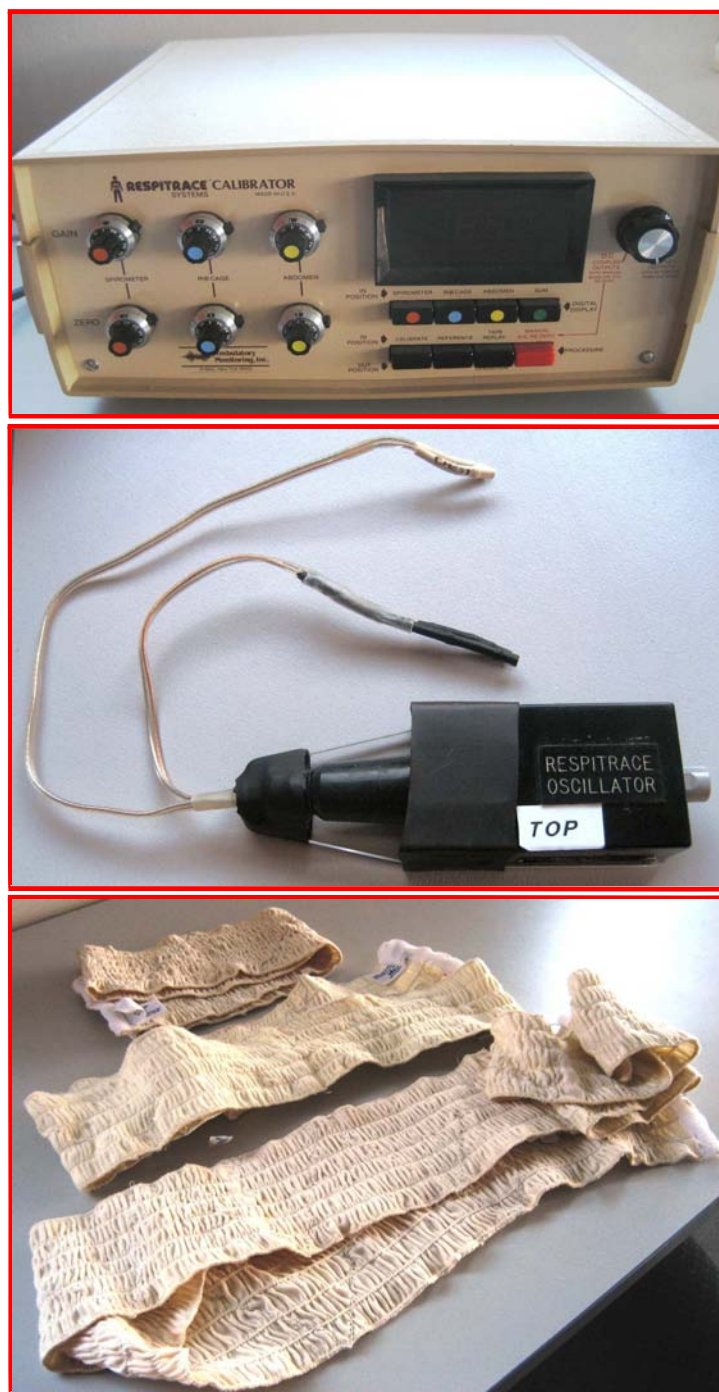


Figure 5.1. Respirace. Respirace calibrator, oscillator and impedance belts for recording respiratory signals.

Herein, ECG (leads I and II) and respiratory signals (from abdomen impedance belts recorded using Respirace, see Fig. 5.1) were sampled at 1 kHz and recorded using a PowerLab data acquisition system (ADInstruments, Sydney, Australia), see Fig. 5.2, and the ChartPro 6.0 software (ADInstruments, Sydney, Australia).

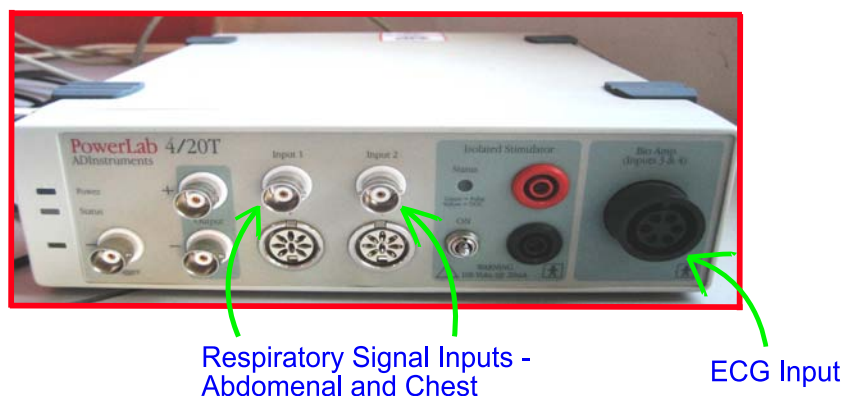


Figure 5.2. PowerLab data acquisition system. PowerLab data acquisition system used for ECG and respiratory signals.

To further validate our results we studied the data from 213 patients with suspected obstructive sleep apnea syndrome (OSAS) discussed in Chapter 4, Section 4.2.2.

5.2.2 Processing of ECG and respiratory signal

The ECG and respiratory signals are processed as described in Chapter 1, Sections 1.4.1 and 1.4.2. The RR time series are visually scanned for artifacts. Although the R-peaks have been correctly identified, we have encountered a few ectopic beats that are manually replaced with the average RR interval calculated from the beats prior to and after the ectopy. The respiratory signals are low-pass filtered at 1.0 Hz to remove noise.

5.2.3 Cardiorespiratory coordination analysis

We studied the coordination between cardiac and respiratory cycles using cardiorespiratory coordination analysis described in Chapter 1.1, Section 1.7.2.

We employ three parameters for characterising cardiorespiratory coordination: Firstly, we calculate the percentage of coordination by adding up the time of all coordinated epochs observed and then dividing it by the total duration of the segments. Secondly, we measure the average duration of all coordinated epochs by calculating the arithmetic mean of the durations of coordinated epochs. Further, the phase locking ratio for each coordinated epoch is recorded.

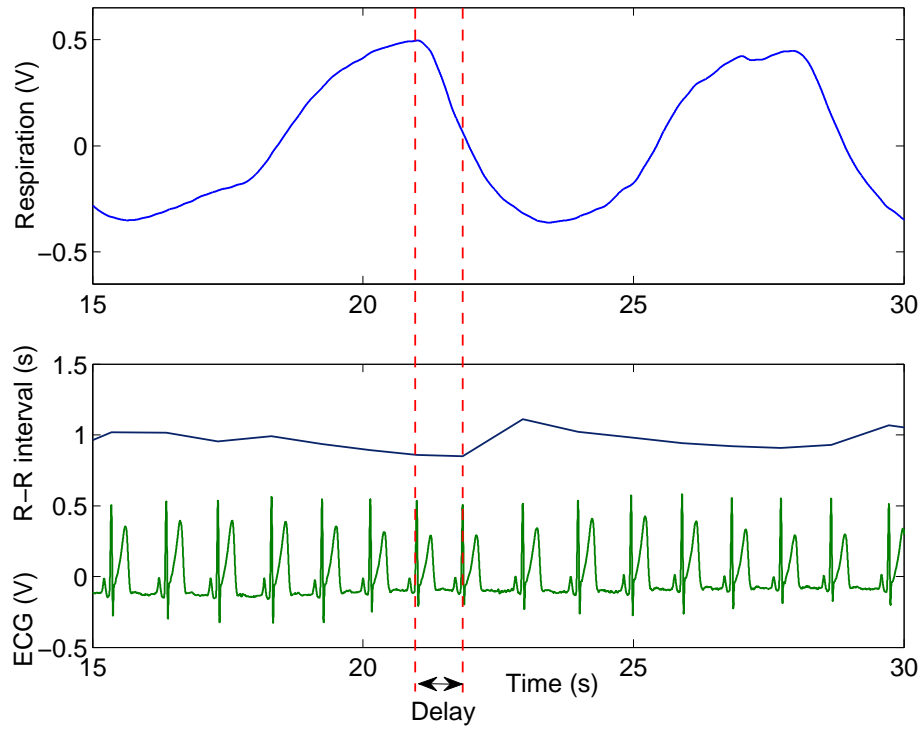


Figure 5.3. Time delay between ECG and respiration. Respiratory signal (top panel) and ECG signal together with RR interval (bottom panel). The delay is calculated as the time between the expiratory onset of respiration and the start of the increase in RR interval.

5.2.4 Calculation of time delays for enhanced detection of coordination

Cross-correlation function

The most common and widely used tool for the calculation of time delay is the cross-correlation function. The linear association between the respiratory phases, $\phi_r(k)$, and RR-intervals, RR, can be assessed by determining the Pearson correlation coefficients for the correlation between RR and $\cos \phi_r(k)$, $r_{RC} = c(\text{RR}(i), \cos \phi_r(k_i))$, RR and $\sin \phi_r(k)$, $r_{RS} = c(\text{RR}(i), \sin \phi_r(k_i))$, and $\cos \phi_r(k)$ and $\sin \phi_r(k)$, $r_{CS} = c(\cos \phi_r(k_i), \sin \phi_r(k_i))$, and subsequently the angular-linear correlation coefficient, r_{RP} , defined as (Zar 1999)

$$r_{RP} = \sqrt{\frac{r_{RC}^2 + r_{RS}^2 - 2r_{RC}r_{RS}r_{CS}}{1 - r_{CS}^2}}. \quad (5.1)$$

The parameters r_{RC} , r_{RS} and r_{CS} are substituted by $r'_{RC} = c(\text{RR}(i+\tau), \cos \phi_r(k_i))$, $r'_{RS} = c(\text{RR}(i+\tau), \sin \phi_r(k_i))$, $r'_{CS} = c(\cos \phi_r(k_i), \sin \phi_r(k_i))$ to introduce a delay of τ R-peaks,

where $\tau = -6, -5, \dots, 0, \dots, +5, +6$ beats. The time delay between respiration and heart beats is illustrated in Figure 5.3. Circular statistics analysis is performed using the CircStat MATLAB[®] toolbox and codes described in Berens (2009).

Symbolic coupling traces

The method of symbolic coupling traces is based on the analysis of structural patterns through transformation of time series into discretized symbols. From the vectors of the RR time series and the series of respiratory phases ϕ_r at the instants of R-peaks, RP, two symbolic sequences, s^{HR} (HR denoting the heart rate) and s^{RP} , were formed using the transformation rule below, based on the differences between successive RR intervals and R-instant respiratory phases, respectively,

$$s_i^{\text{HR}} = \begin{cases} 0 & \text{if } \text{RR}_{i+1} - \text{RR}_i > 0, \\ 1 & \text{if } \text{RR}_{i+1} - \text{RR}_i < 0, \\ 2 & \text{if } \text{RR}_{i+1} - \text{RR}_i = 0. \end{cases} \quad (5.2)$$

$$s_i^{\text{RP}} = \begin{cases} 0 & \text{if } |\text{RP}_{i+1} - \text{RP}_i| > 0, \\ 1 & \text{if } |\text{RP}_{i+1} - \text{RP}_i| < 0, \\ 2 & \text{if } |\text{RP}_{i+1} - \text{RP}_i| = 0. \end{cases} \quad (5.3)$$

Using the symbol vectors s^{HR} and s^{RP} , we constructed words of length 3, w^{HR} and w^{RP} —each containing 3 successive symbols. Subsequently, the word distribution density as described in (Baumert *et al.* 2002) was estimated after introducing delays, τ ($\tau = -6, -5, \dots, 0, \dots, +5, +6$ beats), in R-peaks—providing probabilities that a certain word in the series w^{HR} at time $(t + \tau)$ appears in w^{RP} at time t (Wessel *et al.* 2009).

The negative delays in the RR time series were achieved by shifting the respiratory phases while preserving the original RR intervals. For our analysis we selected the τ -delayed RR time series that either provided the highest correlation between the delayed RR intervals and respiratory phases or showed highest probability of word similarity between the two series using symbolic coupling traces. Subsequently, the parameters for quantifying the cardiorespiratory coordination were obtained after replacing the original with the delayed RR time series, i.e. by shifting the appropriate R-peaks based on the delay, τ .

Table 5.1. Respiratory intervals. Mean values (\pm SD) of the respiratory intervals during supine and upright postures in eight subjects.

Subjects	Respiratory Interval (s)	
	Supine	Upright
Subject 1	2.69 \pm 0.2	3.24 \pm 0.1
Subject 2	3.91 \pm 0.2	4.37 \pm 0.2
Subject 3	5.95 \pm 0.7	5.29 \pm 0.2
Subject 4	3.83 \pm 0.4	4.01 \pm 0.1
Subject 5	4.71 \pm 0.6	5.09 \pm 0.5
Subject 6	3.64 \pm 0.7	3.79 \pm 0.5
Subject 7	4.37 \pm 0.3	4.98 \pm 0.2
Subject 8	3.48 \pm 0.1	3.57 \pm 0.3

5.2.5 Statistical analysis

GraphPad Prism version 5.01 for Windows (GraphPad Software, San Diego California USA, www.graphpad.com) is used for statistical analysis. The measures of cardiorespiratory coordination obtained with the original synchrogram technique for different body postures are compared to those obtained with the modified technique using non-parametric repeated measure analysis of variance (Wilcoxon matched pairs test, Friedman test and Dunn's multiple comparison test). Values with $p < 0.05$ are considered statistically significant. Data are expressed as mean \pm standard deviation (SD).

5.3 Results

5.3.1 Effect of changes in body posture on RR interval

The change in body posture from supine to upright is associated with significant shortening of RR intervals (0.87 ± 0.07 vs. 0.67 ± 0.05 s respectively, $p < 0.001$). Increase in head-up tilt angles from 0 to 30 and 60° also show significant shortening in R-R intervals (0 vs. 30 and 60°: 0.90 ± 0.06 vs. 0.83 ± 0.05 and 0.71 ± 0.05 s, $p < 0.01$ and $p < 0.001$, respectively).

5.3 Results

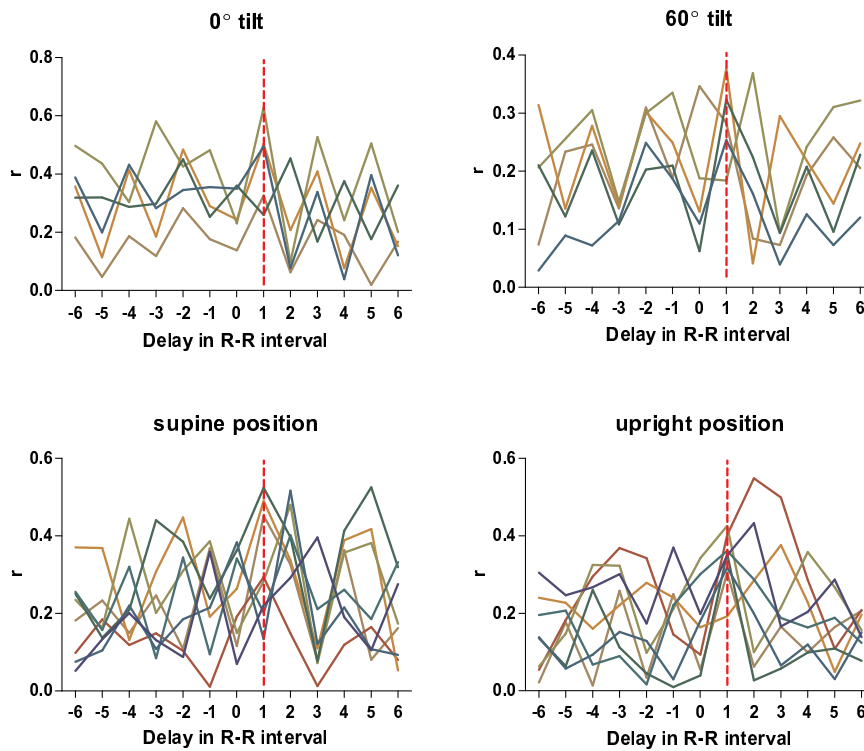


Figure 5.4. Correlation plots. Correlation between respiratory phases and delayed RR time series. In most cases, the highest correlation was observed after introducing a delay of one R-peak in the RR time series.

5.3.2 Effect of changes in body posture on respiratory interval

In spontaneously breathing subjects, the average respiratory interval increase with the change in body posture from supine to upright for all but one subject, in whom a slight decrease in respiratory interval is observed (subject 3: supine vs. upright: 5.95 ± 0.7 vs. 5.29 ± 0.2 s), see Table 5.1. Due to this variation in one subject, the overall difference in respiratory intervals with the change in body posture fails to reach statistical significance.

5.3.3 Calculation of time-delay using cross-correlation analysis and symbolic coupling traces

The cross-correlation functions between respiratory phases and RR intervals and the probabilities of simultaneous words in both the series obtained with delays in the range of -6 to +6 are calculated for all the subjects and plotted as shown in Figures 5.4 and 5.5,

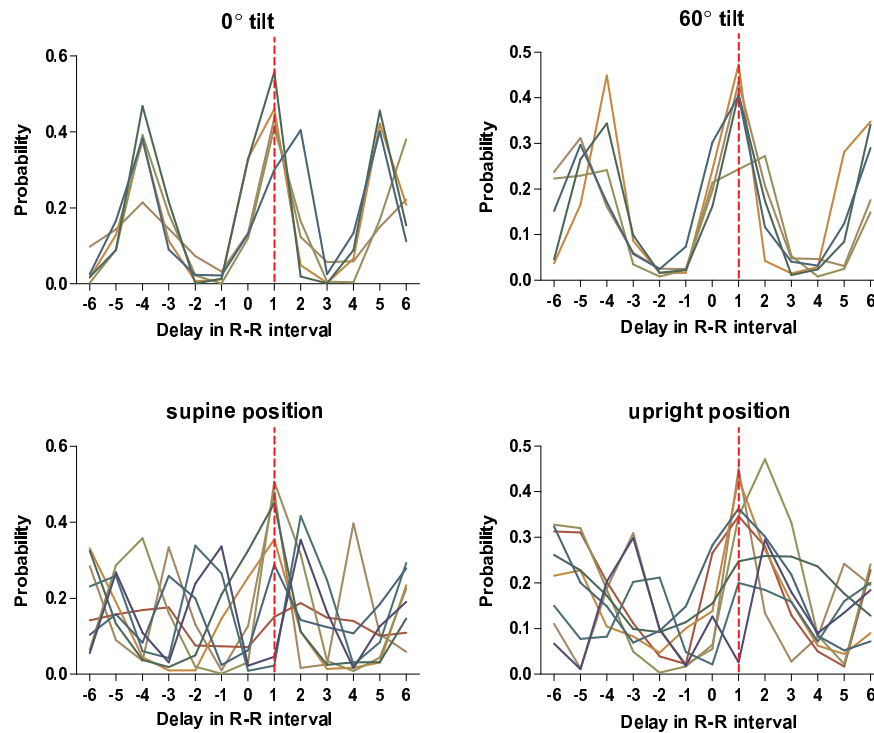


Figure 5.5. Probability plots. Probability of occurrence of similar words from the series of respiratory phases and delayed RR time series. In most cases, the highest probability was observed after introducing a delay of one R-peak in the RR time series.

respectively. From a total of 31 analysed states (5 subjects \times 3 tilt positions + 8 subjects \times 2 body positions), the highest correlation (max. $r = 0.63$, $p < 0.0001$) between the values of RR intervals and respiratory phases is mostly observed for $\tau = +1$ beat (61.3%) (i.e. one positive delay in R-peak), followed by $\tau = +2$ beats (25.8%), while the highest probability (max. 0.56) of concurrent/synchronous words is mostly achieved for $\tau = +1$ (67.7%) and +2 (25.8%) beats.

5.3.4 Percentage of cardiorespiratory coordination

Original synchrogram

The coordination between cardiac and respiratory cycles significantly decrease with the change in body posture from supine to upright (11.9 ± 5.1 vs. 6.9 ± 3.6 %, $p < 0.05$) as shown in Figure 5.6 during spontaneous breathing. Increase in head-up tilt angles during controlled breathing also show a significant decrease in cardiorespiratory coordination (0 vs. 60°: 16.9 ± 4.4 vs. 11.8 ± 4.0 %, $p < 0.05$) as shown in Figure 5.6.

5.3 Results

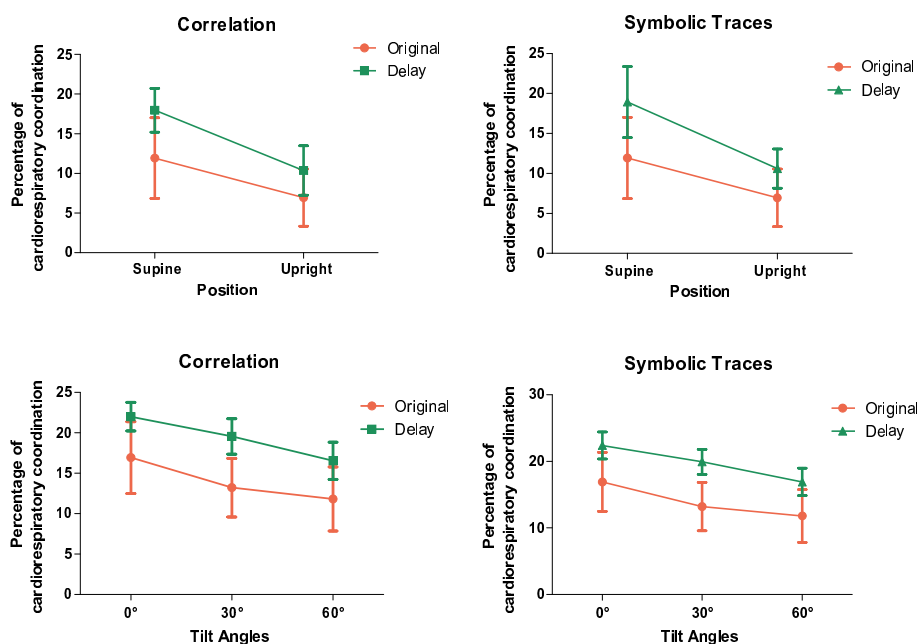


Figure 5.6. Percentage of coordination for different body positions. Percentage of coordination using original and delayed RR intervals (calculated using cross-correlation and symbolic traces) for supine and upright postures and different body tilt-angles. Higher tilt-angles showed a lower percentage of coordination. By appropriate delaying of the RR time series, an increase in the overall percentage of coordination was observed together with a decrease in standard deviation. The lines connecting the points are notional for illustrative purposes only, for grouping pairs of points. The lines are not intended for describing a linear relationship.

Modified synchrogram

After choosing the delayed RR interval that provided either the highest correlation with the respiratory phases or the highest probability of concurrent/synchronous words, cardiorespiratory coordination show a relative increase with a reduction in standard deviation when considering all subjects (supine position—mean using original data vs. mean using delayed data through analysis of cross-correlation and symbolic traces: 11.9 vs. 18.0 %, $p < 0.05$ and 18.9 %, $p < 0.05$, respectively, and SD: 5.1 vs. 2.8 %, $p < 0.05$ and 4.4 %, $p < 0.05$, respectively) as seen in Figure 5.6.

5.3.5 Average duration of coordinated epochs

Original synchrogram

The average duration of coordination between cardiac and respiratory cycles significantly decrease with the change in body posture from supine to upright during spontaneous breathing (7.5 ± 3.1 vs. 5.0 ± 2.1 s, $p < 0.01$) as shown in Figure 5.7. Increase in head-up tilt angles during controlled breathing also show a significant decrease in the average duration of coordinated epoch (0 vs. 60°: 8.6 ± 3.4 vs. 5.9 ± 2.3 s, $p < 0.05$) as shown in Figure 5.7.

Modified synchrogram

The delay in RR interval based on either the highest correlation between the delayed RR time series and respiratory phases or the highest probability of synchronous words cause an overall, but not significant, increase in average duration of coordination (supine position—mean using original data vs. mean using delayed data through analysis of cross-correlation and symbolic traces: 7.5 vs. 9.2 s, $p > 0.05$ and 9.2 s, $p > 0.05$, respectively, and SD: 3.1 vs. 2.3 s, $p > 0.05$ and 2.3 s, $p > 0.05$, respectively) as shown in Figure 5.7.

5.3.6 Phase-locking ratio

The different phase-locking ratios observed in the subjects include 2:1, 3:1, 4:1, 5:1, 6:1, 7:2 and 9:2. The most frequent phase locking ratios observed in the supine posture during spontaneous breathing are 3:1 (3 subjects), 4:1 (3 subjects) and 5:1 (2 subjects), and during metronomic breathing 4:1 (4 subjects) and 9:2 (1 subject), as seen in Table 5.2. The change in posture from supine to upright and higher tilt angles show slight variations in the phase-locking ratios (Table 5.2). The phase-locking ratios observed with the modified synchrogram technique also varied but are not notably different from those observed with the original method (Table 5.2).

5.3.7 Cardiorespiratory coordination in patients with OSAS using modified synchrogram

Using the modified synchrogram, there is a slight but significant increase in cardiorespiratory coordination in patients with OSAS during night-time sleep (see Figure 5.8).

5.4 Discussion

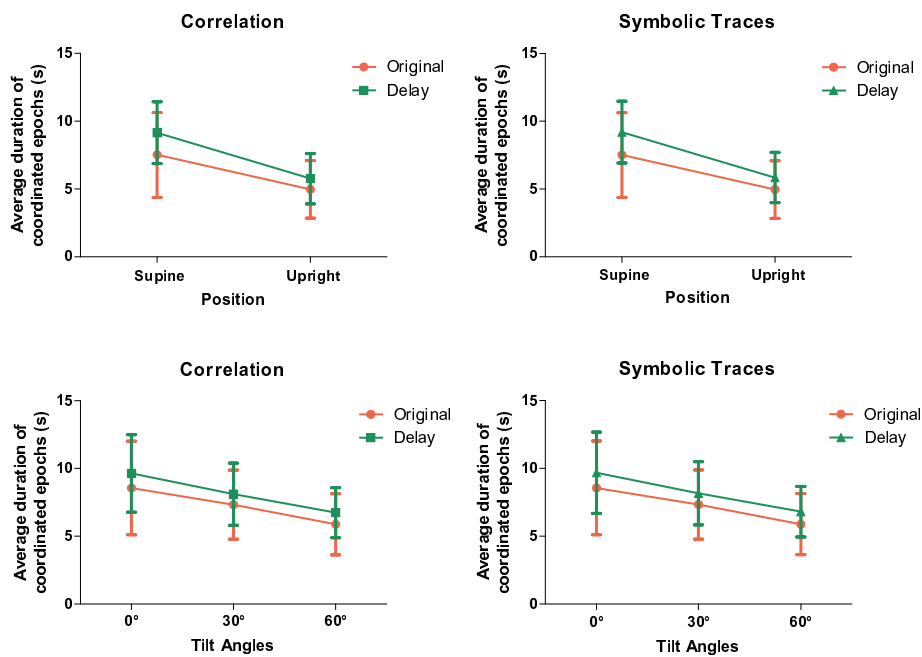


Figure 5.7. Average duration of coordination for different body positions. Average duration of coordinated epochs using original and delayed RR intervals for different body postures and tilt-angles. Higher tilt-angles cause a significant decrease in the average duration of coordinated epochs. However, delaying of RR time series has no significant effect on the duration of coordination. The lines connecting the points are notional for illustrative purposes only, for grouping pairs of points. The lines are not intended for describing a linear relationship.

5.4 Discussion

The major findings of this study are: (1) the detection of epochs of cardiorespiratory coordination can be increased by appropriate delaying of RR intervals, (2) a RR interval delay of one was required to maximise the detection process in most cases, and (3) the percentage and average duration of cardiorespiratory coordination decreases with the change in body posture from supine to upright.

Our results show that the upright posture, as compared to supine, causes a shortening in the RR intervals with no significant change in respiratory intervals, which is consistent with the findings by Gilad *et al.* (2005). It is well known that a postural change in human body, from upright to supine, causes an increase in vagus nerve activity and a decrease in sympathetic nerve activity (Robinson *et al.* 1966, Rowell 1993, Buchheit *et al.* 2009).

Table 5.2. Frequent phase locking ratios. Most frequent phase locking ratios using original and modified synchrograms in two groups of subjects for different body positions.

(a) Group 1

Subjects	Supine		Upright	
	Original	Modified	Original	Modified
Subject 1	3:1(59%)	3:1(63%)	4:1(75%)	4:1(83%)
Subject 2	3:1(60%)	4:1(70%)	2:1(70%)	3:1(87%)
Subject 3	4:1(44%)	4:1(40%)	5:1(56%)	4:1(34%)
Subject 4	5:1(37%)	5:1(47%)	6:1(50%)	5:1(50%)
Subject 5	4:1(65%)	3:1(75%)	5:1(60%)	5:1(67%)
Subject 6	3:1(40%)	3:1(47%)	4:1(75%)	4:1(78%)
Subject 7	4:1(55%)	4:1(67%)	2:1(50%)	3:1(50%)
Subject 8	5:1(50%)	5:1(45%)	6:1(36%)	6:1(55%)

(b) Group 2

Subjects	0° tilt		30° tilt		60° tilt	
	Original	Modified	Original	Modified	Original	Modified
Subject 1	4:1(60%)	5:1(90%)	2:1(75%)	3:1(75%)	6:1(50%)	4:1(40%)
Subject 2	9:2(65%)	9:2(50%)	5:1(80%)	5:1(67%)	5:1(83%)	5:1(67%)
Subject 3	4:1(79%)	4:1(67%)	5:1(94%)	5:1(95%)	6:1(96%)	6:1(93%)
Subject 4	4:1(91%)	4:1(89%)	5:1(60%)	9:2(67%)	5:1(83%)	5:1(89%)
Subject 5	4:1(75%)	4:1(80%)	2:1(40%)	3:1(45%)	2:1(67%)	2:1(75%)

There are mechanical effects of posture on both the respiratory and cardiovascular systems. Passive head up tilt (HUT) greater than 60° increases minute ventilation and tidal volume and increases functional residual capacity (Chadha *et al.* 1985, Loeppky and Luft 1975, Miyamoto *et al.* 1982, Yoshizaki *et al.* 1998, Chang *et al.* 2005). The mechanisms are not clear, but it has been suggested that descent of the diaphragm may alter the point at which tidal breathing occurs on the volume pressure curve (Navajas *et al.* 1988), leading to an increase in lung compliance. This is consistent with the observation that moving from a supine to a sitting posture produces a progressive

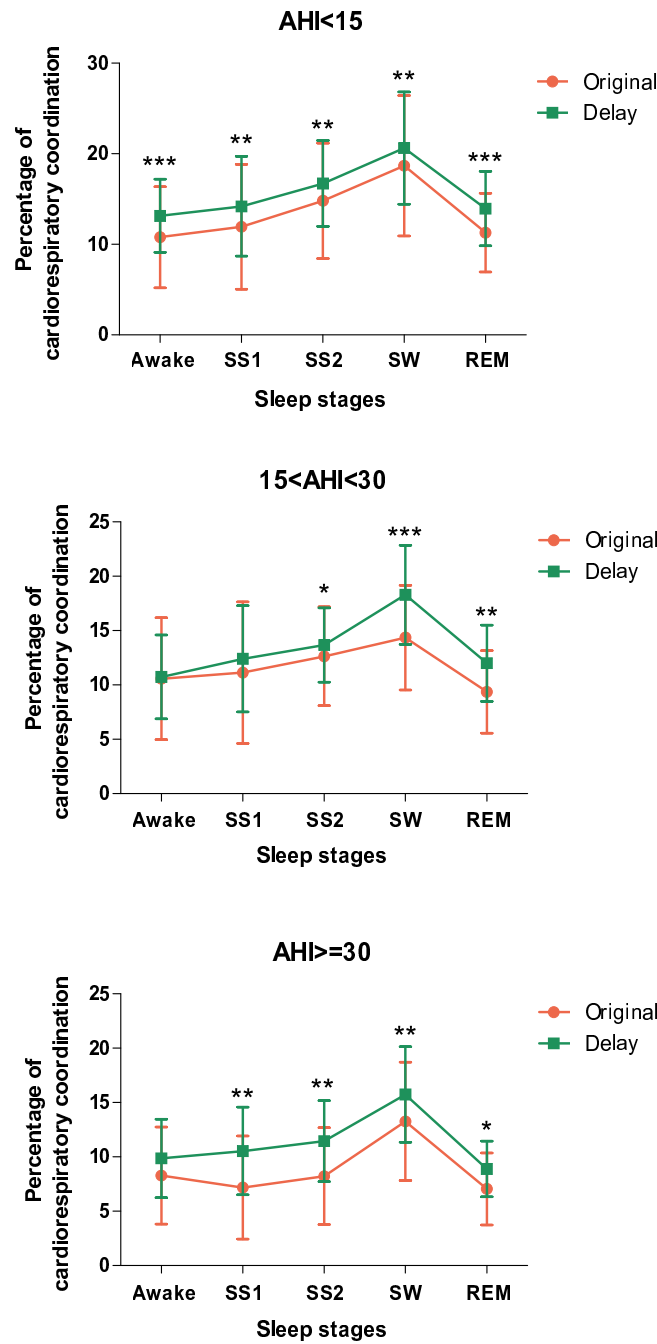


Figure 5.8. Percentage of coordination in patients with OSAS. Percentage of cardiorespiratory coordination using original and delayed RR intervals in patients with mild, moderate and severe OSAS. Severe OSAS show a lower percentage of coordination. By appropriate delaying of RR time series, an increase in the overall percentage of coordination is observed. In some cases there is a decrease in standard deviation. Here, *,** and *** indicate $p < 0.05$, $p < 0.01$, and $p < 0.0001$, respectively.

reduction of rib cage displacement and a concomitant increase of abdominal contribution to breathing mechanics (Sharp *et al.* 1975, Vellody *et al.* 1978, De Troyer 1983, Butler *et al.* 2001). However, effects on tidal volume and ventilation for passive HUT, as opposed to active standing, tend to be minor. Romei *et al.* (2010) showed that absolute tidal volume and minute ventilation were increased when sitting without back support (by about 20% for each), but these effects were not seen when the values were normalised to subject body weight, and no change was seen with 80° sitting with back support. In this study, respiratory rate is not changed by posture. Importantly, these effects appear to be wholly mechanical—no change in neural drive to the respiratory muscles has been demonstrated following passive tilting or active standing (Butler *et al.* 2001). Although many studies have been done on the effect of posture on heart rate variability (HRV), demonstrating, for example a phase shift in respiratory sinus arrhythmia (RSA) with posture (Kotani *et al.* 2008), no studies have examined the effect of posture on cardiorespiratory phase coordination.

In this study, a significant decrease in cardiorespiratory coordination is observed in upright and higher tilt-angled postures as compared to a supine posture. Also, there are variations in the average phase-locking ratio with the change in body posture. Cysarz *et al.* (2004b) reported that a strong cardiorespiratory coordination can be obtained through a breathing pattern caused by poetry recitation as compared to controlled breathing. Our results suggest that autonomic nerve activity has an influence on cardiorespiratory coordination. This observation has further been supported by a recent study (Kabir *et al.* 2009).

The analysis of physiological systems are complicated as they are highly non-linear and non-stationary and are usually contaminated with intrinsic and measurement noise. As a result, the conventional techniques such as linear cross-correlation analysis often prove to be inadequate for characterizing their complex dynamics (Hoyer *et al.* 1998b, Rosenblum *et al.* 1998). Symbolic coupling traces analysis, which is based on simplified description of the system's dynamics through symbolic representation by employing a coarse-graining procedure (Baumert *et al.* 2002, Baumert *et al.* 2005), has been suggested to be more reliable due to its insensitivity towards noise and non-stationeries compared to cross-correlation analysis (Wessel *et al.* 2009). By employing cross-correlation functions and symbolic coupling traces, we find that the highest correlation between RR intervals and respiratory phases is obtained through a delay of usually one heart beat in RR time series. The delay in heart rhythm in regard to the respiratory cycle

5.5 Chapter summary

is apparent in the example displayed in Fig. 5.3. Rybski *et al.* (2003) suggested that the coordination between two time-delayed systems can be increased by introducing a synchronization index into the phase synchronization method. The method based on synchronization index has been compared with the traditional cross-correlation technique and also with a technique based on a model reconstruction and suggested to be the most efficient technique (Cimponeriu *et al.* 2004).

A recent study has also reported the existence of delay between the respiratory phase and RR interval pattern (Gilad *et al.* 2005). Consequently, we add the appropriate delay in RR time series for the cardiorespiratory coordination analysis which show a significant increase in the detection of the phase-locking between cardiac and respiratory rhythms and yields more consistent results. However, there is no significant change in the average duration of coordination or phase-locking ratio after the delay. This would suggest that the cardiac and respiratory cycles are usually phase-locked within short intermittent periods (Hoyer *et al.* 1997, Schafer *et al.* 1998). Although the physiological origin of cardiorespiratory coordination still needs to be explored in more detail, the increase in detection of the interaction between cardiac and respiratory rhythms after incorporating the delay in R-peaks could be explained by the possible involvement of mechanisms such as the well known respiratory influence on cardiac timing known as respiratory sinus arrhythmia and influences of heart on respiratory timing through the baroreceptor nerves (Tzeng *et al.* 2007).

From a statistical point of view the study is sufficiently powered to detect a significant increase in cardiorespiratory coupling with the phase delay method compared to the standard method. This study is able to show this effect in two independent study groups under different conditions (active standing vs. tilt; spontaneous breathing vs. metronomic breathing) and also in a large cohort of patients with OSAS.

5.5 Chapter summary

In this Chapter, we have shown that a change in body posture is associated with the changes in cardiorespiratory coordination in humans and there exists a delay in heart rhythm in regard to the respiratory cycle which should be taken into account during the study of phase coordination between cardiac and respiratory rhythms. This Chapter introduces a modification in the synchrogram technique that substantially enhances

the sensitivity of the detection of cardiorespiratory coordination, and this may facilitate unravelling its physiological role.

Although the time delay introduced in this Chapter provides enhanced detection of cardiorespiratory coordination, we are interested in a relatively simple approach that could show improved performance and also provide us with some additional information. Data analysis using symbolic dynamics has become a topic of interest in recent years due to its reliability. In the following Chapter, we develop a novel technique based on joint symbolic dynamics for the detection of cardiorespiratory coordination.

Cardiorespiratory interaction using joint symbolic dynamics

CARDIAC and respiratory rhythms are highly non-linear and non-stationary. As a result traditional time domain techniques are often inadequate to characterize their complex dynamics. In this Chapter, we introduce a novel technique to investigate the interactions between RR intervals and respiratory phases based on their joint symbolic dynamics. First, to evaluate the technique, we simulate two non-linearly coupled systems using the Lorenz system and an autoregressive process. Both time series are transformed into ternary symbol vectors based on the changes between two successive time points. Subsequently, words of different symbol lengths are formed and the correspondence between the two series of words is determined to quantify their interaction. Second, this technique is applied on 13 healthy subjects in different body postures during spontaneous and controlled breathing to study the interaction between cardiac and respiratory cycles. To validate our results respiratory sinus arrhythmia (RSA) is further studied using the phase-averaged characterization of the RSA pattern.

6.1 Introduction

The association between cardiac and respiratory rhythms has long been recognised (Schafer *et al.* 1998, Schafer *et al.* 1999, Lotric and Stefanovska 2000). Some of the conventional signal-processing techniques such as power spectral density and cross-correlation analysis have shown linear dependencies between heart and respiratory rate (Akselrod *et al.* 1987, Baselli *et al.* 1986). However, as these biological signals are inherently non-linear, non-stationary and contain superimposed noise, the techniques mentioned above often prove to be inadequate for characterizing their complex dynamics (Hoyer *et al.* 1998c, Rosenblum *et al.* 1998). Dynamic relationships between heart rate and respiratory rate were assessed by various approaches, and consequently there is still substantial terminological and conceptual confusion in this field. For this reason, we consider it important to clearly define terms used in the current work. We will use *cardio-respiratory interaction* as the most generalized umbrella term. The quantification of cardiorespiratory interaction appears to have clinical merit for risk stratification of cardiac mortality (Casolo *et al.* 1992, Moser *et al.* 1994) and diagnosing obstructive sleep apnea (Cysarz *et al.* 2004a, Bartsch *et al.* 2007, Kabir *et al.* 2010b).

We are interested in a new and relatively simple approach that could also provide us with some additional information about cardiorespiratory interactions. While assessment of coherence function can lead us to the detection of changes in cardiorespiratory interaction with postural changes, it lacks the temporal information contained in the pattern of either the RR intervals and respiratory phases or their interaction. The concept of symbolic dynamics allows for an easy interpretation of physiological data by a simplified description of the system's dynamics and offers a framework for exploring the nature of a system through a means of simplified analysis (Kurths *et al.* 1995, Voss *et al.* 1996, Baumert *et al.* 2002, Baumert *et al.* 2005, Baier *et al.* 2006). The basic idea of this concept is to partition the state space into a finite number of regions, each of which is represented by a pre-defined symbol. In this case the dynamics of the system is studied by the alteration of symbols rather than representing a trajectory by infinite sequences of numbers. By employing a coarse-graining procedure some of the time series' detailed information is lost while the robust properties of the dynamics are preserved (Voss *et al.* 1996, Baumert *et al.* 2002). In this Chapter we introduce a novel approach to quantify cardiorespiratory interaction that is based on the joint symbolic dynamics of respiratory phase and heart rate.

6.2 Methods

6.2.1 Simulated data analysis using Lorenz system and an autoregressive model

Simulated data is an useful way to determine the credibility of a technique. We use the Lorenz system to represent one of the non-linear dynamic system. The Lorenz system is defined by the equations of a three-dimensional dynamical system, represented by three variables, x , y and z , that exhibits chaotic behavior. The equations, introduced by Lorenz (Lorenz 1963), that govern the Lorenz system are given as

$$\begin{aligned}\frac{dx}{dt} &= \sigma(y - x), \\ \frac{dy}{dt} &= x(\rho - z) - y, \\ \frac{dz}{dt} &= xy - \beta z.\end{aligned}\tag{6.1}$$

where σ and ρ are the Prandtl and Rayleigh numbers.

By solving the three differential equations, the three components of the Lorenz-system, x , y and z are obtained. For our analysis we considered the x -component of the Lorenz system. A second order auto-regressive process was used to generate the time series of the second non-linear system y_n , coupled with x_n , given by

$$y_n = 1.095y_{n-1} - 0.4000y_{n-2} + 0.700\zeta_n + 0.300x_n^2.\tag{6.2}$$

where ζ is white noise and x is normalized to its standard deviation.

The time series of the two coupled systems x_n and y_n are shown in Figure 6.1. Initially, we calculate the probability of appearance of similar words, P , at a particular instant in both the series, by dividing the total number of words in a series (n_x) or (n_y) by the total combination of words from both the series, given by

$$P = \frac{n_x \text{ or } n_y}{n_x \times n_y}.\tag{6.3}$$

Consequently, joint symbolic dynamics is applied on the coupled systems to determine the percentage of interaction between the two systems. In order to determine whether

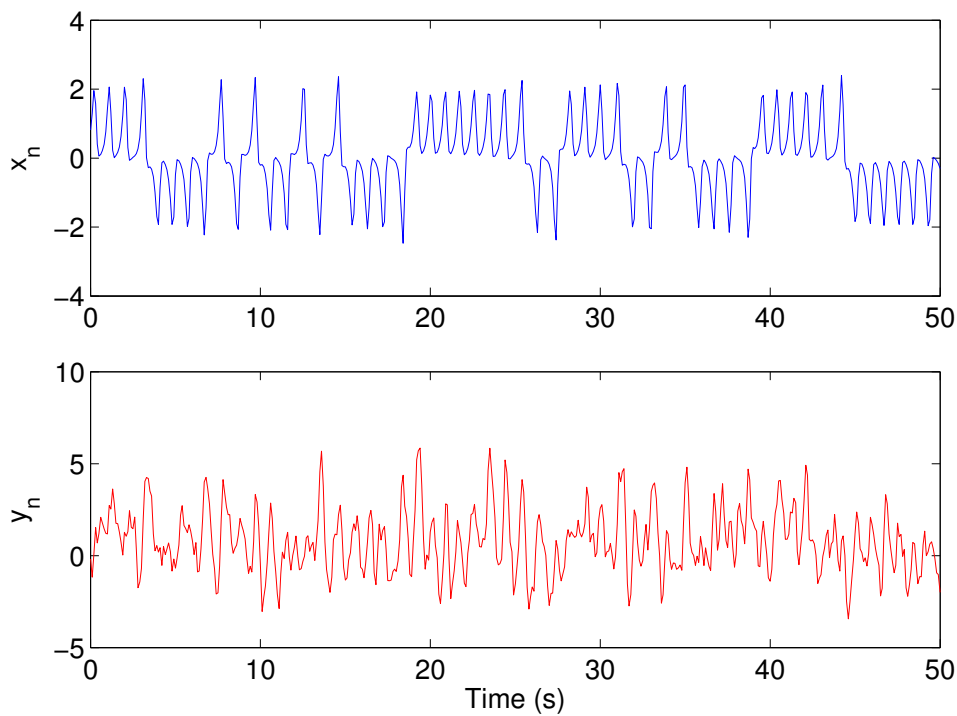


Figure 6.1. Simulated data analysis. Figure representing the time series of nonlinear system, y_n , coupled with the x -component of the Lorenz system, x_n .

joint symbolic dynamics is an effective approach for detecting interaction between nonlinear systems, we randomize the data by shuffling the values of x_n 50 times. For the purpose of statistical analysis, and considering that the values of white noise change in every realization, we generate 20 realizations to obtain a sequence of results.

6.2.2 Subjects / Experimental protocol

Data from 13 healthy subjects discussed in Chapter 5, Section 5.2.1 are used in this study.

6.2.3 Data analysis

Recording of ECG and Respiration

The ECG and respiratory signals are processed as described in Chapter 1, Sections 1.4.1 and 1.4.2. Respiratory signals are low-pass filtered at 1.0 Hz to remove noise.

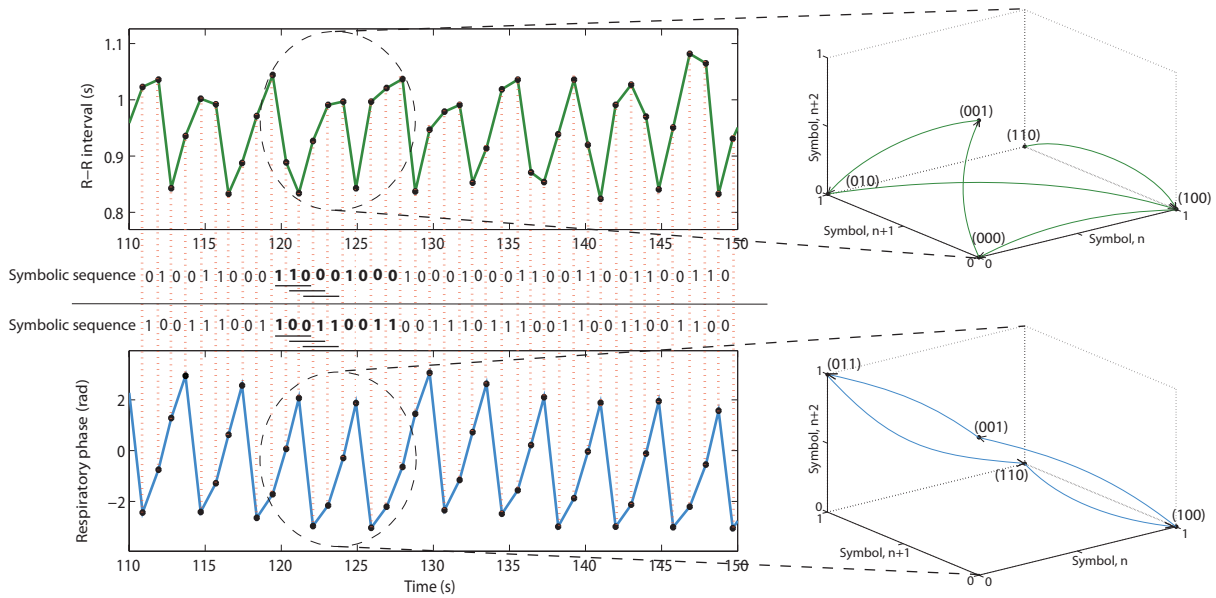


Figure 6.2. Schematic illustration of symbolic dynamics. The top left panel shows the RR intervals as obtained from the time points of R-peaks while the bottom left panel represents the respiratory phase cycle and the respiratory phases at the time points of R-peaks (dots represent the time points while dotted lines show the correspondence between the two time series). Both the time series can be transformed into symbolic sequences as defined in the methods section. In this study, three consecutive symbols were used to form words (underlined in the symbolic sequence). The right panel illustrates the phase space representation of symbolic dynamics using 10 consecutive cardiac cycles (shown in bold symbols in the left panel).

If k_i is the k^{th} sample of ECG corresponding to the appearance of an i^{th} R-peak, then $\phi_r(k_i)$ represents the k^{th} phase of respiration at the instant of the i^{th} R-peak. In this Chapter, the parameter 'RP' contains the series of respiratory phases at the instants of R-peaks.

Calculation of time delays for enhanced detection of coordination

The time delay in the RR time series was calculated using cross-correlation analysis discussed in Chapter 5, Section 5.2.4.

Joint symbolic dynamics

Symbolic analysis involves transformation of time series into a series of discretized symbols to extract information about the behaviour of the system generating the time

series. In this process, the phase space of the dynamical system is partitioned into a finite number of cells in order to obtain a coordinate grid of the phase space. Using the method of time delayed phase space embedding the time series generated by a dynamical system would form an orbit, known as a phase trajectory, within a closed and bounded space. Each cell visited by the trajectory at a time instant can be denoted by a specific symbol among a set of defined symbols (Ray 2004). Subsequently, the phase space trajectory can be mapped onto a symbol space by generating a sequence of symbols corresponding to partitions in the space defining each state of the system (Kitchens 1998, Robinson 1999, Devaney 2003). This is illustrated in Figure 6.2.

Phase space embedding requires knowledge of the system's dimension, which is difficult to obtain from physiological data. In this paper we follow a more pragmatic approach, using an embedding delay of one and varying the embedding dimension with the aim to optimize the classification of our experimental data.

For simulated data analysis, two symbolic sequences s^x and s^y are formed from the vectors of the two time series x and y using the transformation rule below, based on the differences between successive x and y values, respectively,

$$s_i^x = \begin{cases} 0 & \text{if } x_{i+1} - x_i < 0, \\ 1 & \text{if } x_{i+1} - x_i > 0, \\ 2 & \text{if } x_{i+1} - x_i = 0. \end{cases} \quad (6.4)$$

$$s_i^y = \begin{cases} 0 & \text{if } y_{i+1} - y_i < 0, \\ 1 & \text{if } y_{i+1} - y_i > 0, \\ 2 & \text{if } y_{i+1} - y_i = 0. \end{cases} \quad (6.5)$$

For real data analysis, the vectors of the RR time series and the series of respiratory phases ϕ_r at the instants of R-peaks, RP, are used to form two symbolic sequences, s^{HR} (HR denoting the heart rate) and s^{RP} , using the transformation rule below, based on the differences between successive RR intervals and R-instant respiratory phases, respectively,

$$s_i^{\text{HR}} = \begin{cases} 0 & \text{if } \text{RR}_{i+1} - \text{RR}_i > V, \\ 1 & \text{if } \text{RR}_{i+1} - \text{RR}_i < V, \\ 2 & \text{if } \text{RR}_{i+1} - \text{RR}_i = V. \end{cases} \quad (6.6)$$

$$s_i^{\text{RP}} = \begin{cases} 0 & \text{if } | \text{RP}_{i+1} - \text{RP}_i | > V, \\ 1 & \text{if } | \text{RP}_{i+1} - \text{RP}_i | < V, \\ 2 & \text{if } | \text{RP}_{i+1} - \text{RP}_i | = V, \end{cases} \quad (6.7)$$

where V is a threshold value. For the purpose of this study we have used $V = 0, 2, 4, 6, 8, 10$ ms.

The formation of words from the symbol vectors and the analyses of their interaction are similar for both the simulated and real data, and hence only the real data (RR intervals and respiratory phases) has been used below in order to explain the procedure.

Using the symbol vectors s^{HR} and s^{RP} , we construct series of words (bins), w_k^{HR} and w_k^{RP} of lengths $k=1, 2, \dots, 5$ —containing k successive symbols. Consequently, 3^k different word types are obtained for each vector.

After applying the delay in RR intervals leading to the highest correlation between respiratory phases and delayed RR intervals, the interaction between RR intervals and respiratory phases during supine and upright posture is studied using symbolic dynamics for the lengths of words and threshold values mentioned earlier. Subsequently, the word length and threshold value that provided the highest significance level is chosen for our analysis.

The interaction between cardiac and respiratory cycles is studied by comparing the j^{th} ($j = 1, 2, \dots, n$, where n is total number of words) word from the distributions, w_j^{HR} and w_j^{RP} , of a particular word length k . If the sequence of symbols in w_j^{HR} corresponded to w_j^{RP} (i.e. $w_j^{\text{HR}} = w_j^{\text{RP}}$), the two words and hence the cardiac and respiratory epochs are considered to be coordinated. The total interaction is calculated by dividing the total count of coordinated words by the total number of words and subsequently determining the percentage of interaction for different body postures.

Theoretically, the cardiac and respiratory cycles are also considered to be coordinated when the two series are in complete phase opposition. In this study, however, we limit the assessment of cardiorespiratory interaction to the case of identical words in both the series, such that the proposed approach resembles the concept of respiratory sinus arrhythmia (RSA).

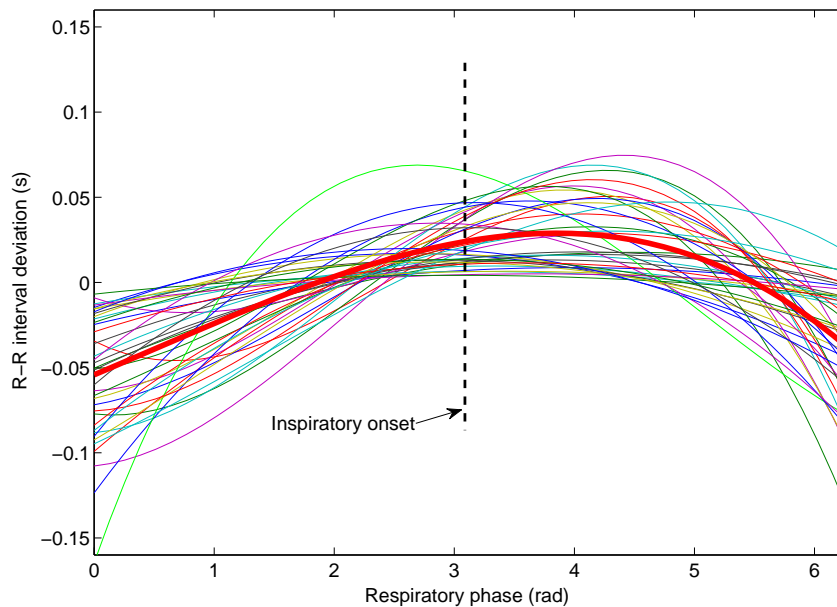


Figure 6.3. Phase-averaged respiratory sinus arrhythmia plot. Respiratory sinus arrhythmia (RSA) of a subject during supine position for 39 respiratory cycles clustered together (thin lines) and the overall RSA (thick red line) obtained by averaging the clustered RSA. Each thin line indicates the RR interval deviation for one respiratory cycle. The origin is the expiratory onset of respiration.

RSA pattern analysis

The pattern of RSA is evaluated by selective averaging of RR interval changes from multiple respiratory cycles over the respiratory phase. As explained in more detail in Gilad *et al.* (2005), for all n respiratory cycles, the RR intervals in each respiratory cycle are interpolated into 50 data points using cubic spline interpolation. The 50 data points for each of all the n respiratory cycles correspond to 2π (Fig. 6.3)—the origin in the figure being the expiratory onset of respiration. The overall RSA pattern is obtained by taking the average of all the RSA patterns for n respiratory cycles (Fig. 6.3). For the purpose of our analysis we defined two RSA parameters: RSA amplitude and phase. The RSA amplitude is calculated by taking the difference between the maximum and the minimum peaks of the overall RSA pattern. The phase of RSA is defined as the respiratory phase at the point of maximum overall RSA.

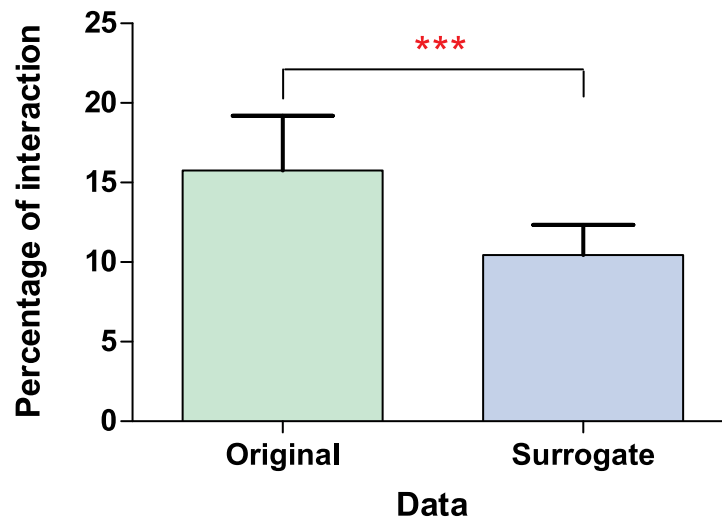


Figure 6.4. Interaction between coupled systems using symbolic dynamics. Interaction between two coupled systems using original and surrogate data. A significant decrease in interaction was observed using surrogate data as compared to original coupled data. Here, *** represents $p < 0.0001$.

Statistical analysis

GraphPad Prism version 5.01 for Windows (GraphPad Software, San Diego California USA, www.graphpad.com) is used for statistical analysis. The interaction between cardiac and respiratory rhythms between different body postures is compared using non-parametric repeated measure analysis of variance (Wilcoxon matched pairs test, Friedman test and Dunn's multiple comparison test). Values with $p < 0.05$ are considered statistically significant. Data are expressed as mean \pm SD.

6.3 Results

6.3.1 Theoretical probability analysis

For our simulated data analysis to determine the interaction between two coupled non-linear systems, we use words of length '3' as suggested by previous studies (Baumert *et al.* 2002, Caminal *et al.* 2005). Since 3 symbols (0, 1 and 2) are used to form words of length 3, the probability of appearance of one word out of total possible words in a series is $\frac{1}{3^3} = 0.037$. Consequently, the probability of appearance of similar words in both the series at a particular instant would be $\frac{3^3}{3^3 \times 3^3} = 3.7\%$. However, we observe

6.3 Results

that although the symbol '2', representing no difference between two successive values in a series, is assigned in the formula, it rarely appeared in the symbolic sequences. Based on this observation the probability is recalculated to be $\frac{2^3}{2^3 \times 2^3} = 12.5\%$.

6.3.2 Analysis of joint symbolic dynamics of the non-linearly coupled system

Using the joint symbolic dynamics approach for the coupled systems defined by Equations 6.1 and 6.2, an overall interaction of $15.8 \pm 3.4\%$ is observed for 20 realizations (Figure 6.4). After shuffling the values of x_n 50 times and calculating its interaction with the original y_n for 20 realizations using joint symbolic dynamics approach, a significant decrease in the percentage of interaction is observed (15.8 ± 3.4 vs. $10.5 \pm 1.9\%$, $p < 0.0001$), see Figure 6.4.

6.3.3 Effect of changes in body posture on respiratory and RR interval

The effect of changes in body posture from supine to upright and with the increase in head-up tilt angles from 0 to 30 and 60 degrees on respiratory and RR interval has been discussed in Chapter 5 section 5.3.1.

6.3.4 Symbolic dynamics approach—Optimisation of word length and threshold value, and analysis of cardiorespiratory interaction

The interaction between respiratory phases and delayed RR intervals is determined by calculating the percentage of similarity of the sequence of symbols between the respective words of the two series. The word length and threshold values are optimized using the recordings of 8 subjects obtained during standing and in the supine position. The Wilcoxon p value between standing and supine recordings is the output variable under consideration. A word length of 3 provides consistently low p -values for different threshold values (Fig. 6.5). Setting the threshold value to 6 ms (Fig. 6.5, upper panel) and the word length to 3, provides the most significant result ($p = 0.008$). The suitability of this parameter setting is validated with the second data set consisting of

Table 6.1. Joint symbolic dynamics approach. Transformation of RR intervals (RR_i) and respiratory phases (RP_i) into symbol vectors, s_i^{RR} and s_i^{RP} , and words of length 3, w_{3j}^{RR} and w_{3j}^{RP} , respectively. The words can be placed in a 27×27 table matrix. In the table, the 'star' indicates that sequence of symbols in w_{3j}^{RR} corresponds to w_{3j}^{RP} and hence is considered coordinated. The 'plus' sign indicates the pair of words with a difference in sequence of symbols. The blank spaces indicate that the respective combination of words do not appear in the selected RR/RP series.

RR_i

0.834	0.788	0.808	0.85	0.858	0.856	0.798	0.77	0.858	0.832
s_i^{RR} : 0	1	1	1	0	0	0	1	0	
s_i^{HR} : 1	0	0	0	1	1	1	0	1	
w_{3j}^{HR} :-	-	100	000	001	011	111	110	101	

| RP |_i

1.979	1.323	0.146	1.688	2.820	2.276	1.259	0.130	1.407	2.907
s_i^{RP} : 1	1	0	0	1	1	1	0	0	
w_{3j}^{RP} :-	-	110	100	001	011	111	110	100	

$w_{3j}^{RP} \backslash w_{3j}^{HR}$	000	001	010	011	100	101	110	111	200	...	211	...	222
000													
001		*											
010													
011				*									
100	+					+							
101													
110					+		*						
111								*					
200													
...													
211													
...													
222													

6.3 Results

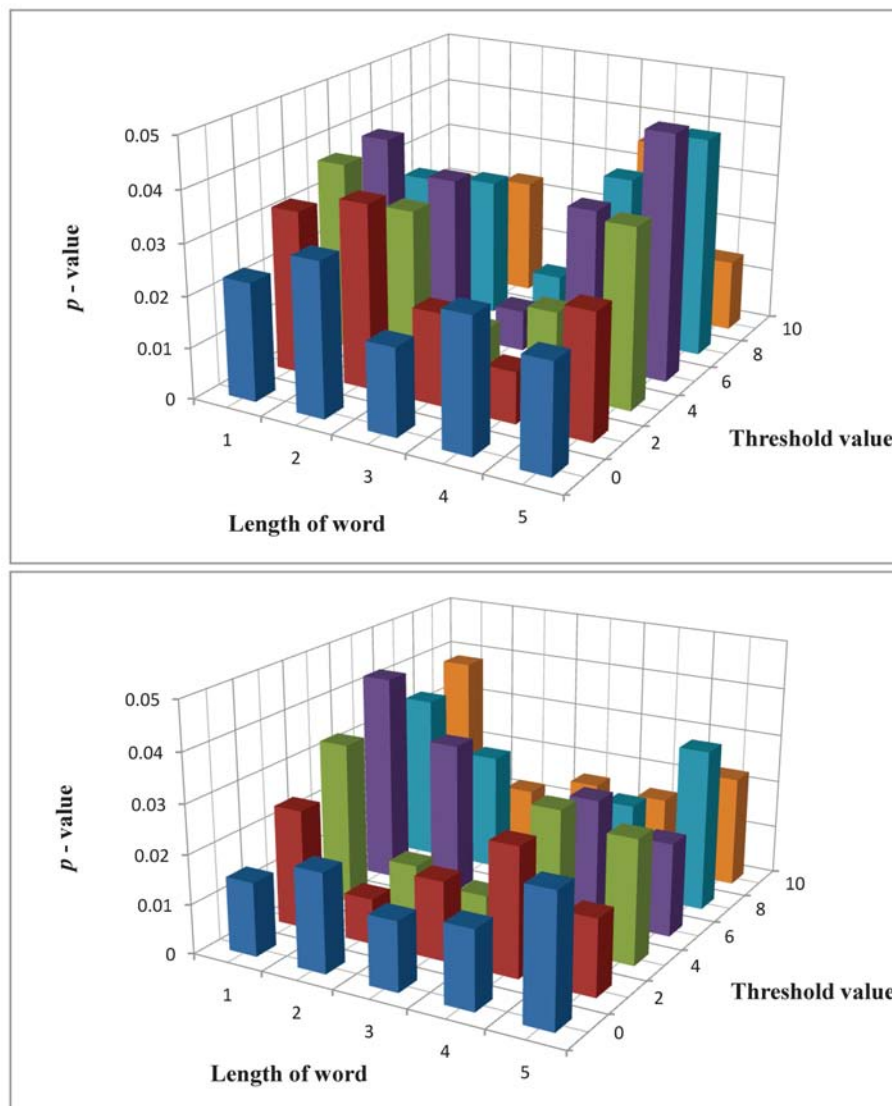


Figure 6.5. Significance test results. Wilcoxon test results (p values) obtained from cardiorespiratory interaction analysis for different lengths of words and threshold values in two groups of subjects: Group 1—supine vs. upright posture with spontaneous normal breathing (upper panel); Group 2—head-up tilt test with controlled metronomic breathing (lower panel).

recordings during graded head-up tilt (Fig. 6.5, bottom panel). The word types span over a 27×27 vector matrix from $[000, 000]^T$ to $[222, 222]^T$ (Table 6.1). There is a significant decrease in cardiorespiratory interaction with the change in body posture from supine to upright (26.4 ± 4.7 vs. 20.5 ± 5.4 %) during spontaneous breathing (Fig. 6.6). Head-up tilt during controlled breathing also shows a significant decrease in cardiorespiratory interaction (0 vs. 60° : 41.8 ± 5.3 vs. 23.5 ± 6.1 %), as seen in Fig. 6.6.

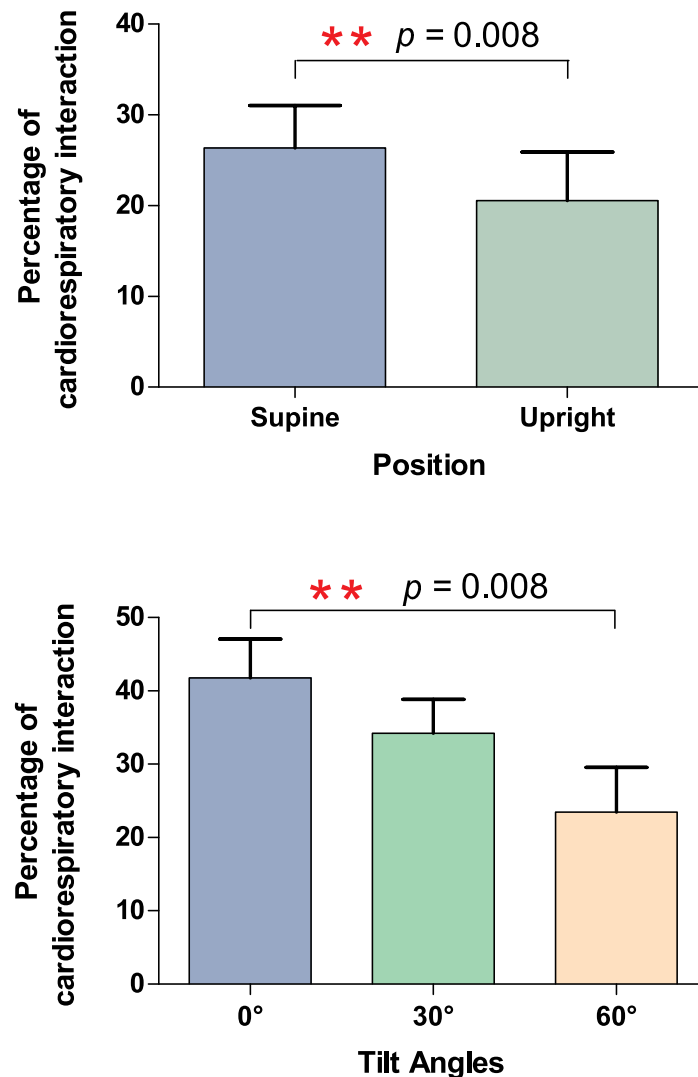


Figure 6.6. Cardiorespiratory coordination using symbolic dynamics. Percentage of cardiorespiratory interaction using the symbolic dynamic approach for the supine and upright postures (top) and different graded head-up tilt (bottom).

6.3.5 Effect of changes in body posture on RSA

The magnitude of RSA maxima in upright posture is significantly lower than in supine posture (0.08 ± 0.01 vs. 0.11 ± 0.02 s, $p < 0.05$, respectively) see Fig. 6.7, upper panel. On the other hand, the phase of the RSA pattern maxima is significantly higher in upright posture as compared to supine posture (5.1 ± 0.7 vs. 4.0 ± 0.6 rad, $p < 0.05$, respectively), see Fig. 6.7, bottom panel.

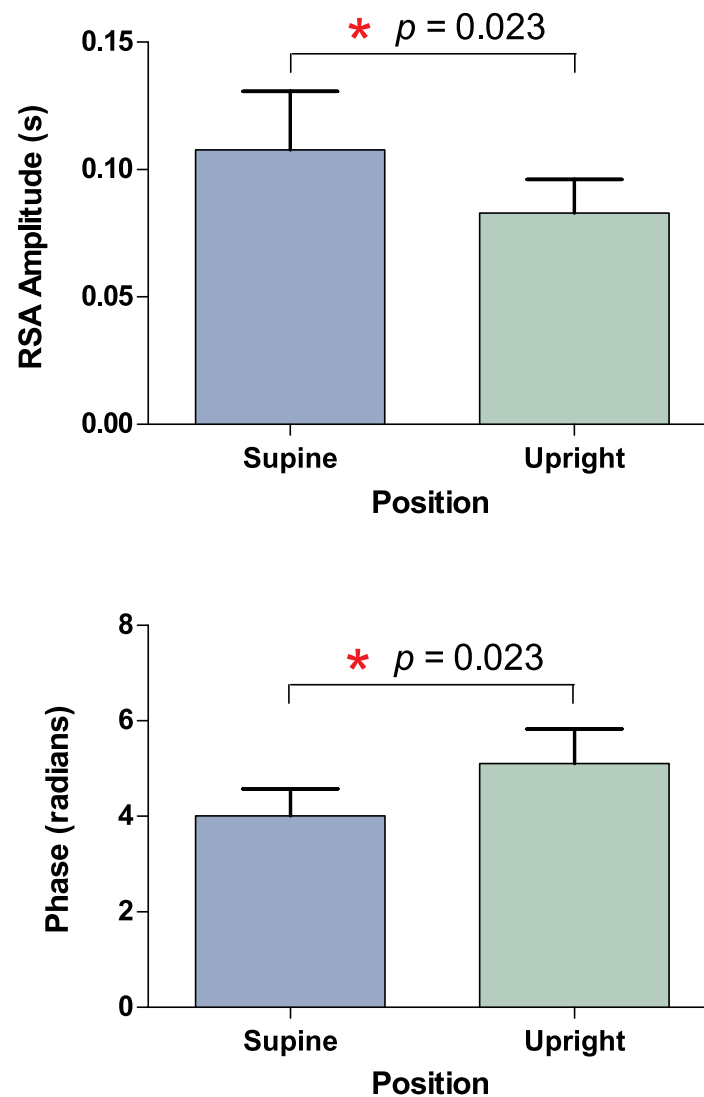


Figure 6.7. RSA in supine and upright posture. Amplitude (top) and phase delay (bottom) of RSA of healthy subjects in supine and upright postures.

Increase in head-up tilt angles from 0 to 60° also results in significant decrease in magnitude and significant increase in phase of the RSA pattern maxima (magnitude: 0.12 ± 0.02 vs. 0.07 ± 0.01 s, $p < 0.05$ and phase: 2.97 ± 0.73 vs. 4.51 ± 0.23 rad, $p < 0.05$, respectively), see Fig. 6.8.

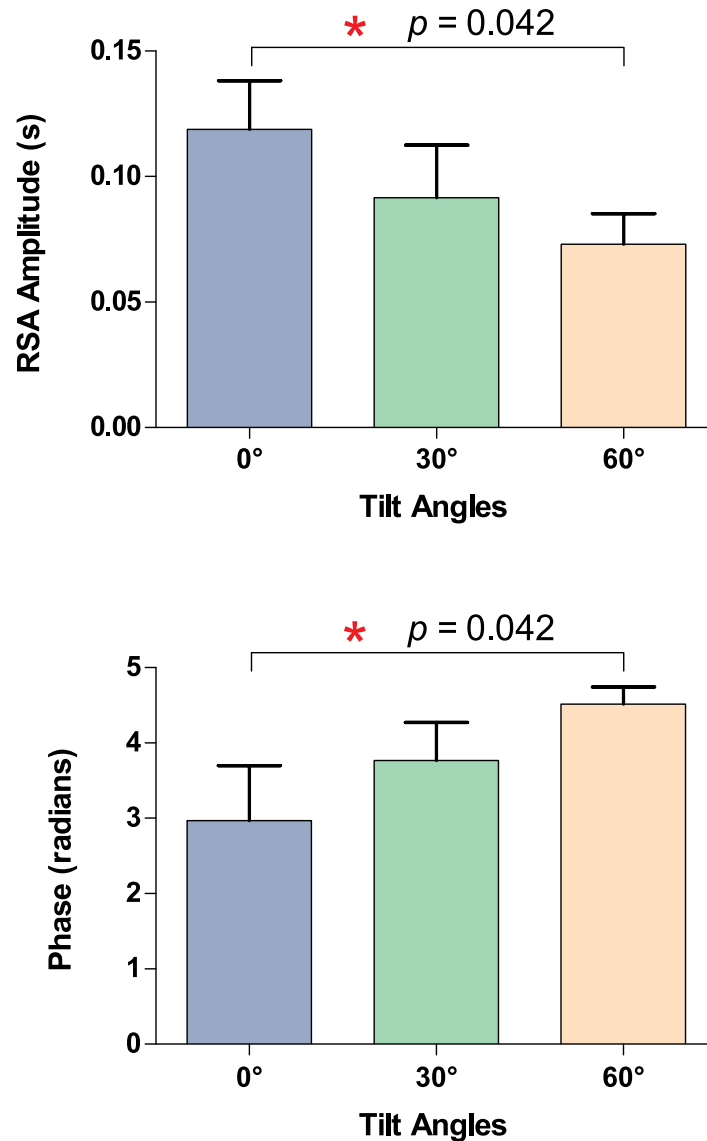


Figure 6.8. RSA during head-up tilt. Amplitude (top) and phase delay (bottom) of RSA in healthy subjects during graded head-up tilt.

6.3.6 Correlation between results obtained using symbolic dynamics and RSA analysis

The cross-correlation between the results of cardiorespiratory interaction analysis for each body posture obtained using joint symbolic dynamics approach and RSA pattern analysis is calculated and presented in Table 6.2. Although moderate correlations are

6.4 Discussion

Table 6.2. Correlation analysis. Correlation between the results of cardiorespiratory interaction analysis obtained using joint symbolic dynamics approach and RSA pattern analysis.

RSA pattern analysis	Joint symbolic dynamics approach					<i>p</i> -values
	Supine	Upright	0°	30°	60°	
Supine	0.12					0.19
Upright		0.09				0.11
0°			-0.30			0.29
30°				-0.39		0.18
60°					-0.27	0.23

observed between the measures obtained using the two techniques, the results of cross-correlation analysis are not statistically significant.

6.4 Discussion

In this chapter we introduce a novel approach for the investigation of interaction between cardiac and respiratory cycles based on their joint symbolic dynamics (JSD). Our main finding is that the joint symbolic dynamics approach reveals significant differences in the cardiorespiratory interaction in different body postures. It appears that JSD is more sensitive to postural changes than phase-averaged RSA pattern analysis.

Symbolic dynamics has become a standard tool for the identification and interpretation of key dynamic structures and behaviours of dynamical systems, particularly when studying chaotic systems (Kitchens 1998, Robinson 1999, Devaney 2003). Analysis of respiratory data by symbolic dynamics has been suggested to provide better results than time-domain analysis (Caminal *et al.* 2005). In a study by Caminal *et al.* (2005), the transformation of the respiratory time series into symbols and their analysis was based on different parameters—non-dimensional parameter α , number of overlapped symbols in consecutive words τ , and probability threshold of word occurrences p^{TH} —whose values had to be suitably selected. Our study uses a novel methodology that is based on the changes in consecutive respiratory phases corresponding to the changes in RR intervals and involves optimization of the transformation rules, threshold values and word lengths and delay. The optimum word length identified in this study is '3' and is well in line with several previous studies that used a

pragmatic approach instead of true phase space embedding (Baumert *et al.* 2002, Caminal *et al.* 2005, Caminal *et al.* 2010).

However, to validate the effectiveness of the proposed approach, it is important to use simulated data (Pikovsky *et al.* 2001). In addition, cross-correlation and coherence functions, which determine the presence of a particular functional relationship between two time series, are based on linear measures and hence can detect little or no couplings between non-linear systems. In order to further evaluate the sensitivity and effectiveness of joint symbolic dynamics in detecting coupling between non-linear systems, we use surrogate data for our analysis. First, we determine the probability of appearance of similar words in both the time series. For words of length '3' and using '3' different symbols, the probability of interaction appeared to be very low (3.7%). However, two successive values in either of the time series of simulated data are hardly similar and hence one of the defined symbols in each of the two series remained unused. Based on this observation, a probability of interaction of 12.5% is estimated. Second, using shuffled values (surrogate) of x_n , and hence affecting the coupling, an interaction of 10.5% with y_n is obtained, which is close to the estimated probability. Consequently, as hypothesized, a higher percentage of interaction (15.8%) is observed when the systems are coupled. This would suggest that the joint symbolic dynamics approach can effectively detect interaction between two non-linear coupled systems.

In Chapter 5 we found that introducing a time delay between cardiac and respiratory symbol strings increases the amount of observed cardiorespiratory interaction. It has recently been demonstrated that introducing a time delay may be useful to detect coordination between two time series when the coupling of the underlying systems includes a delay (Rybski *et al.* 2003). Consequently, we introduce a delay in the RR time series accordingly for subsequent symbolic cardiorespiratory interaction analysis.

Our results show that the upright posture, as compared to supine, causes a shortening in RR intervals with no significant change in respiratory intervals, which is consistent with the findings by Gilad *et al.* (2005). It is well known that a postural change from supine to upright causes a decrease in vagus nerve activity and an increase in sympathetic nerve activity (Robinson *et al.* 1966, Rowell 1993, Buchheit *et al.* 2009) and this is the most likely cause of the decrease in RR interval.

Using a symbolic dynamics approach, a significant decrease in cardiorespiratory interaction is observed in the upright position and also with increasing tilt angles compared to supine posture. This finding is in line with several other studies that used different

6.5 Chapter summary

approaches to investigate cardiorespiratory interaction during head-up tilt. Porta *et al.* (2000) used a non-linear approach to assess the casual interactions between heart period and respiration based on the evaluation of conditional entropy. Censi *et al.* (2003) employed a multivariate embedding approach, and Krishnamurthy *et al.* (2004) investigated coherence spectrum of heart rate variability and respiration.

Our analysis of the phase-averaged RSA pattern confirms previous studies (Saul *et al.* 1991, Gilad *et al.* 2005). The upright position is associated with a decrease in amplitude of RSA indicating less influence of respiration on heart rate in upright posture. The phase delay of the RSA pattern with regard to the respiratory signal is significantly higher in the upright posture, compared with the supine posture and is in line with the findings by Gilad *et al.* (2005).

Comparing the results obtained by the analysis of symbolic dynamics to those obtained with the phase-averaging method, the significance level is higher when using the novel method ($p = 0.008$ vs. $p = 0.023$ in group 1, and $p = 0.008$ vs. $p = 0.042$ in group 2, respectively), suggesting improved performance in detecting changes in cardiorespiratory interactions. In addition, the lack of correlation between the symbolic dynamics measure and the amplitude and phase of the RSA pattern suggest that the proposed methodology provides additional information about the cardiorespiratory coordination—hence establishing a framework for further studies.

The results in this study are obtained by analysing the data from a small number of subjects. Although the study is sufficient to detect statistically significant differences, the results need to be validated using another group of subjects. For the quantification of symbolic dynamics we considered only patterns that resemble RSA due to its predominant role in cardiorespiratory interaction. Future work should extend this approach to bidirectional interactions (Mrowka *et al.* 2003).

6.5 Chapter summary

In this Chapter, we have introduced a novel methodology based on joint symbolic dynamics of heart rate and respiratory rate that provides a new representation of cardiorespiratory interaction and shows significant differences in cardiorespiratory coordination for different body postures and appears to be more sensitive to postural changes than phase-averaged RSA analysis.

In the following Chapter we will apply this technique in children and adults with obstructive sleep apnea syndrome (OSAS) to determine the technique's efficiency as screening tool for OSAS and possibly gain some understanding about the underlying physiological mechanism and relationship between cardiorespiratory interaction and sleep apnea.

Chapter 7

Sleep apnea detection using joint symbolic dynamics

THIS Chapter investigates the interaction between heart rhythm and respiration using an approach based on joint symbolic dynamics (JSD) in adults with mild, moderate and severe obstructive sleep apnea syndrome (OSAS), in healthy children and in children with sleep disordered breathing (SDB). It also reports cardiorespiratory response to spontaneous arousals in healthy children.

7.1 Introduction

It has been reported that about one third of the human population suffers from various sleep disorders possibly due to increase in obesity, increased stress or decreased physical activity (Jurkovicova and Celec 2004). Obstructive sleep apnea is disorder of breathing during sleep, which is characterized by prolonged partial and intermittent obstruction of upper airway that affects normal sleep patterns (American Thoracic Society 1996). Apnea/hypopnea indexes greater than 1 in children and greater than 5 in adults are considered to be abnormal (Witmans *et al.* 2003). Respiratory disorders such as upper airway obstruction/sleep disordered breathing and chronic lung disease are thought to be worse during sleep than wakefulness (Marcus 2001, Chervin *et al.* 2006). Patients suffering from obstructive sleep apnea syndrome (OSAS) are more likely to suffer from hypertension and heart diseases (Marcus 2001).

With the increasing evidence of the association of arousals with sleep disorders such as daytime sleepiness and cardiovascular dysfunction, investigation of the physiological events related to arousals from sleep has gained much interest (Baumert *et al.* 2010). Although arousal from sleep is considered to be an important physiological response to adverse stimuli, excessive arousals can affect normal sleep physiology. Arousal from sleep is associated with transient and abrupt cardiorespiratory changes, including an increase in heart rate and blood pressure (Horner 2003). While the cardiorespiratory response to arousal has been investigated substantially in adults, comparatively little work has been done in children. It is now becoming evident that children with SDB may also be at increased risk of adverse cardiovascular outcomes, including abnormal heart rate and blood pressure regulation and cardiac remodeling, and that arousals may also contribute to this pathology (Aljadeff *et al.* 1997, Marcus *et al.* 1998, Amin *et al.* 2002, Amin *et al.* 2004, Amin *et al.* 2005). However, elucidating the pathways underlying the development of cardiovascular disorders in SDB requires an understanding of cardiorespiratory response to spontaneous arousals in healthy individuals.

In Chapter 6, we introduced a novel approach that is based on the joint symbolic dynamics (JSD) of respiratory phase and heart rate to quantify cardiorespiratory interaction. Symbolic dynamics, which provides the opportunity for an easy interpretation of physiological data by allowing a simplified description of the dynamics of a system by means of a few symbols, has been suggested to provide improved performance in detecting changes in cardiorespiratory interactions (Chapter 6).

The aim of this Chapter is to investigate: a) the efficiency of JSD approach in determining the effect of sleep stages and severity of obstructive sleep apnea syndrome on cardiorespiratory interaction in adults, b) the effect of sleep disordered breathing on cardiorespiratory interaction in children, and c) cardiorespiratory interaction during pre- and post-spontaneous arousals from sleep in healthy children.

7.2 Methods

7.2.1 Subjects

In this study, data from 213 adults with suspected OSAS, 40 healthy children (controls) and 40 children with sleep disordered breathing (SDB) as described in Chapter 4, Section 4.2.2 are used. The study conformed to the principles outlined in the Declaration of Helsinki.

7.2.2 Overnight polysomnography and data processing

Details on the study protocol, overnight polysomnography in adults and children, and processing of ECG and respiratory signals have been reported in Chapter 4, Section 4.2.3. In this Chapter, abdominal respiratory signal is used for the analysis of cardiorespiratory interaction.

For our data analysis, we first investigate 213 adults with obstructive sleep apnea syndrome (OSAS) to determine the effect of sleep stages and severity of OSAS on cardiorespiratory interaction using joint symbolic dynamics approach. The approach is later employed in 40 healthy children and another 40 children with SDB. All the artefact such as movement are removed for data analysis.

In children with sleep disordered breathing (SDB), cardiorespiratory interaction is studied and compared with healthy controls,

1. first, by calculating cardiorespiratory interaction for every sleep stage and comparing the results with those of healthy controls,
2. second, after removing all the spontaneous arousals and SDB related events (apnea, hypopnea and respiratory arousal episodes) together with epochs before and

7.2 Methods

after each, to determine whether there are any significant differences in cardiorespiratory interaction during normal/quiet sleep episodes between healthy and SDB children.

For the analysis of cardiorespiratory interaction during pre- and post-spontaneous arousal episodes, only stage 2 sleep (during which the arousals are mostly observed) from healthy children is considered. Furthermore, the spontaneous arousal episodes are selected such that the first 30-second epoch before and after each arousal episode is artefact-free and belongs to stage 2 sleep. For statistical analysis, the first 10 arousal episodes from stage 2 sleep of each subject are considered. Subjects with less than 10 arousal episodes after applying the above criteria are excluded from this analysis. Since the data lengths are short, results in each subject are averaged to obtain overall cardiorespiratory interactions before and after the arousal episodes. To further understand the physiology behind the cardiorespiratory response to spontaneous arousals, epochs 30-60 seconds before and after each arousal episode are also investigated, under the condition that the epochs are artefact-free and belongs to stage 2 sleep.

7.2.3 Joint symbolic dynamics

The RR time series and respiratory phases at the instants of R-peaks are transformed into symbolic sequences and words based on the transformation rule described in Chapter 6, Table 6.1 and Section 6.2.3. However, in children, words of length '2' (instead of '3' as in adults) are used (see Table 7.1) to analyze cardiorespiratory interaction, since they show more significant results as determined by the procedure described in Chapter 6, Section 6.3.4.

7.2.4 Statistical analysis

GraphPad Prism version 5.01 for Windows (GraphPad Software, San Diego California USA, www.graphpad.com) is used for statistical analysis. We investigate the relation between cardiorespiratory interaction and sleep stage using repeated measures ANOVA. Post-hoc analysis and group differences in cardiorespiratory interaction are tested using ANOVA. Values with $p < 0.05$ are considered statistically significant. Data are expressed as mean \pm standard deviation (SD). To determine the effect of OSAS severity on cardiorespiratory interaction, the adult cohort was trichotomized

Table 7.1. Word formations using joint symbolic dynamics. Transformation of RR intervals (RR_i) and respiratory phases (RP_i) into symbol vectors, s_i^{RR} and s_i^{RP} , and words of length 2, w_{2j}^{RR} and w_{2j}^{RP} , respectively. The words can be placed in a 9×9 table matrix. In the table, the 'star' indicates that sequence of symbols in w_{2j}^{RR} corresponds to w_{2j}^{RP} and hence is considered coordinated. The 'plus' sign indicates the pair of words with a difference in sequence of symbols. A blank entry indicates that the respective combination of words do not appear in the selected RR/RP series.

RR_i									
	0.73	0.69	0.71	0.75	0.76	0.75	0.70	0.67	
s_i^{RR} :	0	1	1	1	0	0	0		
s_i^{HR} :	1	0	0	0	1	1	1		
w_{2j}^{HR} :-		10	00	00	01	11	11		

RP_i									
	1.89	1.21	0.43	1.71	2.92	2.35	1.18	0.15	
s_i^{RP} :	1	1	0	0	1	1	1		
w_{2j}^{RP} :-		11	10	00	01	11	11		

w_{2j}^{RP} \ w_{2j}^{HR}	w_{2j}^{HR}	00	01	02	10	11	12	20	21	22
00	*									
01		*								
02										
10	+									
11					+	**				
12										
20										
21										
22										

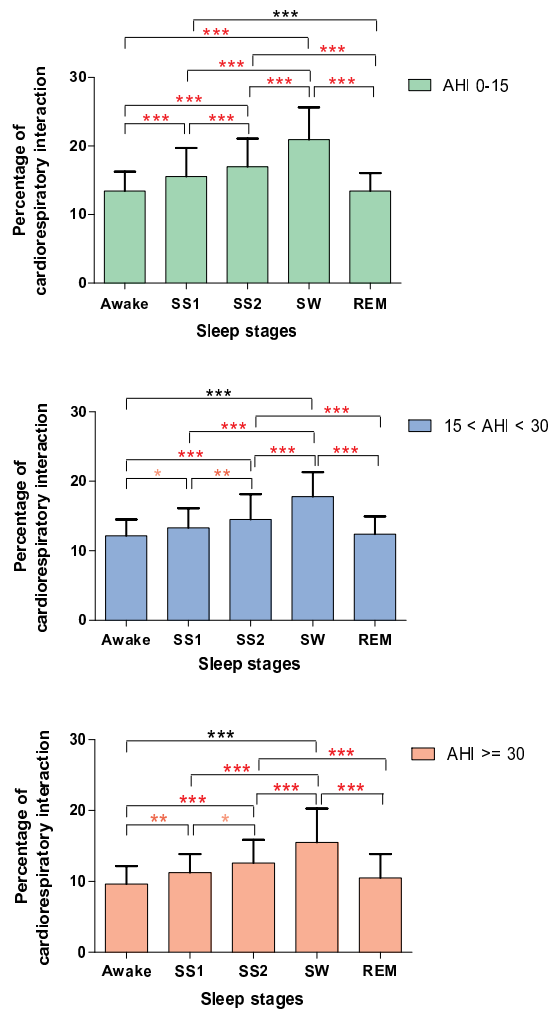


Figure 7.1. Sleep related comparison of cardiorespiratory interaction in adults with OSA.

Cardiorespiratory interaction is strongly associated with sleep stages for all the three groups. Here, *,** and *** indicate $p < 0.05$, $p < 0.01$, $p < 0.0001$, respectively.

based on the apnea-hypopnea index (AHI): no/mild OSAS ($AHI \leq 15$), moderate OSAS ($15 < AHI < 30$), and severe OSAS ($AHI \geq 30$); see Chapter 4 for details. Further, the adult cohort with mild OSAS is divided into subgroups, while the healthy children cohort is dichotomized based on gender and on median values of age and BMI, to study the effects of gender, age and BMI on cardiorespiratory interaction.

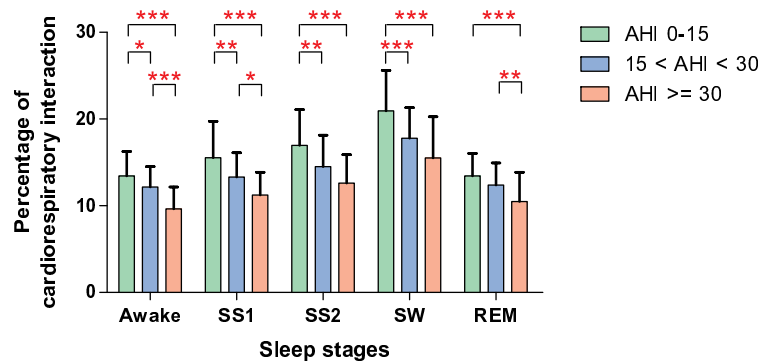


Figure 7.2. Association between cardiorespiratory interaction and severity of OSA in adults.

Using symbolic dynamics approach, a strong association between cardiorespiratory interaction and severity of OSAS was observed in adults. Here, *,** and *** represent $p < 0.05$, $p < 0.01$, $p < 0.0001$, respectively.

7.3 Results—Adults

7.3.1 Sleep stage effects on cardiorespiratory interaction in adults with OSAS

Cardiorespiratory interaction is strongly associated with sleep stages. A significant increase in cardiorespiratory interaction is observed during slow-wave sleep (SW) as compared to any other sleep stages (patients with mild OSAS—SW vs. stage 1, stage 2 and REM sleep: 20.9 ± 4.7 vs. 15.5 ± 4.2 , 17.0 ± 4.1 and 13.4 ± 2.6 %, $p < 0.0001$, respectively), see Figure 7.1.

7.3.2 Group effects on cardiorespiratory interaction in adults with OSAS

A strong association is observed between cardiorespiratory interaction and degree of severity of obstructive sleep apnea. Cardiorespiratory interaction is significantly lower in patients with severe OSAS compared to patients with no or mild OSAS (SW sleep—severe vs. mild: 15.5 ± 4.7 vs. 20.9 ± 4.7 %, $p < 0.0001$, respectively), see Figure 7.2.

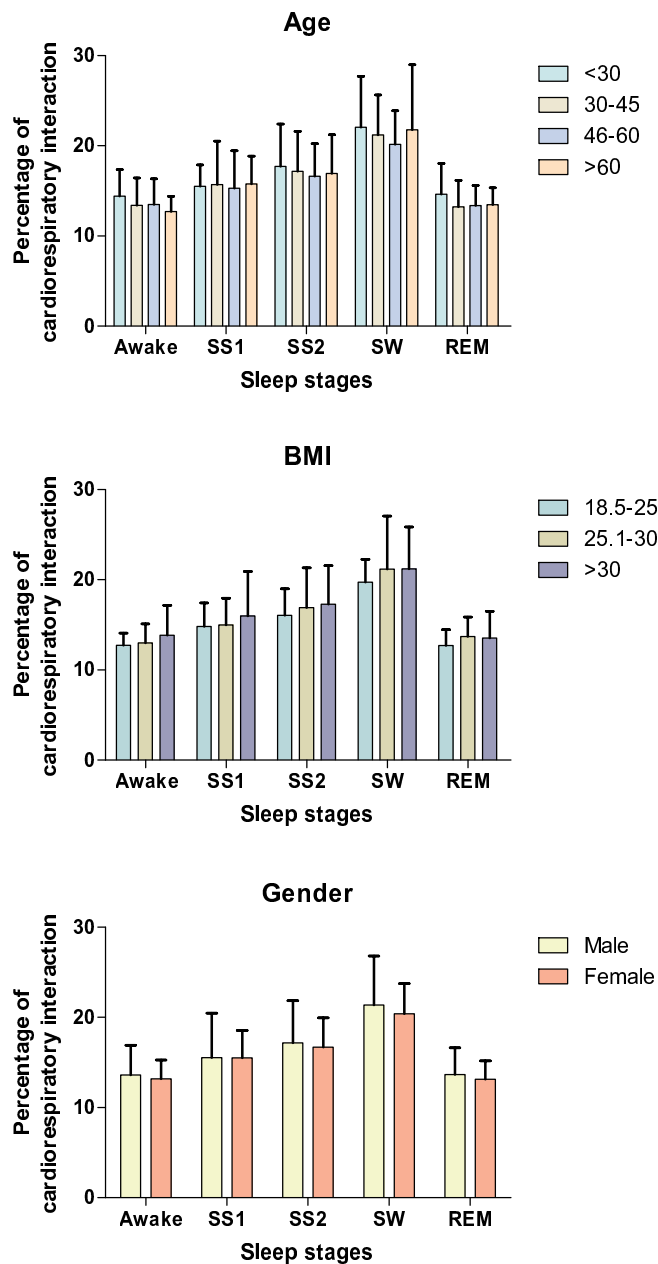


Figure 7.3. Association between cardiorespiratory interaction and age, BMI or gender in adults. Using symbolic dynamics approach to quantify cardiorespiratory interaction, no association is observed between cardiorespiratory interaction and age, BMI and gender in adults.

7.3.3 Age, gender and BMI effects on cardiorespiratory interaction in adults

To investigate the age effect on cardiorespiratory interaction, the group of adults with mild OSAS (AHI<15) is divided into four arbitrary subgroups: <30 years, 30-45 years,

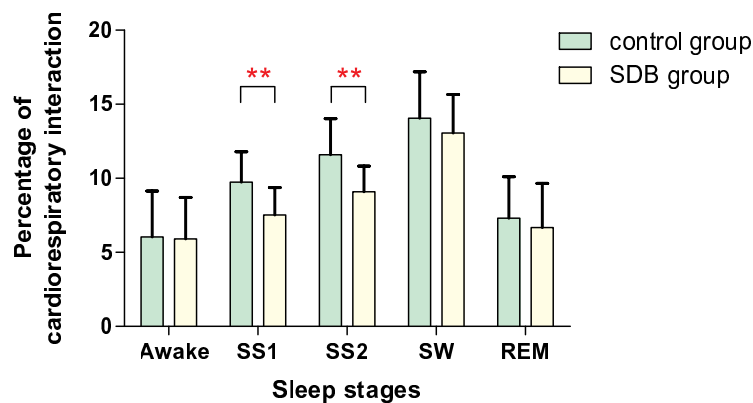


Figure 7.4. Analysis of cardiorespiratory interaction in children considering respiratory arousal episodes. Comparison of cardiorespiratory interaction (mean+SD) between healthy children and children with SDB for different stages of sleep, considering only the respiratory arousals together with the normal sleep episodes. Here, ** represents $p < 0.01$.

46-60 years and >60 years. Similarly, the association of cardiorespiratory interaction with BMI is assessed by dividing the cohort into four groups based on the statistical categories of BMI values: underweight (<18.5 kg/m²), normal (18.5-25 kg/m²), overweight (25.1-30 kg/m²) and obese (>30 kg/m²). No significant difference in cardiorespiratory interaction is observed between any two of either the age or BMI categories (Figure 7.3). Also, there is no association between gender and cardiorespiratory interaction (Figure 7.3).

7.4 Results—Children

Demographics and polysomnographic (PSG) results for the overnight PSG in healthy and SDB children are reported in Chapter 4, Section 4.4.1.

7.4.1 Effect of SDB—Group effects on cardiorespiratory interaction between healthy children and children with SDB

The interaction between cardiac and respiratory cycles is significantly reduced in children with SDB as compared to healthy controls during stage 1 (7.6 ± 1.8 vs. 9.4 ± 2.2 %, respectively) and stage 2 (9.2 ± 1.7 vs. 11.3 ± 2.5 %, respectively) sleep (Figure 7.4).

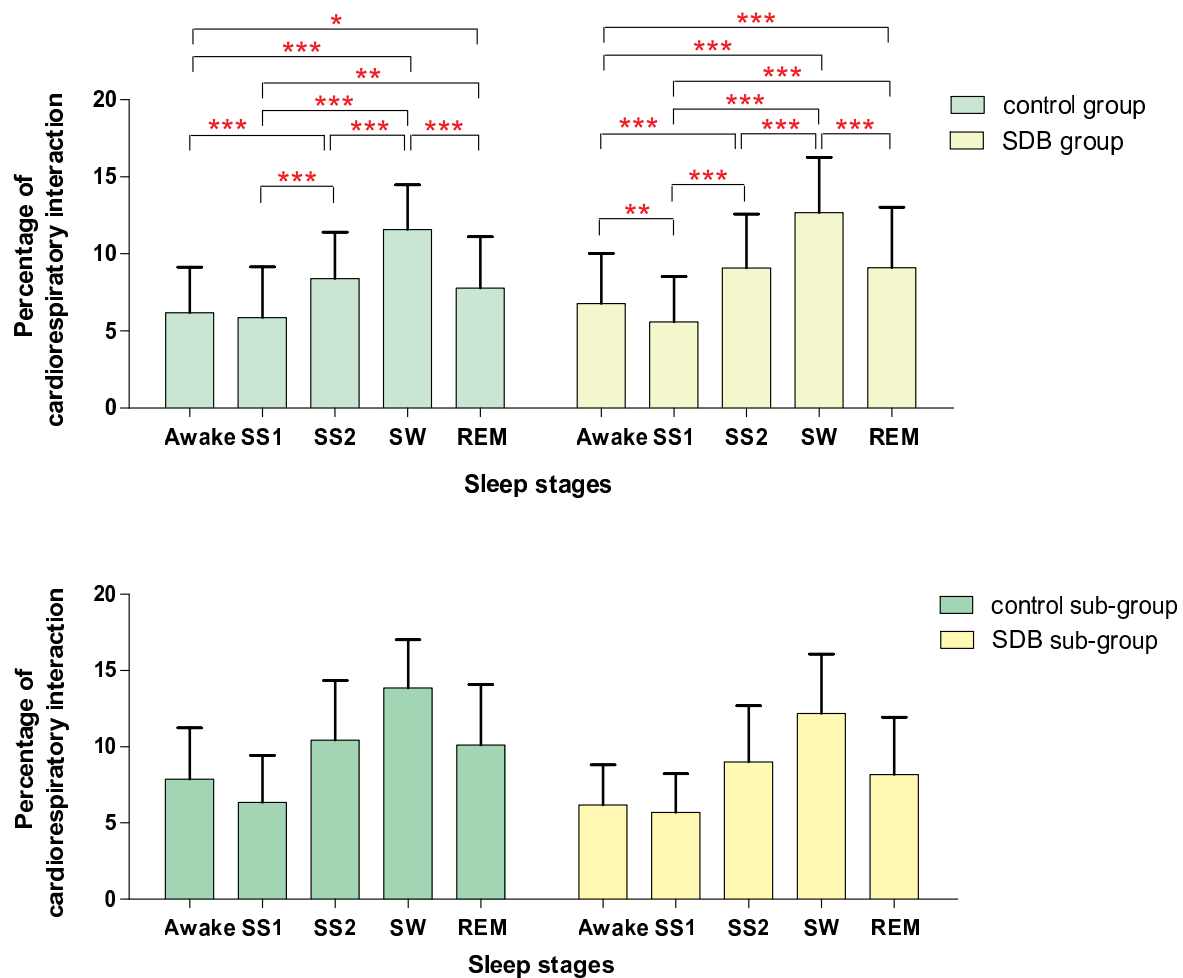


Figure 7.5. Analysis of cardiorespiratory interaction in children after excluding SDB related events. Group and sleep related comparison of cardiorespiratory interaction (mean+SD) in healthy and SDB children, analyzed after removing all the artefact, spontaneous arousals and SDB related events. The top panel shows the results (mean+SD) for cardiorespiratory interaction in all the children. Here, *, ** and *** represent $p < 0.05$, $p < 0.001$ and $p < 0.0001$, respectively. Further, the two groups are divided into two sub-groups of 20 children each (bottom panel)—20 healthy children and another 20 children with SDB with the highest apnea/hypopnea index (AHI). Again, no significant differences between the respective sleep stages of the two groups are observed. Note that the purpose of the figure in the bottom panel is to determine group differences and hence the comparison between sleep stages of a particular group has not been reported.

Table 7.2. Comparison of cardiorespiratory interaction in healthy children. Mean values (\pm standard deviation) of the percentage of cardiorespiratory interaction during different sleep stages in 40 healthy children dichotomized based on gender or the median values of age or BMI z-scores

Sleep stages	Age (yrs)		BMI z-score		Gender	
	<7.3	>7.3	<0.37	>0.37	Male	Female
Awake	5.4 \pm 2	6.9 \pm 3	7.3 \pm 3	5.1 \pm 2	6.6 \pm 3	5.8 \pm 3
SS1	5.5 \pm 3	6.2 \pm 4	6.9 \pm 4	4.8 \pm 2	6.0 \pm 4	5.7 \pm 3
SS2	7.9 \pm 2	8.8 \pm 4	9.3 \pm 4	7.5 \pm 2	8.2 \pm 3	8.6 \pm 3
SW	11.7 \pm 3	11.5 \pm 3	11.9 \pm 3	11.2 \pm 3	11.7 \pm 3	11.4 \pm 3
REM	7.2 \pm 3	8.4 \pm 4	8.6 \pm 4	6.9 \pm 3	8.0 \pm 3	7.6 \pm 4

7.4.2 Analysis of cardiorespiratory interaction in healthy children and in children with SDB after excluding SDB related events

Sleep stage effects on cardiorespiratory interaction in children during normal quiet sleep

A strong association between cardiorespiratory interaction and sleep stages is observed in healthy and SDB children. A significant increase in cardiorespiratory interaction is observed during SW sleep as compared to any other sleep stages (SW vs. stage 1, stage 2 and REM sleep—controls: 11.6 ± 2.9 vs. 5.9 ± 3.3 , 8.4 ± 3.0 and 7.8 ± 3.3 %, $p < 0.0001$; SDB: 12.7 ± 3.6 vs. 5.6 ± 2.9 , 9.1 ± 3.5 and 9.1 ± 3.9 %, $p < 0.0001$, respectively), as seen in Figure 7.5 (upper panel).

Group effects on cardiorespiratory interaction between healthy children and children with SDB during normal quiet sleep

There are no significant differences in cardiorespiratory interaction between respective sleep stages of control and SDB children, as seen in Figure 7.5 (upper panel). Further, the two groups, consisting of 40 children each, are divided into two sub-groups containing 20 children from the control group and another 20 children from the SDB group with the highest apnea/hypopnea index (AHI), and subsequently compared the cardiorespiratory interaction between the two subgroups. Again, no significant differences in cardiorespiratory interaction are observed between respective sleep stages of the subgroups of control and SDB children, see Figure 7.5 (bottom panel).

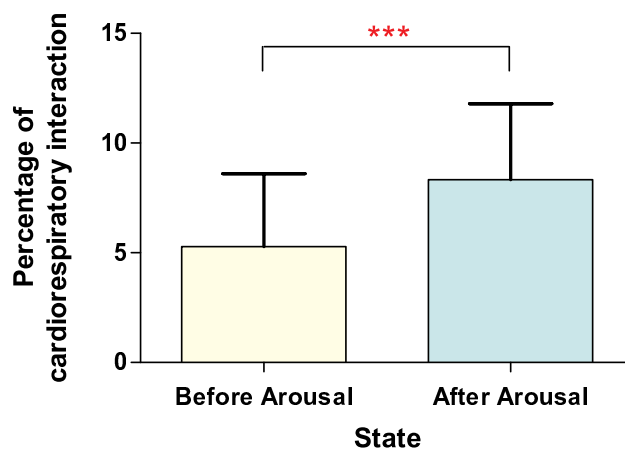


Figure 7.6. Cardiorespiratory response to spontaneous arousals in healthy children. Comparison of cardiorespiratory interaction (mean+SD) 30 seconds before and after spontaneous arousals during stage 2 sleep in healthy children. A significant increase in cardiorespiratory interaction is observed immediately after as compared to before an arousal episode. Here, *** represents $p < 0.0001$.

Age, gender and BMI effects on cardiorespiratory interaction in healthy children

The group of healthy children ($n = 40$) is divided into sub-groups based on the median values of age (median: 7.3 yrs) and BMI z-score (median: 0.37). No significant differences are observed in cardiorespiratory interaction between the corresponding sleep stages of the subgroups (Table 7.2).

7.4.3 Analysis of cardiorespiratory response to spontaneous arousals in healthy children

Six subjects have less than 10 arousals and are excluded from the analysis. Investigating cardiorespiratory interaction before and after spontaneous arousals during stage 2 sleep, a significant increase in cardiorespiratory interaction is observed during 30-second post-arousal episode as compared to 30-second pre-arousal episode (8.3 ± 3.5 vs. 5.3 ± 3.3 %, $p < 0.0001$, respectively), see Fig. 7.6.

After including additional epochs between 30-60 seconds from stage 2 sleep before and after each spontaneous arousal episode, a total of 10 subjects has to be excluded as they failed to satisfy the criteria mentioned in Section 7.2.2. A significant increase in cardiorespiratory interaction is observed during the first 30-second post-arousal

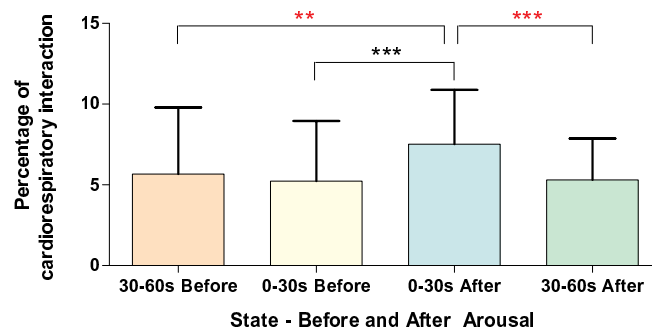


Figure 7.7. Cardiorespiratory response to spontaneous arousals in healthy children. Comparison of cardiorespiratory interaction (mean+SD) 0-30 and 30-60 seconds before and after each spontaneous arousal during stage 2 sleep in healthy children. A significant increase in cardiorespiratory interaction is observed 0-30 seconds after as compared to 0-30 and 30-60 seconds before and 30-60 seconds after an arousal episode. Here, ** and *** represent $p < 0.01$ and $p < 0.0001$, respectively.

episode as compared to both the 30-second pre-arousal episode (7.5 ± 3.4 vs. 5.2 ± 3.7 % ($p < 0.0001$) and 5.7 ± 4.1 % ($p < 0.01$), respectively), see Fig. 7.7. The next 30-second post-arousal episode showed a significant decrease in cardiorespiratory interaction as compared to the first 30-second post-arousal episode (5.3 ± 2.6 vs. 7.5 ± 3.4 %, $p < 0.0001$, respectively), see Fig. 7.7. However, there are no significant differences in cardiorespiratory interaction during 30-60 seconds episode after arousal as compared to 0-30 and 30-60 seconds before arousal.

7.5 Discussion

In this Chapter, we investigate cardiorespiratory interaction in adults with suspected obstructive sleep apnea syndrome (OSAS) and in healthy children and children with sleep disordered breathing (SDB) during night-time sleep using a novel approach based on joint symbolic dynamics. The major findings using joint symbolic dynamics approach (JSD) are: (1) a strong association between cardiorespiratory interaction and sleep stages is observed, which is the highest during slow-wave (SW) sleep—a finding already reported in Chapter 4; (2) cardiorespiratory interaction is affected by OSAS and significantly decreased in patients with severe OSAS compared to patients with no/mild OSAS; (3) a significant decrease in the interaction between cardiac and respiratory cycles is observed during stage 1 and stage 2 stages of sleep in children with

SDB as compared to healthy controls; (4) there are no significant differences in cardiorespiratory interaction during normal/quiet sleep episodes in children with SDB (after removing SDB related events) as compared to healthy children; and (5) there are no effects of age, gender or BMI on cardiorespiratory interaction, which is in line with the findings reported in Chapter 4 and by Bartsch *et al.* (2007).

Employing JSD approach in adults with OSAS, healthy children and children with SDB for the detection and analysis of the association between cardiorespiratory interaction and sleep stages showed similar results but with improved performance as compared to the results obtained using the synchrogram technique reported in Chapter 4.

Cardiorespiratory interaction is significantly decreased in children with SDB during stage 1 and stage 2 sleep (during which the arousals and apnea mostly occur) as compared to healthy controls. After removing SDB related events, no significant differences in cardiorespiratory interaction between healthy children and children with SDB are observed. It thus appears that the interaction between cardiac and respiratory cycles has the ability to recover soon after an arousal episode. It is apparent from the analysis of cardiorespiratory interaction during two consecutive 30-second (0-30 and 30-60 s) pre- and post-arousal episodes, where a significant increase in cardiorespiratory interaction during the first 30-second post-arousal episode is followed by a return to baseline level. It has been reported by Baumert *et al.* (2010) that the respiratory rate significantly increased for a brief period following arousal and demonstrated maximal response at the first breath following arousal with a return to baseline level by the third breath post-arousal. In another study, a significant increase in heart rate/shortening in RR interval after arousal (spontaneous and respiratory) has also been observed (Nalivaiko *et al.* 2007, Baumert *et al.* 2007b). The brief changes in heart and respiratory rates after arousal are the possible cause of a brief but significant increase in cardiorespiratory interaction. Also, it appears that there is a temporal relationship between cardiorespiratory interaction and spontaneous arousals and can be related to the findings by Kesler *et al.* (1999) that induced changes in arterial blood pressure in human adults are capable of eliciting arousal from sleep. However, further studies are required to understand the cause of spontaneous arousal during quiet sleep and its association with cardiorespiratory interaction.

7.6 Chapter summary

In this Chapter, we have successfully used JSD approach for the quantification of cardiorespiratory interaction in adults with OSAS and children with SDB. In line with Chapter 6, the JSD approach has shown improved performance. Also, this is the first study to report the relation between cardiorespiratory interaction and spontaneous arousals in healthy children. It appears that the interaction between cardiac cycle and respiration is associated with spontaneous arousal and significantly increases during the first 30 seconds but returns to baseline about 30 seconds after the arousal episode.

This Chapter has verified the ability of our proposed JSD approach to provide improved performance even in patients with OSAS. Although, Respiratory sinus arrhythmia (RSA) is a widely studied topic and has been investigated in children in recent studies, a detailed study on the association of RSA with sleep stages, arousals and sleep disordered breathing in children has never been explored. In the next Chapter we will study respiratory sinus arrhythmia in healthy children and children with SDB using phase-averaged RSA technique.

Chapter 8



Respiratory sinus arrhythmia in children

THIS Chapter investigates respiratory sinus arrhythmia in healthy children and children with sleep disordered breathing using phase-averaged characterization of the respiratory sinus arrhythmia pattern.

8.1 Introduction

Respiratory sinus arrhythmia (RSA), i.e. subtle rhythmic heart rate accelerations / decelerations that oscillate at the respiratory frequency and defined by the high-frequency component of heart rate variability, is a widely studied topic that has been linked to cardiac vagal tone in studies using autonomic blockade (Akselrod *et al.* 1981). The influence of the vagus nerve activity on RSA has been demonstrated through its significant attenuation or elimination by pharmacological blockade (Hayano *et al.* 1991, Berntson *et al.* 1997). Basal RSA reflects the status of the parasympathetic nervous system at rest and has been suggested as an appropriate index of vagal activity for research with children (Grossman and Taylor 2007). Also, breathing frequency has a profound influence on the magnitude of RSA, independent of actual changes in cardiac vagal outflow (Angelone and Coulter 1964, Pitzalis *et al.* 1998, Pinna *et al.* 2006).

Frequent arousals triggered by episodes of upper airway obstruction are believed to play a key role via repetitive sympathetic nervous system activation and destabilisation of cardiorespiratory control (Loredo *et al.* 1999, Blasi *et al.* 2003, Pack and Gislason 2009). The cardiovascular effects of obstructive sleep apnea syndrome (OSAS) have been widely studied (Bonsignore *et al.* 1994, Blasi *et al.* 2002). In the previous Chapter we have gained some understanding about the effect of sleep disordered breathing on cardiorespiratory interaction in children. Although a few studies have examined RSA in children (Nakra *et al.* 2008, Staton *et al.* 2009, Gentzler *et al.* 2011), a detailed study on the association of RSA with sleep stages, arousals and sleep disordered breathing in children has never been explored. In this Chapter we will study the influence of sleep stages, spontaneous arousals and sleep disordered breathing on RSA in children.

8.2 Methods

Children in this study were participating in an investigation of sleep, breathing and psychological performance before and after treatment for suspected sleep disordered breathing by adenotonsillectomy. Further details on the study protocol are given in Chapter 4, Section 4.2.3.

8.2.1 Subjects

In this study, data from two groups of children—one with 40 healthy controls and another comprising of 40 children with sleep disordered breathing (SDB)—as described in Chapter 4, Section 4.2.2 are used. The study conformed to the principles outlined in the Declaration of Helsinki and was approved by the Human Ethics Committee, Women's and Children's Hospital, Adelaide. Parental consent and child assent were obtained from all participants.

8.2.2 Overnight polysomnography and data processing

Details on the study protocol, overnight polysomnography in children, and processing of ECG and respiratory signals have been reported in Chapter 4, Section 4.2.3. Epochs containing artifacts such as movement or associated with movement are excluded during data analysis. While both groups experienced spontaneous arousals during sleep, the group of children with SDB also suffered from SDB related events which include episodes of apnea, hypopnea and respiratory arousals.

The group of healthy children (40 controls) are further divided into sub-groups based on gender or either the median values of age (median: 7.3 yrs) or BMI z-score (median: 0.37) to study the effects of gender, age and BMI on cardiorespiratory interaction, respectively.

The study/data analysis is structured as follows:

1. In healthy children, the effect of sleep stages on RSA is studied by calculating and comparing the average magnitude and phase delay of RSA for every sleep stage.
2. Ten episodes of spontaneous arousals together with 30 and 60 seconds of pre- and post-arousal normal quiet sleep epochs are selected in healthy children to study the effect of spontaneous arousals on RSA. Details on selection of epochs for analysis has been clearly described in Chapter 7, Section 7.2.2.
3. The group of healthy children is dichotomized based on gender or medians of age or BMI index to study their effect on RSA.
4. In children with SDB, average magnitude and phase delay of RSA is calculated for every sleep stage to investigate the effect of sleep stages and also sleep disordered breathing by comparing the results with those of healthy controls.

8.2 Methods

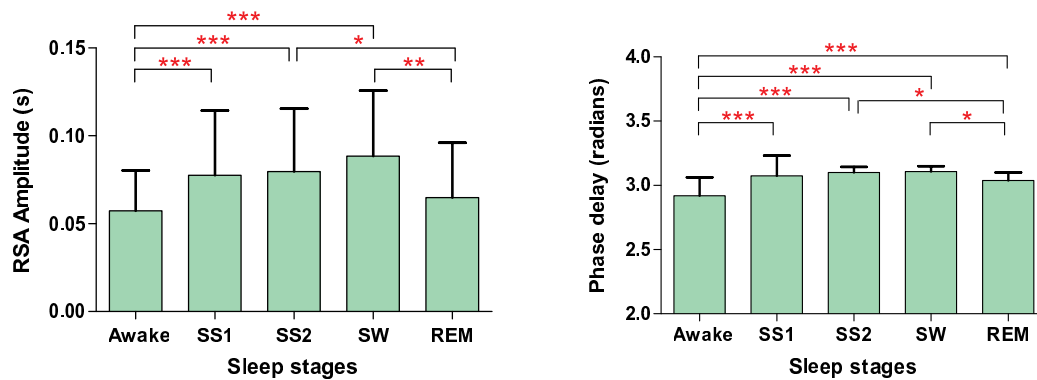


Figure 8.1. Sleep stages effects on RSA in healthy children. Magnitude of RSA shows strong association with sleep stage and is highest during slow-wave (SW) sleep. Also, RSA phase delay is significantly reduced during REM sleep as compared to stage 2 and SW sleep. Here, *, ** and *** represent $p < 0.05$, $p < 0.01$ and $p < 0.0001$, respectively.

5. For further analysis to determine whether there are any significant differences in RSA during normal quiet sleep episodes between healthy and SDB children, data are analysed after removing all the sleep disordered breathing events (apnea, hypopnea and respiratory arousals) and spontaneous arousal episodes together with epochs before and after each.

8.2.3 Phase-averaged RSA

The evaluation of the pattern of RSA has already been discussed in Chapter 6, Section 6.2.3.

8.2.4 Statistical analysis

Two-way analysis of variance (ANOVA) for repeated measures is used to test for differences in RSA across groups and between sleep stages. Post-hoc analysis is performed using ANOVA. Data are expressed as mean \pm standard deviation (SD). Values with $p < 0.05$ are considered statistically significant.

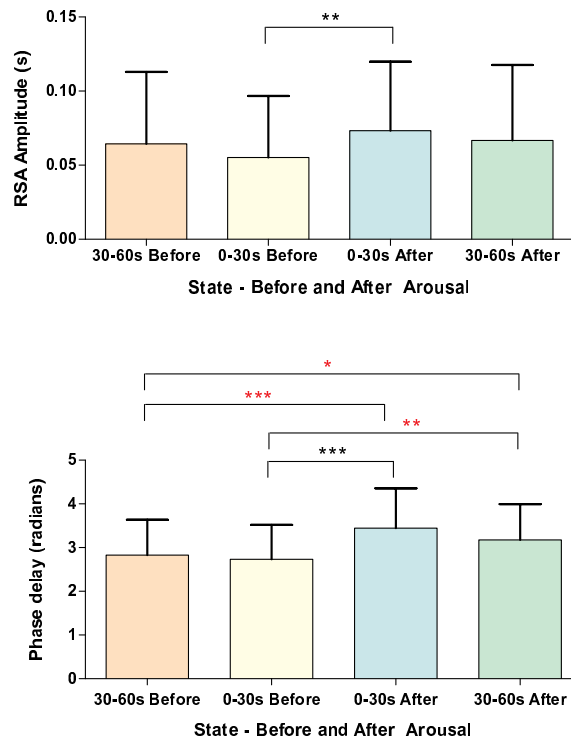


Figure 8.2. Effect of spontaneous arousals on RSA in healthy children. Magnitude and phase delay of RSA show strong association with spontaneous arousals and increase significantly during the first 30 seconds post-arousal compared to 30 seconds pre-arousal episode. Here, *,** and *** represent $p < 0.05$, $p < 0.01$ and $p < 0.0001$, respectively.

8.3 Results

8.3.1 Effect of sleep stage on RSA in healthy children

Mean amplitude of RSA show a strong association with sleep stages in healthy children and is significantly increased during SW sleep as compared to REM sleep (0.09 ± 0.04 vs. 0.06 ± 0.03 s, $p < 0.01$, respectively), see Fig. 8.1. A significant decrease in RSA phase delay during REM sleep compared to stage 2 and SW sleep is observed in healthy children (3.0 ± 0.06 vs. 3.1 ± 0.04 and 3.1 ± 0.04 rad, $p < 0.05$, respectively), see Fig. 8.1.

8.3 Results

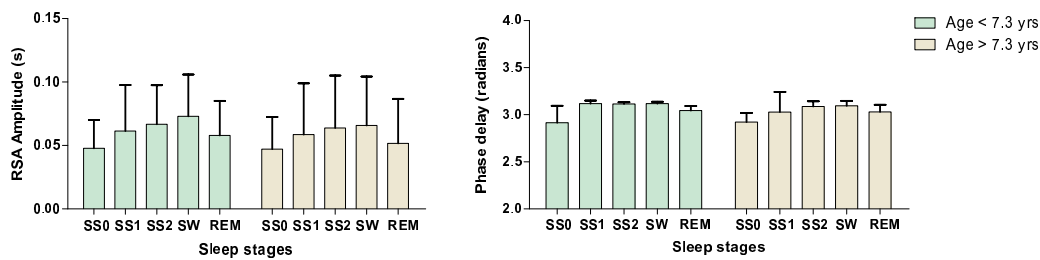


Figure 8.3. Age effect on RSA in healthy children. Comparing RSA magnitude and phase delay between two sub-groups comprising of 20 healthy children each, dichotomized based on the median age (median: 7.3 yrs), no significant differences are observed.

Table 8.1. Correlation analysis. Correlation between age and the magnitude and phase delay of RSA for different stages of sleep.

	Correlation coefficients and p -values	RSA magnitude				
		Awake	SS1	SS2	SW	REM
Age	r	-0.20	-0.20	-0.23	-0.27	-0.25
	p	0.24	0.22	0.16	0.10	0.12
	Correlation coefficients and p -values	RSA phase delay				
		Awake	SS1	SS2	SW	REM
Age	r	-0.07	-0.22	-0.21	-0.11	-0.11
	p	0.66	0.18	0.21	0.50	0.49

8.3.2 Effect of spontaneous arousals on RSA in healthy children

Respiratory sinus arrhythmia is associated with spontaneous arousals. Mean amplitude and phase delay of RSA is significantly increased during the first 30 seconds post-arousal episode compared to 30 seconds pre-arousal episode (mean amplitude: 0.07 ± 0.05 vs. 0.06 ± 0.04 s ($p < 0.01$) and phase delay: 3.4 ± 0.9 vs. 2.7 ± 0.8 rad ($p < 0.0001$), respectively), see Fig. 8.2.

8.3.3 Effect of age, gender and BMI on RSA in healthy children

There are no significant differences in magnitude and phase delay of RSA between the respective sleep stages of the two age groups (dichotomized based on median value: 7.3 yrs) of 20 healthy children each, as seen in Fig. 8.3. However, negative correlations

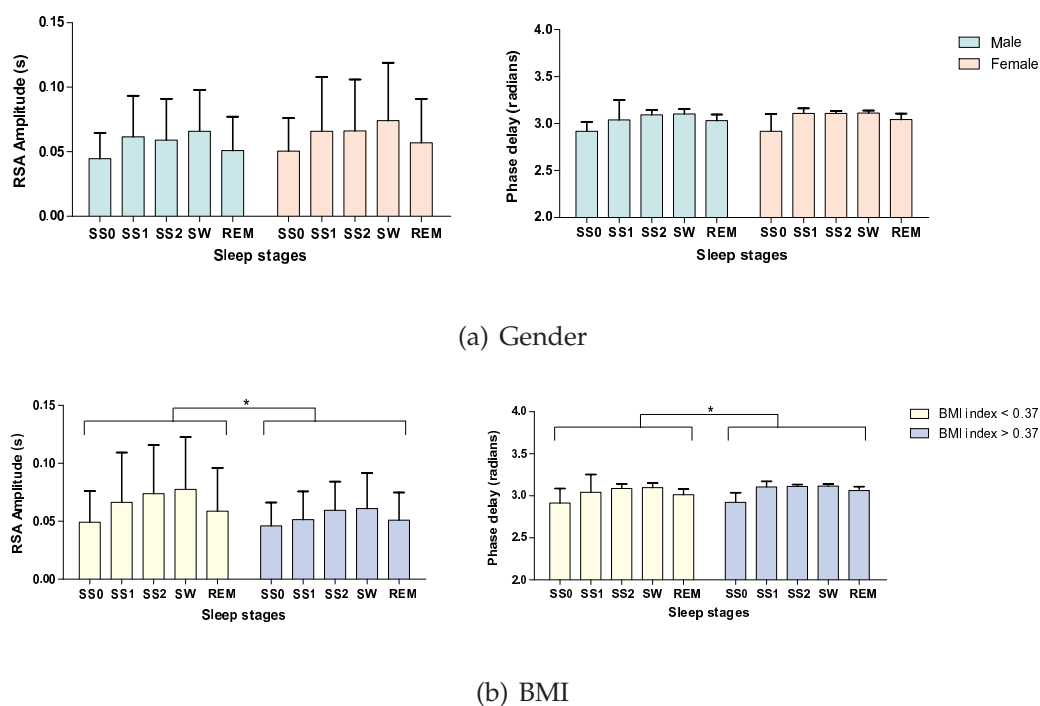


Figure 8.4. Gender and BMI effects on RSA in healthy children. Gender has no significant effect on the magnitude and phase delay of RSA. On the other hand, children with higher BMI index show a significant decrease in RSA magnitude and a significant increase in phase delay as compared to children with lower BMI index. Here, * represents $p < 0.05$.

between age and magnitude/phase delay of RSA for all the sleep stages are observed, as seen in Table 8.1. Also, gender has no significant effect on magnitude or phase delay of RSA in healthy children, see Fig. 8.4(a). However, children with higher BMI index show significant decrease in magnitude (for example, slow-wave sleep: 0.08 ± 0.05 vs. 0.06 ± 0.02 s) and significant increase in phase delay (for example, slow-wave sleep: 3.1 ± 0.05 vs. 3.2 ± 0.02 rad) of RSA compared to children with lower BMI index, as seen in Figure 8.4(b).

8.3.4 Effect of sleep stage on RSA in SDB children before removing SDB related events and comparison with healthy controls

The magnitude of RSA shows strong association with sleep stages in children with SDB and is significantly higher during slow-wave (SW) sleep compared to rapid-eye-movement (REM) sleep (0.08 ± 0.04 vs. 0.06 ± 0.04 s, $p < 0.05$, respectively), see Fig. 8.5. There are no significant differences in phase delay of RSA between sleep stages in

8.3 Results

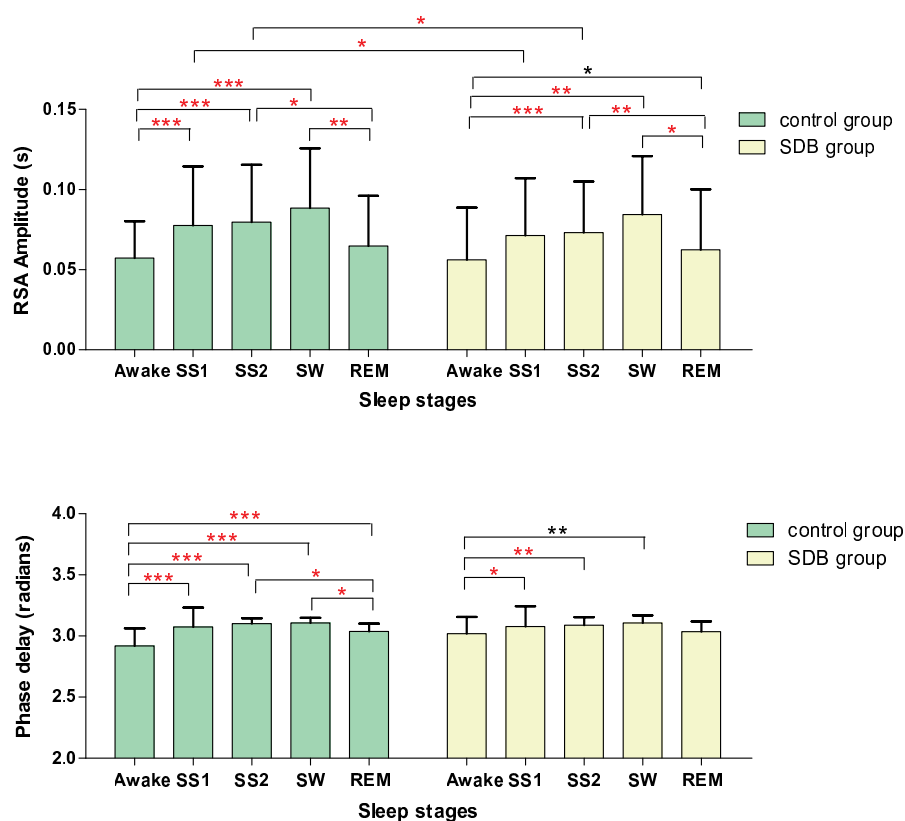


Figure 8.5. Group and sleep stage effects on RSA in children before removing SDB related events. Significant differences in RSA amplitude and phase delay between sleep stages are observed in children with SDB. Also, significant decrease in magnitude of RSA during stage 1 and stage 2 sleep of children with SDB compared to healthy children (healthy group) are observed. However, there are no significant differences in phase delay of RSA between the two groups. Here, *,** and *** represent $p < 0.05$, $p < 0.01$ and $p < 0.0001$, respectively.

children with SDB except for the awake stage, during which it is significantly lower compared to stage 1, stage 2 and SW sleep (3.0 ± 0.1 vs. 3.1 ± 0.2 rad ($p < 0.05$), 3.1 ± 0.1 rad ($p < 0.01$) and 3.1 ± 0.1 rad ($p < 0.01$), respectively), see Fig. 8.5.

Compared with healthy controls, significant decrease in magnitude of RSA during stage 1 and stage 2 sleep is observed in children with SDB (stage 1: 0.08 ± 0.04 vs. 0.07 ± 0.04 s ($p < 0.05$) and stage 2: 0.08 ± 0.04 vs. 0.07 ± 0.03 s ($p < 0.05$), respectively), see Fig. 8.5 (top panel), with no significant changes in phase delay.

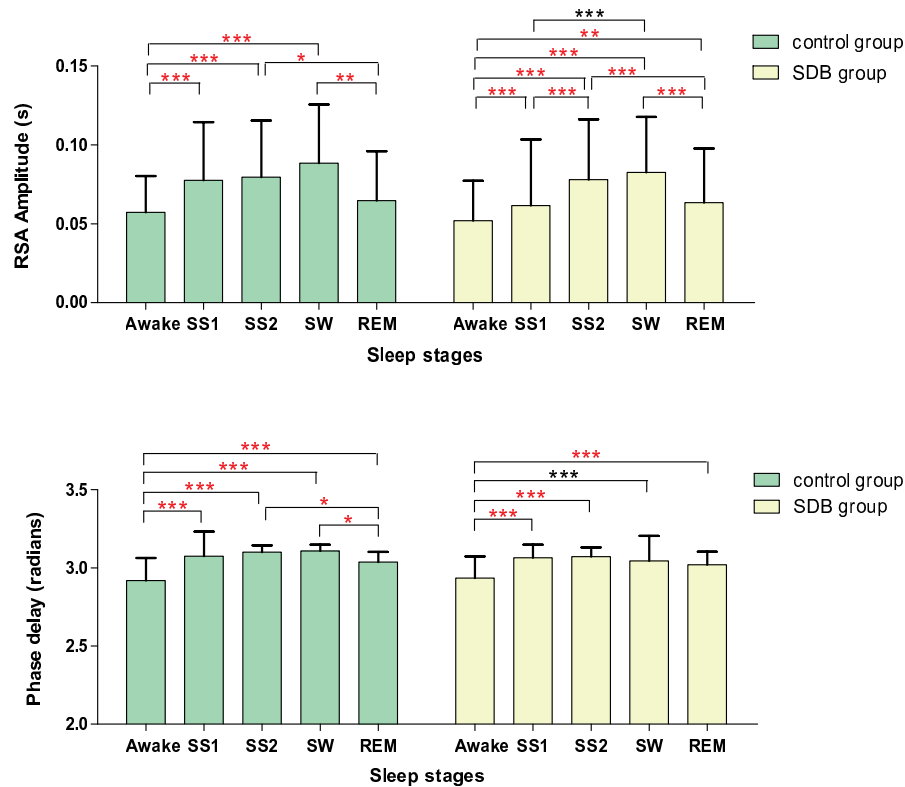


Figure 8.6. Group and sleep stage effects on RSA in children after removing SDB related events. Significant differences in magnitude and phase delay of RSA between sleep stages are observed in children with SDB. However, there are no significant differences in mean amplitude or phase delay of RSA between healthy children and children with SDB. Here, *, ** and *** represent $p < 0.05$, $p < 0.01$ and $p < 0.0001$, respectively.

8.3.5 Effect of sleep stage on RSA in SDB children after removing SDB related events and comparison with healthy controls

Analysing normal quiet sleep episodes in children with SDB, a significant increase in mean amplitude of RSA is observed during SW sleep as compared to REM sleep (0.08 ± 0.04 vs. 0.06 ± 0.03 s, $p < 0.0001$, respectively) as can be seen in Figure 8.6. However, there is no significant effect of sleep stage on RSA phase delay except for awake state, during which it is significantly lower compared to other sleep stages (Figure 8.6).

Excluding SDB related events from analysis in children with SDB has shown a significant increase in magnitude of RSA during stage 2 sleep compared to RSA magnitude computed with SDB related events (0.08 ± 0.03 vs. 0.07 ± 0.03 s, $p < 0.05$, respectively),

which has further removed the differences in magnitude of RSA during stage 1 and stage 2 sleep between healthy children and children with SDB, as seen in Figure 8.6.

8.4 Discussion

This is the first study to investigate respiratory sinus arrhythmia (RSA) in healthy children and children with sleep disordered breathing (SDB), and the association between spontaneous arousals and RSA during night-time sleep. The major findings are: (1) there is a strong association between RSA and sleep stages in healthy children and children with SDB; (2) RSA is the highest during slow-wave (SW) sleep; (3) there is a significant increase in RSA during 30 seconds post-arousal (spontaneous) episode compared to 30 seconds pre-arousal epoch; (4) RSA decreases with the increase in BMI index in healthy children; (5) a significant decrease in RSA is observed during stage 1 and stage 2 sleep in children with SDB as compared to healthy controls; and (6) there are no significant differences in RSA during normal/quiet sleep episodes in children with SDB (after removing SDB related events) as compared to healthy children, which is in line with the response of cardiorespiratory interaction reported in Chapter 7.

Variation in the sympathetic-vagal balance happens throughout the sleep cycles from non-rapid-eye-movement (NREM) sleep to rapid-eye-movement (REM) sleep (Brandenberger *et al.* 2001) with a switch from pronounced cardiac vagal tone during slow-wave (SW) sleep to sympathetic dominance during REM sleep (Buchheit *et al.* 2004). Slow-wave sleep—a parasympathetic state and the deepest stage of sleep is characterized by high electrocardiographic (ECG) stationarity and spontaneous regular respiratory patterns (Zemaityte *et al.* 1984, Buchheit *et al.* 2004). The presence of high parasympathetic tone during SW sleep (Zemaityte *et al.* 1984, Vanoli *et al.* 1995, Verrier *et al.* 1996) explains the prominence of RSA during SW sleep compared to other sleep stages in this study. Consequently, the suppression of cardiac efferent vagal tone explains the decrease in RSA during REM sleep in healthy children and children with SDB.

According to Morgan *et al.* (1996), arousal from sleep is linked to increase in heart rate in healthy subjects. We observe significant increase in RSA 0-30 seconds after an arousal episode possibly due to an increase in ventilatory response, which is in line with an earlier study by Blasi *et al.* (2002).

Aging is associated with the changes in sympathovagal balance, with a significant increase in sympathetic nervous system input to the cardiovascular system in old age (Pfeifer *et al.* 1983, De Meersman 1993). In adults, Hellman and Stacy (1976) reported a significant decrease in RSA with age. However, according to Marshall and Stevenson-Hinde (1998), the mean RSA increased across children with age span from 4.5 to 7 yrs while another study of subjects between 8 to 17 yrs of age reported no significant change in RSA (Salomon 2005). In our study, no significant differences in RSA between the two age groups (3.4-7.3 yrs and 7.3-12.6 yrs) consisting of 20 healthy children each, are observed. Further, using cross-correlation analysis, we find lack of correlation between age and RSA, suggesting that RSA is independent of age.

In this study, a significant decrease in RSA in children with sleep disordered breathing (SDB) has been observed during stage 1 and stage 2 sleep, as compared to healthy controls. In previous studies, increased sympathetic activity has been reported in adults and children with obstructive sleep apnea (Somers *et al.* 1995, Coy *et al.* 1996, Kadi-tis *et al.* 2009), which possibly explains the decrease in RSA in children with SDB. Since SDB related events (apnea, hypopnea and respiratory arousal episodes) are the main episodes during sleep that differentiate children with SDB from healthy controls, RSA is re-analysed in children with SDB during sleep after excluding the SDB related events from our analysis. Subsequently, no significant differences in RSA between healthy children and children with SDB is observed suggesting that the mechanism responsible for RSA remains unaffected during normal/quiet sleep episodes.

8.5 Chapter Summary

In this Chapter, we have investigated respiratory sinus arrhythmia (RSA) in healthy children and children with sleep disordered breathing (SDB). It appears that RSA significantly increases immediately after spontaneous arousal episode but returns to baseline after about 30 seconds—similar to our observation for cardiorespiratory interaction in children (Chapter 7). Also, it is observed that RSA is affected by SDB related events in children with SDB, but shows similar behavior to that of healthy controls during normal quiet sleep episodes.

The next Chapter will summarize the key findings of this Thesis and suggest directions for future work.

Chapter 9



Thesis conclusion and future work

THIS chapter summarizes the key findings of this Thesis and suggests directions for future work.

9.1 Introduction

Although the association between cardiac and respiratory rhythms and the clinical merit of its quantification has long been recognized, the development of an efficient technique for the effective detection and easy interpretation of cardiorespiratory interaction and its underlying physiological mechanisms has been a major challenge in this field of Biomedical Engineering. The primary factors that affect the detection and analysis of cardiorespiratory are signal noise and non-linear/non-stationary nature of physiological systems. Therefore, to overcome these issues, it is required to develop a technique that is less sensitive to noise, robust and possibly provides additional information about the interaction between cardiac rhythms and respiration. This Thesis has proposed an approach based on joint symbolic dynamics that shows improved performance in the detection of cardiorespiratory interaction compared to the synchrogram or phase-averaged respiratory sinus arrhythmia (RSA) technique. This Chapter summarizes the research and main findings of this Thesis that led to the successful discovery of the novel technique and discusses possible future directions for continued development of techniques for clinical research applications and understanding of physiological mechanisms in human body.

9.2 Thesis summary and conclusions

Chapter 1 provides brief review of the electrocardiogram (ECG) and respiratory signals and their processing techniques. It also discusses coupling between cardiac and respiratory signals and some of their quantification techniques.

Understanding the physiology and underlying mechanisms responsible for cardiorespiratory coordination is an important step towards improving its detection. It has long been known that cardiorythm is influenced by respiration (a phenomenon termed as respiratory sinus arrhythmia) that can further have influence on cardiorespiratory interaction. In Chapter 2, the influence of heart rate and respiration has been investigated independently in rats: first, applying isoflurane—a volatile anesthetic that affects the heart rate; second, changing the ventilation rates to investigate cardiorespiratory interaction under paced respiration. We have demonstrated that with the increase in the level of isoflurane there is a marked increase in heart rate and cardiorespiratory coordination. It has also been illustrated that the interaction between cardiac and respiratory cycles varies with the change in ventilation rates but is significantly increased

at a suitable choice of breathing frequency. Since the autonomic nervous system has a great influence on heart rate, investigating its role on the interaction between cardiac and respiratory cycles has been considered crucial. We have demonstrated that blockade of the parasympathetic nervous system caused a decrease while blockade of the sympathetic nervous system caused an increase in cardiorespiratory interaction, indicating that cardiorespiratory rhythms are strongly modulated and coordinated by the autonomic nervous system.

Although there have been several studies on respiratory physiology, one aspect of it received very little attention—the association between respiratory pattern and voluntary movement. In Chapter 3, we have investigated the impact of movement on respiratory rate and cardiorespiratory interaction in awake rats. This is the first study where a novel framework for analyzing respiratory-motor relations in small laboratory animals has been developed. To quantify motor activity, we have developed an index which we called the *movement power index*. From the study, we have illustrated a high extent of variability in the respiratory rate and heart rate during voluntary movement, and a strong association between respiration and movement. At rest or at low-intensity movements respiratory rate is observed to be lower and more variable compared to high-intensity movements when it is invariably high. It has been observed that the onset of respiratory rate acceleration either coincide with the onset of a movement or even slightly precede it, but is never delayed. However, significant changes in heart rate are only observed during longer bouts of movement. Also, a significant decrease in cardiorespiratory interaction has been illustrated during high-intensity movement as compared to low-intensity movement.

Quantification of cardiorespiratory interaction has been suggested to have clinical merit e.g. estimating the prognosis of cardiac diseases after myocardial infarction in patients. In Chapter 4 cardiorespiratory interaction during sleep has been assessed as a marker of cardiorespiratory system disturbances in a large cohort of adults children suffering from obstructive sleep apnea syndrome (OSAS). Although there has been a significant decrease in the interaction between cardiac and respiratory cycles with the severity of OSAS in adults, it remains unaffected during normal/quiet sleep episodes in children with sleep disordered breathing as compared to healthy controls. This suggests that the assessment of cardiorespiratory interaction may provide an ECG based screening tool for OSAS.

9.2 Thesis summary and conclusions

It has previously been reported that delays in coupling between two systems can have significant influence on their dynamical behaviour. Studies have shown that there exists a delay between phase of respiration and RR interval. Accordingly, in Chapter 5, we have introduced a modification of the synchrogram by incorporating an additional adaptive delay in the cardiac oscillator based on the maximisation of the cross-correlation or symbolic coupling traces between the phases of respiration and the delayed RR intervals. We have illustrated that the modification in the synchrogram technique by including an adaptive delay in the cardiac oscillator substantially enhances the sensitivity of the detection of cardiorespiratory coordination.

Data analysis using symbolic dynamics has become a topic of interest in recent years due to its reliability. Although the time delay introduced in Chapter 5 has provided enhanced detection of cardiorespiratory interaction, our interest in a relatively simple approach that potentially shows reliable improved performance and provides additional information resulted in the development of a novel technique based on joint symbolic dynamics (JSD) for the detection of cardiorespiratory interaction. In Chapter 6, we have introduced a novel approach to quantify cardiorespiratory interaction that is based on the joint symbolic dynamics of respiratory phase and heart rate. We have illustrated that the JSD approach reveals significant differences in the cardiorespiratory interaction in different body postures and is more sensitive to postural changes than phase-averaged respiratory sinus arrhythmia pattern analysis.

In order to test the efficiency of JSD approach and its ability to quantify cardiorespiratory interaction in patients suffering from obstructive sleep apnea syndrome (OSAS), we have applied the JSD approach in children and adults with OSAS discussed in Chapter 4. As expected, our proposed JSD approach has verified the ability to provide improved performance even in patients with OSAS. We have further demonstrated that cardiorespiratory interaction is associated with spontaneous arousals.

Respiratory sinus arrhythmia (RSA) reflects the status of the parasympathetic nervous system at rest and has been suggested as an appropriate index of vagal activity for research with children. In Chapter 8 we have studied the influence of sleep stages and sleep disordered breathing (SDB) on RSA in children. We have demonstrated that RSA is associated with sleep stage and is affected by SDB related events in children with SDB but remains unaffected during normal quiet sleep episodes as compared to healthy controls.

9.3 Potential future directions

In summary, this Thesis has explored the interaction between cardiac rhythm and respiration in humans and rats, and has discussed some of the mechanisms that are directly or indirectly associated with it. Our proposed methodology based on joint symbolic dynamics has shown improved performance in the detection of cardiorespiratory interaction and hence can be useful for clinical research applications. Here, we discuss in brief, some of the directions in which this work can be advanced further.

9.3.1 Early detection of diseases

In this Thesis we have investigated adults suffering from obstructive sleep apnea syndrome (OSAS) and observed a significant decrease in cardiorespiratory response/interaction with the severity of OSAS. In future studies, it would be interesting to investigate if cardiorespiratory interaction is affected even before the development/early stages of OSAS and whether the treatment of OSAS improves the interaction between cardiac and respiratory cycles.

9.3.2 Assessment of stress and mental-disorders

Breathing is influenced by and responds to emotions such as happiness, anxiety or fear. The relationship between emotion and respiration is reflected in numerous expressions such as “breathtaking” and “a sigh of relief”. Abnormal breathing has been observed in various behavioural and mental disorders, e.g. panic disorder and depression. Future study on cardiorespiratory interaction in subjects suffering from stress or mental-disorders may provide us with information on physiological processes and patho-physiological changes.

9.3.3 Cardiorespiratory interaction during inspiration and expiration

Previous techniques used for the quantification of interaction between cardiac rhythms and respiration (for example, synchrogram technique or phase-averaged analysis of RSA pattern) utilize complete/full respiratory cycles for analysis. With the joint symbolic dynamics approach, partial respiratory cycles can be used which gives the opportunity to analyse cardiorespiratory interaction independently for inspiration and

9.4 Summary of author's original contributions

expiration. The experiment can be carried out for different inspiration to expiration time ratios for investigating if cardiorespiratory interaction varies between inspiration and expiration and if varying inspiration to expiration ratios has any effect on cardiorespiratory interaction.

9.4 Summary of author's original contributions

In summary, the key contributions are as follows:

- **Influence of autonomic nervous system and isoflurane on cardiorespiratory interaction:** Through experimental studies, carried out in rats, this Thesis demonstrates that isoflurane, forced ventilation and autonomic nervous system has influence on cardiorespiratory interaction (Kabir *et al.* 2008, Kabir *et al.* 2009),
- **Effect of voluntary movement on respiration:** A novel framework for analyzing respiratory-motor relations in small laboratory animals has been developed for the first time. This Thesis illustrates a strong association between movement and respiration, and also between movement and cardiorespiratory interaction (Kabir *et al.* 2010a, Kabir *et al.* 2010c),
- **Cardiorespiratory interaction as a marker for sleep apnea:** This Thesis demonstrates that quantification of cardiorespiratory interaction in patients suffering for obstructive sleep apnea syndrome (OSAS) can be used to identify the severity of OSAS (Kabir *et al.* 2010b),
- **Time delay correction of synchrogram:** This Thesis illustrates that the modification in the synchrogram technique by including an adaptive delay in the cardiac oscillator substantially enhances the sensitivity of the detection of cardiorespiratory coordination (Kabir *et al.* 2011c),
- **Joint symbolic dynamics:** This Thesis introduces a novel approach to quantify cardiorespiratory interaction that is based on the joint symbolic dynamics of respiratory phase and heart rate. We have illustrated its ability to provide improved performance by comparing it with other techniques (Kabir *et al.* 2011d, Kabir *et al.* 2011b, Kabir *et al.* 2011a),
- **Respiratory sinus arrhythmia in children:** A detailed study on RSA during sleep in healthy children and children suffering from sleep disordered breathing (SDB)

has been carried out for the first time. This Thesis demonstrates that RSA is associated with sleep stages and SDB in children.

9.5 In closing

This Chapter summarises the major findings and conclusions of this Thesis accompanied by recommendations for future work. This Thesis has made a number contributions towards understanding some of the physiological functioning in a human body, through quantification of cardiorespiratory interaction. The work herein is unique and original, laying groundwork for an improved detection of cardiorespiratory interaction for future clinical research applications.

Appendix A



Influence of age on cardiorespiratory interaction

THIS appendix investigates the influence of age on the interaction between cardiac and respiratory cycles in healthy subjects using the approach based on joint symbolic dynamics.

A.1 Introduction

Symbolic dynamics, a concept which provides a simplified description of the system's dynamics through transformation of the time series into a symbol sequence achieved by a coarse-graining procedure, has successfully been applied in several studies (Voss *et al.* 1996, Baumert *et al.* 2002, Baumert *et al.* 2005) and in the quantification of cardiorespiratory interaction (Schiek *et al.* 1998, Kabir *et al.* 2011d). It has been suggested in Chapter 6 that data analyses using joint symbolic dynamics (JSD) provide improved performance compared to time-domain techniques (Caminal *et al.* 2005, Kabir *et al.* 2011d).

Also, in Chapter 5, it has been suggested that the delay in heart rhythm in regard to the respiratory cycle should be taken into account in the study of interaction between cardiac and respiratory rhythms, as this substantially enhances the sensitivity of the detection of cardiorespiratory interaction (Kabir *et al.* 2011c).

In this Chapter, we apply the approach based on joint symbolic dynamics in healthy subjects while taking the delay in heart cycle into account to study the effect of age on cardiorespiratory interaction. It is hypothesized that cardiorespiratory interaction decreases with age.

A.2 Methods

A.2.1 Subjects

Here, ECG and respiratory signals of two groups of healthy subjects, 20 young (range: 21-34 yrs, mean: 27 yrs) and 20 elderly (range: 68-85 yrs, mean: 74 yrs) from the Physionet database (<http://physionet.org/physiobank/database/fantasia/>) were collected for this study. Each group consisted of 10 men and 10 women. Subjects were non-smokers and had no medical condition/history.

A.2.2 Processing of ECG and respiratory signal

The sampling rate of ECG and respiratory signals were 250 Hz and the recording time was 120 minutes in the supine position for each subject. Custom written computer software developed under MATLAB[®] is used to detect the R-peaks from the recorded

ECG signal using parabolic fitting, described in Chapter 1, Section 1.4.1. The RR time series are visually scanned for artifacts.

To remove noise, as discussed in Chapter 1, Section 1.4.2, respiratory signals are low-pass filtered at 1.0 Hz using a zero-phase forward and reverse digital filter, which first filtered the raw signal in the forward direction using a 4th order Butterworth filter, and subsequently filtered the reversed signal. The phases of the filtered respiratory signal are calculated using the Hilbert transform.

A.2.3 Calculation of time delays for enhanced detection of cardiorespiratory interaction

The time delay in the RR time series is calculated using cross-correlation analysis discussed in Chapter 5, Section 5.2.4.

A.2.4 Joint symbolic dynamics

The RR time series and respiratory phases at the instants of R-peaks are transformed into symbolic sequences and words based on the transformation rule described in Chapter 6, Table 6.1 and Section 6.2.3.

A.2.5 Statistical analysis

GraphPad Prism version 5.01 for Windows (GraphPad Software, San Diego California USA, www.graphpad.com) is used for statistical analysis. Considering normally distributed data, we investigate cardiorespiratory interaction between two age groups using Student's t-test. Values with $p < 0.05$ are considered statistically significant. Data are expressed as mean \pm standard deviation (SD).

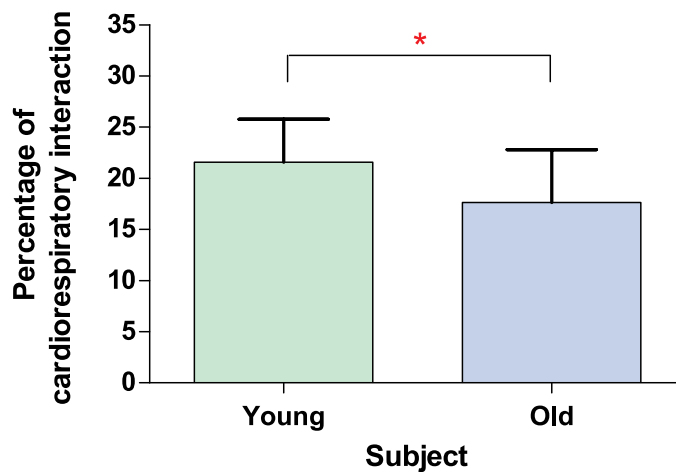


Figure A.1. Cardiorespiratory interaction vs. age. Figure showing the affect of age on cardiorespiratory interaction using original RR intervals. Elderly subjects show a lower percentage of interaction compared to young subjects. Here, * represents $p < 0.05$.

A.3 Results

A.3.1 Age effect on cardiorespiratory interaction using original RR interval

Using original RR interval, the interaction between cardiac and respiratory cycles shows significant decrease in elderly subjects as compared to young subjects (17.6 ± 5.1 vs. 21.6 ± 4.2 %, $p < 0.05$, respectively), see Figure A.1.

A.3.2 Age effect on cardiorespiratory interaction using delayed RR interval

After choosing the delayed RR interval that provides the highest correlation with the respiratory phases, cardiorespiratory interaction shows a relative and more significant decrease in elderly subjects as compared to young subjects (16.5 ± 6.6 vs. 22.8 ± 6.7 %, $p < 0.01$, respectively), see Figure A.2.

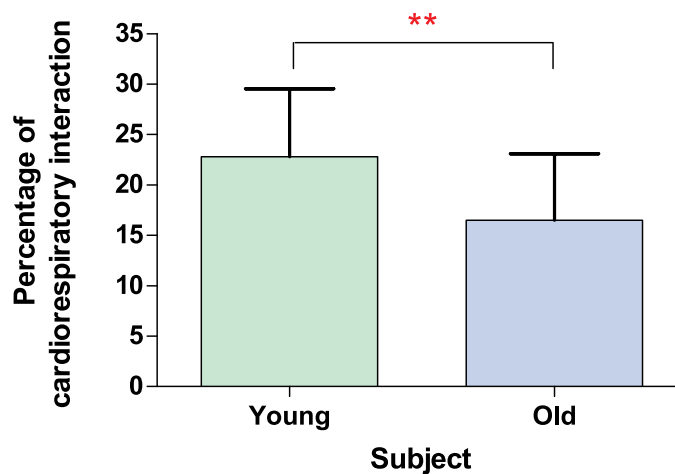


Figure A.2. Cardiorespiratory interaction vs. age using delayed RR interval. Figure showing the effect of age on cardiorespiratory interaction using delayed RR intervals. By appropriate delaying of the RR time series, an increase in the overall percentage of interaction in young subjects and more significant difference in cardiorespiratory interaction between young and elderly subjects is observed. Here, ** represents $p < 0.01$.

A.4 Discussion

In this Chapter, the approach based on joint symbolic dynamics, designed for the detection of cardiorespiratory interaction, is used to determine the influence of age. A significant decrease in cardiorespiratory interaction is observed in elderly subjects as compared to young subjects.

Respiratory sinus arrhythmia (RSA), modulation of heart rate by respiration, is influenced by age and is more prominent in children than in adults (Hrushesky *et al.* 1984, Yasuma and Hayano 2004). Our analysis based on joint symbolic dynamics shows a significant decrease in cardiorespiratory interaction in elderly subjects compared to young subjects. Also, more significant differences are observed after introducing a time delay between cardiac and respiratory symbol strings based on the highest correlation between RR intervals and respiratory phases, which is in line with our previous studies (Kabir *et al.* 2011d, Kabir *et al.* 2011c).

From this study it appears that the approach based on joint symbolic dynamics provides a simple technique for the effective quantification of interaction between two non-linearly coupled systems.


A.5 Summary

The study shows that cardiorespiratory interaction in healthy subjects is influenced by age and is more prominent in young subjects as compared to elderly subjects. It further emphasizes that joint symbolic dynamics provides a simple and more efficient tool to quantify the relation between cardiac and respiratory rhythms.

Appendix B



Respiratory sinus arrhythmia and cardiorespiratory phase coordination



THIS appendix investigates the relation between respiratory sinus arrhythmia (RSA) and cardiorespiratory phase coordination (CRC) by comparing RSA during CRC, with the RSA immediately before and after the CRC episode.

B.1 Introduction

Respiratory sinus arrhythmia (RSA) is the change in heart rate variability (HRV) induced by respiration (Grossman and Taylor 2007); during which the heart rate increases at inspiration and decreases at expiration (Bonsignore *et al.* 1995). Also, respiration and cardiac rhythms are weakly coupled (known as synchronization), whose patterns differ at different breathing rhythms and are transient rather than permanent phenomena, with a driving effect of respiration on HRV (Schafer *et al.* 1998, Censi *et al.* 2000). Respiratory sinus arrhythmia is a physiological phenomena reflecting cardiorespiratory interaction (Hayano and Yasuma 2003). Cardiorespiratory interaction similar to RSA has been reported in species of vertebrates from fishes to mammals and birds (Taylor *et al.* 1999), indicating a strong biological phenomenon throughout the evolution (Hayano and Yasuma 2003).

Respiratory sinus arrhythmia (RSA), which is the synchronization between respiration and HRV, has long being been investigated in previous studies (Hirsch and Bishop 1981, Saul *et al.* 1991, Taha *et al.* 1995, Bettermann *et al.* 2000, Neff *et al.* 2003, Yasuma and Hayano 2004, Kabir *et al.* 2011d) but its relation with cardiorespiratory phase coordination has never been studied. In this Chapter, we investigate the association between RSA and cardiorespiratory phase coordination by comparing the RSA prior to, during and after a coordinated epoch.

B.2 Methods

B.2.1 Subjects / Experimental protocol

Ten healthy subjects (5 males, 5 females) participated in this study. The age of the subjects ranged between 19-24 years. The study conformed to the principles outlined in the Declaration of Helsinki and was approved by the institution's human research ethics committee. Subjects gave informed consent.

The protocol included 10 minutes of ECG and respiration recording for different body postures. The subjects underwent graded head-up tilt test at angles: 0, 30 and 60° during controlled metronomic breathing at 15 bpm. The subjects were instructed not to speak and to remain absolutely motionless during the recording.

Herein, ECG (leads I and II) and respiratory signals (from abdomen impedance belts) were sampled at 1 kHz and recorded using a PowerLab data acquisition system (ADInstruments, Sydney, Australia) and the ChartPro 6.0 software (ADInstruments, Sydney, Australia), as described in Chapter 5.

B.2.2 Processing of ECG and Respiratory signal

The ECG and respiratory signals are processed as described in Chapter 1, Sections 1.4.1 and 1.4.2. The RR time series are visually scanned for artifacts. Although the R-peaks are correctly identified, we have encountered a few ectopic beats that are manually replaced with the average RR interval calculated from the beats prior to and after the ectopy. The respiratory signals are low-pass filtered at 1.0 Hz to remove noise.

B.2.3 Cardiorespiratory phase coordination and RSA pattern analysis

The coordination between cardiac and respiratory cycles is determined using cardiorespiratory coordination analysis described in Chapter 1.1, Section 1.7.2. The duration of each coordinated epoch is noted and epochs of similar duration before and after each coordinated epoch are selected for RSA analysis. The coordinated epochs that are shorter than 5 seconds are excluded for this analysis.

The evaluation of the pattern of RSA has already been discussed in Chapter 6, Section 6.2.3.

Statistical analysis

GraphPad Prism version 5.01 for Windows (GraphPad Software, San Diego California USA, www.graphpad.com) is used for statistical analysis. The magnitude and phase delay of RSA before, during and after cardiorespiratory phase coordination for different body postures are compared using non-parametric repeated measure analysis of variance (Wilcoxon matched pairs test, Friedman test and Dunn's multiple comparison test). Values with $p < 0.05$ are considered statistically significant. Data are expressed as mean \pm standard deviation (SD).

B.3 Results

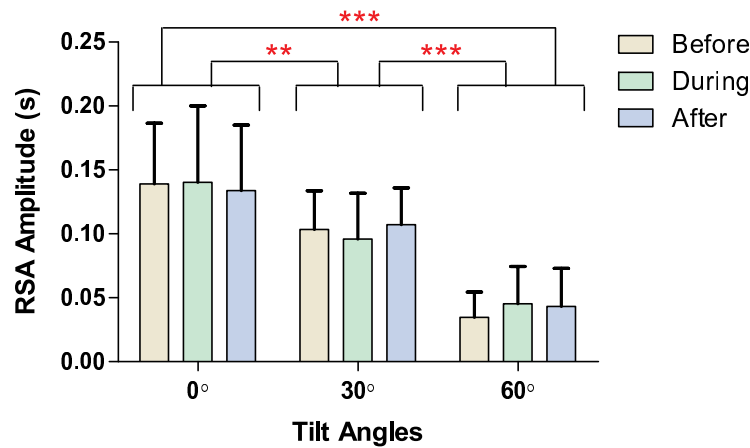


Figure B.1. RSA magnitude and cardiorespiratory phase coordination. Although the magnitude of RSA significantly decreased with the increase in tilt angles, there was no significant change in RSA amplitude before, during and after the occurrence of cardiorespiratory phase coordination.

B.3 Results

B.3.1 Duration of coordinated epochs

Since the main focus of this study is to analyse magnitude and phase delay of RSA, the results for percentage of cardiorespiratory phase coordination has not been reported. However, the average duration of coordinated epochs is reported, being required for selecting the duration of epochs before and after a coordinated epoch for RSA analysis.

Increase in head-up tilt angles during controlled breathing show a significant decrease in average duration of coordinated epoch (0 vs. 60°: 9.2 ± 2.3 vs. 7.0 ± 2.1 %, $p < 0.05$).

For more information on the effect of postural changes on cardiorespiratory phase coordination, please refer to Chapter 5.

B.3.2 Association between RSA and cardiorespiratory phase coordination

Increase in head-up tilt angles from 0 to 30 and 60° results in significant decrease in magnitude and significant increase in phase delay of RSA in all the three stages: prior to, during and in post-coordinated episodes, as seen in Figures B.1 and B.2. However,

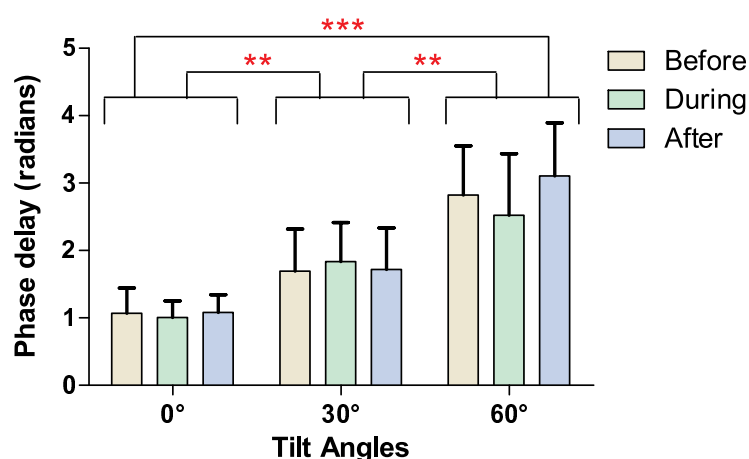


Figure B.2. RSA phase and cardiorespiratory phase coordination. Although there was a significant increase in the phase delay of RSA with the increase in tilt angles, no significant change in RSA phase delay was observed before, during and after the occurrence of cardiorespiratory phase coordination.

there are no significant differences in magnitude or phase delay of RSA among the pre-, during and post-stages of coordinated epochs for all the head-up tilt angles.

B.4 Discussion

This is a preliminary study investigating the association between respiratory sinus arrhythmia and cardiorespiratory phase coordination. We have analysed respiratory sinus arrhythmia (RSA) for different body postures during a cardiorespiratory phase coordination of duration equal to or greater than 5 seconds, and for episodes of similar duration before and after the coordinated epoch. According to this study, no significant differences in RSA prior to, during and in post-coordinated epoch are observed.

According to Yasuma and Hayano (2004), RSA improves respiratory efficiency by the pairing of increases in heart rate with inhalation. However, this phase relationship only occurs under specific circumstances and is specifically relevant for sympathetically mediated heart rate variability, or for respiratory sinus arrhythmia associated with slow breathing (Vaschillo *et al.* 2004). The phase relationship between heart rate and respiration is nonlinear but shows frequency dependence (Eckberg 1983). It is reported that the prolongation of the RR interval begins shortly after the onset of expiration and is independent of respiratory frequency, while the shortening of the RR interval begins progressively earlier in reference to the onset of inspiration with

B.5 Summary

the decrease in respiratory frequency (Eckberg 1983). This would suggest that the timing of the maximum instantaneous heart rate occurs instantly after end of inspiration (Vaschillo *et al.* 2004). Also, an increase in detection of the interaction between cardiac and respiratory rhythms has been observed after incorporating the delay in R-peak in regard to the onset of respiration (Chapter 5), which could be explained by the possible involvement of mechanisms such as the well known respiratory influence on cardiac timing (respiratory sinus arrhythmia) and influences of heart on respiratory timing through the baroreceptor nerves (Tzeng *et al.* 2007). Accordingly, we expected to observe a higher RSA during cardiorespiratory phase coordination compared to RSA during pre- and post-coordinated episodes. However, in this study, no significant differences are observed.

Our observation is supported by an earlier study by Rosenblum *et al.* (1998) who stated: 'It appears that subjects with epochs of synchronization between the cardiac and respiratory rhythm have no remarkable respiratory modulated heart rate fluctuations, whereas the subjects with the higher RSA exhibit no distinct epochs of cardiorespiratory synchronization'. According to Schafer *et al.* (1999), the phase locking of cardiac rhythms and respiration, and the respiratory modulation of heart rate, are 'two competing aspects of cardiorespiratory interaction'. However, further studies are required to better understand the underlying mechanisms and relation between RSA and cardiorespiratory phase coordination.

B.5 Summary

In this appendix, we have investigated the association between respiratory sinus arrhythmia (RSA) and cardiorespiratory phase coordination. From this study, it appears that RSA during a cardiorespiratory phase coordination is not significantly different from RSA before and after a coordinated episode.

Appendix C



Matlab Codes

THIS appendix presents some of the Matlab algorithms used in this Thesis. These algorithms are available as m-files on the attached DVD-ROM.

C.1 Detection of R-peaks

```
%%%%%%%%%%%%%%%%%%%%%%%%%%%%%%%%%%%%%%%%%%%%%%%%%%%%%%%%%%%%%%%%%%%%%%%%
%      Matlab code for detection of R-peaks of ECG signal      %
%      using parabolic fitting                                %
%                                                            %
% Muammar M. Kabir                                          %
% The University of Adelaide                                %
% September 2008                                           %
%%%%%%%%%%%%%%%%%%%%%%%%%%%%%%%%%%%%%%%%%%%%%%%%%%%%%%%%%%%%%%%%%%%%%%%%

clear all
close all
clc

time=[]; ECG=[];

% Extract time and ECG signal from saved file 'A'
A=load('A.txt');
time=A(:,1);
ECG=A(:,2);
sfreq=1000;

% Filter ECG signal
ECGFilter=[];
[b,a] = butter(4,(30/(sfreq/2)));
ECGFilter = filtfilt(b,a,ECG);

% Setting for Parabolic fitting
width=10; % It can be varied based on resolution
halfWindow=(1/width):(1/width):1;
fullWindow=sqrt([halfWindow,1,flipr(halfWindow)]);

% Processing ECG with parabola
rebuiltECG=[]; ECGpar1=[]; ECGpar2=[];
parabolaWin = [-(+width:width).^2]', ones(2*width+1,1)];
parabolaWin = fullWindow(:,[1 1]) .* parabolaWin;
parabolaWinInv = inv(parabolaWin'*parabolaWin)*parabolaWin';
for parCT=(width+1):(length(ECGFilter)-width)
    ECGwin = ECGFilter((parCT-width):(parCT+width));
    ECGwin = fullWindow.*ECGwin;
    ECGpoints = parabolaWinInv*ECGwin;
end
```

```

    ECGpar1(parCT) = ECGpoints(1);
    ECGpar2(parCT) = ECGpoints(2);
end
rebuiltECG = ECGpar1.*ECGpar2; % scaled ECG

%Sort rebuiltECG
sortedrebuiltECG=[];
sortedrebuiltECG=sort(rebuiltECG);

%Assign '0' to 95% of the lower ECG values
ECGvalue95p = sortedrebuiltECG(round(length(sortedrebuiltECG)*0.95));
rebuiltECG(find(rebuiltECG<ECGvalue95p)) = 0;

%Find R-peaks (maximum point)
cqSamples = round(0.25*sfreq); %consecutive samples - 25% sampling ...
    frequency
RpeaksIndex=[]; RpeakCT=1;
RWstartPT = 1; % R-wave start point
RWendPT = 0; % R-wave end point
for rpCT=(1+cqSamples):length(rebuiltECG)-cqSamples
    if any(rebuiltECG(rpCT)) & ~any(rebuiltECG((rpCT-cqSamples):(rpCT-1)))
        RWstartPT = rpCT;
    end
    if any(rebuiltECG(rpCT)) & ~any(rebuiltECG((rpCT+1):(rpCT+cqSamples)))
        RWendPT = rpCT;
        [val,idx] = max(rebuiltECG(RWstartPT:RWendPT));
        RpeaksIndex(RpeakCT) = idx + RWstartPT - 1;
        RpeakCT = RpeakCT+1;
    end
end

timeRpeak=[]; ECGrpeak=[];
timeRpeak = time(RpeaksIndex); %time of R-peaks
ECGrpeak = ECGFilter(RpeaksIndex); %R-peaks

figure(1);
plot(time,ECGFilter); hold on; plot(timeRpeak,ECGrpeak,'.r'); hold off

%RR interval
rrint=[];
tint=[];
for i=1:length(timeRpeak)-1

```

C.1 Detection of R-peaks

```
    rrint(i)=timeRpeak(i+1)-timeRpeak(i);  
    tint(i)=timeRpeak(i+1);  
end  
  
figure(2);  
plot(tint,rrint);
```

C.2 Detection of inspiratory and expiratory onsets

```

%%%%%%%%%%%%%%%%%%%%%%%%%%%%%%%%%%%%%%%%%%%%%%%%%%%%%%%%%%%%%%%%%%%%%%%%
%   Matlab code for detection of inspiratory onset (minima)           %
%   and expiratory onset (maxima)                                     %
%                                                                 %
% Muammar M. Kabir                                                  %
% The University of Adelaide                                         %
% November 2008                                                      %
%%%%%%%%%%%%%%%%%%%%%%%%%%%%%%%%%%%%%%%%%%%%%%%%%%%%%%%%%%%%%%%%%%%%%%%%

clear all
close all
clc

time=[]; Respiration=[];

% Extract time and respiratory signal from saved file 'A'
A=load('A.txt');
time=A(:,1);
Respiration=A(:,2);
sfreq=1000;

%Setting start time to 0+(1/sfreq)
time=time-time(1)+(1/sfreq);
tmax = max(time);
tmin = min(time);
tdiff = tmax - tmin;

%Filter Respiration
RespFilter=[];
[b,a] = butter(4,(1/(sfreq/2)));
RespFilter = filtfilt(b,a,Respiration);

figure(1);
plot(time,Respiration); hold on; plot(time,RespFilter,'r'); hold off;

xder=[];
xder = diff(RespFilter);

%Minima Detection
maxminr = [];

```

C.2 Detection of inspiratory and expiratory onsets

```
maxminpos = [];  
maxminpost=[];  
  
j=1;  
for i=1:length(xder)  
    if xder(i)<1.5 & xder(i)>=0 % xder(i)<1.5 xder(i)<1.0  
        maxminr(j) = RespFilter(i);  
        maxminpos(j) = i;  
        maxminpost(j)= time(i); % position in time (s)  
        j=j+1;  
    end  
end  
  
figure(2);  
plot(RespFilter);  
hold on;  
plot(maxminpos,maxminr,'.r');  
hold off;  
  
maxi=[]; maxipos=[]; maxipost=[];  
mini=[]; minipos=[]; minipost=[];  
k=1;  
  
if length(maxminr)==0  
    continue;  
end  
  
mini(1) = maxminr(1);  
minipos(1) = maxminpos(1);  
minipost(1) = maxminpost(1);  
  
for i=2:length(maxminr)-1  
    if (maxminr(i-1)-maxminr(i))<(maxminr(i)-maxminr(i+1))...  
        & (maxminr(i)-maxminr(i+1))>0  
        maxi(k) = maxminr(i);  
        maxipos(k) = maxminpos(i);  
        maxipost(k) = maxminpost(i);  
        mini(k+1) = maxminr(i+1);  
        minipos(k+1) = maxminpos(i+1);  
        minipost(k+1) = maxminpost(i+1);  
        k=k+1;  
    end  
end
```



```
    end
end

minifinal=[]; miniposfinal=[]; minipostfinal=[]; l1=1;
cont1=0;
for c1=1:length(minipost)-1
    if cont1==1
        cont1=0;
        continue;
    end
    if abs(minipost(c1+1)-minipost(c1))<0.1
%         cont1=1;
        if mini(c1+1)<mini(c1)
            minifinal(l1)=mini(c1+1);
            miniposfinal(l1)=minipos(c1+1);
            minipostfinal(l1)=minipost(c1+1);
            l1=l1+1;
            cont1=1;
        else
            minifinal(l1)=mini(c1);
            miniposfinal(l1)=minipos(c1);
            minipostfinal(l1)=minipost(c1);
            l1=l1+1;
        end
    else
        minifinal(l1)=mini(c1);
        miniposfinal(l1)=minipos(c1);
        minipostfinal(l1)=minipost(c1);
        l1=l1+1;
    end
end
minifinal(l1) = mini(end);
miniposfinal(l1) = minipos(end);
minipostfinal(l1) = minipost(end);
maxifinal=[]; maxiposfinal=[]; maxipostfinal=[]; l2=1;
cont2=0;
for c2=1:length(maxipost)-1
    if cont2==1
        cont2=0;
        continue;
    end
```

C.2 Detection of inspiratory and expiratory onsets

```
if abs(maxipost(c2+1)-maxipost(c2))<0.3
    cont2=1;
    if maxi(c2+1)>maxi(c2)
        maxifinal(l2)=maxi(c2+1);
        maxiposfinal(l2)=maxipos(c2+1);
        maxipostfinal(l2)=maxipost(c2+1);
        l2=l2+1;
    else
        maxifinal(l2)=maxi(c2);
        maxiposfinal(l2)=maxipos(c2);
        maxipostfinal(l2)=maxipost(c2);
        l2=l2+1;
    end
else
    maxifinal(l2)=maxi(c2);
    maxiposfinal(l2)=maxipos(c2);
    maxipostfinal(l2)=maxipost(c2);
    l2=l2+1;
end
end
maxifinal(l2) = maxi(end);
maxiposfinal(l2) = maxipos(end);
maxipostfinal(l2) = maxipost(end);
minifinaltemp=[]; tc1=1;
for tt1=1:length(minifinal)-1
    for tt2=1:length(maxifinal)
        if maxipostfinal(tt2)>minipostfinal(tt1)...
            & maxipostfinal(tt2)<minipostfinal(tt1+1)
            if maxifinal(tt2)-minifinal(tt1)<0.03
                minifinaltemp(tc1)=minifinal(tt1);
                tc1=tc1+1;
            elseif maxifinal(tt2)-minifinal(tt1+1)<0.03
                minifinaltemp(tc1)=minifinal(tt1+1);
                tc1=tc1+1;
            else
                continue;
            end
        end
    end
end
end
minifinal2=[]; miniposfinal2=[]; minipostfinal2=[]; n1=1;
```

```
bk1=0;
for c3=1:length(minifinal)
    bk1=0;
    for c4=1:length(minifinaltemp)
        if minifinal(c3)==minifinaltemp(c4)
            bk1=1;
            break;
        end
    end
    if bk1==1 | minifinal(c3)>0
        continue;
    else
        minifinal2(n1)=minifinal(c3);
        miniposfinal2(n1)=miniposfinal(c3);
        minipostfinal2(n1)=minipostfinal(c3);
        n1=n1+1;
    end
end

%Reprocessing minima
minifinaltemp2=[]; tc1=1;
for tt1=1:length(minipostfinal2)-1
    if minipostfinal2(tt1+1)-minipostfinal2(tt1)<2.0
        if minifinal2(tt1)<minifinal2(tt1+1)
            minifinaltemp2(tc1)=minifinal2(tt1+1);
            tc1=tc1+1;
        else
            minifinaltemp2(tc1)=minifinal2(tt1);
            tc1=tc1+1;
        end
    end
end

minifinal3=[]; miniposfinal3=[]; minipostfinal3=[]; n1=1;
bk1=0;
for c3=1:length(minifinal2)
    bk1=0;
    for c4=1:length(minifinaltemp2)
        if minifinal2(c3)==minifinaltemp2(c4)
            bk1=1;
        end
    end
end
```

C.2 Detection of inspiratory and expiratory onsets

```
        break;
    end
end
if bk1==1 | minifinal2(c3)>0      %%% Changed
    continue;
else
    minifinal3(n1)=minifinal2(c3);
    miniposfinal3(n1)=miniposfinal2(c3);
    minipostfinal3(n1)=minipostfinal2(c3);
    n1=n1+1;
end
end

%Final processing minima
minifinaltemp3=[]; tc1=1;
for tt1=1:length(minipostfinal3)-1
    if minipostfinal3(tt1+1)-minipostfinal3(tt1)<2.0
        if minifinal3(tt1)<minifinal3(tt1+1)
            minifinaltemp3(tc1)=minifinal3(tt1+1);
            tc1=tc1+1;
        else
            minifinaltemp3(tc1)=minifinal3(tt1);
            tc1=tc1+1;
        end
    else
        continue;
    end
end

minifinal4=[]; miniposfinal4=[]; minipostfinal4=[]; n1=1;
bk1=0;
for c3=1:length(minifinal3)
    bk1=0;
    for c4=1:length(minifinaltemp3)
        if minifinal3(c3)==minifinaltemp3(c4)
            bk1=1;
            break;
        end
    end
end
if bk1==1 | minifinal3(c3)>0      %%% Changed
    continue;
else
```

```

        minifinal4(n1)=minifinal3(c3);
        miniposfinal4(n1)=miniposfinal3(c3);
        minipostfinal4(n1)=minipostfinal3(c3);
        n1=n1+1;
    end
end

% ===== Maxima Processing ===== %

maxifinal2=maxifinal;
maxiposfinal2=maxiposfinal;
maxipostfinal2=maxipostfinal;

%Reprocessing maxima
maxifinaltemp2=[]; tc1=1;
for tt1=1:length(maxipostfinal2)-1
    if maxipostfinal2(tt1+1)-maxipostfinal2(tt1)<2.0
        if maxifinal(tt1)>maxifinal2(tt1+1)
            maxifinaltemp2(tc1)=maxifinal2(tt1+1);
            tc1=tc1+1;
        else
            maxifinaltemp2(tc1)=maxifinal2(tt1);
            tc1=tc1+1;
        end
    else
        continue;
    end
end

maxifinal3=[]; maxiposfinal3=[]; maxipostfinal3=[]; n1=1;
bk1=0;
for c3=1:length(maxifinal2)
    bk1=0;
    for c4=1:length(maxifinaltemp2)
        if maxifinal2(c3)==maxifinaltemp2(c4)
            bk1=1;
            break;
        end
    end
    if bk1==1 | maxifinal2(c3)<0
        continue;
    else

```

C.2 Detection of inspiratory and expiratory onsets

```
    maxifinal3(n1)=maxifinal2(c3);
    maxiposfinal3(n1)=maxiposfinal2(c3);
    maxipostfinal3(n1)=maxipostfinal2(c3);
    n1=n1+1;
end
end

%Final processing maxima
maxifinaltemp3=[]; tc1=1;
for tt1=1:length(maxipostfinal3)-1
    if maxipostfinal3(tt1+1)-maxipostfinal3(tt1)<2.0
        if maxifinal3(tt1)>maxifinal3(tt1+1)
            maxifinaltemp3(tc1)=maxifinal3(tt1+1);
            tc1=tc1+1;
        else
            maxifinaltemp3(tc1)=maxifinal3(tt1);
            tc1=tc1+1;
        end
    else
        continue;
    end
end

maxifinal4=[]; maxiposfinal4=[]; maxipostfinal4=[]; n1=1;
bk1=0;
for c3=1:length(maxifinal3)
    bk1=0;
    for c4=1:length(maxifinaltemp3)
        if maxifinal3(c3)==maxifinaltemp3(c4)
            bk1=1;
            break;
        end
    end
    if bk1==1 | maxifinal3(c3)<0
        continue;
    else
        maxifinal4(n1)=maxifinal3(c3);
        maxiposfinal4(n1)=maxiposfinal3(c3);
        maxipostfinal4(n1)=maxipostfinal3(c3);
        n1=n1+1;
    end
end
end
```

```
figure(3);
plot(time,RespFilter);
hold on;
plot(minipostfinal4,minifinal4,'.r');
plot(maxipostfinal4,maxifinal4,'.r');
hold off;
xlabel('Time'); ylabel('Respiration');

%Respiratory period
resPeriod=[];
for rpd=1:length(maxipostfinal4)-1
    resPeriod(rpd)=maxipostfinal4(rpd+1)-maxipostfinal4(rpd);
end

avgResPeriod=0; avgResFreq=0;
avgResPeriod=mean(resPeriod(~isnan(resPeriod)));
avgResFreq=1/avgResPeriod;

%minima between two maximas
%Calculating inspiration and expiration times
mxbm=[]; mxbct=1; mxst=1;
expTime=[]; inspTime=[];
for mbm1=1:length(maxipostfinal4)-1
    for mbm2=mxst:length(minipostfinal4)
        if minipostfinal4(mbm2)>maxipostfinal4(mbm1) & ...
            minipostfinal4(mbm2)<maxipostfinal4(mbm1+1)
            mxbm(mxbct)=minipostfinal4(mbm2);
            expTime(mxbct)=minipostfinal4(mbm2)-maxipostfinal4(mbm1);
            inspTime(mxbct)=maxipostfinal4(mbm1+1)-minipostfinal4(mbm2);
            mxbct=mxbct+1;
            mxst=mbm2;
            break;
        else
            continue;
        end
    end
end
end
```

C.3 Respiration analysis during movement in rats

```
%%%%%%%%%%%%%%%%%%%%%%%%%%%%%%%%%%%%%%%%%%%%%%%%%%%%%%%%%%%%%%%%%%%%%%%%
%           Matlab code for respiration analysis during           %
%           voluntary movement in rats                           %
%                                                                 %
% Muammar M. Kabir                                             %
% The University of Adelaide                                   %
% June 2009                                                  %
%%%%%%%%%%%%%%%%%%%%%%%%%%%%%%%%%%%%%%%%%%%%%%%%%%%%%%%%%%%%%%%%%%%%%%%%

% Rat Movement analysis
% Using average movement between two inspiratory onsets
% square->integration->integrated interval->median of points
% square->points->integration->sum of integrated points

% movement, same cont. movement and non-movement
% 0.1s - 0.4s(max.) non-movement = movement

% slope of movement integral for each individual movement

clear all
close all
clc

% load RR and QT time series from QTanalysis output results
[fname,pname] = uigetfile('*','Verzeichnis whlen');
tachofiles = dir(pname);
anz=length(tachofiles);

for lp=3:1:anz
    filename=tachofiles(lp).name;
    file=strcat(pname,filename);
    [pathstr, name, ext, versn] = fileparts(file);
    % read RR,QT data
    % load(strcat(pathstr,'\',name,'.mat'));

    clear ratc ratctime ratcResp ratcResRate ratcECG
    clear ratcHR ratcPiezo t1 ratcPiezosqr
    clear inintsum inintsumdiv mmint

    ratc = [];
```



```

ratc = load(strcat(pathstr,'\',name,'.txt')); % file containing data

disp(strcat(pathstr,'\',name,'.txt'));

ratctime=ratc(:,1); % Respiration
ratcResp=ratc(:,2); % Respiration
ratcResRate=ratc(:,3); % Respiration Rate
ratcECG=ratc(:,4); % ECG
ratcHR=ratc(:,5); % Heart rate
ratcPiezo=ratc(:,6); % Piezo

sfreq=1000;

ratctime = ratctime - ratctime(1) + 1/sfreq;

%Filtering respiratory signal
ratcResp2=[];
[b,a] = butter(4,0.02);
ratcResp2 = filtfilt(b,a,ratcResp);

%%===== MOVEMENT Analysis =====%%
ratcPiezosqr=[];
ratcPiezosqr=ratcPiezo.*ratcPiezo;

ratcPiezosqr2=[];
rPsCt=1;
for i=1:length(ratcPiezosqr)
    if ratcPiezosqr(i)>=0
        ratcPiezosqr2(rPsCt)=ratcPiezosqr(i);
        rPsCt=rPsCt+1;
    else
        ratcPiezosqr2(rPsCt)=0;
        rPsCt=rPsCt+1;
    end
end
ratcPiezosqr2=ratcPiezosqr2';

thres=0.008;%12*(median(ratcPiezosqr2)-(Plgmct*10^(chkct-chkct2-1)));
wintime1=0;

```

C.3 Respiration analysis during movement in rats

```
wintime2=ratctime(1);
winlength=0.05;
movct=0;
movctplus=0;
movctminus=0;
totmovtime=0; % total movement time
totmovct=0; % total movement count
sepmovtime=[]; % separate movement time
sepmovct=1; % separate movement count
sepmovtime(sepmovct)=0;
sepmovtime2=[]; % separate movement time
sepmovct2=1; % separate movement count
sepmovtime2(sepmovct2)=0;
ymov=0;
nonmov=0;

tmctmv=[]; tmvct=1;
tmctnmv=[]; tnmvct=1;
movstTime=[];
movendTime=[];
stendct=0;
for tmct=1:winlength*1000:length(ratctime)-(winlength*1000)
    movstore=[];
    wintime1=wintime2;
    wintime2=wintime1+winlength;
    movstore=ratcPiezosqr(round(wintime1*1000):round(wintime2*1000));
    if max(movstore)>thres
        movctplus=movctplus+1;
        movct=movct+1;
        sepmovtime(sepmovct)=sepmovtime(sepmovct)+winlength;
        tmctmv(tmvct)=tmct/sfreq;
        tmvct=tmvct+1;
    else
        movctminus=movctminus+1;
        movct=movct+1;
        sepmovct=sepmovct+1;
        sepmovtime(sepmovct)=0;
        tmctnmv(tnmvct)=tmct/sfreq;
        tnmvct=tnmvct+1;
    end
    if movct==4
        if (movctplus-movctminus)>2
```

```

if ymov==1 & nonmov<3      % same continuous movement
    totmovct=totmovct;
    totmovtime=totmovtime+(movctplus*winlength);
    sepmovtime2(sepmovct2)=sepmovtime2(sepmovct2)+...
        (movctplus*winlength);
    movendTime(stendct)=tmctmv(end)+winlength;
    movct=0;
    movctplus=0;
    movctminus=0;
    tmctmv=[]; tmvct=1;
    tmctnmv=[]; tnmvct=1;
else
    totmovct=totmovct+1;    % new movement
    totmovtime=totmovtime+(movctplus*winlength);
    sepmovct2=sepmovct2+1;
    sepmovtime2(sepmovct2)=0;
    sepmovtime2(sepmovct2)=sepmovtime2(sepmovct2)+...
        (movctplus*winlength);
    stendct=stendct+1;
    movstTime(stendct)=tmctmv(1);
    movct=0;
    movctplus=0;
    movctminus=0;
    ymov=1;
    nonmov=0;
    tmctmv=[]; tmvct=1;
    tmctnmv=[]; tnmvct=1;
end
else          % non movement
    movct=0;
    movctplus=0;
    movctminus=0;
    nonmov=nonmov+1;
    if nonmov<3
        ymov=ymov;
    else
        ymov=0;
    end
    tmctmv=[]; tmvct=1;
    tmctnmv=[]; tnmvct=1;
end
%         if (movctplus-movctminus)>2

```

C.3 Respiration analysis during movement in rats

```
%          totmovtime=totmovtime+(movctplus*winlength);
%          sepmovtime2(sepmovct2)=sepmovtime2(sepmovct2)+...
%          (movctplus*winlength);
%          movct=0;
%          movctplus=0;
%          movctminus=0;
%      else
%          movct=0;
%          movctplus=0;
%          movctminus=0;
%          sepmovct2=sepmovct2+1;
%          sepmovtime2(sepmovct2)=0;
%      end
    else
        continue;
    end
end

movstTime2=[];
movendTime2=[];
stendct2=1;
for msect=1:length(movendTime)
    if movendTime(msect)==0
        continue;
    else
        movstTime2(stendct2)=movstTime(msect);
        movendTime2(stendct2)=movendTime(msect);
        stendct2=stendct2+1;
    end
end

movstTime3=[];
movendTime3=[];
stendct3=1;
if length(movstTime2)>0
    movstTime3(stendct3)=movstTime2(1);
    for msect2=1:length(movstTime2)-1
        if movstTime2(msect2+1)-movendTime2(msect2)<=0.7 %1.0
            if msect2+1==length(movstTime2)
                movendTime3(stendct3)=movendTime2(msect2);
            else
                continue;
            end
        end
    end
end
```

```

        end
    else
        movendTime3(stendct3)=movendTime2(msect2);
        if msect2+1==length(movstTime2)
            break;
        else
            stendct3=stendct3+1;
            movstTime3(stendct3)=movstTime2(msect2+1);
        end
    end
end
end

mvtincl=[];
if length(movendTime3)>0
    for mvtin=1:length(movstTime3)
        mvtincl(mvtin)= movendTime3(mvtin)-movstTime3(mvtin);
    end
end

inintsum=[];
inintsumdiv=[];
cumsummov=[];
cumsummovdiv=[];
isct=1;
in2=1;
if length(movendTime3)>0
    for in=1:length(movendTime3)
        insq=[];
        inct=1;
        stpt=in2;
        inint=[];
        for in2=stpt:length(ratctime)
            if ratctime(in2)>movendTime3(in)
                break;
            elseif ratctime(in2)>=movstTime3(in) &...
                ratctime(in2)<=movendTime3(in)
                insq(inct)=ratcPiezosqr(in2);
                inct=inct+1;
            else
                continue;
            end
        end
    end
end

```

C.3 Respiration analysis during movement in rats

```
        end
        inint=cumtrapz(insq);
        inintsum(isct)=median(diff(inint)); %inintsum(isct)=sum(inint);
%       inintsum(isct)=median(insq);
        inintsumdiv(isct)=inintsum(isct)/(movendTime3(in)-movstTime3(in));
        cumsummov(isct)=inint(end);
        cumsummovdiv(isct)=cumsummov(isct)/(movendTime3(in)-movstTime3(in));
        isct=isct+1;
    end
else
    continue;
end

%=====

%       figure(4);plot(mvtincl,inintsum, '.'); xlabel('mm interval(s)');...
%           ylabel('integrated interval of movement');

%       figure(5);plot(mvtincl,inintsumdiv, '.'); xlabel('mm interval(s)');...
%           ylabel('sum of integrated interval of movement div by ...
interval');

fidl = fopen('RatDataAnalysis.txt','a');
for i=1:length(mvtincl)
    fprintf(fidl,'%2.3f \t %2.3f \t ',mvtincl(i),inintsumdiv(i));
    fprintf(fidl,'\n');
end
fclose(fidl);

%       fidl = fopen('RatDataAnalysis2.txt','a');
%       for i=1:length(mvtincl)
%           fprintf(fidl,'%2.3f \t %2.3f \t ',mvtincl(i),cumsummovdiv(i));
%           fprintf(fidl,'\n');
%       end
%       fclose(fidl);

%       fidl = fopen('MovementTime2.txt','a');
%       for i=1:length(sepmovtime2)
%           fprintf(fidl,'%2.3f \t ',sepmovtime2(i));
%           fprintf(fidl,'\n');
```

```
% end
% fclose(fid1);

% fid1 = fopen('TimeNMovPerMin.txt','a');
% fprintf(fid1,'%2.3f \t %2.3f \t %2.1f ...
\t',ratctime(end),totmovtime,totmovct);
% fprintf(fid1,'%2.1f \t',((totmovtime/ratctime(end))*60));
% fprintf(fid1,'%2.1f \t',((totmovct/ratctime(end))*60));
% fprintf(fid1,'%2.2f \t',mean(sepmovtime2));
% fprintf(fid1,'\n');
% fclose(fid1);

end

figure(6);
rdap=load('RatDataAnalysis.txt');
plot(rdap(:,1),rdap(:,2),'.');

% figure(7);
% rdap2=load('RatDataAnalysis2.txt');
% plot(rdap2(:,1),rdap2(:,2),'.');
```

C.4 Phase-averaged RSA analysis

```
%%%%%%%%%%%%%%%%%%%%%%%%%%%%%%%%%%%%%%%%%%%%%%%%%%%%%%%%%%%%%%%%%%%%%%%%%
%   Matlab code for analysing respiratory sinus arrhythmia       %
%   using phase-averaged RSA technique                           %
%                                                                 %
% Muammar M. Kabir                                             %
% The University of Adelaide                                    %
% March 2010                                                  %
%%%%%%%%%%%%%%%%%%%%%%%%%%%%%%%%%%%%%%%%%%%%%%%%%%%%%%%%%%%%%%%%%%%%%%%%%

clear all
close all
clc

ECG=[]; time=[]; Respiration=[];

time=A(:,1);
Respiration=A(:,2);
ECG=A(:,4);
sfreq=1000;
iPol=50; %interpolation

maxipostfinal4=[];
maxipostfinal4=maximaDetection(time,Respiration);

D = rpeak(ECGfilter,1000);
trp = time(D); %time of R-peaks
rp = ECGfilter(D); %R-peaks

%RR interval
rrint=[];
tint=[];
for i=1:length(trp)-1
    rrint(i)=trp(i+1)-trp(i);
    tint(i)=trp(i+1);
end

%Using Maximas
%Origin = Maxima
%Using interpolation - 50
%Low-pass filtering @ 1Hz
```



```

Tcnt=1;
Tmat=[]; rrmatrix=[];
Tmat(:,:)=0; rrmatrix(:,:)=0; tmct=1;
for cct1=1:length(maxipostfinal4)-1
    for cct2=Tcnt:length(tint)
        if tint(cct2)<maxipostfinal4(cct1)
            continue;
        elseif tint(cct2)>=maxipostfinal4(cct1)...
            & tint(cct2)<maxipostfinal4(cct1+1)
            Tmat(tmct,cct1)=tint(cct2);
            rrmatrix(tmct,cct1)=rrrint(cct2);
            tmct=tmct+1;
            %         if tmct==1
            %             tmct=tmct+1;
            %         else
            %             rrmatrix(tmct,cct1)=Tmat(tmct,cct1)-Tmat(tmct-1,cct1);
            %             tmct=tmct+1;
            %         end
            %         tmct=tmct+1;
        else
            Tcnt=cct2;
            tmct=1;
            break;
        end
    end
end

[rro0,rcol0]=size(rrmatrix);
rripolmat=[]; tmipolmat=[];
rripolmat(:,:)=0; tmipolmat(:,:)=0;
for rct1=1:rcol0
    rripolmattemp0=[];
    tmipolmattemp0=[];
    rpmct=1;
    for rct2=2:rro0
        if rct2==1 | rrmatrix(rct2,rct1)>0
            rripolmattemp0(rpmct)=rrmatrix(rct2,rct1);
            tmipolmattemp0(rpmct)=Tmat(rct2,rct1);
            rpmct=rpmct+1;
        else

```

C.4 Phase-averaged RSA analysis

```
        break;
    end
end
tempA0=[];tempB0=[];
if length(tmipolmattemp0)<2
    continue;
else
    tempA0=tmipolmattemp0(1):((tmipolmattemp0(end)-tmipolmattemp0(1))...
        /(iPol-1)):tmipolmattemp0(end);
    tempB0=spline(tmipolmattemp0,rripolmattemp0,tempA0);
end
for tpct=1:length(tempA0)
    tmipolmat(tpct,rct1)=tempA0(tpct);
    rripolmat(tpct,rct1)=tempB0(tpct);
end
end

[n,m]=size(rripolmat);
x0=[]; x0(n,1)=0;
for rct1=1:n
    x0ct=0;
    for rct2=1:m
        if rripolmat(rct1,rct2)==0
            continue;
        else
            x0(rct1,1)=x0(rct1,1)+rripolmat(rct1,rct2);
            x0ct=x0ct+1;
        end
    end
end
if x0ct==0
    continue;
else
    x0(rct1,1)=x0(rct1,1)/x0ct;
end
end

%phaseDom=0:(2*pi)/(iPol-1):2*pi; % Phase Domain 0-2pi
phaseDom=0:(2*pi)/(n-1):2*pi;

% RRI Deviation
rrmatMean=[];
```

```

rridevmat=[]; rridevmat(:,:)=0;
for rriect1=1:m
    rrmatTemp=[]; rmct=1;
    for rriect2=1:n
        if rripolmat(rriect2,rriect1)==0
            continue;
        else
            rrmatTemp(rmct)=rripolmat(rriect2,rriect1);
            rmct=rmct+1;
        end
    end
    rrmatMean(rriect1)=mean(rrmatTemp);

    for rriect3=1:length(rrmatTemp)
        rridevmat(rriect3,rriect1)=rrmatTemp(rriect3)-rrmatMean(rriect1);
    end
end

x0dev(n,1)=0;
for rct1=1:n
    x0ct=0;
    for rct2=1:m
        if rridevmat(rct1,rct2)==0
            continue;
        else
            x0dev(rct1,1)=x0dev(rct1,1)+(rridevmat(rct1,rct2));
            x0ct=x0ct+1;
        end
    end
    if x0ct==0
        continue;
    else
        x0dev(rct1,1)=x0dev(rct1,1)/x0ct;
    end
end

RSAampInit=max(x0dev)-min(x0dev); % RSA amplitude before removing outliers

phaseDelayInit=0;
for xdct=1:length(x0dev)
    if x0dev(xdct)==min(x0dev)
        phaseDelayInit=phaseDom(xdct);
    end
end

```

C.4 Phase-averaged RSA analysis

```
        break;
    end
end

phaseDelay2Init=0;
for xdct2=1:length(x0dev)
    if x0dev(xdct2)==max(x0dev)
        phaseDelay2Init=phaseDom(xdct2);
        break;
    end
end

figure(7);
plot(phaseDom,rripolmat); xlabel('Respiratory phase [rad]');...
    ylabel('RR Intervals (s)');
figure(8);
plot(phaseDom,rridevmat*1000); xlabel('Respiratory phase [rad]');...
    ylabel('RRI deviation (ms)');

figure(9);
plot(phaseDom,x0); xlabel('Respiratory phase [rad]');...
    ylabel('Avg RR Intervals (s)');
figure(10);
plot(phaseDom,x0dev*1000); xlabel('Respiratory phase [rad]');...
    ylabel('Avg RRI deviation (ms)');

%Hilbert Transform RSA
htAvRSA=hilbert(x0);
magRSA=abs(htAvRSA); % magnitude
phsRSA=angle(htAvRSA); % Phase

phi0=angle(max(htAvRSA)); % phase of maximum value

% Variance
[x0R,x0C]=size(x0);
Vj(1,m)=0;
for i1=1:m
    for i2=1:n
        if rripolmat(i2,i1)==0
            continue;
        elseif i1>x0R
            Vj(1,i1)=0;
        end
    end
end
```

```

        else
            Vj(1,i1)=Vj(1,i1)+((x0(i1,1)-rripolmat(i2,i1)).^2);
        end
    end
end

%Phase Respiration
htRes=hilbert(RespFilter);
phiJ=[]; Rmct=1; %maxRPmat=[]; phase of jth respiration cycle max value
Tcnt=1;
for cct3=1:length(maxipostfinal4)-1
    mmHTmat=[]; Hmct=1;
    for cct4=Tcnt:length(time)
        if time(cct4)<maxipostfinal4(cct3)
            continue;
        elseif time(cct4)>=maxipostfinal4(cct3)...
            & time(cct4)<maxipostfinal4(cct3+1)
            mmHTmat(Hmct)=htRes(cct4);
            Hmct=Hmct+1;
        else
            Tcnt=cct4;
            break;
        end
    end
    phiJ(Rmct)=angle(max(mmHTmat));
    Rmct=Rmct+1;
end

%Phase difference
deltaPHI=[];
for i=1:m
    deltaPHI(i)=abs(phi0-phiJ(i));
end

%Sort
sortVj=sort(Vj);
delVj=sortVj(round(0.9*m):end);
mcol=[]; mcct=1; %deleted 'm' collections
for dt1=1:length(delVj)
    for dt2=1:length(Vj)
        if Vj(1,dt2)==delVj(dt1)
            mcol(mcct)=dt2;

```

C.4 Phase-averaged RSA analysis

```
        mcct=mcct+1;
        break;
    else
        continue;
    end
end
end

deltaPHI2=[]; dPct=1; dPstart=1;
for dt1=1:length(mcol)+1
    for dt2=dPstart:length(deltaPHI)
        if dt1<=length(mcol) & dt2==mcol(dt1)
            dPstart=dt2+1;
            break;
        else
            deltaPHI2(dPct)=deltaPHI(dt2);
            dPct=dPct+1;
        end
    end
end

sortdeltaPHI2=sort(deltaPHI2);
delDPHI=sortdeltaPHI2(round(0.8*m):end);
for dt1=1:length(delDPHI)
    for dt2=1:length(deltaPHI) % Note the use of deltaPHI and not deltaPHI2
        if deltaPHI(dt2)==delDPHI(dt1)
            mcol(mcct)=dt2;
            mcct=mcct+1;
            break;
        else
            continue;
        end
    end
end

% Subset RR intervals
rrmatsub(:,:)=0; rrsct3=1;
for rrsct1=1:m
    entr=0;
    for rrsct2=1:length(mcol)
        if rrsct1==mcol(rrsct2)
            entr=1;
        end
    end
end
```

```

        break;
    else
        continue;
    end
end
if entr==1
    continue;
else
    for dmat=1:n
        rrmatsub(dmat,rrsct3)=rripolmat(dmat,rrsct1);
    end
    rrsct3=rrsct3+1;
end
end

[n1,m1]=size(rrmatsub);
x1(n1,1)=0;
for i1=1:n1
    xlct=0;
    for i2=1:m1
        if rrmatsub(i1,i2)==0
            continue;
        else
            x1(i1,1)=x1(i1,1)+rrmatsub(i1,i2);
            xlct=xlct+1;
        end
    end
    x1(i1,1)=x1(i1,1)/xlct;
end

% RRI Deviation
rrmatsubMean=[];
rridevmatsub(:,:)=0;
for rriect1=1:m1
    rrmatsubTemp=[]; rmct=1;
    for rriect2=1:n1
        if rrmatsub(rriect2,rriect1)==0
            continue;
        else
            rrmatsubTemp(rmct)=rrmatsub(rriect2,rriect1);
            rmct=rmct+1;
        end
    end
end

```

C.4 Phase-averaged RSA analysis

```
end
rrmatsubMean(rrict1)=mean(rrmatsubTemp);

for rriect3=1:length(rrmatsubTemp)
    rridevmatsub(rrict3,rrict1)=rrmatsubTemp(rrict3)-rrmatsubMean(rrict1);
end
end

[n11,m11]=size(rridevmatsub);
xldev(n11,1)=0;
for rct1=1:n11
    xlct=0;
    for rct2=1:m11
        if rridevmatsub(rct1,rct2)==0
            continue;
        else
            xldev(rct1,1)=xldev(rct1,1)+(rridevmatsub(rct1,rct2));
            xlct=xlct+1;
        end
    end
    xldev(rct1,1)=xldev(rct1,1)/xlct;
end

RSAamp=max(xldev)-min(xldev); % RSA amplitude

phaseDom2=0:(2*pi)/(n11-1):2*pi;

phaseDelay=0;
for xdct=1:length(xldev)
    if xldev(xdct)==min(xldev)
        phaseDelay=phaseDom2(xdct);
        break;
    end
end

phaseDelay2=0;
for xdct2=1:length(xldev)
    if xldev(xdct2)==max(xldev)
        phaseDelay2=phaseDom2(xdct2);
        break;
    end
end
end
```



```
figure(11);  
plot(phaseDom2,rridevmatsub*1000);...  
    xlabel('Respiratory phase [rad]'); ylabel('RRI deviation (ms)');
```

```
figure(12);  
plot(phaseDom2,xldev*1000); xlabel('Respiratory phase [rad]');...  
    ylabel('Avg RRI deviation (ms)');
```

C.5 Joint symbolic dynamics approach

```
%%%%%%%%%%%%%%%%%%%%%%%%%%%%%%%%%%%%%%%%%%%%%%%%%%%%%%%%%%%%%%%%%%%%%%%%%
%       Matlab code for Joint Symbolic Dynamic Approach           %
%                                                                 %
% Muammar M. Kabir                                             %
% The University of Adelaide                                   %
% April 2011                                                 %
%%%%%%%%%%%%%%%%%%%%%%%%%%%%%%%%%%%%%%%%%%%%%%%%%%%%%%%%%%%%%%%%%%%%%%%%%

clear all
close all
clc

% load RR and QT time series from QTanalysis output results
[fname,pname] = uigetfile('*','Verzeichnis whlen');
tachofiles = dir(pname);
anz=length(tachofiles);

fidl = fopen('JSDanalysis.xls','a');
fprintf(fidl,'File ID \t');
fprintf(fidl,'Total time (s) \t ');
fprintf(fidl,'Mean RR Interval (s) \t');
fprintf(fidl,'Shift \t ');
fprintf(fidl,'Length of word \t ');
fprintf(fidl,'Threshold (ms) \t ');
fprintf(fidl,'Percent RSA using current word length \t ');
fprintf(fidl,'Average duration of coordination (s) \t ');
fprintf(fidl,'Median duration of coordination (s) \t ');
fprintf(fidl,'Max. duration of coordination (s) \t ');
fprintf(fidl,'Average duration of interaction (s) \t ');
fprintf(fidl,'Median duration of interaction (s) \t ');
fprintf(fidl,'Max. duration of interaction (s) \t ');
fprintf(fidl,'\n');
fprintf(fidl,'\n');
fclose(fidl);

for fileCT=3:1:anz
    filename=tachofiles(fileCT).name;
    file=strcat(pname,filename);
    [pathstr, name, ext, versn] = fileparts(file);
```

```
clear A D ECG Respiration RespFilter totsynchroncount totsynchrontime
clear synchroncount rrint rspmf
clear miniposfinal miniposfinal4 minipostfinal minipostfinal4
clear lockRatio freqLockRatio recordRSapercent

disp(strcat(pathstr, '\', name, '.txt')); % Display current file

A = [];
A = load(strcat(pathstr, '\', name, '.txt')); % Load data

time=[]; Respiration=[]; ECG=[];
A=A(60000:end-30000,:);
time=A(:,1);
Respiration=A(:,2);
ECG=A(:,4);
sfreq=1000;

time=time-time(1)+(1/sfreq);
tmax = max(time);
tmin = min(time);
tdiff = tmax - tmin;

%ECG processing
D = rpeak(ECG,1000);
trp = time(D); %time of R-peaks
rp = ECG(D); %R-peaks

figure(1);
plot(time,ECG); hold on; plot(trp,rp,'.r'); hold off
xlabel('Time (s)'); ylabel('ECG');

%RR interval
rrint=[];
for i=1:length(trp)-1
    rrint(i)=trp(i+1)-trp(i);
    tint(i)=trp(i+1);
end

%Filter Respiration
RespFilter=[];
[b,a] = butter(4,(1/(sfreq/2)));
```

C.5 Joint symbolic dynamics approach

```
RespFilter = filtfilt(b,a,Respiration);

RespFilter = RespFilter - mean(RespFilter);

figure(2);
plot(time,Respiration); hold on; plot(time,RespFilter,'r'); hold off;

%Respiratory phase
htRs = []; phRs = [];
htRs = hilbert(RespFilter);
phRs = angle(htRs); % phase
phil = phRs(D); % corresponding respiratory reading
phil = phil(2:end);

%=====%
%%%%%%%% Correlation - SHIFT %%%%%%%%%
%=====%

recordCorr=[];
for delyLP=1:5 %8
    [recordCorr(delyLP),xp]...
        =circ_corrcl(rrint(1+delyLP:end),phil(1:end-delyLP)');
end

shft=0;
for delyLP1=1:length(recordCorr)
    if recordCorr(delyLP1)==max(recordCorr)
        shft=delyLP1-1;
        break;
    end
end

%=====% Shift =====%
rrint=rrint(1+shft:end);
tint=tint(1+shft:end);
trp=trp(1+shft:end);
phil=phil(1:end-shft);
%=====%

fid1 = fopen('JSDanalysis.xls','a');
```

```

fprintf(fid1, '%s \t', name);
fprintf(fid1, '%2.3f \t ', tdiff);
fprintf(fid1, '%2.3f \t ', mean(rrint));
fprintf(fid1, '%2.1f \t ', shft);
fprintf(fid1, '\n');
fclose(fid1);

```

```

%=====
%%%%%%%% Symbolic Analysis %%%%%%%%%
%=====

```

```

recordRSAword=[];
timeWORD=[];

```

```

for symbolicWord=1:5

```

```

    fid1 = fopen('JSDanalysis.xls', 'a');
    fprintf(fid1, '\t \t \t \t');
    fprintf(fid1, '%2.1f \t ', symbolicWord);
    fprintf(fid1, '\n');
    fclose(fid1);

```

```

for threshold=2:2:10

```

```

    % Threshold
    rrintShort=[];
    rrintShort=round(rrint/(threshold/1000))*(threshold/1000);

```

```

    % Symbolics for RR interval – two symbols
    % Symbolics for Heart Rate – two symbols
    % 0 means rrint decrease; 1 means rrint increase;
    symRR=[]; symRRct=1; symHR=[]; timeATsym=[];

```

```

    for sRRct=1:length(rrintShort)-1
        if (rrintShort(sRRct+1)-rrintShort(sRRct))<0
            symRR(symRRct)=0;
            symHR(symRRct)=1;
            timeATsym(symRRct)=tint(sRRct+1);
            symRRct=symRRct+1;
        elseif (rrintShort(sRRct+1)-rrintShort(sRRct))>0
            symRR(symRRct)=1;
            symHR(symRRct)=0;
            timeATsym(symRRct)=tint(sRRct+1);

```

C.5 Joint symbolic dynamics approach

```
        symRRct=symRRct+1;
    else
        symRR(symRRct)=2;
        symHR(symRRct)=2;
        timeATsym(symRRct)=tint(sRRct+1);
        symRRct=symRRct+1;
    end
end

% Symbolics for Respiratory phases
% 0 means expiration, +1 means inspiration
symRsPh=[]; symRsPhct=1;
for sRPct=1:length(phil)-1
    if (abs(phil(sRPct))-abs(phil(sRPct+1)))<0
        symRsPh(symRsPhct)=0;
        symRsPhct=symRsPhct+1;
    else
        symRsPh(symRsPhct)=1;
        symRsPhct=symRsPhct+1;
    end
end

% Word formation for RR interval using 2 symbols
wordRR=[]; wordRRcnt=1;
for cntRR=1:length(symRR)-(symbolicWord-1)
    wordRR(wordRRcnt)=0;
    for wordFormLoop=1:symbolicWord
        wordRR(wordRRcnt)...
            =wordRR(wordRRcnt)+symRR(cntRR+wordFormLoop-1).*...
            (10^(symbolicWord-wordFormLoop));
    end
    wordRRcnt=wordRRcnt+1;
end

% figure(4); hist(wordRR2);

% Word formation for Heart Rate using 2 symbols
wordHR=[]; wordHRcnt=1; timeWORDst=[]; timeWORDend=[];
for cntHR=1:length(symHR)-(symbolicWord-1)
    wordHR(wordHRcnt)=0;
    for wordFormLoop=1:symbolicWord
        wordHR(wordHRcnt)=wordHR(wordHRcnt)+...
```

```

        symHR(cntHR+wordFormLoop-1).*...
        (10^(symbolicWord-wordFormLoop));
    end
    timeWORDst(symbolicWord,wordHRcnt)=timeATsym(cntHR); ...
        % Start time of a 'word' epoch
    timeWORDend(symbolicWord,wordHRcnt)=...
        timeATsym(cntHR+symbolicWord-1); ...
        % End time of a 'word' epoch
    wordHRcnt=wordHRcnt+1;
end
% figure(5); hist(wordHR2);

% Word formation for Respiratory phase using 2 symbols
wordRsPh=[]; wordRsPhcnt=1;
for cntRsPh=1:length(symRsPh)-(symbolicWord-1)
    wordRsPh(wordRsPhcnt)=0;
    for wordFormLoop=1:symbolicWord
        wordRsPh(wordRsPhcnt)=wordRsPh(wordRsPhcnt)+...
            symRsPh(cntRsPh+wordFormLoop-1).*...
            (10^(symbolicWord-wordFormLoop));
    end
    wordRsPhcnt=wordRsPhcnt+1;
end
% figure(6); hist(wordRsPh2);

%Duration of interaction – based on word length of '1'
ent=0;
timeStart=0; timeEnd=0;
DurCordn=[]; DurCorCnt=1;
for cntRR=1:length(symHR)
    if (symHR(cntRR)==0 && symRsPh(cntRR)==0) || ...
        (symHR(cntRR)==1 && symRsPh(cntRR)==1)
        if ent==0
            timeStart=timeATsym(cntRR);
            ent=1;
        else
            timeEnd=timeATsym(cntRR);
        end
    else
        ent=0;
        if timeStart==0 || timeEnd==0

```

C.5 Joint symbolic dynamics approach

```
        continue;
    else
        DurCordn(DurCorCnt)=timeEnd-timeStart;
        DurCorCnt=DurCorCnt+1;
        timeStart=0;
        timeEnd=0;
    end
end
end

% Total count RSA/not-RSA for 2 symbols and...
% 'n' symbols used to form word
cntRSAword=0; % HR increase/decrease with ...
% Resp increase/decrease in terms of words
cntNotRSAword=0; % HR increase/decrease with ...
% Resp decrease/increase in terms of words
recordRSAword=[]; % 1 means RSA, 0 means not RSA
timeRSAst=[]; timeRSAend=[];
timeNotRSAst=[]; timeNotRSAend=[];
for cntRSA=1:length(wordHR)
    if wordHR(cntRSA)==wordRsPh(cntRSA)
        cntRSAword=cntRSAword+1;
        recordRSAword(symbolicWord,cntRSA)=1;
        timeRSAst(cntRSAword)=timeWORDst(symbolicWord,cntRSA);
        timeRSAend(cntRSAword)=timeWORDend(symbolicWord,cntRSA);
    else
        cntNotRSAword=cntNotRSAword+1;
        recordRSAword(symbolicWord,cntRSA)=0;
        timeNotRSAst(cntNotRSAword)=timeWORDst(symbolicWord,cntRSA);
        timeNotRSAend(cntNotRSAword)=timeWORDend(symbolicWord,cntRSA);
    end
end

%Duration of interaction – based on total length of word
DurIntr=[];
DurIntr=timeRSAend-timeRSAst;

fid1 = fopen('JSDanalysis.xls','a');
fprintf(fid1,'\t\t\t\t\t');
fprintf(fid1,'%2.1f\t',threshold);
fprintf(fid1,'%2.3f\t',(cntRSAword/...
    (cntRSAword+cntNotRSAword)*100);
```



```
fprintf(fid1, '%2.3f \t ', mean(DurCordn));
fprintf(fid1, '%2.3f \t ', median(DurCordn));
fprintf(fid1, '%2.3f \t ', max(DurCordn));
fprintf(fid1, '%2.3f \t ', mean(DurIntr));
fprintf(fid1, '%2.3f \t ', median(DurIntr));
fprintf(fid1, '%2.3f \t ', max(DurIntr));
fprintf(fid1, '\n');
fclose(fid1);

clear rrintShort symRR symHR timeATsym symRsPh DurIntr
clear wordRR wordHR timeWORD wordRsPh DurCordn recordRSAword

end
end
end
```


Bibliography

- ADDISON-P. S. (2002). The continuous wavelet transform, in S. Laurenson. (ed.), *The Illustrated Wavelet Transform Handbook*, Institute of Physics Publishing, London, pp. 6–20.
- AKSELROD-S., ELIASH-S., OZ-O., AND COHEN-S. (1987). Hemodynamic regulation in SHR: Investigation by spectral analysis, *American Journal of Physiology—Heart and Circulatory Physiology*, **253**(1), pp. H176–H183.
- AKSELROD-S., GORDON-D., UBEL-F., SHANNON-D., BERGER-A., AND COHEN-R. (1981). Power spectrum analysis of heart rate fluctuation: a quantitative probe of beat-to-beat cardiovascular control, *Science*, **213**(4504), pp. 220–222.
- ALJADJEFF-G., GOZAL-D., SCHECHTMAN-V. L., BURRELL-B., M.-H. R., AND WARD-S. L. (1997). Heart rate variability in children with obstructive sleep apnea, *Sleep*, **20**, pp. 151–157.
- ALVAREZ-RAMIREZ-J., RODRIGUEZ-E., AND ECHEVERRIA-J. C. (2009). Delays in the human heartbeat dynamics, *Chaos*, **19**(2), article number 028502.
- AMERICAN SLEEP DISORDERS ASSOCIATION. (1993). Reading and scoring leg movements, *Sleep*, **16**, pp. 748–759.
- AMERICAN SLEEP DISORDERS TASK FORCE. (1992). EEG arousals: Scoring rules and examples: A preliminary report from the sleep disorders atlas task force of the american sleep disorders association, *Sleep*, **15**, pp. 173–184.
- AMERICAN THORACIC SOCIETY. (1996). Standards and indications for cardiopulmonary sleep studies in children., *Am. J. Respir. Crit. Care Med.*, **153**, pp. 866–878.
- AMIN-R. S., CARROLL-J. L., JEFFRIES-J. L., GRONE-C., BEAN-J. A., CHINI-B., BOKULIC-R., AND DANIELS-S. R. (2004). Twenty-four-hour ambulatory blood pressure in children with sleep-disordered breathing, *Am. J. Respir. Crit. Care Med.*, **169**(8), pp. 950–956.
- AMIN-R. S., KIMBALL-T. R., BEAN-J. A., JEFFRIES-J. L., WILLGING-J. P., COTTON-R. T., WITT-S. A., GLASCOCK-B. J., AND DANIELS-S. R. (2002). Left ventricular hypertrophy and abnormal ventricular geometry in children and adolescents with obstructive sleep apnea, *Am. J. Respir. Crit. Care Med.*, **165**(10), pp. 1395–1399.
- AMIN-R. S., KIMBALL-T. R., KALRA-M., JEFFRIES-J. L., CARROLL-J. L., BEAN-J. A., WITT-S. A., GLASCOCK-B. J., AND DANIELS-S. R. (2005). Left ventricular function in children with sleep-disordered breathing., *The American Journal of Cardiology*, **95**(6), pp. 801–804.
- ANGELONE-A., AND COULTER-N. A. (1964). Respiratory sinus arrhythmia: A frequency dependent phenomenon, *Journal of Applied Physiology*, **19**(3), pp. 479–482.
- ANTUNES-V. R., BONAGAMBA-L. G. H., AND MACHADO-B. H. (2005). Hemodynamic and respiratory responses to microinjection of ATP into the intermediate and caudal NTS of awake rats, *Brain Research*, **1032**(1-2), pp. 85–93.

Bibliography

- AYDIN-M., ALTIN-R., OZEREN-A., KART-L., BILGE-M., AND UNALACAK-M. (2004). Cardiac autonomic activity in obstructive sleep apnea: time-dependent and spectral analysis of heart rate variability using 24-hour holter electrocardiograms, *Tex. Heart Inst. J.*, **31**(2), pp. 132–136.
- BAHRAMINASAB-A., KENWRIGHT-D., STEFANOVSKA-A., GHASEMI-F., AND MCCLINTOCK-P. V. E. (2008). Phase coupling in the cardiorespiratory interaction, *IET Systems Biology*, **2**(1), pp. 48–54.
- BAIER-V., BAUMERT-M., CAMINAL-P., VALLVERDU-M., FABER-R., AND VOSS-A. (2006). Hidden markov models based on symbolic dynamics for statistical modeling of cardiovascular control in hypertensive pregnancy disorders, *IEEE Transactions on Biomedical Engineering*, **53**(1), pp. 140–143.
- BALOCCHI-R., MENICUCCI-D., SANTARCANGELO-E., SEBASTIANI-L., GEMIGNANI-A., GHELARDUCCI-B., AND VARANINI-M. (2004). Deriving the respiratory sinus arrhythmia from the heartbeat time series using empirical mode decomposition, *Chaos, Solitons & Fractals*, **20**(1), pp. 171 – 177.
- BARTSCH-R., KANTELHARDT-J. W., PENZEL-T., AND HAVLIN-S. (2007). Experimental evidence for phase synchronization transitions in the human cardiorespiratory system, *Phys. Rev. Lett*, **98**(5), article number 054102.
- BASELLI-G., CERUTTI-S., CIVARDI-S., LIBERATI-D., LOMBARDI-F., MALLIANI-A., AND PAGANI-M. (1986). Spectral and cross-spectral analysis of heart rate and arterial blood pressure variability signals, *Comput. Biomed. Res.*, **19**(6), pp. 520–534.
- BAUMERT-M., BAIER-V., TRUEBNER-S., SCHIRDEWAN-A., AND VOSS-A. (2005). Short- and long-term joint symbolic dynamics of heart rate and blood pressure in dilated cardiomyopathy, *IEEE Transactions on Biomedical Engineering*, **52**(12), pp. 2112–2115.
- BAUMERT-M., KOHLER-M., KABIR-M., KENNEDY-D., AND PAMULA-Y. (2010). Cardiorespiratory response to spontaneous cortical arousals during stage 2 and rapid eye movement sleep in healthy children, *J. Sleep Res.*, **19**(3), pp. 415–424.
- BAUMERT-M., NALIVAICO-E., AND ABBOTT-D. (2007a). Effects of vagal blockade on the complexity of heart rate variability in rats, in R. Magjarevic., T. Jarm., P. Kramar., and A. Zupanic. (eds.), *11th Mediterranean Conference on Medical and Biomedical Engineering and Computing 2007*, Vol. 16 of *IFMBE Proceedings*, Springer Berlin Heidelberg, pp. 26–29.
- BAUMERT-M., SMITH-J., CATCHESIDE-P., MCEVOY-D., ABBOTT-D., AND NALIVAICO-E. (2007b). Changes in RR and QT intervals after spontaneous and respiratory arousal in patients with obstructive sleep apnea, *Computers in Cardiology*, Durham, NC, pp. 677–680.
- BAUMERT-M., SMITH-J., CATCHESIDE-P., MCEVOY-R. D., ABBOTT-D., SANDERS-P., AND NALIVAICO-E. (2008). Variability of QT interval duration in obstructive sleep apnea: an indicator of disease severity, *Sleep*, **31**(7), pp. 959–966.
- BAUMERT-M., WALTHER-T., HOPFE-J., STEPAN-H., FABER-R., AND VOSS-A. (2002). Joint symbolic dynamic analysis of beat-to-beat interactions of heart rate and systolic blood pressure in normal pregnancy, *Medical and Biological Engineering and Computing*, **40**(2), pp. 241–245.

- BAUM-K., SELLE-K., LEYK-D., AND ESSFELD-D. (1995). Comparison of blood pressure and heart rate responses to isometric exercise and passive muscle stretch in humans, *European Journal of Applied Physiology and Occupational Physiology*, **70**, pp. 240–245.
- BECKERS-F., VERHEYDEN-B., RAMAEKERS-D., SWYNGHEDAUW-B., AND AUBERT-A. E. (2006). Effects of autonomic blockade on non-linear cardiovascular variability indices in rats, *Clinical and Experimental Pharmacology and Physiology*, **33**(5-6), pp. 431–439.
- BERENS-P. (2009). Circstat: A matlab toolbox for circular statistics, *Journal of Statistical Software*, **31**(10), pp. 1–21.
- BERNARDI-L., PORTA-C., GABUTTI-A., SPICUZZA-L., AND SLEIGHT-P. (2001). Modulatory effects of respiration, *Autonomic Neuroscience: Basic & Clinical*, **90**(1), pp. 47–56.
- BERNTSON-G. G., BIGGER, J. T.-J., ECKBERG-D. L., GROSSMAN-P., KAUFMANN-P. G., MALIK-M., NAGARAJA-H. N., PORGES-S. W., SAUL-J. P., STONE-P. H., AND VAN DER MOLEN-M. W. (1997). Heart rate variability: origins, methods, and interpretive caveats, *Psychophysiology*, **34**(6), pp. 623–648.
- BERNTSON-G. G., CACIOPPO-J. T., AND QUIGLEY-K. S. (1993). Respiratory sinus arrhythmia: Autonomic origins, physiological mechanisms, and psychophysiological implications, *Psychophysiology*, **30**(2), pp. 183–196.
- BETTERMANN-H., CYSARZ-D., AND LEEUWEN-P. V. (2000). Detecting cardiorespiratory coordination by respiratory pattern analysis of heart period dynamics: The musical rhythm approach, *Int. J. Bifurcation Chaos*, **10**, pp. 2349–2360.
- BETTERMANN-H., CYSARZ-D., AND VAN LEEUWEN-P. (2002). Comparison of two different approaches in the detection of intermittent cardiorespiratory coordination during night sleep, *BMC Physiol*, **2**(18). DOI:10.1186/1472-6793-2-18.
- BHUIYAN-S. M. A., KHAN-J. F., AND ADHAMI-R. R. (2010). A novel approach of edge detection via a fast and adaptive bidimensional empirical mode decomposition method, *Advances in Adaptive Data Analysis*, **2**, pp. 171–192.
- BLASI-A., JO-J., BAYDUR-A., JUAREZ-R., AND KHOO-M. (2002). Effects of arousal from sleep on autonomic cardiovascular control in obstructive sleep apnea syndrome, *Proceedings of the Second Joint 24th Annual Conference and the Annual Fall Meeting of the Biomedical Engineering Society EMBS/BMES Conference, 2002.*, Vol. 2, pp. 1525–1526.
- BLASI-A., JO-J., VALLADARES-E., MORGAN-B. J., SKATRUD-J. B., AND KHOO-M. C. K. (2003). Cardiovascular variability after arousal from sleep: Time-varying spectral analysis, *Journal of Applied Physiology*, **95**(4), pp. 1394–1404.
- BONSIGNORE-M., MARRONE-O., INSALACO-G., AND BONSIGNORE-G. (1994). The cardiovascular effects of obstructive sleep apnoeas: Analysis of pathogenic mechanisms, *European Respiratory Journal*, **7**(4), pp. 786–805.
- BONSIGNORE-M. R., ROMANO-S., MARRONE-O., AND INSALACO-G. (1995). Respiratory sinus arrhythmia during obstructive sleep apnoeas in humans, *Journal of Sleep Research*, **4**, pp. 68–70.

Bibliography

- BRADLEY-T. D., AND FLORAS-J. S. (2009). Obstructive sleep apnoea and its cardiovascular consequences, *The Lancet*, **373**(9657), pp. 82–93.
- BRANDENBERGER-G., BUCHHEIT-M., EHRHART-J., SIMON-C., AND PIQUARD-F. (2005). Is slow wave sleep an appropriate recording condition for heart rate variability analysis?, *Autonomic Neuroscience*, **121**(1-2), pp. 81–86.
- BRANDENBERGER-G., EHRHART-J., PIQUARD-F., AND SIMON-C. (2001). Inverse coupling between ultradian oscillations in delta wave activity and heart rate variability during sleep, *Clinical Neurophysiology*, **112**(6), pp. 992–996.
- BUCHHEIT-M., HADDAD-H. A., LAURSEN-P. B., AND AHMAIDI-S. (2009). Effect of body posture on postexercise parasympathetic reactivation in men, *Exp. Physiol.*, **94**, pp. 795–804.
- BUCHHEIT-M., SIMON-C., PIQUARD-F., EHRHART-J., AND BRANDENBERGER-G. (2004). Effects of increased training load on vagal-related indexes of heart rate variability: A novel sleep approach, *American Journal of Physiology—Heart and Circulatory Physiology*, **287**(6), pp. H2813–H2818.
- BUSETTO-L., ENZI-G., INELMEN-E. M., COSTA-G., NEGRIN-V., SERGI-G., AND VIANELLO-A. (2005). Obstructive sleep apnea syndrome in morbid obesity: effects of intragastric balloon, *Chest*, **128**(2), pp. 618–623.
- BUTLER-J. E., MCKENZIE-D. K., AND GANDEVIA-S. C. (2001). Discharge frequencies of single motor units in human diaphragm and parasternal muscles in lying and standing, *J. Appl. Physiol.*, **90**(1), pp. 147–154.
- CAMINAL-P., GIRALDO-B., VALLVERD-M., BENITO-S., SCHROEDER-R., AND VOSS-A. (2010). Symbolic dynamic analysis of relations between cardiac and breathing cycles in patients on weaning trials, *Annals of Biomedical Engineering*, **38**(8), pp. 2542–2552.
- CAMINAL-P., VALLVERDU-M., GIRALDO-B., BENITO-S., VAZQUEZ-G., AND VOSS-A. (2005). Optimized symbolic dynamics approach for the analysis of the respiratory pattern, *IEEE Transactions on Biomedical Engineering*, **52**(11), pp. 1832–1839.
- CARSKADON-M., AND DEMENT-W. (2005). *Principles and Practice of Sleep Medicine*, 4 edn, Elsevier Saunders, Philadelphia, chapter Normal human sleep: An overview, pp. 13–23.
- CASOLO-G. C., STRODER-P., SIGNORINI-C., CALZOLARI-F., ZUCCHINI-M., BALLI-E., SULLA-A., AND LAZZERINI-S. (1992). Heart rate variability during the acute phase of myocardial infarction, *Circulation*, **85**(6), pp. 2073–2079.
- CENSI-F., CALCAGNINI-G., LINO-S., SEYDNEJAD-S., KITNEY-R., AND CERUTTI-S. (2000). Transient phase locking patterns among respiration, heart rate and blood pressure during cardiorespiratory synchronisation in humans, *Medical and Biological Engineering and Computing*, **38**(4), pp. 416–426.
- CENSI-F., CALCAGNINI-G., STRANO-S., BARTOLINI-P., AND BARBARO-V. (2003). Nonlinear coupling among heart rate, blood pressure, and respiration in patients susceptible to neuromediated syncope, *Annals of Biomedical Engineering*, **31**(9), pp. 1097–1105.

- CERUTTI-C., GUSTIN-M. P., PAULTRE-C. Z., LO-M., JULIEN-C., VINCENT-M., AND SASSARD-J. (1991). Autonomic nervous system and cardiovascular variability in rats: a spectral analysis approach, *American Journal of Physiology—Heart and Circulatory Physiology*, **261**(4), pp. H1292–H1299.
- CHADHA-T. S., LANG-E., BIRCH-S., AND SACKNER-M. A. (1985). Respiratory drive in nonsmokers and smokers assessed by passive tilt and mouth occlusion pressure. response to rebreathing carbon dioxide, *Chest*, **87**(1), pp. 6–10.
- CHANG-A. T., BOOTS-R. J., BROWN-M. G., PARATZ-J. D., AND HODGES-P. W. (2005). Ventilatory changes following head-up tilt and standing in healthy subjects, *Eur. J. Appl. Physiol.*, **95**(5-6), pp. 409–417.
- CHERVIN-R. D., RUZICKA-D. L., GIORDANI-B. J., WEATHERLY-R. A., DILLON-J. E., HODGES-E. K., MARCUS-C. L., AND GUIRE-K. E. (2006). Sleep-disordered breathing, behavior, and cognition in children before and after adenotonsillectomy, *Pediatrics*, **117**(4), pp. e769–e778.
- CIMPONERIU-L., ROSENBLUM-M., AND PIKOVSKY-A. (2004). Estimation of delay in coupling from time series, *Physical Review E*, **70**(4), article number 046213.
- CLARKE-S., AND TROWILL-J. A. (1971). Sniffing and motivated behavior in the rat, *Physiology & Behavior*, **6**(1), pp. 49–52.
- CORUZZI-P., GUALERZI-M., BERNKOPF-E., BRAMBILLA-L., BRAMBILLA-V., BROIA-V., LOMBARDI-C., AND PARATI-G. (2006). Autonomic cardiac modulation in obstructive sleep apnea: Effect of an oral jaw-positioning appliance, *Chest*, **130**(5), pp. 1362–1368.
- COY-T. V., DIMSDALE-J. E., ANCOLI-ISRAEL-S., AND CLAUSEN-J. (1996). Sleep apnoea and sympathetic nervous system activity: A review, *J. Sleep Res.*, **5**(1), pp. 42–50.
- CYSARZ-D., BETTERMANN-H., LANGE-S., GEUE-D., AND VAN LEEUWEN-P. (2004a). A quantitative comparison of different methods to detect cardiorespiratory coordination during night-time sleep, *Biomed. Eng. Online*, **3**(44), article number 44.
- CYSARZ-D., VON BONIN-D., LACKNER-H., HEUSSER-P., MOSER-M., AND BETTERMANN-H. (2004b). Oscillations of heart rate and respiration synchronize during poetry recitation, *Am J Physiol Heart Circ Physiol*, **287**(2), pp. H579–H587.
- DE MEERSMAN-R. E. (1992). Respiratory sinus arrhythmia alteration following training in endurance athletes, *European Journal of Applied Physiology*, **64**(5), pp. 434–436.
- DE MEERSMAN-R. E. (1993). Aging as a modulator of respiratory sinus arrhythmia, *Journal of Gerontology*, **48**(2), pp. B74–B78.
- DE TROYER-A. (1983). Mechanical role of the abdominal muscles in relation to posture, *Respir Physiol*, **53**(3), pp. 341–353.
- DEVANEY-R. L. (2003). *An Introduction to Chaotic Dynamical Systems*, Westview Press.
- ECHVERRIA-J., CROWE-J., WOOLFSON-M., AND HAYES-GILL-B. (2001). Application of empirical mode decomposition to heart rate variability analysis, *Medical and Biological Engineering and Computing*, **39**, pp. 471–479.

Bibliography

- ECKBERG-D. L. (1983). Human sinus arrhythmia as an index of vagal cardiac outflow, *Journal of Applied Physiology*, **54**(4), pp. 961–966.
- ECKBERG-D. L. (2003). The human respiratory gate, *The Journal of Physiology*, **548**(2), pp. 339–352.
- EINTHOVEN-W., FAHR-G., AND DE WAART-A. (1950). On the direction and manifest size of the variations of potential in the human heart and on the influence of the position of the heart on the form of the electrocardiogram, *Am. Heart J.*, **40**(2), pp. 163–211.
- ELDRIDGE-F., AND WALDROP-T. (1991). Neural control of breathing during exercise, in B. Whipp., and K. Wasseman. (eds.), *Excercise: Pulmonary Physiology and Pathophysiology*, Marcel Dekker, NY, pp. 309–370.
- EMWAVE. (2011). The science behind the emwave pc stress relief system, Institute of HeartMath. <http://www.emwavepc.org/emwave-pc-science-research.html>.
- FAUCHIER-L., MELIN-A., EDER-V., ANTIER-D., AND BONNET-P. (2006). Heart rate variability in rats with chronic hypoxic pulmonary hypertension., *Ann. Cardiol. Angeiol. (Paris)*, **55**(5), pp. 249–254.
- FERGUSON-K. A., ONO-T., LOWE-A. A., RYAN-C. F., AND FLEETHAM-J. A. (1995). The relationship between obesity and craniofacial structure in obstructive sleep apnea, *Chest*, **108**(2), pp. 375–381.
- FISHER-N. I. (1993). *Statistical Analysis of Circular Data*, Cambridge University Press.
- FOURNIER-S., ALLARD-M., GULEMETOVA-R., JOSEPH-V., AND KINKEAD-R. (2007). Chronic corticosterone elevation and sex-specific augmentation of the hypoxic ventilatory response in awake rats, *The Journal of Physiology*, **584**(3), pp. 951–962.
- GABOR-D. (1946). Theory of communication, *Journal of the Institute of Electrical Engineers (London)*, **93**, pp. 429–457.
- GALLETLY-D. C., AND LARSEN-P. D. (1997). Cardioventilatory coupling during anaesthesia, *British Journal of Anaesthesia*, **79**(1), pp. 35–40.
- GALLETLY-D. C., AND LARSEN-P. D. (1998). Relationship between cardioventilatory coupling and respiratory sinus arrhythmia, *British Journal of Anaesthesia*, **80**, pp. 164–168.
- GALLETLY-D. C., AND LARSEN-P. D. (1999). The determination of cardioventilatory coupling from heart rate and ventilatory time series, *Research in Experimental Medicine*, **199**(2), pp. 95–99.
- GALLETLY-D. C., AND LARSEN-P. D. (2001). Cardioventilatory coupling in heart rate variability: methods for qualitative and quantitative determination, *British Journal of Anaesthesia*, **87**(6), pp. 827–833.
- GENEST-S.-E., GULEMETOVA-R., LAFOREST-S., DROLET-G., AND KINKEAD-R. (2007). Neonatal maternal separation induces sex-specific augmentation of the hypercapnic ventilatory response in awake rat, *Journal of Applied Physiology*, **102**(4), pp. 1416–1421.
- GENTZLER-A. L., ROTTENBERG-J., KOVACS-M., GEORGE-C. J., AND MOREY-J. N. (2011). Atypical development of resting respiratory sinus arrhythmia in children at high risk for depression, *Dev. Psychobiol.*, . DOI: 10.1002/dev.20614.

- GILAD-O., SWENNE-C. A., DAVRATH-L. R., AND AKSELROD-S. (2005). Phase-averaged characterization of respiratory sinus arrhythmia pattern, *Am. J. Physiol. Heart Circ. Physiol.*, **288**(2), pp. H504–H510.
- GOTTESMANN-C. (1999). Neurophysiological support of consciousness during waking and sleep, *Progress in Neurobiology*, **59**(5), pp. 469–508.
- GROSSMAN-P., AND TAYLOR-E. W. (2007). Toward understanding respiratory sinus arrhythmia: Relations to cardiac vagal tone, evolution and biobehavioral functions, *Biological Psychology*, **74**(2), pp. 263–285.
- GUYTON-A. C., AND HALL-J. E. (2006). States of brain activity - sleep, brain waves, epilepsy, psychoses, in W. Schmitt., and R. Grulicow. (eds.), *Textbook of medical physiology*, Elsevier Saunders, pp. 739–747.
- HAMANN-C., BARTSCH-R. P., SCHUMANN-A. Y., PENZEL-T., HAVLIN-S., AND KANTELHARDT-J. W. (2009). Automated synchrogram analysis applied to heartbeat and reconstructed respiration, *Chaos*, **19**(1), article number 015106.
- HAYANO-J., AND YASUMA-F. (2003). Hypothesis: Respiratory sinus arrhythmia is an intrinsic resting function of cardiopulmonary system, *Cardiovascular Research*, **58**(1), pp. 1–9.
- HAYANO-J., MUKAI-S., SAKAKIBARA-M., OKADA-A., TAKATA-K., AND FUJINAMI-T. (1994). Effects of respiratory interval on vagal modulation of heart rate, *Am. J. Physiol. Heart Circ. Physiol.*, **267**(1), pp. H33–H40.
- HAYANO-J., SAKAKIBARA-Y., YAMADA-A., YAMADA-M., MUKAI-S., FUJINAMI-T., YOKOYAMA-K., WATANABE-Y., AND TAKATA-K. (1991). Accuracy of assessment of cardiac vagal tone by heart rate variability in normal subjects, *The American Journal of Cardiology*, **67**(2), pp. 199–204.
- HAYANO-J., YASUMA-F., OKADA-A., MUKAI-S., AND FUJINAMI-T. (1996). Respiratory sinus arrhythmia: A phenomenon improving pulmonary gas exchange and circulatory efficiency, *Circulation*, **94**(4), pp. 842–847.
- HELLMAN-J. B., AND STACY-R. W. (1976). Variation of respiratory sinus arrhythmia with age, *Journal of Applied Physiology*, **41**(5), pp. 734–738.
- HILTON-S. M., MARSHALL-J. M., AND TIMMS-R. J. (1983). Ventral medullary relay neurones in the pathway from the defence areas of the cat and their effect on blood pressure, *J. Physiol.*, **345**, pp. 149–166.
- HIRSCH-J. A., AND BISHOP-B. (1981). Respiratory sinus arrhythmia in humans: How breathing pattern modulates heart rate, *Am. J. Physiol. Heart Circ. Physiol.*, **241**(4), pp. H620–H629.
- HOFFMANN-J., GRIMM-W., MENZ-V., KNOP-U., AND MAISCH-B. (1996). Heart rate variability and major arrhythmic events in patients with idiopathic dilated cardiomyopathy, *Pacing Clin. Electrophysiol.*, **19**(11 Pt 2), pp. 1841–1844.
- HORN-E. M., AND WALDROP-T. G. (1998). Suprapontine control of respiration, *Respiration Physiology*, **114**(3), pp. 201–211.

Bibliography

- HORNER-R. L. (2003). *Sleep Apnea: Pathogenesis, Diagnosis and Treatment*, Marcel Dekker, New York, chapter Arousal mechanisms and autonomic consequences, pp. 179–216.
- HOYER-D., BAUER-R., WALTER-B., AND ZWIENER-U. (1998a). Estimation of nonlinear couplings on the basis of complexity and predictability—a new method applied to cardiorespiratory coordination, *IEEE Transaction on Biomedical Engineering*, **45**(5), pp. 545–552.
- HOYER-D., HADER-O., AND ZWIENER-U. (1997). Relative and intermittent cardiorespiratory coordination, *IEEE Eng Med Biol Mag*, **16**(6), pp. 97–104.
- HOYER-D., HOYER-O., AND ZWIENER-U. (2000). A new approach to uncover dynamic phase coordination and synchronization, *IEEE Transaction on Biomedical Engineering*, **47**(1), pp. 68–74.
- HOYER-D., KAPLAN-D., SCHAAFF-F., AND EISELT-M. (1998b). Determinism in bivariate cardiorespiratory phase-space sets, *IEEE Eng. Med. Biol. Mag.*, **17**(6), pp. 26–31.
- HOYER-D., LEDER-U., HOYER-H., POMPE-B., SOMMER-M., AND ZWIENER-U. (2002). Mutual information and phase dependencies: measures of reduced nonlinear cardiorespiratory interactions after myocardial infarction, *Medical Engineering & Physics*, **24**(1), pp. 33–43.
- HOYER-D., POMPE-B., HERZEL-H., AND ZWIENER-U. (1998c). Nonlinear coordination of cardiovascular autonomic control, *IEEE Engineering in Medicine and Biology*, **17**(6), pp. 17–21.
- HRUSHESKY-W. J., FADER-D., SCHMITT-O., AND GILBERTSEN-V. (1984). The respiratory sinus arrhythmia: A measure of cardiac age, *Science*, **224**(4652), pp. 1001–1004.
- HSIEH-C. W., MAO-C. W., YOUNG-M. S., YEH-T. L., AND YEH-S. J. (2003). Respiratory effect on the pulse spectrum, *J. Med. Eng. Technol.*, **27**(2), pp. 77–84.
- HUANG-N. E., SHEN-Z., LONG-S. R., WU-M. C., SHIH-H. H., ZHENG-Q., YEN-N.-C., TUNG-C. C., AND LIU-H. H. (1998). The empirical mode decomposition and the Hilbert spectrum for nonlinear and non-stationary time series analysis, *Proceeding of Royal Society London A*, **454**, pp. 903–995.
- HUBBARD-B. B. (1998). *The World According to Wavelets: The Story of a Mathematical Technique in the Making*, A K Peters, Natick, Massachusetts.
- IKEMOTO-S., AND PANKSEPP-J. (1994). The relationship between self-stimulation and sniffing in rats: does a common brain system mediate these behaviors?, *Behav. Brain Res.*, **61**(2), pp. 143–162.
- JAVORKA-M., TRUNKVALTEROVA-Z., TONHAJZEROVA-I., JAVORKOVA-J., JAVORKA-K., AND BAUMERT-M. (2008). Short-term heart rate complexity is reduced in patients with type 1 diabetes mellitus, *Clinical Neurophysiology*, **119**(5), pp. 1071–1081.
- JURKOVICOVA-I., AND CELEC-P. (2004). Sleep apnea syndrome and its complications, *Acta Med Austriaca*, **31**(2), pp. 45–50.
- KABIR-M. M., BEIG-M. I., BAUMERT-M., TROMBINI-M., MASTORCI-F., SGOIFO-A., WALKER-F. R., DAY-T. A., AND NALIVAICO-E. (2010a). Respiratory pattern in awake rats: Effects of motor activity and of alerting stimuli, *Physiology & Behavior*, **101**(1), pp. 22–31. DOI: 10.1016/j.physbeh.2010.04.004.

- KABIR-M. M., BEIG-M. I., NALIVAICO-E., ABBOTT-D., AND BAUMERT-M. (2008). Isoflurane increases cardiorespiratory coordination in rats, *Proc. SPIE Biomedical Applications of Micro- and Nano-engineering IV and Complex Systems*, Vol. 7270, Melbourne, Australia.
- KABIR-M. M., BEIG-M. I., NALIVAICO-E., ABBOTT-D., AND BAUMERT-M. (2009). Cardiorespiratory coordination in rats is influenced by autonomic blockade, in C. T. Lim., and J. C. H. Goh. (eds.), *13th International Conference on Biomedical Engineering*, Vol. 23 of *IFMBE Proceedings*, Springer Berlin Heidelberg, pp. 456–459.
- KABIR-M. M., DIMITRI-H., SANDERS-P., ANTIC-R., ABBOTT-D., AND BAUMERT-M. (2011a). Quantification of cardio-respiratory interactions in patients with mild obstructive sleep apnea syndrome using joint symbolic dynamics, *Computing in Cardiology*, Vol. 38, pp. 41–44.
- KABIR-M. M., DIMITRI-H., SANDERS-P., ANTIC-R., NALIVAICO-E., ABBOTT-D., AND BAUMERT-M. (2010b). Cardiorespiratory phase-coupling is reduced in patients with obstructive sleep apnea, *PLoS ONE*, 5(5), article number e10602.
- KABIR-M. M., KOHLER-M., ABBOTT-D., AND BAUMERT-M. (2011b). Quantification of cardiorespiratory interactions in healthy children during night-time sleep using joint symbolic dynamics, *Engineering in Medicine and Biology Society (EMBC), 2011 Annual International Conference of the IEEE*, pp. 1459–1462.
- KABIR-M. M., NALIVAICO-E., ABBOTT-D., AND BAUMERT-M. (2010c). Impact of movement on cardiorespiratory coordination in conscious rats, *Engineering in Medicine and Biology Society (EMBC), 2010 Annual International Conference of the IEEE*, pp. 1938–1941.
- KABIR-M., SAINT-D., NALIVAICO-E., ABBOTT-D., AND BAUMERT-M. (2011c). Time delay correction of the synchrogram for optimized detection of cardiorespiratory coordination, *Medical & Biological Engineering & Computing*, 49, pp. 1249–1259. DOI: 10.1007/s11517-011-0822-3.
- KABIR-M., SAINT-D., NALIVAICO-E., ABBOTT-D., VOSS-A., AND BAUMERT-M. (2011d). Quantification of cardiorespiratory interactions based on joint symbolic dynamics, *Annals of Biomedical Engineering*, 39(10), pp. 2604–2614. DOI: 10.1007/s10439-011-0332-3.
- KADITIS-A. G., ALEXOPOULOS-E. I., DAMANI-E., HATZI-F., CHAIDAS-K., KOSTOPOULOU-T., TZIGEROGLOU-A., AND GOURGOULIANIS-K. (2009). Urine levels of catecholamines in greek children with obstructive sleep-disordered breathing, *Pediatric Pulmonology*, 44(1), pp. 38–45.
- KENWRIGHT-D., BAHRAMINASAB-A., STEFANOVSKA-A., AND MCCLINTOCK-P. (2008). The effect of low-frequency oscillations on cardio-respiratory synchronization, *The European Physical Journal B—Condensed Matter and Complex Systems*, 65(3), pp. 425–433.
- KEPECS-A., UCHIDA-N., AND MAINEN-Z. F. (2007). Rapid and precise control of sniffing during olfactory discrimination in rats, *J Neurophysiol*, 98(1), pp. 205–213.
- KESLER-B., ANAND-A., LAUNOIS-S. H., AND WEISS-J. W. (1999). Drug-induced arterial pressure elevation is associated with arousal from nrem sleep in normal volunteers, *Journal of Applied Physiology*, 87(3), pp. 897–901.

Bibliography

- KITCHENS-B. P. (1998). *Symbolic Dynamics: One-Sided, Two-Sided and Countable State Markov Shifts*, Springer.
- KOTANI-K., TAKAMASU-K., ASHKENAZY-Y., STANLEY-H. E., AND YAMAMOTO-Y. (2002). Model for cardiorespiratory synchronization in humans, *Phys. Rev. E*, **65**(5 Pt 1), article number 051923.
- KOTANI-K., TAKAMASU-K., JIMBO-Y., AND YAMAMOTO-Y. (2008). Postural-induced phase shift of respiratory sinus arrhythmia and blood pressure variations: insight from respiratory-phase domain analysis, *Am. J. Physiol. Heart Circ. Physiol.*, **294**(3), pp. H1481–H1489.
- KRISHNAMURTHY-S., WANG-X., BHAKTA-D., BRUCE-E., EVANS-J., JUSTICE-T., AND PATWARDHAN-A. (2004). Dynamic cardiorespiratory interaction during head-up tilt-mediated presyncope, *American Journal of Physiology—Heart and Circulatory Physiology*, **287**(6), pp. H2510–H2517.
- KURTHS-J., VOSS-A., SAPARIN-P., WITT-A., KLEINER-H. J., AND WESSEL-N. (1995). Quantitative analysis of heart rate variability, *Chaos: An Interdisciplinary Journal of Nonlinear Science*, **5**(1), pp. 88–94.
- KUWAHARA-M., ICHI HASHIMOTO-S., ISHII-K., YAGI-Y., HADA-T., HIRAGA-A., KAI-M., KUBO-K., OKI-H., TSUBONE-H., AND SUGANO-S. (1996). Assessment of autonomic nervous function by power spectral analysis of heart rate variability in the horse, *Journal of the Autonomic Nervous System*, **60**(1-2), pp. 43–48.
- LEDER-U., HOYER-D., SOMMER-M., BAIER-V., HAUEISEN-J., ZWIENER-U., AND FIGULLA-H. R. (2000). Cardiorespiratory desynchronization after acute myocardial infarct, *Z. Kardiol.*, **89**(7), pp. 630–637.
- LOEPPKY-J. A., AND LUFT-U. C. (1975). Fluctuations in O₂ stores and gas exchange with passive changes in posture, *J Appl Physiol*, **39**(1), pp. 47–53.
- LOREDO-J. S., ZIEGLER-M. G., ANCOLI-ISRAEL-S., CLAUSEN-J. L., AND DIMSDALE-J. E. (1999). Relationship of arousals from sleep to sympathetic nervous system activity and BP in obstructive sleep apnea, *Chest*, **116**(3), pp. 655–659.
- LORENZ-E. N. (1963). Deterministic nonperiodic flow, *Journal of the Atmospheric Sciences*, **20**, pp. 130–141.
- LOTRIC-M. B., AND STEFANOVSKA-A. (2000). Synchronization and modulation in the human cardiorespiratory system, *Physica A*, **283**, pp. 451–461.
- LUMENG-J. C., AND CHERVIN-R. D. (2008). Epidemiology of pediatric obstructive sleep apnea, *Proc. Am. Thorac. Soc.*, **5**(2), pp. 242–252.
- MALLIANI-A., PAGANI-M., LOMBARDI-F., AND CERUTTI-S. (1991). Cardiovascular neural regulation explored in the frequency domain, *Circulation*, **84**(2), pp. 482–492.
- MANGIN-L., CLERICI-C., SIMILOWSKI-T., AND POON-C.-S. (2009). Chaotic dynamics of cardioventilatory coupling in humans: effects of ventilatory modes, *Am. J. Physiol. Regul. Integr. Comp. Physiol.*, **296**(4), pp. R1088–R1097.
- MANRIQUEZ-A. I., AND ZHANG-Q. (2007). An algorithm for qrs onset and offset detection in single lead electrocardiogram records, *Conf. Proc. IEEE Eng. Med. Biol. Soc.*, **2007**, pp. 541–544.

- MARAGOS-P., KAISER-J. F., AND QUATIERI-T. F. (1993a). Energy separation in signal modulations with application to speech analysis, *IEEE Transaction on Biomedical Engineering*, **41**(10), pp. 3024–3051.
- MARAGOS-P., KAISER-J. F., AND QUATIERI-T. F. (1993b). On amplitude and frequency demodulation using energy operators, *IEEE Transaction on Biomedical Engineering*, **41**(4), pp. 1532–1550.
- MARANO-G., GRIGIONI-M., TIBURZI-F., VERGARI-A., AND ZANGHI-F. (1996). Effects of isoflurane on cardiovascular system and sympathovagal balance in New Zealand white rabbits, *Journal of Cardiovascular Pharmacology*, **28**(4), pp. 513–518.
- MARCUS-C., GREENE-M., AND CARROLL-J. (1998). Blood pressure in children with obstructive sleep apnea, *Am. J. Respir. Crit. Care Med.*, **157**(4), pp. 1098–1103.
- MARCUS-C. L. (2001). Sleep-disordered breathing in children, *Am. J. Respir. Crit. Care Med.*, **164**(1), pp. 16–30.
- MARSHALL-P. J., AND STEVENSON-HINDE-J. (1998). Behavioral inhibition, heart period, and respiratory sinus arrhythmia in young children, *Developmental Psychobiology*, **33**(3), pp. 283–292.
- MCNICHOLAS-W. T., BONSIGNORE-M. R., AND THE MANAGEMENT COMMITTEE OF EU COST ACTION B26. (2007). Sleep apnoea as an independent risk factor for cardiovascular disease: current evidence, basic mechanisms and research priorities, *European Respiratory Journal*, **29**(1), pp. 156–178.
- MIYAMOTO-Y., TAMURA-T., HIURA-T., NAKAMURA-T., HIGUCHI-J., AND MIKAMI-T. (1982). The dynamic response of the cardiopulmonary parameters to passive head-up tilt, *Jpn. J. Physiol.*, **32**(2), pp. 245–258.
- MONTANDON-G., BAIRAM-A., AND KINKEAD-R. (2008). Neonatal caffeine induces sex-specific developmental plasticity of the hypoxic respiratory chemoreflex in adult rats, *American Journal of Physiology*, **295**(3), pp. R922–R934.
- MONTANO-N., LOMBARDI-F., RUSCONE-T. G., CONTINI-M., FINOCCHIARO-M. L., BASELLI-G., PORTA-A., CERUTTI-S., AND MALLIANI-A. (1992). Spectral analysis of sympathetic discharge, R-R interval and systolic arterial pressure in decerebrate cats, *Journal of the Autonomic Nervous System*, **40**(1), pp. 21–31.
- MOODY-G. B., MARK-R. G., ZOCCOLA-A., AND MANTERO-S. (1985). Derivation of respiratory signals from multi-lead ECGs, *Computers in Cardiology*, **12**, pp. 113–116.
- MORGAN-B. J., CRABTREE-D. C., PULEO-D. S., BADR-M. S., TOIBER-F., AND SKATRUD-J. B. (1996). Neurocirculatory consequences of abrupt change in sleep state in humans, *Journal of Applied Physiology*, **80**(5), pp. 1627–1636.
- MORTOLA-J. P., AND FRAPPELL-P. B. (1998). On the barometric method for measurements of ventilation, and its use in small animals, *Can. J. Physiol. Pharmacol.*, **76**(10-11), pp. 937–944.
- MOSER-M., LEHOFER-M., SEDMINEK-A., LUX-M., ZAPOTOCZKY-H., KENNER-T., AND NOORDERGRAAF-A. (1994). Heart rate variability as a prognostic tool in cardiology: A contribution to the problem from a theoretical point of view, *Circulation*, **90**(2), pp. 1078–1082.

Bibliography

- MROWKA-R., CIMPONERIU-L., PATZAK-A., AND ROSENBLUM-M. G. (2003). Directionality of coupling of physiological subsystems: age-related changes of cardiorespiratory interaction during different sleep stages in babies, *American Journal of Physiology—Regulatory, Integrative and Comparative Physiology*, **285**(6), pp. R1395–R1401.
- MROWKA-R., PATZAK-A., AND ROSENBLUM-M. (2000). Quantitative analysis of cardiorespiratory synchronization in infants, *International Journal of Bifurcation and Chaos*, **10**(11), pp. 2479–2488.
- NAKRA-N., BHARGAVA-S., DZUIRA-J., CAPRIO-S., AND BAZZY-ASAAD-A. (2008). Sleep-disordered breathing in children with metabolic syndrome: The role of leptin and sympathetic nervous system activity and the effect of continuous positive airway pressure, *Pediatrics*, **122**(3), pp. e634–e642.
- NALIVAICO-E., CATCHESIDE-P. G., ADAMS-A., JORDAN-A. S., ECKERT-D. J., AND MCEVOY-R. D. (2007). Cardiac changes during arousals from non-REM sleep in healthy volunteers, *Am. J. Physiol. Regul. Integr. Comp. Physiol.*, **292**(3), pp. R1320–R1327.
- NARKIEWICZ-K., AND SOMERS-V. K. (2003). Sympathetic nerve activity in obstructive sleep apnoea, *Acta Physiologica Scandinavica*, **177**(3), pp. 385–390.
- NARKIEWICZ-K., MONTANO-N., COGLIATI-C., VAN DE BORNE-P. J. H., DYKEN-M. E., AND SOMERS-V. K. (1998). Altered cardiovascular variability in obstructive sleep apnea, *Circulation*, **98**(11), pp. 1071–1077.
- NAVAJAS-D., FARRE-R., ROTGER-M. M., MILIC-EMILI-J., AND SANCHIS-J. (1988). Effect of body posture on respiratory impedance, *J. Appl. Physiol.*, **64**(1), pp. 194–199.
- NEFF-R. A., WANG-J., BAXI-S., EVANS-C., AND MENDELOWITZ-D. (2003). Respiratory sinus arrhythmia: Endogenous activation of nicotinic receptors mediates respiratory modulation of brainstem cardioinhibitory parasympathetic neurons, *Circ. Res.*, **93**(6), pp. 565–572.
- NGAMPAMUAN-S., BAUMERT-M., BEIG-M. I., KOTCHABHAKDI-N., AND NALIVAICO-E. (2008). Activation of 5-HT(1A) receptors attenuates tachycardia induced by restraint stress in rats, *Am. J. Physiol. Regul. Integr. Comp. Physiol.*, **294**(1), pp. R132–R141.
- NIEBUR-E., SCHUSTER-H. G., AND KAMMEN-D. M. (1991). Collective frequencies and metastability in networks of limit-cycle oscillators with time delay, *Physical Review Letters*, **67**(20), pp. 2753–2756.
- O'DRISCOLL-D. M., FOSTER-A. M., NG-M. L., YANG-J., BASHIR-F., NIXON-G. M., DAVEY-M. J., ANDERSON-V., WALKER-A. M., TRINDER-J., AND HORNE-R. S. (2009). Acute cardiovascular changes with obstructive events in children with sleep disordered breathing, *Sleep*, **32**, pp. 1265–1271.
- PACK-A. I., AND GISLASON-T. (2009). Obstructive sleep apnea and cardiovascular disease: A perspective and future directions, *Progress in Cardiovascular Diseases*, **51**(5), pp. 434–451.
- PENTTILA-J., HELMINEN-A., JARTTI-T., KUUSELA-T., HUIKURI-H. V., TULPPO-M. P., COFFENG-R., AND SCHEININ-H. (2001). Time domain, geometrical and frequency domain analysis of cardiac vagal outflow: Effects of various respiratory patterns, *Clinical Physiology*, **21**(3), pp. 365–376.

- PENZEL-T., KANTELHARDT-J. W., LO-C. C., VOIGT-K., AND VOGELMEIER-C. (2003). Dynamics of heart rate and sleep stages in normals and patients with sleep apnea, *Neuropsychopharmacology*, **28 Suppl 1**, pp. S48–S53.
- PEREDA-E., CRUZ-D. M. D. L., VERA-L. D., AND GONZALEZ-J. J. (2005). Comparing generalized and phase synchronization in cardiovascular and cardiorespiratory signals, *IEEE Transactions on Biomedical Engineering*, **52(4)**, pp. 578–583.
- PFEIFER-M. A., WEINBERG-C. R., COOK-D., BEST-J. D., REENAN-A., AND HALTER-J. B. (1983). Differential changes of autonomic nervous system function with age in man, *The American Journal of Medicine*, **75(2)**, pp. 249–258.
- PIKOVSKY-A., ROSENBLUM-M., AND KURTHS-J. (2001). *Synchronization: A Universal Concept in Non-linear Sciences*, Cambridge University Press, chapter Synchronization of chaotic systems, pp. 137–152.
- PIKOVSKY-A. S., ROSENBLUM-M. G., OSIPOV-G. V., AND KURTHS-J. (1997). Phase synchronization of chaotic oscillators by external driving, *Physica D: Nonlinear Phenomena*, **104(3-4)**, pp. 219–238.
- PINNA-G. D., MAESTRI-R., LA ROVERE-M. T., GOBBI-E., AND FANFULLA-F. (2006). Effect of paced breathing on ventilatory and cardiovascular variability parameters during short-term investigations of autonomic function, *American Journal of Physiology—Heart and Circulatory Physiology*, **290(1)**, pp. H424–H433.
- PITZALIS-M. V., MASTROPASQUA-F., MASSARI-F., PASSANTINO-A., COLOMBO-R., MANNARINI-A., FORLEO-C., AND RIZZON-P. (1998). Effect of respiratory rate on the relationships between RR interval and systolic blood pressure fluctuations: A frequency-dependent phenomenon, *Cardiovascular Research*, **38(2)**, pp. 332–339.
- PIZZUTI-G. P., CIFALDI-S., AND NOLFE-G. (1985). Digital sampling rate and ECG analysis, *Journal of Biomedical Engineering*, **7(3)**, pp. 247–250.
- PORTA-A., GUZZETTI-S., MONTANO-N., PAGANI-M., SOMERS-V., MALLIANI-A., BASELLI-G., AND CERUTTI-S. (2000). Information domain analysis of cardiovascular variability signals: Evaluation of regularity, synchronisation and co-ordination, *Medical and Biological Engineering and Computing*, **38(2)**, pp. 180–188.
- PUNJABI-N. M. (2008). The epidemiology of adult obstructive sleep apnea, *Proc. Am. Thorac. Soc.*, **5(2)**, pp. 136–143.
- RAY-A. (2004). Symbolic dynamic analysis of complex systems for anomaly detection, *Signal Processing*, **84(7)**, pp. 1115–1130.
- RECHTSCHAFFEN-A., AND KALES-A. (1968). *A Manual of Standardized Terminology, Techniques and Scoring System for Sleep Stages in Human Subjects*, Brain Information Service/Brain Research Institute, Los Angeles.
- REDDY-D. V. R., SEN-A., AND JOHNSTON-G. L. (2000). Dynamics of a limit cycle oscillator under time delayed linear and nonlinear feedbacks, *Physica D: Nonlinear Phenomena*, **144(3-4)**, pp. 335–357.

Bibliography

- ROBINSON-B. F., EPSTEIN-S. E., BEISER-G. D., AND BRAUNWALD-E. (1966). Control of heart rate by the autonomic nervous system: Studies in man on the interrelation between baroreceptors mechanisms and exercise, *Circ. Res.*, **19**, pp. 400–411.
- ROBINSON-C. (1999). *Dynamical Systems: Stability, Symbolic Dynamics, and Chaos*, CRC press.
- ROCHE-F., DUVERNEY-D., COURT-FORTUNE-I., PICHOT-V., COSTES-F., LACOUR-J. R., ANTONIADIS-J. A., GASPOZ-J. M., AND BARTHELEMY-J. C. (2002). Cardiac interbeat interval increment for the identification of obstructive sleep apnea, *Pacing Clin. Electrophysiol.*, **25**(8), pp. 1192–1199.
- ROCHE-F., GASPOZ-J. M., COURT-FORTUNE-I., MININI-P., PICHOT-V., DUVERNEY-D., COSTES-F., LACOUR-J. R., AND BARTHELEMY-J. C. (1999). Screening of obstructive sleep apnea syndrome by heart rate variability analysis, *Circulation*, **100**(13), pp. 1411–1415.
- ROMEI-M., MAURO-A. L., D'ANGELO-M. G., TURCONI-A. C., BRESOLIN-N., PEDOTTI-A., AND ALIVERTI-A. (2010). Effects of gender and posture on thoraco-abdominal kinematics during quiet breathing in healthy adults, *Respir. Physiol. Neurobiol.*, **172**(3), pp. 184–191.
- ROSENBLUM-M. G., AND KURTHS-J. (1998). Analysing synchronization phenomena from bivariate data by means of the Hilbert transform, in H. Kantz., J. Kurths., and G. Mayer-Kress. (eds.), *Nonlinear Analysis of Physiological Data*, Springer, Berlin, pp. 91–99.
- ROSENBLUM-M. G., CIMPONERIU-L., BEZERIANOS-A., PATZAK-A., AND MROWKA-R. (2002). Identification of coupling direction: Application to cardiorespiratory interaction, *Physical Review E*, **65**, article number 041909.
- ROSENBLUM-M. G., KURTHS-J., PIKOVSKY-A., SCHAFER-C., TASS-P., AND ABEL-H. H. (1998). Synchronization in noisy systems and cardiorespiratory interaction, *IEEE Eng. Med. Biol. Mag.*, **17**(6), pp. 46–53.
- ROSENBLUM-M. G., PIKOVSKY-A., KURTHS-J., SCHAFER-C., AND TASS-P. A. (2001). Phase synchronization: From theory to data analysis, in F. Moss., and S. Gielen. (eds.), *Handbook of Biological Physics*, Vol. 4 of *Neuro-informatics*, Elsevier Science, pp. 279–321.
- ROSENBLUM-M. G., PIKOVSKY-A. S., AND KURTHS-J. (1996). Phase synchronization of chaotic oscillators, *Physical Review Letters*, **76**(11), pp. 1804–1807.
- ROSENBLUM-M. G., PIKOVSKY-A. S., AND KURTHS-J. (2004). Synchronization approach to analysis of biological systems, *Fluctuation and Noise Letters*, **4**(1), pp. L53–L62.
- ROUX-J. C., PEYRONNET-J., PASCUAL-O., DALMAZ-Y., AND PEQUIGNOT-J. M. (2000). Ventilatory and central neurochemical reorganisation of O₂ chemoreflex after carotid sinus nerve transection in rat, *J. Physiol.*, **522**, pp. 493–501.
- ROWELL-L. B. (1993). Reflex control during orthostasis, in L. B. Rowell. (ed.), *Human Cardiovascular Control*, Oxford University Press, New York, pp. 37–80.
- RYBSKI-D., HAVLIN-S., AND BUNDE-A. (2003). Phase synchronization in temperature and precipitation records, *Physica A: Statistical Mechanics and its Applications*, **320**, pp. 601–610.

- RZECZINSKI-S., JANSON-N. B., BALANOV-A. G., AND MCCLINTOCK-P. V. E. (2002). Regions of cardiorespiratory synchronization in humans under paced respiration, *Physical Review E*, **66**(5), article number 051909.
- SALOME-N., NGAMPRAMUAN-S., AND NALIVAICO-E. (2007). Intra-amygdala injection of GABAA agonist, muscimol, reduces tachycardia and modifies cardiac sympatho-vagal balance during restraint stress in rats, *Neuroscience*, **148**(2), pp. 335–341. DOI: 10.1016/j.neuroscience.2007.06.022.
- SALOMON-K. (2005). Respiratory sinus arrhythmia during stress predicts resting respiratory sinus arrhythmia 3 years later in a pediatric sample, *Health Psychology*, **24**(1), pp. 68–76.
- SANDERCOCK-G. R., AND BRODIE-D. A. (2006). The role of heart rate variability in prognosis for different modes of death in chronic heart failure, *Pacing Clin. Electrophysiol.*, **29**(8), pp. 892–904.
- SAUL-J. P., BERGER-R. D., ALBRECHT-P., STEIN-S. P., CHEN-M. H., AND COHEN-R. J. (1991). Transfer function analysis of the circulation: unique insights into cardiovascular regulation, *American Journal of Physiology—Heart and Circulatory Physiology*, **261**(4), pp. H1231–H1245.
- SCHAFFER-C., ROSENBLUM-M. G., ABEL-H. H., AND KURTHS-J. (1999). Synchronization in the human cardiorespiratory system, *Phys. Rev. E Stat. Phys. Plasmas Fluids Relat. Interdiscip. Topics*, **60**(1), pp. 857–870.
- SCHAFFER-C., ROSENBLUM-M. G., KURTHS-J., AND ABEL-H. H. (1998). Heartbeat synchronized with ventilation, *Nature*, **392**(6673), pp. 239–240.
- SCHIEK-M., DREPPER-F. R., ENGBERT-R., ABEL-H. H., AND SUDER-K. (1998). *Nonlinear Analysis of Physiological Data*, Springer, chapter Cardiorespiratory synchronization, pp. 191–209.
- SGOIFO-A., STILLI-D., MEDICI-D., GALLO-P., AIMI-B., AND MUSSO-E. (1996). Electrode positioning for reliable telemetry ECG recordings during social stress in unrestrained rats, *Physiology & Behavior*, **60**(6), pp. 1397–1401. DOI: 10.1016/S0031-9384(96)00228-4.
- SHARP-J. T., GOLDBERG-N. B., DRUZ-W. S., AND DANON-J. (1975). Relative contributions of rib cage and abdomen to breathing in normal subjects, *J. Appl. Physiol.*, **39**(4), pp. 608–618.
- SHIOGAI-Y., STEFANOVSKA-A., AND MCCLINTOCK-P. V. E. (2010). Nonlinear dynamics of cardiovascular ageing, *Physics Reports*, **488**(2-3), pp. 51–110. DOI: 10.1016/j.physrep.2009.12.003.
- SIGLER-L. H. (1957). *The Electrocardiogram*, 2 edn, Grune & Stratton, New York. Its interpretation and Clinical Application.
- SNYDER-F., HOBSON-J. A., MORRISON-D. F., AND GOLDFRANK-F. (1964). Changes in respiration, heart rate, and systolic blood pressure in human sleep, *J. Appl. Physiol.*, **19**(3), pp. 417–422.
- SOMERS-V. K., DYKEN-M. E., CLARY-M. P., AND ABOUD-F. M. (1995). Sympathetic neural mechanisms in obstructive sleep apnea, *Journal of Clinical Investigation*, **96**(4), pp. 1897–1904.
- STANDARDIZATION OF PRECORDIAL LEADS. (1938). Joint recommendations of the American Heart Association and the Cardiac Society of Great Britain and Ireland: Standardization of precordial leads, *Am. Heart J.*, **15**, p. 107.

Bibliography

- STATON-L., EL-SHEIKH-M., AND BUCKHALT-J. A. (2009). Respiratory sinus arrhythmia and cognitive functioning in children, *Developmental Psychobiology*, **51**(3), pp. 249–258.
- STEFANOVSKA-A., HAKEN-H., MCCLINTOCK-P. V. E., HOZIC-M., BAJROVIC-F., AND RIBARIC-S. (2000). Reversible transitions between synchronization states of the cardiorespiratory system, *Phys. Rev. Lett.*, **85**(22), pp. 4831–4834.
- TAHA-B. H., SIMON-P. M., DEMPSEY-J. A., SKATRUD-J. B., AND IBER-C. (1995). Respiratory sinus arrhythmia in humans: An obligatory role for vagal feedback from the lungs, *Journal of Applied Physiology*, **78**(2), pp. 638–645.
- TAKAHASHI-T., HAYANO-J., OKADA-A., SAITOH-T., AND KAMIYA-A. (2005). Effects of the muscle pump and body posture on cardiovascular responses during recovery from cycle exercise, *Eur. J. Appl. Physiol.*, **94**(5-6), pp. 576–583.
- TAKAHASHI-T., OKADA-A., SAITOH-T., HAYANO-J., AND MIYAMOTO-Y. (2000). Difference in human cardiovascular response between upright and supine recovery from upright cycle exercise, *Eur. J. Appl. Physiol.*, **81**(3), pp. 233–239.
- TASS-P., ROSENBLUM-M. G., WEULE-J., KURTHS-J., PIVOSKY-A., VOLKMANN-J., SCHNITZLER-A., AND FREUND-H.-J. (1998). Detection of n:m phase locking from noisy data: Application to magnetoencephalography, *Physical Review Letters*, **81**(15), pp. 3291–3294.
- TAYLOR-E. W., JORDAN-D., AND COOTE-J. H. (1999). Central control of the cardiovascular and respiratory systems and their interactions in vertebrates, *Physiological Reviews*, **79**(3), pp. 855–916.
- TOLEDO-E., AKSELROD-S., PINHAS-I., AND ARAVOT-D. (2002). Does synchronization reflect a true interaction in the cardiorespiratory system?, *Med Eng Phys*, **24**(1), pp. 45–52.
- TSUJI-H., LARSON-M. G., VENDITTI, F. J.-J., MANDERS-E. S., EVANS-J. C., FELDMAN-C. L., AND LEVY-D. (1996). Impact of reduced heart rate variability on risk for cardiac events: The framingham heart study, *Circulation*, **94**(11), pp. 2850–2855.
- TZENG-Y. C., LARSEN-P. D., AND GALLETTY-D. C. (2003). Cardioventilatory coupling in resting human subjects, *Exp. Physiol.*, **88**(6), pp. 775–782.
- TZENG-Y. C., LARSEN-P. D., AND GALLETTY-D. C. (2007). Mechanism of cardioventilatory coupling: Insights from cardiac pacing, vagotomy, and sinoaortic denervation in the anesthetized rat, *Am. J. Physiol. Heart Circ. Physiol.*, **292**(4), pp. H1967–H1977.
- TZENG-Y. C., SIN-P. Y. W., AND GALLETTY-D. C. (2009). Human sinus arrhythmia: Inconsistencies of a teleological hypothesis, *Am. J. Physiol. Heart Circ. Physiol.*, **296**(1), pp. H65–H70.
- UMETANI-K., SINGER-D. H., MCCRATY-R., AND ATKINSON-M. (1998). Twenty-four hour time domain heart rate variability and heart rate: Relations to age and gender over nine decades, *J. Am. Coll. Cardiol.*, **31**(3), pp. 593–601.
- VANOLI-E., ADAMSON-P. B., BA-LIN., PINNA-G. D., LAZZARA-R., AND ORR-W. C. (1995). Heart rate variability during specific sleep stages: A comparison of healthy subjects with patients after myocardial infarction, *Circulation*, **91**(7), pp. 1918–1922.

- VARADY-P., BONGAR-S., AND BENYO-Z. (2003). Detection of airway obstructions and sleep apnea by analyzing the phase relation of respiration movement signals, *IEEE Transactions on Instrumentation and Measurement*, **52**(1), pp. 2–6.
- VASCHILLO-E., VASCHILLO-B., AND LEHRER-P. (2004). Heartbeat synchronizes with respiratory rhythm only under specific circumstances, *Chest*, **126**(4), pp. 1385–1387.
- VELLODY-V. P., NASSERY-M., DRUZ-W. S., AND SHARP-J. T. (1978). Effects of body position change on thoracoabdominal motion, *J. Appl. Physiol.*, **45**(4), pp. 581–589.
- VERRIER-R. L., AND JOSEPHSON-M. E. (2009). Impact of sleep on arrhythmogenesis, *Circulation: Arrhythmia and Electrophysiology*, **2**(4), pp. 450–459.
- VERRIER-R. L., MULLER-J. E., AND HOBSON-J. (1996). Sleep, dreams, and sudden death: The case for sleep as an autonomic stress test for the heart, *Cardiovascular Research*, **31**(2), pp. 181–211.
- VOSS-A., KURTHS-J., KLEINER-H., WITT-A., WESSEL-N., SAPARIN-P., OSTERZIEL-K., SCHURATH-R., AND DIETZ-R. (1996). The application of methods of non-linear dynamics for the improved and predictive recognition of patients threatened by sudden cardiac death, *Cardiovascular Research*, **31**(3), pp. 419–433.
- WALLER-A. D. (1887). A demonstration on man of electromotive changes accompanying the heart's beat, *The Journal of Physiology*, **8**(5), pp. 229–234.
- WELKER-W. I. (1964). Analysis of sniffing of the albino rat, *Behaviour*, **22**(3/4), pp. 223–244.
- WESSEL-N., SUHRBIER-A., RIEDL-M., MARWAN-N., MALBERG-H., BRETTHAUER-G., PENZEL-T., AND KURTHS-J. (2009). Detection of time-delayed interactions in biosignals using symbolic coupling traces, *Europhysics Letters*, **87**(1), article number 10004.
- WIKLUND-U., OLOFSSON-B. O., FRANKLIN-K., BLOM-H., BJERLE-P., AND NIKLASSON-U. (2000). Autonomic cardiovascular regulation in patients with obstructive sleep apnoea: a study based on spectral analysis of heart rate variability, *Clin. Physiol.*, **20**(3), pp. 234–241.
- WILSON-F. N., WISHART-S. W., AND HERRMANN-G. R. (1926). *Proc. Soc. Exper. Biol. & Med.*, **27**, p. 276.
- WITMANS-M. B., KEENS-T. G., DAVIDSON WARD-S. L., AND MARCUS-C. L. (2003). Obstructive hypopneas in children and adolescents: Normal values, *Am. J. Respir. Crit. Care Med.*, **168**, p. 1540.
- WU-M.-C., AND HU-C.-K. (2006). Empirical mode decomposition and synchrogram approach to cardiorespiratory synchronization, *Physical Review E*, **73**, article number 051917.
- YASUMA-F., AND HAYANO-J.-I. (2004). Respiratory sinus arrhythmia: Why does the heartbeat synchronize with respiratory rhythm?, *Chest*, **125**(2), pp. 683–690.
- YEUNG-M. K. S., AND STROGATZ-S. H. (1999). Time delay in the Kuramoto model of coupled oscillators, *Physical Review Letters*, **82**(3), pp. 648–651.
- YOSHIZAKI-H., YOSHIDA-A., HAYASHI-F., AND FUKUDA-Y. (1998). Effect of posture change on control of ventilation, *Jpn. J. Physiol.*, **48**(4), pp. 267–273.

-
- YOUNG-T., PALTA-M., DEMPSEY-J., SKATRUD-J., WEBER-S., AND BADR-S. (1993). The occurrence of sleep-disordered breathing among middle-aged adults, *N. Engl. J. Med.*, **328**(17), pp. 1230–1235.
- ZAR-J. H. (1999). Circular distributions: Hypothesis testing, in T. Ryu. (ed.), *Biostatistical Analysis*, 4th edn, Prentice-Hall, New Jersey, pp. 616–663.
- ZEMAITYTE-D., VARONECKAS-G., AND SOKOLOV-E. (1984). Heart rhythm control during sleep, *Psychophysiology*, **21**(3), pp. 279–289.
- ZHANG-J., YU-X., AND XIE-D. (2010). Effects of mental tasks on the cardiorespiratory synchronization, *Respiratory Physiology & Neurobiology*, **170**(1), pp. 91–95. DOI: 10.1016/j.resp.2009.11.003.
- ZHANG-Y., LI-H., AND BI-L. (2008). Adaptive instantaneous frequency estimation based on EMD and TKEO, *Proceedings of the 2008 Congress on Image and Signal Processing, CISP '08*, IEEE Computer Society, Washington, DC, USA, Vol. 1, pp. 60–64.

Glossary

ANOVA	analysis of variance
ANS	autonomic nervous system
AHI	apnea-hypopnea index
BMI	body-mass index
CRC	cardiorespiratory coordination
CVC	cardioventilatory coupling
ECG	electrocardiogram
EMD	empirical mode decomposition
EOG	electrooculogram
HF	high-frequency power
HR	heart rate
HRV	heart rate variability
IMF	intrinsic mode function
JSD	joint symbolic dynamics
LF	low-frequency power
MPI	movement-power index
OSAS	obstructive sleep apnea syndrome
PLMI	periodic leg movement index
PLMS	periodic leg movements
PNS	peripheral nervous system
PSG	polysomnography
PSNS	parasympathetic nervous system
REM	rapid-eye-movement sleep
RP	respiratory phase
RR	ECG R to R interval
RSA	respiratory sinus arrhythmia
SaO ₂	arterial oxygen saturation
SNS	sympathetic nervous system
SD	standard deviation
SDB	sleep disordered breathing
SS1	stage 1 sleep

Glossary

SS2	stage 2 sleep
SW	slow-wave sleep
TcCO ₂	transcutaneous carbondioxide
TST	total sleep time

Index

- apnea/hypopnea index (AHI), 63, 65, 68, 128, 132, 137
- arousal
 - respiratory, 61, 66, 78, 129, 145, 146, 153
 - spontaneous, 4, 61, 65, 66, 77, 78, 86, 128–130, 140, 144, 145, 152, 158
- autonomic
 - blockade, 26, 28, 34, 35, 37, 144
 - modulation, 61, 85
 - nerve activity, 61, 103
 - nervous system (ANS), 3, 23, 26, 157, 160
 - neuropathy, 62
- cardiac
 - activity, 5, 13, 46, 123, 128, 158
 - cycle, 4, 29, 35, 45, 66, 86, 92, 104, 111, 122, 135, 139, 156, 157, 159, 166, 171
 - disease, 16, 21, 61, 108, 157
 - rhythm, 2, 5, 82, 90, 104, 108, 156, 159, 164, 170, 174
 - vagal tone, 22, 56, 144, 152
- cardiorespiratory
 - coordination, 4, 16, 18, 19, 23, 26, 29, 35, 36, 40, 53, 56, 61, 66, 82, 90, 100, 103
 - coupling, 2, 16, 36, 59, 90, 104, 123, 156, 158
 - interaction, 21, 108, 118, 122, 128, 130, 139, 144, 152
 - synchrogram, 17, 66, 90
 - synchronization, 2–4, 12, 31, 36, 87, 90, 104, 170, 174
- electrocardiogram (ECG), 5, 21, 23, 27, 28, 41, 43, 61, 87, 91, 111, 129, 145, 152, 156, 157, 164, 171
- empirical mode decomposition (EMD), 9, 11, 28
- expiration, 22, 160, 170
- expiratory onset, 7, 93, 114
- heart, 5, 26
- beat, 13, 16, 17, 20, 22, 103
- disease, 61, 62, 75, 85, 90, 128
- rate, 3, 5, 15, 21, 26, 30, 31, 36, 40, 45, 46, 50, 60, 64, 75, 84, 89, 94, 108, 112, 124, 128, 140, 144, 152, 156, 157, 160, 167, 170, 173
- rate variability (HRV), 5, 26, 29, 34, 103, 124, 144, 170, 173
- rhythm, 3, 7, 14, 16, 21, 40, 56, 84, 103, 164
- Hilbert transform, 8, 15, 83, 85, 165
- inspiration, 22, 159, 170, 174
- inspiratory onset, 7, 13, 20, 43, 44, 83, 173
- isoflurane, 23, 26, 27, 29, 36, 37, 41, 156, 160
- joint symbolic dynamics (JSD), 4, 122, 128, 139, 158, 164
- metronomic breathing, 90, 99, 104, 118
- obstructive sleep apnea syndrome (OSAS), 3, 23, 60, 62, 68, 82, 84, 92, 99, 128, 129, 139, 144, 157–160
- parasympathetic
 - nervous system (PSNS), 26, 28, 32
- phase-locking, 16, 21, 29, 37, 69, 71, 84, 86, 92, 99
- piezoelectric, 42, 44–46, 64
- polysomnography, 59, 64, 67, 79, 129, 145
- respiration, 3, 4, 6, 13, 16, 21, 23, 26, 33, 37, 40, 47, 53, 75, 84, 90, 94, 111, 114, 124, 145, 156, 157, 159, 160, 167, 170, 173
- respiratory phase, 17, 23, 93, 96, 98, 99, 103, 104, 108, 111, 114, 122, 128, 130, 158, 160
- respiratory sinus arrhythmia (RSA), 4, 14, 21, 24, 36, 56, 77, 82, 84, 103, 113, 114, 119, 121, 122, 124, 141, 144, 145, 147, 152, 153, 156, 160, 167, 170, 172–174
- respiratory trace
 - calibrator, 91

- impedance belts, 91
- oscillator, 91
- RR interval, 5, 20, 28, 33, 45, 47, 50, 51, 56, 61, 67, 68, 75, 84, 85, 92–94, 96, 99, 100, 113, 114, 116, 122, 123, 131, 140, 158, 166, 167, 171, 173
- sleep
 - rapid-eye-movement (REM), 60, 81, 85, 133, 147, 152
 - slow-wave (SW), 60, 64, 81, 85, 133, 139, 147, 152
 - stage 1 (SS1), 60, 71, 81, 135, 139, 150, 153
 - stage 2 (SS2), 60, 71, 78, 83, 130, 135, 138, 139, 150, 153
- sleep disordered breathing (SDB), 24, 61, 62, 77, 82, 86, 128, 129, 139, 145, 152, 153, 158, 161
- surrogate data, 67, 72, 74, 83, 84, 115, 123
- sympathetic
 - blockade, 34, 35, 37
 - nerve activity, 100, 123, 153
 - nervous system (SNS), 22, 23, 26, 28, 32, 34, 36, 60, 144, 153, 157
 - tone, 86
- time delay correction, 23, 93, 111, 123, 165, 167
- transducer, 42, 86
- vagal
 - blockade, 28, 32, 34, 35, 37
 - modulation, 14
 - nerve activity, 100, 123, 144, 158
 - system, 22, 23, 26, 28, 32, 34, 36
 - tone, 56, 144, 152
- ventilation, 3, 15, 23, 29, 31, 35, 37, 56, 101, 156
- wavelet, 41, 44, 47

Biography

Muammar Muhammad Kabir received his Bachelors of Engineering degree with Honours in Electrical and Electronics Engineering from The University of Adelaide, Australia, in 2007.

Soon after completing his Bachelors degree, he joined the Centre of Biomedical Engineering and the Centre of Heart Rhythm Disorders, and the School of Electrical and Electronic Engineering under a Research Training Scheme to study towards his PhD under the supervision of Dr Mathias Baumert and Prof Derek Abbott.



His major interests lie in the field of biomedical signal processing. He has worked in collaboration with Royal Adelaide Hospital and Women's and Children Hospital, Adelaide, and University of Newcastle, New South Wales, Australia.

During his candidature, he received the 'IEEE South Australia Travel Assistance Award' in 2010 and 2011 and the 'Walter and Dorothy Duncan Trust Travel Grant' in 2010 and 2011 . Also, in 2011, he was selected as one of the 15 prestigious finalists for the IEEE Engineering in Medicine and Biology Society (EMBS) student paper competition, held in Boston, co-sponsored by the National Science Foundation. He has authored and co-authored 13 peer-reviewed publications, and has given 9 presentations at conferences.


Muammar Muhammad Kabir is a member of the IEEE (Institute of Electrical and Electronics Engineers).

Muammar M. Kabir

muammar.kabir@adelaide.edu.au

<http://www.adelaide.edu.au/directory/muammar.kabir>

Scientific Genealogy of Muammar Muhammad Kabir

— Formalised supervisor relationship
 Mentoring relationship
 Nobel prize

